

UNIVERSITÉ DU QUÉBEC A MONTRÉAL

PHENOLOGY OF PRIMARY AND SECONDARY MERISTEMS AND ITS
IMPLICATION FOR FOREST MANAGEMENT AND ECOSYSTEM
CARBON SEQUESTRATION

THÈSE
PRÉSENTÉE
COMME EXIGENCE PARTIELLE
DU DOCTORAT EN BIOLOGIE
EXTENSIONNÉ DE L'UNIVERSITÉ DU QUÉBEC À CHICOUTIMI

PAR
ROBERTO SILVESTRO

MARS 2024

REMERCIEMENTS

Words cannot express my gratitude to my director Sergio Rossi and my co-director Maurizio Mencuccini for their invaluable patience and feedback. With you, I have acquired a comprehensive understanding of the entire process of creating and developing a scientific project, from conceiving an idea to publishing the final results. I have come to appreciate the diverse approaches and methodologies employed in scientific research, and your guidance and expertise have played a significant role in shaping my own approach. I am grateful for the knowledge and skills I have gained through our collaboration, as they have undoubtedly contributed to my personal and professional growth in the field of scientific inquiry.

I am deeply grateful to my evaluation committee, consisting of Rossella Guerrieri and Marcin Klinz, for their unique contributions to my research. Their insightful feedback, constructive criticism, and guidance have been instrumental in the development and refinement of many parts of my research project.

I am immensely grateful for the precious support and camaraderie I have received from my colleagues and lab members throughout my journey. The days spent together in the lab, field, and office have been enriched by your presence, making them both enjoyable and educational. I would also like to extend my thanks to the students who have joined us for short-term internships, research assistants, and the many individuals from our department of fundamental science who have had a profound impact on me and served as a source of inspiration.

I would like to take a moment to express my heartfelt gratitude to all my friends. They have been a source of immense joy and support in my life. Their presence has brought light, laughter, and countless cherished memories into my days.

Desidero esprimere la mia gratitudine alla mia amata famiglia, composta da Imma, Antonello e Manuel. Sono consapevole che ancora oggi stanno cercando di comprendere appieno la natura del mio lavoro e di come mi guadagni da vivere, ma, nonostante ciò, sono stati sempre al mio fianco, condividendo le gioie e le delusioni lungo tutto il percorso della mia vita, dalla mia infanzia fino all'età adulta. La loro costante presenza e il loro sostegno incondizionato hanno rappresentato un'ancora di stabilità e ispirazione in ogni fase del mio cammino. Grazie al loro supporto, ho trovato la forza necessaria per

affrontare le sfide, perseverare nei momenti difficili e celebrare i traguardi raggiunti. Il loro amore, la fiducia e l'incoraggiamento mi hanno alimentato nel perseguire i miei obiettivi e nel credere in me stesso.

Je souhaite exprimer toute ma gratitude envers ma famille québécoise, Johanne et Bertrand, pour leur soutien indéfectible dans les défis quotidiens, petits et grands, de la vie. Leur présence et leur soutien constant ont été d'une valeur inestimable. De plus, je suis extrêmement chanceux d'avoir une équipe de soutien enthousiaste et collaborative qui m'accompagne dans tous mes projets créatifs. Leur encouragement et leur collaboration ont été une source d'inspiration et de motivation.

Un immense merci à ma compagne Katleen, qui est présente à mes côtés chaque jour. Sa présence rend mes journées stressantes beaucoup plus supportables. Sa capacité à transformer notre maison en un véritable refuge d'amour et de tranquillité est une véritable bénédiction. Je suis profondément reconnaissant de l'amour et du réconfort qu'elle apporte à ma vie.

Je souhaite également exprimer ma profonde gratitude envers mes chats pour tout le divertissement et le soutien émotionnel qu'ils m'apportent au quotidien.

DÉDICACE

A Mele Noé

Perché, in bosco,
le prime avventure,
i primi esperimenti,
le prime scoperte
sono state con te.

Luna luna
Damm nu piatt d maccarùn

TABLE DES MATIÈRE

REMERCIEMENTS.....	II
DÉDICACE	I
LISTE DES FIGURES	X
LISTE DES TABLEAUX.....	XVI
RÉSUMÉ	XIX
ABSTRACT.....	1
INTRODUCTION	3
0.1 Plant phenology and its role in a changing world	4
0.2 The phenology of leaves	5
0.3 The phenology of wood formation.....	7
0.4 Objectives and hypothesis.....	9
0.5 Experimental approach.....	11
0.6 Structure of the thesis.....	19
0.7 Figures.....	20
0.8 Annexes.....	21
0.8.1 References Table S 1.1	22
0.9 References	25
CHAPTER I BIOCLIMATIC DISTANCE AND PERFORMANCE OF APICAL SHOOT EXTENSION: DISENTANGLING THE ROLE OF GROWTH RATE AND DURATION IN ECOTYPIC DIFFERENTIATION	31
1.1 Abstract	33
1.2 Introduction.....	35
1.3 Materials and methods	39
1.3.1 Provenances selection	39
1.3.2 Bud phenology and height growth.....	39
1.3.3 Statistical analyses	40
1.4 Results	42
1.4.1 Climate-shift effect	42
1.4.2 ANCOVA models.....	42
1.4.3 Phenological periods.....	43
1.4.4 Height growth	44
1.4.5 ANCOVA models and PCA scores	44
1.5 Discussion	45
1.6 Conclusion.....	50
1.6.1 Acknowledgements.....	51

1.6.2	Author contribution statement	51
1.6.3	Conflict of interest	51
1.7	Figures.....	52
1.8	Tables	57
1.9	Annexes.....	59
1.10	References	64
CHAPTER II LOCAL ADAPTATION SHAPES FUNCTIONAL TRAITS AND RESOURCE ALLOCATION IN BLACK SPUCE		70
2.1	Abstract	72
2.2	Introduction.....	73
2.3	Materials and methods	77
2.3.1	Provenances and common garden.....	77
2.3.2	Data collection	78
2.3.3	Late frost damage assessment.....	79
2.3.4	Statistical analyses	79
2.4	Results.....	81
2.4.1	Phenological timings and growth performances.....	81
2.4.2	Lifetime first reproduction.....	82
2.4.3	Late frost event and frost damages	82
2.4.4	Frost damage and bud phenology	83
2.4.5	Frost damage and height growth performances	83
2.5	Discussion	84
2.5.1	Tree size and reproductive maturity	84
2.5.2	Phenology and frost tolerance.....	86
2.5.3	A blessing in disguise or a curse in hiding?.....	88
2.5.4	Acknowledgements.....	89
2.5.5	Author contribution.....	90
2.5.6	Competing interests	90
2.5.7	Data availability.....	90
2.6	Figures.....	91
2.7	Annexes.....	97
2.8	References	104
CHAPTER III UPSCALING XYLEM PHENOLOGY: SAMPLE SIZE MATTERS 111		111
3.1	Abstract	113
3.2	Introduction.....	115
3.2.1	Wood formation: standards and limits	117
3.3	Materials and methods	120
3.3.1	Study area	120
3.3.2	Sampling and data collection.....	120
3.3.3	Variability in xylem phenology.....	121

3.3.4	The margin of error and minimum sample size	122
3.4	Results	124
3.4.1	Timings of xylogenesis	124
3.4.2	Variability in xylem phenology.....	124
3.4.3	Tree size and spatial variability	125
3.4.4	The margin of error and sample size.....	126
3.5	Discussion	128
3.5.1	Does tree size shape tree growth dynamics?	128
3.5.2	Should we sample closely located trees?	130
3.5.3	Is phenology an issue of carbon sink?	132
3.5.4	Xylogenesis: sample size matters	133
3.5.5	Acknowledgements.....	136
3.5.6	Authors contribution	136
3.6	Figures.....	137
3.7	Tables	145
3.8	Annexes.....	148
3.9	References	154
CHAPTER IV A LONGER WOOD GROWING SEASON DOES NOT LEAD TO HIGHER CARBON SEQUESTRATION		162
4.1	Abstract	165
4.2	Introduction.....	166
4.3	Materials and methods	169
4.3.1	Study area	169
4.3.2	Xylem phenology.....	169
4.3.3	Xylem cell anatomy	170
4.3.4	Statistical Analyses	171
4.4	Results	173
4.4.1	Wood formation dynamics.....	173
4.4.2	Cell production and anatomical traits	174
4.4.3	Wood formation dynamics, production and cell traits	175
4.5	Discussion	178
4.5.1	More is less: phenology, productivity and cell traits	178
4.5.2	Variability at the onset and end of the growing season.....	180
4.5.3	Growing season length and carbon sequestration.....	181
4.6	Conclusions	183
4.6.1	Acknowledgements.....	183
4.6.2	Author contribution.....	184
4.6.3	Competing interests	184
4.6.4	Data availability	184
4.7	Figures.....	185
4.8	Annexes.....	192

4.9	References	195
CHAPTER V PARTIAL ASYNCHRONY OF FOREST CARBON SOURCES AND SINKS AT THE INTRA-ANNUAL TIME SCALE		201
5.1	Abstract	208
5.2	Introduction	209
5.3	Materials and Methods	213
5.3.1	Data selection.....	213
5.3.2	Bioclimatic analyses	213
5.3.3	Assessment of seasonal patterns	214
5.4	Results and discussion.....	218
5.4.1	Bioclimatic analysis	218
5.4.2	Sources and sinks seasonal dynamics within and among biomes	218
5.4.3	Cambial activity and C assimilation	220
5.4.4	The sequence of C allocation in wood.....	222
5.4.5	Variance and predictors of phenological events	224
5.4.6	A reconciliation between C-sources and sinks	226
5.4.7	Acknowledgements.....	230
5.4.8	Author Contributions	230
5.4.9	Competing Interests	231
5.4.10	Data Availability	231
5.5	Figures.....	232
5.6	Tables	237
5.7	Annexes.....	238
5.7.1	Supplementary materials 1 - Site selection and dataset assembly	238
5.7.2	Supplementary material 2 – Data sources and sites.....	246
5.7.3	Supplementary material 3 – Extended results.....	253
5.8	References	287
GENERAL CONCLUSION		295
6.1	Local adaptation and phenological variability among provenances	295
6.2	Within population phenological variability and wood growth.....	296
6.3	Carbon sources and sinks	297
BIBLIOGRAPHIE.....		299

LISTE DES FIGURES

- Figure 0.1 Timeline history of the development of plant phenological observation, experiments, and modelling (Table S 0.1 provides a detailed list of references for these events). 20
- Figure 1.1 The three hypotheses testing the relationship between duration and rate of growth vs height growth in black spruce populations originating from a latitudinal gradient. 52
- Figure 1.2 Sites of origin of the five black spruce provenances [Simoncouche (abbreviated as SIM), Bernatchez (BER), Mistassibi (MIS), Camp Daniel (DAN) and Mirage (MIR)] in the coniferous boreal forest of Québec (Canada) and annual mean temperature of the region..... 53
- Figure 1.3 Climate-related variability between sites of origin [Simoncouche (SIM), Bernatchez (BER), Mistassibi (MIS), Camp Daniel (DAN) and Mirage (MIR)] based on 19 bioclimatic variables (refer to Table 1 for bioclimatic variables abbreviations). Variables vector are colour-coded according to their contribution to total variance. 54
- Figure 1.4 Duration of bud phenology predicted by Ordinary Least Squares (OLS) models in black spruce populations according to mean annual temperature at the site of origin..... 55
- Figure 1.5 Duration of shoot extension, growth rate and height growth predicted by Ordinary Least Squares (OLS) models in black spruce populations according to the mean annual temperature at the site of origin. 56
- Figure 2.1 Origin sites of the five black spruce provenances [Simoncouche (abbreviated as SIM), Bernatchez (BER), Mistassibi (MIS), Camp Daniel (DAN) and Mirage (MIR)] in Quebec, Canada, and annual temperature across the study region. All provenances were planted in a common garden located in SIM (crossed circle).... 91
- Figure 2.2 Comparison of basal diameter and total height across the five black spruce provenances [Simoncouche (abbreviated as SIM), Bernatchez (BER), Mistassibi (MIS), Camp Daniel (DAN) and Mirage (MIR)]. Boxplots represent upper and lower quartiles; whiskers achieve the 10th and 90th percentiles; the median and mean values are drawn as horizontal black lines and black diamond, respectively. 92
- Figure 2.3 Number of trees in reproduction and tree growth in the five black spruce provenances [Simoncouche (abbreviated as SIM), Bernatchez (BER), Mistassibi (MIS), Camp Daniel (DAN) and Mirage (MIR)]. The boxplots illustrate the upper and lower quartiles, with whiskers indicating the 10th and 90th percentiles. The median and the mean are represented by horizontal black lines and a black diamond, respectively..... 93
- Figure 2.4 Bud phenology in trees according to their visible damage by the late frost in 2021. Mean values are denoted by dots, while vertical lines indicate the standard deviations..... 94
- Figure 2.5 Apical shoot extension in 2022 in trees with different damage by the late frost in 2021. The boxplots illustrate the upper and lower quartiles, with whiskers

- indicating the 10th and 90th percentiles. The median and the mean are represented by horizontal black lines and a black diamond, respectively. 95
- Figure 2.6 Apical shoot extension in trees with different damage by the late frost in 2021 for the study years 2017-2022. The boxplots illustrate the upper and lower quartiles, with whiskers indicating the 10th and 90th percentiles. The median and the mean are represented by horizontal black lines and a black diamond, respectively. 96
- Figure 3.1 Location of the experimental plots in the Montmorency Forest (QC, Canada). 137
- Figure 3.2 Transverse section of a weekly sampled microcore, observed at $\times 400$ magnification, for counting the developing tracheids, and classified as (CA) cambium, (EC) enlarging cells, (WTC) wall-thickening and lignifying cells, and (MC) mature cells of the previous year. 138
- Figure 3.3 Number of cambial, enlarging, wall thickening and lignifying, and mature cells observed in 159 balsam firs during 2018. Dots and bars represent average and standard deviation, respectively..... 139
- Figure 3.4 Frequency distributions of the phenological dates determined in 159 balsam firs during 2018. Horizontal boxplots represent upper and lower quartiles, and the mean and median are drawn as orange dots and vertical black lines, respectively. 140
- Figure 3.5 Standardized major axis (SMA) regressions among timings of onset (orange dots) and ending (blue dots) of xylem phenology and total number of cells in the tree ring at the end of the growing season in 159 balsam firs at Montmorency forest. 141
- Figure 3.6 Standardized major axis (SMA) regressions among total duration of cell enlargement and cell wall thickening and lignification, and total number of cells in the tree ring at the end of the growing season in 159 balsam firs at Montmorency forest. 142
- Figure 3.7 Sample size for the onset of xylem formation. Boxplots represent upper and lower quartiles of bootstrapped mean and standard deviation outputs for the onset of enlargement, wall-thickening and first mature cell. The minimum sample size is calculated at different confidence levels and margins of error. 143
- Figure 3.8 Sample size for the ending of xylem formation. Boxplots represent upper and lower quartiles of bootstrapped mean and standard deviation outputs for the ending of enlargement and wall thickening and lignification. The minimum sample size is calculated at different confidence levels and margins of error. 144
- Figure 4.1 Duration of xylem formation (cell enlargement and secondary cell-wall deposition) across the growth ring in 27 balsam firs at the Montmorency Forest (QC, Canada). Boxplots represent upper and lower quartiles; whiskers achieve the 10th and 90th percentiles; the median and mean values are drawn as horizontal black lines and black dots, respectively. The trends result from loess function (span 0.9), with the grey background representing the standard deviation. The dotted line represents the boundary between earlywood and latewood. 185
- Figure 4.2 Xylem cell production and latewood cell percentage in 27 balsam firs at the Montmorency Forest (QC, Canada). 186
- Figure 4.3 Wood anatomical traits and morphometric density across the growth ring in 27 balsam firs at the Montmorency Forest (QC, Canada). Boxplots represent upper and

- lower quartiles; whiskers achieve the 10th and 90th percentiles; the median and mean values are drawn as horizontal black lines and black dots, respectively. The trends result from loess function (span 0.9), with the grey background representing the standard deviation. The dotted line represents the boundary between earlywood and latewood. 187
- Figure 4.4 Relationships between cell production and anatomical traits in 27 balsam firs at the Montmorency forest (QC, Canada). 188
- Figure 4.5 Standardized major axis (SMA) regressions among timings of onset (orange dots) and ending (blue dots) of xylem phenology, earlywood and latewood phenology as a function of the total number of cells in the growth ring at the end of the growing season in 27 balsam firs at Montmorency forest (QC, Canada). 189
- Figure 4.6 Relationships between the amount of earlywood and latewood (expressed as cell number and percentage of total cell production) and earlywood and latewood phenology in 27 balsam firs at Montmorency forest (QC, Canada). 190
- Figure 4.7 Relationships between the amount of earlywood and latewood (expressed as cell number and percentage of total cell production) and annual cell production in 27 balsam firs at Montmorency forest (QC, Canada). 191
- Figure 5.1 Study sites in the Northern hemisphere where the dynamics of wood formation (81 sites), non-structural carbohydrates (57 sites) and C fluxes (39 sites) were determined. C fluxes were also estimated from the FluxSat product for each pixel corresponding to the 87 sites where wood formation was determined. Below, a Whittaker biome plot illustrates the mean annual temperature (°C) and mean annual precipitation (cm) for all 177 study sites. 232
- Figure 5.2 Peak (dot or triangle) and period of maximum activity (horizontal lines) for C fluxes, NSC dynamics and wood formation phenological phases. Minimum concentration is shown for soluble sugars. On the right, for each event the difference among biomes is shown. On the left, for each biome, the temporal consecutive events during the growing season are shown. NEE, GPP and RECO represent the Net Ecosystem Exchange, Gross Primary Production and Ecosystem Respiration. ST and SS represent starch and soluble sugars, respectively. Cell WTL represents the phenological stage of cell wall thickening and lignification. 233
- Figure 5.3 Differences (i.e., subtraction) between the timing of different percentiles and peak (i.e., 100th percentile) of C fluxes, i.e., NEE, GPP, RECO and those of phenological phases of wood formation, i.e., cambial activity, cell enlargement and cell wall thickening and lignification in boreal, temperate and Mediterranean biomes. Negative deltas indicate that C fluxes occurred earlier, while positive deltas that C fluxes occurred later, relative to wood formation, for each percentile shown in the figure. 234
- Figure 5.4 Synchronisms among the timing of peak of Gross Primary Production (GPP) and phenological phases of wood formation (i.e., cambial activity, cell enlargement, and cell wall thickening and lignification) in 87 sites across boreal, temperate and Mediterranean biomes. The dashed line represents a bisecting line (1:1). 235
- Figure 5.5 Relative importance in terms of Mean Decrease Accuracy (%IncMSE) of predictors in the random forest regression models for the timing of peak of FluxSat Gross Primary Production (GPP) and phenological phases of wood formation (i.e., cambial activity, cell wall thickening and lignification). 236

Figure S 1.1 Walter and Lieth climatic diagrams of the five black spruce sites of origin (BER, DAN, MIR, MIS and SIM) from the boreal coniferous forest of Quebec, Canada.	59
Figure S 1.2 Distribution of Studentized residuals of the Ordinary Least Squares (OLS) models. The studentized residuals were uniformly distributed around zero and, generally, residuals exceeding the range between -2 and 2 (i.e., the 95% confidence interval) were < 5.0%.	60
Figure S 1.3 Duration of bud phenology, duration of shoot extension, growth rate and height growth predicted by Ordinary Least Squares (OLS) models in black spruce populations according to the Principal Component Analysis (PCA) scores of the five black spruce sites of origin (BER, DAN, MIR, MIS and SIM).	61
Figure S 2.1 Days of occurrence of the onset and the ending for both budbreak and bud set for each black spruce provenance predicted by the Ordinary Least Squares (OLS) models.	98
Figure S 2.2 Duration of budbreak, shoot extension, and bud set for each black spruce provenance predicted by the Ordinary Least Squares (OLS) models.	99
Figure S 2.3 Apical shoot growth for each black spruce provenance during the study years 2017-2022.	100
Figure S 3.1 Sample size related to the margin of error according to a range of different standard deviations.	148
Figure S 3.2 Relative frequency of diameter classes (left) and height classes (right) among the 159 individual trees sampled in Montmorency forest, Quebec, Canada.	149
Figure S 3.3 Diameter at breast height, tree height and cell production in 159 trees at Montmorency Forest.	150
Figure S 3.4 Linear regressions among timings of the onset of xylem developmental phases and stem diameter and tree height in 159 balsam firs at Montmorency forest (QC, Canada).	151
Figure S 3.5 Linear regressions among timings of the ending of xylem developmental phases and stem diameter and tree height in 159 balsam firs at Montmorency forest (QC, Canada).	152
Figure S 3.6 Timings of xylem phenology in 159 trees at Montmorency forest.	153
Figure S 4.1 Modelized timings of xylem phenology in earlywood and latewood of 27 balsam firs at the Montmorency Forest, QC, Canada.	192
Figure S 4.2 Studentized residuals vs duration of wood formation phases resulting from the fitting of loess function. The dotted lines represent the range between -1.96 and 1.96.	193
Figure S 4.3 Studentized residuals vs wood anatomical traits resulting from the fitting of loess function. The dotted lines represent the range between -1.96 and 1.96.	194
Figure S 5.1 Within Sum of Square (WSS) of the optimal number of clusters determined for climate-related wood formation sites grouping.	240

Figure S 5.2 Whittaker biome plot showing the comparison between the study site classification in the present study (i.e. boreal, temperate and Mediterranean biomes) and Whittaker biome classification according to mean annual temperature (°C) and annual precipitation (cm).....	244
Figure S 5.3 Climate-related variability among 81 wood formation sites of 7 CHELSA (database V2.1) bioclimatic variables summarized in a PCA biplot. The color of the site ID is consistent with color codes used for bioclimatic clusters (boreal –blue labels–, temperate –red labels– and Mediterranean –green labels– biomes). Scores correspond to the first (PC1) and second (PC2) axes of the PCA.....	254
Figure S 5.4 Seasonal pattern of cambial activity and cell differentiation stages (i.e., enlargement and secondary wall thickening and lignification), normalized according to the biome and study site in conifers as a function of the biome (i.e., Boreal, Temperate and Mediterranean).	260
Figure S 5.5 Seasonal dynamics of NSC concentration (i.e., starch and soluble sugars, normalized according to biome, organ, study and quantification method) in conifers as a function of organ (i.e., needles, stem, roots) and biome (i.e., Boreal, Temperate and Mediterranean).	263
Figure S 5.6 Seasonal pattern of Net Ecosystem Exchange (NEE), Ecosystem Respiration (RECO), and Gross Primary Production (GPP), normalized according to the biome, flux type (i.e., NEE, RECO and GPP) and study site in conifers as a function of the biome (i.e., Boreal, Temperate and Mediterranean).	264
Figure S 5.7 Area under the curve (AUC) of the period of maximum activity (MA) of the processes of Gross Primary Production (GPP) and phenological phases of cell enlargement and cell wall thickening and lignification during wood formation in boreal, temperate and Mediterranean biomes.....	266
Figure S 5.8 Fitting details for cambial activity and cell differentiation phenological phase in boreal, temperate and Mediterranean biomes.....	267
Figure S 5.9 Fitting details for starch and soluble sugars in needles in boreal, temperate and Mediterranean biomes.	268
Figure S 5.10 Fitting details for starch and soluble sugars in stem in boreal, temperate and Mediterranean biomes.	269
Figure S 5.11 Fitting details for starch and soluble sugars in roots in boreal, temperate and Mediterranean biomes.	270
Figure S 5.12 Fitting details for Net Ecosystem Exchange (NEE), Ecosystem Respiration (RECO) and Gross Primary Production (GPP) in boreal, temperate and Mediterranean biomes.	271
Figure S 5.13 Synchronisms among the timing of peak of Gross Primary Production (GPP) and phenological phases of wood formation (i.e., cambial activity, cell enlargement, and cell wall thickening and lignification) in 87 sites across boreal (1, blue lines and symbols), temperate (2 and 3, green lines and symbols) and Mediterranean (4, red lines and symbols) biomes. The dashed line represents a bisecting line (1:1).....	285
Figure S 5.14 Relative importance in terms of Mean Decrease Accuracy (%IncMSE) of predictors in the random forest regression models for the timing of peak of FluxNET	

Net Ecosystem Exchange (NEE), Gross Primary Production (GPP), and Ecosystem Respiration (RECO).	286
---	-----

LISTE DES TABLEAUX

Table 1.1 Pearson’s correlation coefficients between the 19 bioclimatic variables proposed by O’Donnell & Ignizio (2012) and the first two principal components (PC1 and PC2) and their contribution to explaining the climatic space across the study sites.	57
Table 1.2 Effects of mean annual temperature of the sites of origin (T), year (Y) and their interaction (T × Y) on bud phenology and components of height growth (shoot extension, height growth, height growth rate) evaluated by ANCOVA models. All models were significant at P < 0.001. The significance of the effect of the factors was obtained by bootstrapping 10,000 times by randomly resampling the original dataset and estimating the 95% confidence intervals of the resulting distributions. Asterisks indicate at least P < 0.05.	58
Table 3.1 Linear regression between xylem phenology and stem diameter (DHB) and height. The “q” represents the slope, SE the standard error. No significant results were observed.	145
Table 3.2 Moran’s correlation coefficients testing for the spatial autocorrelation of xylem phenology for experimental plots and individual trees. No significant results were observed (p < 0.05). Values indicated as Moran’s coefficient and standard deviation.	146
Table 3.3 Minimum sample size for each phenological phase (both onset and end of enlargement, both onset and end of wall thickening and lignification, and onset of maturation) for each confidence level (CL, 70, 80, 85, 90, 95, and 99%) and each desired margin of error (± 1, ± 2, ± 3, ± 4, ± 5 days). For average assessment, we used 300 when the value was > 300.	147
Table 5.1 Results of Standardized Major Axis (SMA) analyses of the bivariate relationships among timing of the peak of GPP and timing of cambial activity, cell enlargement and cell wall thickening and lignification in 87 sites across boreal, temperate and Mediterranean biomes.	237
Table S 0.1 Major historical events in the development of plant phenological studies and their references.	21
Table S 1.1 The 19 bioclimatic variables proposed by O’Donnell & Ignizio (2012) of the five sites in the boreal forest of Quebec, Canada, where the studied populations come from. The climatic parameters at the sites of origin for the period 1979-2013 were extracted using CHELSA Bioclim (Karger et al., 2017) at a spatial resolution of 30 arcsec.	62
Table S 1.2 Effects of PCA axes (PC1 and PC2), year (Y) and their interaction on duration of bud phenology and components of height growth (duration of shoot extension, annual height growth increment, height growth rate) evaluated by ANCOVA models. All models including PC1 scores were significant at P < 0.001, whereas including PC2 scores only the model referring to the duration of bud phenology resulted significant at P < 0.001. The significance of the effect of the factors was obtained by bootstrapping 10,000 times by randomly resampling the original dataset and estimating the 95% confidence intervals of the resulting distributions. Asterisks indicate at least P < 0.05.	63

Table S 2.1 Effects of mean annual temperature of the provenance (Temp), Year and their interaction (Temp×Year) on the phenological phases evaluated by ANCOVA models.....	97
Table S 2.2 Effects of the provenance (Prov), reproductive maturity (Repr) and their interaction (Prov × Repr) on basal diameter and total height evaluated by ANCOVA models.....	101
Table S 2.3 Effects of the Year, damage level (Damage) and their interaction (Year x Damage) on the timing of onset and ending for both bud break and bud set evaluated by ANOVA models.	102
Table S 2.4 Effects of the provenance (Prov), damage level (Damage) and their interaction (Prov x Damage) on growth performances evaluated by ANOVA model.....	103
Table S 2.5 Effects of the year, damage level (Damage) and their interaction (Year x Damage) on growth performances for Mirage (MIR) and Camp Daniel (DAN) provenances evaluated by ANOVA models.....	103
Table S 3.1 Moran`s correlation coefficients tested for the spatial autocorrelation of diameter at breast height, tree height and xylem cell production for experimental plots and individual trees. Values indicated as Moran`s coefficient and standard deviation. * Indicated significant results.	150
Table S 5.1 Pearson correlation coefficients between climatic variable and the first two principal components, eigenvalues, and variance explained.	241
Table S 5.2 Alphabetical list of all the species monitored in the study. 39 species of conifers belonging to 8 different genera were the object of the study.....	245
Table S 5.3 Summary of all curve fitting. RSE indicates the residual standard error. All fittings were significant, at least with a p-value < 0.05.....	256
Table S 5.4 Maximum value (Max), onset, ending and duration of the period of maximum activity (MA), total and period of maximum activity area under the curve (AUC) and their ratio for all the curves describing the seasonal dynamics of wood formation (i.e., cambial activity, cell enlargement, and cell wall thickening and lignification).	259
Table S 5.5 Maximum value (Max), onset, ending and duration of the period of maximum activity (MA), total and period of maximum activity area under the curve (AUC) and their ratio for all the curves describing the seasonal dynamics of NSC (i.e., starch and soluble sugars in needles, stem and roots).....	262
Table S 5.6 Maximum value (Max), onset, ending and duration of the period of maximum activity (MA), total and period of maximum activity area under the curve (AUC) and their ratio for all the curves describing the seasonal dynamics of carbon fluxes (i.e., NEE, GPP and RECO).	265
Table S 5.7 Delta (i.e., subtraction) between the timing of 10th, 25th, 50th, 75th, 90th percentile and peak (i.e., 100th percentile) among C fluxes, i.e., NEE, GPP, RECO and phenological phases of wood formation, i.e., cambial activity, cell enlargement and cell wall thickening and lignification in boreal, temperate and Mediterranean biomes.....	272
Table S 5.8 Results of Standardized Major Axis (SMA) analyses of the bivariate relationships among timing of the peak of GPP and timing of cambial activity, cell	

enlargement and cell wall thickening and lignification in 81 sites according to their bioclimatic classification. * Indicates non-significant ($p > 0.05$) regressions.	285
Table S 5.9 Random forest regression models applied to FluxNET (i.e., NEE, GPP, RECO), FluxSat (i.e., GPP), cambial activity and xylem cell differentiation (i.e., cell enlargement and cell wall thickening and lignification timings of peaks. For each model, the table show the percentage of variance explained, the root mean squared error (RMSE) and the R^2 for both the training and test set.	286

RÉSUMÉ

La phénologie végétale a suscité un intérêt croissant en raison de sa sensibilité aux changements climatiques et de ses implications significatives pour le fonctionnement des écosystèmes. Le timing des phénophases chez les arbres joue un rôle crucial dans l'influence de leurs fonctions biologiques et de leurs interactions écologiques à différentes échelles. Chez les arbres des régions tempérées et boréales, la coordination des activités des organes est essentielle et façonne les schémas saisonniers d'assimilation et d'utilisation des ressources au niveau des arbres, incluant la croissance, la reproduction et le stockage. De plus, des preuves convaincantes suggèrent que les variations phénologiques des feuilles d'une année à l'autre ont un impact direct sur les bilans de carbone, d'eau et d'énergie de l'écosystème. Malgré notre capacité à observer les événements phénologiques à différentes échelles, il reste encore beaucoup à découvrir sur les mécanismes sous-jacents de la phénologie et sur sa relation complexe avec d'autres traits fonctionnels éco-physiologiques. Cette thèse vise à améliorer notre compréhension de la variabilité phénologique entre et au sein des populations, en mettant l'accent spécifiquement sur la croissance primaire et secondaire, et à évaluer comment cette variabilité influence la relation entre les calendriers phénologiques et l'allocation du carbone lors de la croissance.

Cette étude a été menée sur deux sites distincts. Le premier site était une plantation comprenant cinq provenances d'épinettes noires [*Picea mariana* (Mill.)] provenant de différentes latitudes au Québec, Canada. L'objectif principal dans ce site était d'étudier la variation de la phénologie des bourgeons entre les différentes provenances et son impact sur la croissance et la sensibilité aux dommages causés par le gel tardif. Le deuxième site était un peuplement naturel de sapin baumier [*Abies balsamea* (L.) Mill.] au Québec, Canada. Sur ce site, la recherche visait à explorer la variabilité de la phénologie du xylème parmi 159 arbres individuels et à examiner la relation entre la phénologie du bois, la production et les caractéristiques anatomiques. Enfin, le dernier chapitre de cette thèse présente une analyse comparative des dynamiques intra-annuelles des flux de carbone et de la formation du bois dans différents biomes de l'hémisphère nord, comprenant les régions boréales, tempérées et méditerranéennes. L'analyse couvre différentes étapes, de l'assimilation du carbone et de la synthèse de composés non-structuraux à leur incorporation dans les tissus ligneux des conifères.

Les arbres du Nord ont montré un débourrement et une mise en dormance des bourgeons plus précoces, avec une croissance annuelle des pousses plus faible par rapport aux sites plus chauds. La durée de la phénologie des bourgeons était similaire entre les provenances, mais les arbres du Nord avaient une période plus longue d'extension des pousses. En revanche, les provenances des sites du Sud présentaient des taux de croissance plus élevés, ce qui contribuait finalement à de meilleures performances de croissance. De plus, mes résultats ont révélé que les provenances du Nord, qui avaient un débourrement des bourgeons plus précoce, étaient plus sensibles aux dommages causés par un gel tardif du printemps en 2021. Ces dommages par le gel ont eu un impact négatif sur la croissance en hauteur. Cependant, aucun ajustement phénologique significatif n'a été observé l'année suivante.

Les études menées dans la peupleraie naturelle de sapins baumiers ont révélé une variabilité significative dans le moment de la formation du bois parmi les arbres dans une zone de 1 km². La proximité et la taille des arbres n'ont pas affecté la phénologie du

xylème, mais des taux de production cellulaires plus élevés étaient associés à des saisons de croissance plus longues. La production de bois initial représentait 95% de la variation du xylème, avec des arbres productifs produisant plus de bois initial et des cellules plus grandes. Bien que des saisons de croissance plus longues aient entraîné plus de cellules, les cernes des arbres présentaient une densité morphométrique plus faible. Pour évaluer précisément la phénologie du xylème et tenir compte de cette variabilité importante, mon étude a déterminé qu'un échantillon de 23 arbres pouvait fournir des estimations à un niveau de confiance de 95% avec une marge d'erreur d'une semaine. De plus, la synthèse des données mondiales réalisée dans cette thèse a révélé des pics saisonniers synchronisés d'assimilation du carbone et de différenciation des cellules du bois. Elle a également mis en évidence le rôle des glucides non structuraux dans l'amortissement des processus d'assimilation du carbone et d'allocation vers le bois.

Mes études ont révélé des variations écotypiques dans la phénologie des bourgeons et les performances de croissance des populations d'épinettes noires. Ces variations dans la longueur des pousses étaient influencées par le taux de croissance et la durée. La variabilité observée dans les traits fonctionnels suggère des différences dans les stratégies de vie entre les provenances, avec une adaptation locale jouant un rôle crucial dans la survie de l'espèce. Cependant, les implications de ces adaptations pour les conditions climatiques futures et les éventuelles maladaptations ne sont pas entièrement comprises. Il est incertain si ces adaptations seront avantageuses ou poseront des défis face aux changements des conditions environnementales.

Ces études montrent une variabilité dans le moment de la formation du bois au sein des populations d'arbres, suggérant un lien entre la formation du bois et la séquestration du carbone. Cependant, les changements climatiques qui prolongent la saison de croissance ne vont pas nécessairement augmenter la séquestration du carbone par la production de bois. La taille de l'échantillon est importante dans l'étude de la phénologie du xylème pour comprendre les raisons sous-jacentes de cette variabilité et estimer précisément l'allocation du carbone dans les forêts. L'examen des modèles saisonniers à haute résolution des flux de carbone, de la formation du bois et des processus physiologiques est essentiel pour comprendre le cycle du carbone dans les forêts. Cette évaluation contribue à réduire les incertitudes et à prédire les effets du changement climatique sur les forêts à différentes échelles spatiales, améliorant ainsi notre capacité à atténuer les impacts.

Mots clés : Forêt boréale ; Xylogénèse ; Traits fonctionnels ; Phénologie des bourgeons.

ABSTRACT

Plant phenology has received increasing attention due to its sensitivity to climate change and its significant implications for ecosystem functioning. The timing of phenophases in trees plays a crucial role in influencing their biological functions and ecological interactions across various scales. In temperate and boreal trees, the coordination of organ activities is essential, shaping the seasonal patterns of resource assimilation and utilization at the tree level, including growth, reproduction, and storage. Furthermore, compelling evidence suggests that year-to-year leaf phenology variations directly impact the ecosystem's carbon, water, and energy balances. Despite our ability to observe phenological events at different scales, there is still much to uncover regarding the underlying mechanisms of phenology and its intricate relationship with other eco-physiological functional traits. This thesis aims to enhance our understanding of phenological variability among and within populations, specifically focusing on primary and secondary growth, and to evaluate how this variability influences the connection between phenological timings and carbon allocation during growth.

This study was conducted at two distinct sites. The first site consisted of a plantation comprising five black spruce [*Picea mariana* (Mill.)] provenances sourced from different latitudes in Quebec, Canada. These trees were grown in a common garden located at the southern edge of the boreal forest to simulate warmer conditions. The main focus of this site was to investigate the variation in bud phenology among different provenances and its impact on growth performance and susceptibility to late-spring frost damage. The second site was a natural balsam fir [*Abies balsamea* (L.) Mill.] stand in Quebec, Canada. In this site, the research aimed to explore the variability in xylem phenology among 159 individual trees and examine the relationship between wood phenology, production, and anatomical traits. The final chapter of the thesis provides a comparative data synthesis on carbon fluxes and wood formation across different biomes in the Northern Hemisphere. The study covers carbon assimilation, non-structural compound synthesis, and their incorporation into coniferous woody tissues.

Northern trees exhibited earlier budbreak and bud set, with lower annual shoot increment compared to warmer sites. The duration of bud phenology was similar among provenances, but northern trees had a longer period of shoot extension. On the other hand, the provenances from southern sites exhibited higher growth rates, which ultimately contributed to better growth performances. Furthermore, my findings revealed that the northern provenances, which experienced an earlier budbreak, were more susceptible to damage from a late-spring frost event in 2021. This frost damage had a negative impact on height growth performance. However, no significant phenological adjustment was observed in the following year.

The studies conducted in the natural stand of balsam fir revealed significant variability in the timing of wood formation among trees within a 1 km² area. Proximity and tree size did not affect xylem phenology, but higher cell production rates were associated with longer growing seasons. Earlywood production accounted for 95% of xylem variation, with productive trees producing more earlywood and larger cells. Although longer growing seasons led to more cells, tree rings had lower morphometric density. To accurately assess xylem phenology and account for this substantial variability, my study determined that a sample size of 23 trees could provide estimates at a 95% confidence level with a margin of error of one week. Furthermore, the global data synthesis conducted

in this thesis revealed synchronized seasonal peaks of carbon assimilation and wood cell differentiation. It also highlighted the role of non-structural carbohydrates in buffering the processes of carbon assimilation and allocation to wood.

My studies showed ecotypic variation in bud phenology and growth performance of black spruce populations. These variations in shoot length were influenced by growth rate and duration. The observed variability in functional traits suggests differences in life strategies among provenances, with local adaptation playing a crucial role in species' survival. However, the implications of these adaptations for future climate conditions and potential maladaptation are not fully understood. It is uncertain whether these adaptations will be advantageous or pose challenges under changing environmental conditions.

These studies show variability in wood formation timing within tree populations, suggesting a strong link between wood formation and carbon sequestration. However, climate-driven changes that extend the growing season may not necessarily increase carbon sequestration through wood production. Sample size is important in studying xylem phenology to understand the underlying reasons for this variability and accurately estimate carbon allocation in forests. Examining high-resolution seasonal patterns of carbon fluxes, wood formation, and physiological processes is crucial for understanding the carbon cycle in forests. This assessment helps reduce uncertainties and predict climate change effects on forests at different spatial scales, improving our ability to mitigate impacts.

Key words: Boreal forest; Xylogenesis; Functional traits; Bud phenology.

INTRODUCTION

Phenology refers to the study of the timing of recurring life-cycle events and the various factors that influence them, encompassing both biotic and abiotic drivers. The term "phenology" derives from the Greek word φαίνω (phainō), meaning "to show" and "to bring to light", and referring to visible changes in biological development (Tang et al., 2016). Nevertheless, modern phenological research not only involves the description of observable events but also investigates the physiological mechanisms, interconnections, and cascading indirect effects of these events on an ecosystem (Delpierre et al., 2016; Piao et al., 2019). While records of phenological events date back thousands of years, it was not until the 1900s that phenology gained recognition as a scientific discipline (Figure 0.1).

Throughout its history, phenology has evolved from a purely observational discipline focused on documenting the timing of a few key annual natural events in a limited number of species to a comprehensive field incorporating expanded observations, experimental studies, and modelling (Figure 0.1). The close relationship between phenology and various aspects of the ecosystem underscores the importance of monitoring phenological patterns (Delpierre et al., 2016; Gray & Ewers, 2021; Piao et al., 2019). In response to growing concerns about global climate change and its potential impacts, international phenology networks have been established to facilitate collaborative efforts in large-scale, standardized data collection and sharing (Delpierre et al., 2016; Parmesan & Hanley, 2015; Tang et al., 2016). This monitoring is crucial for advancing our understanding of ecological processes and effectively managing resources in the face of climate change and habitat alterations (Gray & Ewers, 2021). Consequently, there has been a significant surge in phenological research in recent decades, accompanied by the development of

new methodologies and technologies to support these endeavours (Figure 0.1). As a result, interdisciplinary frameworks for phenological research have gained prominence in the past two decades, harnessing technological advancements to monitor phenology and its impact on ecosystem functioning across different spatial and temporal scales.

0.1 Plant phenology and its role in a changing world

How do plants recognize the passage of time and the right moment to accomplish growth and reproduction? Like people, plants have their own calendar. A plant's clock is represented by cycles in the environmental conditions, and the timing of phenological events is controlled by climate. Specifically, plants use a set of signals to synchronize the timings of growth and reproduction with favourable environmental conditions.

Plant phenology exhibits a sensitive response to cyclical environmental changes for two primary reasons. First, the aim is to synchronize sexual reproduction among individuals within a population, promoting gene flow (Tang et al., 2016). Second, it serves as a precautionary mechanism to avoid unfavourable seasons (Tang et al., 2016). While the former can utilize any environmental signal, the latter has likely primarily driven the evolution of species populations, necessitating signals that prevent exposure of unhardened or delicate tissues to potentially harmful environmental conditions like freezing temperatures.

The impact of a warming climate on plant phenology is unquestionable (Parmesan & Hanley, 2015; Piao et al., 2019). Various studies have demonstrated that germination (De Frenne et al., 2012; Milbau et al., 2009), leaf emergence (Jeong et al., 2011; Slayback et al., 2003), flowering and fruiting (Cook et al., 2012; Fitter & Fitter, 2002; Xia & Wan, 2013), as well as the general greening of the northern hemisphere (Piao et al., 2015), have all shifted in response to regional warming trends (Menzel et al., 2006; Parmesan, 2006).

These significant changes in phenology under climate change can profoundly impact community structures and ecosystem functions (Suttle et al., 2007; Yang & Rudolf, 2010). Moreover, warming-induced shifts in phenology are a primary factor contributing to the recent increase in vegetation activity and carbon uptake (Piao et al., 2017). Changes in plant phenology can also have feedback effects on the climate system through their role in modifying water and energy exchanges between terrestrial ecosystems and the atmosphere (Peñuelas et al., 2009; Richardson et al., 2013). Therefore, understanding phenology, its underlying drivers, and its impacts on ecosystems is essential for comprehending and modelling the interactions between ecosystems and the climate system.

0.2 The phenology of leaves

Buds play a crucial role among the overwintering tissues of temperate and boreal trees as they harbour the primordia of future leaves or needles. The regulation and maintenance of bud dormancy are paramount for comprehending trees' phenological responses to climate change (Piao et al., 2019). Although not completely understood, it is evident that in most species, phenological timings rely on a combination of signals that can be categorized into three groups: (1) day length (photoperiod), (2) past seasonal experiences (winter chilling temperatures), and (3) current or recent conditions (forcing temperature or water availability) (Flynn & Wolkovich, 2018). When photoperiod is used for spring phenology, winter chilling is also essential since the day length remains the same in spring and autumn. Therefore, the legacy of winter experience, through chilling exposure, is necessary to trigger plants to respond appropriately to spring or autumn cues (Polgar & Primack, 2011; Schwartz & Hanes, 2010). Plants may rely solely on thermal forcing as winter transitions to summer. However, the temperature signal is less reliable as hot early spring weather may induce leaf-out before the risk of freezing has passed a certain

threshold (referred to as a "false spring"; (Allstadt et al., 2015)) or before the onset of the rainy season (Shen et al., 2015). Regardless of the combination of signals utilized by plants, temperature plays a significant role in driving development once the internal requirements have been met (Körner & Basler, 2010).

In autumn, temperate and boreal tree species must synchronize the late-season transition to dormancy before the arrival of periods that pose a risk of freezing damage. Typically, temperature and photoperiod serve as a reliable signal for initiating autumnal hardening in most of these species (Delpierre et al., 2016). However, autumnal phenology lacks easily identifiable visual signals, unlike spring phenology, where phenophases can be visually observed through clear indicators such as budbreak and leaf flushing (Delpierre et al., 2016). The change in leaf colouration during autumn represents only the final stage of a complex series of developmental processes that are more challenging to visually monitor, including winter bud set and leaf abscission layer formation.

Lastly, it is important to acknowledge that the various phenophases, such as budbreak, bud-set, leaf maturation, and leaf senescence, are interconnected. Alterations in the timing of one phase can potentially influence the timing of subsequent phases (Fu et al., 2014; Hänninen & Kramer, 2007). As a result, the environmental cues that drive the timing of each phase also indirectly impact the timing of subsequent phases.

In addition to the abiotic cues mentioned earlier, phenology is also influenced by biological factors such as competition, resource limitation, and genetics (Wolkovich et al., 2014). Within a species, local populations can exhibit divergent phenological timings adapted to optimize survival and reproductive success in their specific environmental conditions (Savolainen et al., 2007). This intraspecific variation in functional traits reflects differences in genotype and phenotypic plasticity across different environments

(Aitken et al., 2008). Local adaptation to contrasting environments, driven by natural selection, increases genetic divergence over time (Aitken et al., 2008). Phenotypic plasticity allows individuals to quickly adjust their phenotypes in response to local conditions, thereby mitigating selective pressures (Pelletier & De Lafontaine, 2023). Therefore, to fully understand phenology and its response to climate change, it is essential to differentiate and integrate both abiotic and biotic drivers into modelling efforts (Schwartz & Hanes, 2010; Steltzer & Post, 2009; Wolkovich et al., 2014).

0.3 The phenology of wood formation

Xylogenesis (i.e., wood formation) is the result of the seasonal activity of the vascular cambium, a secondary meristem derived from the procambium, which in turn derives from the apical meristem (Larson, 1994). Wood growth occurs in a well-defined time window (Rossi et al., 2016). During this period, environmental signals directly affect trees at different time scales: long-term general patterns (climate), recurrent events (seasonality) or punctual events (weather).

The cambium annually or periodically renews both the phloem and the xylem. The cambial zone includes the cambium, made up of a single layer of meristematic cells called “initials” and both phloem and xylem mother cells. When an initial divides, it produces a mother cell and another initial (Larson, 1994), thus assuring a perpetual regeneration of the initials. Given that it is impossible to identify unquestionably which cells represent the true initials based on cell morphology, it is common to refer to all of them as cambial cells.

During development, xylem mother cells undergo differentiation by altering both morphologically and physiologically, gradually assuming definite features and differentiating into the specific elements of the stem tissues. Cells firstly enlarge by

stretching the primary walls, then they produce, thicken and lignify secondary walls and ultimately succumb to programmed cell death (Rossi et al., 2012). During cell enlargement, the cell protoplast is still enclosed in the thin, elastic primary wall. Following positive turgor increased by water movement into the vacuoles, the cell wall stretches, increasing the radial diameter of the tracheid and, consequently, the lumen area. Once their final size has been reached, the cells begin maturing through the formation of a secondary cell wall, its thickening and lignification (Rossi et al., 2012).

Both external and internal factors contribute to the regulation of xylogenesis (Buttò et al., 2020) and are likely involved in determining its timing. Temperature, among these factors, is expected to be a crucial factor in determining the phenology of xylogenesis due to its influence on cell structure (Begum et al., 2013) and fundamental processes such as regulating the division rate of cambium initials (Begum et al., 2013) and gene expression related to active auxin transport (Schrader et al., 2003).

While temperature is a well-recognized ecological factor influencing the timing of the growing season in temperate and boreal climates (Rossi, Deslauriers, Gričar, et al., 2008), it has been revealed that other climatic factors also contribute to the timing of wood formation. For instance, soil drought has been suggested to accelerate the cessation of cambial activity (Balducci et al., 2013; Deslauriers et al., 2016; Vieira et al., 2014). Furthermore, day length, which likely impacts the rate of cambial division (Cuny et al., 2012; Rossi, Deslauriers, Anfodillo, et al., 2006), may serve as a signal for the cessation of cambial activity (Huang et al., 2020).

Beyond climatic signals driving wood formation, since the first pioneer has been observed a significant variability in wood phenology among individuals within a population (Wodzicki & Zajaczkowski, 1970) and has been demonstrated in many species (Gričar et

al., 2009; Lupi et al., 2010; Rathgeber et al., 2011; Rossi, Deslauriers, Anfodillo, et al., 2008). Although part of this variability can be related to the genetic differences among individuals, other factors such as tree size, age, and microsite conditions might influence xylem phenology (Lupi et al., 2013). However, the causes of the observed differences in xylem phenology remain partially unresolved.

0.4 Objectives and hypothesis

My thesis aims to: (i) assess the phenological variability among and within sites for primary and secondary growth and (ii) deepen the relationship between phenological timings and carbon allocation during growth.

Here it follows a list with the specific aims and hypothesis for each chapter composing this thesis:

Chapter 1 - Determining how phenological timing and rate of growth explain the difference in height growth among populations. Three hypotheses are formulated, according to whether the difference in final height growth depends (i) on the growth rate only. Accordingly, I expect to find higher growth rates in the southern populations; (ii) on the duration of growth only. Accordingly, I expect to find longer periods of shoot extension in southern populations; (iii) on both duration and rate of growth.

Chapter 2 - Assessing the differences among five black spruce provenances growing in a common garden in: (i) bud phenology and growth performance, (ii) timings of lifetime first reproduction, and (iii) the consequences of the late-frost event in 2021 on the growth performance and phenological adjustments of trees. I test the hypothesis that (i) the provenance differs in bud phenology and growth performance, (ii) the provenances with faster growth start reproduction at younger ages, and (iii) trees experiencing damage from

frost show an annual growth decline but adjust their phenology to mitigate exposure to late frost events during the successive years.

Chapter 3 - Assessing the variability in wood phenology among trees in an even-aged population by testing the spatial distribution of individuals, their size and the annual xylem production as explanatory variables for the timings of xylem phenology. I raise the hypothesis that xylem phenology is (i) affected by tree size; (ii) spatially heterogeneous within a population; and (iii) related to the rate of annual cell production. Moreover, once variability is assessed and explained, I will quantify the thresholds of sample sizes that can be used as a guideline for sampling during the assessment of wood phenology in the field, and for building and calibrating intra-annual growth models.

Chapter 4 - Determining the relationships and trade-offs among wood formation temporal dynamics, annual productivity, and wood anatomical traits. I test three alternative hypotheses related to the anatomical traits of the xylem. A longer growing season leads to a greater annual tracheid production in which: (i) Earlywood and latewood productions increase proportionally, no differences in morphometric density can be highlighted; (ii) A longer growing season increases carbon assimilation in wood, latewood production augments and thus increases carbon sequestration and morphometric density; or (iii) An earlier onset of the growing season does not result in extra carbon sequestration from wood production, earlywood production increases, resulting in a lower morphometric wood density.

Chapter 5 – Providing a comparative analysis of the intra-annual dynamics of C fluxes and wood formation, from C assimilation and the formation of non-structural compounds to their incorporation in woody tissues in conifers of the Northern hemisphere. Specifically, I use a novel global compilation of (i) ecosystem-scale Net Ecosystem

exchange (NEE), Gross Primary Production (GPP) and Ecosystem Respiration (RECO), (ii) non-structural carbohydrates (NSC) concentrations in various tissues (needles, stems, roots), and (iii) observations of cambial activity (i.e., cambial cell division) and wood formation (i.e., xylem cell differentiation) of 39 conifer species in boreal, temperate, and Mediterranean biomes. I use this dataset to: (i) identify and describe the seasonal patterns of these processes; (ii) assess the co-occurrence of seasonal peaks among processes; and, specifically, (iii) assess the temporal relationship between C assimilation and wood formation at intra-annual scale.

0.5 Experimental approach

The research studies presented in the first four chapters of this thesis were conducted in two specific study areas. In the final chapter, I perform a data synthesis, here is described the data assembly process.

- Simoncouche common garden (Chapter I and II)

This plantation is composed of five provenances of black spruce originated from a latitudinal gradient ranging between the 48th and 53rd parallels in the coniferous boreal forest of Québec, Canada [Simoncouche (SIM), Bernatchez (BER), Mistassibi (MIS), Camp Daniel (DAN) and Mirage (MIR)]. Sampling was conducted in June 2012, randomly selecting 5–10 dominant trees in each stand and collecting 2–10 cones per tree, according to the availability and accessibility of the canopy. On average, 75–145 cones were collected from each stand. The cones were kept in an oven at 80 °C for 4 h, and then shaken in beakers by a vortex mixer to pull out the seeds easily. At the end of June, seeds were sown in plastic containers, and the seedlings were grown under controlled conditions until reaching a suitable size to be planted in the field. In July 2014, seedlings were transferred to a forest gap located in SIM. The common garden area was a 0.5 ha.

The former stand had been harvested, and the ground was left as undisturbed as possible. Seedlings were randomly planted at a distance of 2m×2 m. Two rows of non-experimental black spruce seedlings were also planted on each side of the plantation to avoid an edge effect.

In this site, budbreak and bud set were monitored on a weekly basis from the beginning of May to the end of October 2017-2022. To distinguish between the different phenological phases of the apical bud, I followed the procedure described by Dhont et al. (2010), and I used the apical buds to discriminate the different phenological phases of budbreak during spring and bud set between summer and autumn. Specifically, I considered six budbreak phases: (1) open bud, with a pale spot at the bud tip; (2) elongated bud, with lengthening brown scales; (3) swollen bud, with smooth and pale-coloured scales but no visible needles; (4) translucent bud, with needles visible through the scales; (5) split bud, with open scales but needles still clustered; and (6) exposed shoot, with needles totally emerged from the surrounding scales and spreading outwards. Therefore, I defined five phases of bud set as follows: (1) white bud, presence of a white bud; (2) beige bud, with beige color scale around the bud; (3) brownish bud, with a substantial increase in volume; (4) brown bud, with the beginning of needles spread outwards; and (5) spread needles, with the needles in the whorl spreading outwards.

I defined bud phenology as the period ranging from the first phase of budbreak (i.e., open bud) to the last phase of bud set (i.e., spread needles). The period of shoot extension ranged from the last phase of budbreak (i.e., exposed shoot) to the first phase of bud set (i.e., white bud), corresponding to the period of annual growth of the apical arrow.

I recorded the total height and stem diameter at the collar of each tree. I measured shoot extension during 2017-2022 on the internodes of the main stem using a measuring tape,

with a precision of 2 mm, representing the annual growth of the primary meristem. The growth rate (i.e., mean daily growth during shoot extension) was calculated as a ratio between internode length and the period of shoot extension. I also identified the trees reaching reproductive maturity, based on the presence of cones, from 2020 (the first year in which cones were observed on the trees) to 2022.

- Montmorency Forest (Chapter III and IV)

This study area is located at the Forêt Montmorency in Quebec, Canada (47°16'20"N, 71°08'20" W), within the balsam fir-white birch bioclimatic domain. According to the Köppen Classification System, the climate type is continental, with a short growing season characterized by cool temperatures and high humidity. The mean annual temperature is 0.4 °C. January is the coldest month, with a mean temperature of –15.9 °C. July is the warmest month, with a mean temperature of 14.6 °C. Mean annual precipitation is 1422 mm, of which 465 mm falls in the form of snow. Overall, the stands are composed of 80 % balsam fir [*Abies balsamea* (L.) Mill.], 10 % white birch (*Betula papyrifera* Marsh.) and 10 % spruce [*Picea glauca* (Moench) Voss and *Picea mariana* (Mill.) B.S.P.]. The study area covers 218 ha that was submitted to clear cuts during 1993–1994. The age of the dominant and co-dominant balsam fir stands ranges between 25 and 30 years.

The study consists of 33 permanent plots of 20 × 20 m. In each plot, were chosen 4–5 dominant balsam firs with upright stems for a total sampling of 159 trees. Trees with polycormic stems, partially dead crowns, reaction wood or evident damage due to parasites were avoided. For each tree, we recorded height and diameter at breast height (i.e., 1.3 m above the ground). Wood microcores were collected weekly from April to October 2018 on every tree using a Trephor (Rossi, Anfodillo, et al., 2006). The samples

included mature and developing xylem of the current year, the cambial zone and adjacent phloem, and at least one previous complete tree ring. The microcores were dehydrated through successive immersions in ethanol and d-limonene, embedded in paraffin, cut into 8 μm cross-sections and stained with cresyl violet acetate (0.16 % in water) (Rossi, Deslauriers, & Anfodillo, 2006). I discriminated between developing and mature tracheids under visible and polarized light at magnifications of $\times 400$. Cells were counted across three radial rows and classified as (1) cambium, (2) enlarging, (3) wall-thickening and lignifying or (4) mature (Deslauriers et al., 2003). Cambial cells were characterized by thin cell walls and small radial diameters. The enlargement zone was represented by the absence of glistening under polarized light, which indicates the presence of only primary cell walls. Cells undergoing secondary cell wall formation glistened under polarized light. Cresyl violet acetate reacts with lignin, turning from violet to blue in mature cells. Maturation was reached when the cell walls were entirely blue (Rossi, Deslauriers, & Anfodillo, 2006).

Two additional microcores per tree were collected at the end of summer 2018. I prepared the samples according to the abovementioned experimental protocol. Wood sections were stained in safranin (1% water) and stored on micro slides with a Permount™ mounting medium. We collected digital images of wood transversal sections with a camera fixed on an optical microscope at magnifications of $\times 20$. We measured the lumen radial diameter, lumen tangential diameter, wall radial thickness, and lumen area for all the transversal sections using WinCELL™ (Regent Instruments, Canada).

- Data synthesis – Northern hemisphere

Wood formation data

This study utilizes wood formation data collected from 87 sites encompassing boreal, temperate, and Mediterranean biomes. The data collection followed specific criteria and procedures, both in the field and laboratory, as described below and in accordance with the methodology outlined by Rossi, Anfodillo, et al. (2006) and Rossi, Deslauriers, et al. (2006).

To determine the timings of wood formation, healthy dominant trees were monitored at each site. Throughout the entire growing seasons from 1998 to 2018, the sample size ranged from 1 to 55 trees across all sites. Weekly or occasionally biweekly stem microcores were collected at breast height (1.3 m) using surgical bone-sampling needles or a Trephor tool. These microcores included the mature and developing xylem of the current year, the cambial zone, adjacent phloem, and at least one previous complete tree ring. They were then fixed in solutions of propionic or acetic acid mixed with formaldehyde and stored in ethanol-water at 5 °C. Subsequently, the microcores were dehydrated through successive immersions in ethanol and D-limonene before being embedded in paraffin or glycol methacrylate (samples from Switzerland were not embedded). Transverse sections of 10 to 30 µm thickness were obtained by cutting the microcores using rotary or sledge microtomes.

The obtained sections were stained with cresyl violet acetate or a mixture of safranin and astra/Alcian blue and examined under light microscopy, including bright-field and polarized light. The vascular cambium, a secondary meristem, consists of cambial initials that divide outward and inward to produce phloem and xylem mother cells. These mother cells subsequently form new phloem and xylem tissues. The process of tracheid formation, which involves cell differentiation, can be divided into several phenological phases, including cell enlargement, secondary cell wall thickening and lignification, and programmed cell death, leading to maturity. Cambial cells are characterized by thin cell

walls and small radial diameters. The absence of glistening under polarized light indicates the enlargement zone, where only primary cell walls are present. Cells undergoing secondary cell wall formation exhibit a glistening appearance under polarized light. In mature cells, cresyl violet acetate reacts with lignin, causing a color change from violet to blue. Maturation is reached when the cell walls become entirely blue.

For this study, data pertaining to the phenological phases of cambial activity, cell enlargement, and cell wall thickening and lignification were grouped by biome and site and then normalized using min-max normalization on a scale ranging from 0 to 1.

NSC (Non-structural Carbohydrates)

I compiled the NSC dataset by selecting the conifers section from the dataset used by Martínez-Vilalta et al. (2016) and updated it with more recent data. This resulted in a total of 57 sites distributed across boreal, temperate, and Mediterranean biomes. The dataset included studies that provided seasonal NSC data on wild species measured under natural field conditions. In cases where studies involved experimental manipulations, we only considered results from unmanipulated control groups. Furthermore, to ensure robust temporal coverage and minimize unwanted variability, we applied the following criteria: (1) the study duration was at least four months, (2) the same individuals or populations were measured at least three times throughout the study period, (3) plants were in the mature stage, (4) measurements were taken on needles, main stems, fine roots, or coarse roots, and (5) the reported values were either starch/fructans or soluble sugars.

I extracted individual NSC data points from the text, tables, or figures of each study. In some cases, we directly contacted the authors and used the software GetData Graph Digitizer (Version 2.26) to obtain the necessary data. Typically, NSC concentrations are expressed as a percentage or mg/g dry mass. If the values were reported differently, we

converted them to mg/g for consistency. Finally, the NSC concentrations were grouped by biome, organ, study, extraction method, and quantification method. These additional grouping operations were performed because a study on the comparability of NSC measurements across laboratories (Quentin et al., 2015) concluded that NSC estimates for woody plant tissues may not be directly comparable. To ensure consistency, all the data were normalized using min-max normalization on a scale ranging from 0 to 1.

Flux Data for Evergreen Needleleaf Forests (FLUXNET 2015)

We utilized tier-one level data from the FLUXNET2015 dataset (Pastorello et al., 2020) and extracted daily aggregated data from sites categorized as Evergreen Needleleaf Forests (ENF). These sites consist of forest lands dominated by woody vegetation with a cover of over 60% and a height exceeding 2 meters. To ensure consistency and minimize unwanted variability, we specifically selected data from stands that met the following criteria: (1) belonging to boreal, temperate, or Mediterranean biomes, (2) being at least 15 years old, and (3) not having recently experienced disturbances such as burn sites. Consequently, my dataset comprised a total of 39 sites.

The CO₂ fluxes extracted for each site included Net Ecosystem Exchange (NEE), Ecosystem Respiration (RECO), and Gross Primary Production (GPP). For NEE, we utilized the variable NEE_VUT_REF since it captures the temporal variability and represents the ensemble (Pastorello et al., 2020). There are two main approaches to estimate GPP and RECO (in units of g C m⁻² d⁻¹) through the partitioning of NEE computed with the Ustar (u^*) threshold (VUT): (1) the night-time method (GPP_NT_VUT_REF and RECO_NT_VUT_REF); and (2) the day-time method (GPP_DT_VUT_REF) (Pastorello et al., 2020). The results presented here utilize an average of the night-time and day-time partitioning methods (RECO_NT_VUT_REF and

RECO_DT_VUT_REF for RECO, GPP_NT_VUT_REF and GPP_DT_VUT_REF for GPP).

To facilitate analysis and comparison, the carbon fluxes were grouped by biome, flux type (NEE, GPP, RECO), and site. Furthermore, all data were normalized using min-max normalization on a scale ranging from 0 to 1, ensuring consistent comparisons across variables.

Flux Data in Wood Formation Sites (FLUXSAT V2.0)

We extracted daily Gross Primary Production (GPP) data for each site and each year in which wood formation was monitored. Unlike the dataset obtained from FLUXNET2015, in this case, the samples were collected from coniferous species, while the study area could comprise a mixed forest. The GPP products were obtained using FluxSat v2.0 (Joiner & Yoshida, 2021). FluxSat refers to data derived from FLUXNET eddy covariance tower site data combined with coincident satellite data. This dataset provides global gridded daily estimates of terrestrial GPP and uncertainties at a resolution of 0.05° for the period from 01/03/2000 to the recent past (Joiner & Yoshida, 2021). The GPP estimation was derived from the MODerate-resolution Imaging Spectroradiometer (MODIS) instruments on the NASA Terra and Aqua satellites using the Nadir Bidirectional Reflectance Distribution Function (BRDF)-Adjusted Reflectances (NBAR) product as input for neural networks. These neural networks were trained to upscale GPP estimates obtained from selected FLUXNET 2015 eddy covariance tower sites on a global scale. The GPP value (in $\text{g C m}^{-2} \text{d}^{-1}$) for each site was derived from the interpolation of GPP values from the four nearest pixels (Joiner & Yoshida, 2021).

0.6 Structure of the thesis

This thesis is formed by five chapters devoted to one of the objectives outlined earlier. Each chapter follows the structure of a scientific paper, which has either been published or submitted to a peer-reviewed journal at the time of writing. The formatting of the texts has been standardized to enhance the document's readability. However, if published, a citation to the original manuscript is provided on the title page of each chapter.

0.7 Figures

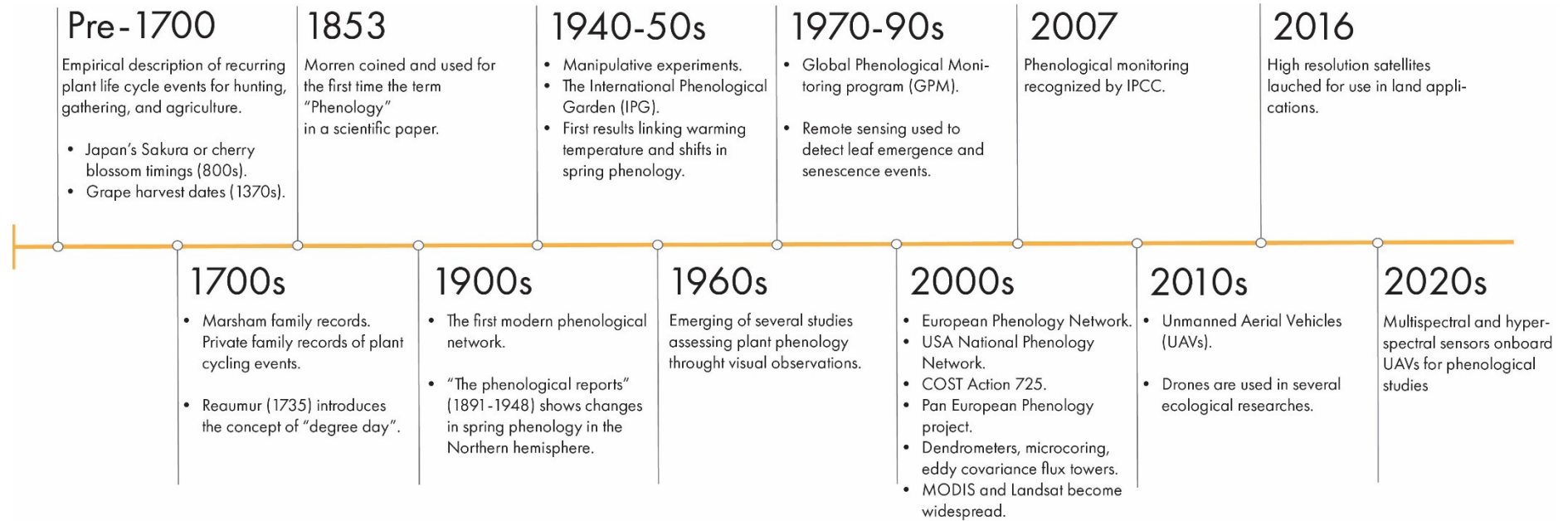


Figure 0.1 Timeline history of the development of plant phenological observation, experiments, and modelling (Table S 0.1 provides a detailed list of references for these events).

0.8 Annexes

Table S 0.1 Major historical events in the development of plant phenological studies and their references.

Time	Events	References
Pre-1700	Cherry tree flowering time	(Aono & Kazui, 2008)
	Grape harvest dates	(Chuine <i>et al.</i> , 2004)
1700s	Marshall's records	(Sparks & Carey, 1995)
	The concept of degree days	(Reaumur, 1735)
1853	Morren coined the word "Phenology"	(Demarée & Rutishauser 2009)
1900s	The first modern phenological network	(Koch <i>et al.</i> , 2008)
	The Phenological Reports	(Clark, 1936; Jeffree 1960)
1940-50s	Manipulative experiment	(Olmsted, 1951)
	The International Phenological Garden (IPG)	(Schnelle & Volkert, 1974)
	Warming temperatures and spring phenology	(McMillan, 1957)
1960s	Visual observations	(Newman & Beard, 1962; Jackson, 1966)
1960-70s	Remote sensing: Landsat	(Dethier <i>et al.</i> , 1973)
	Global Phenological Monitoring program (GPM)	(Chmielewski <i>et al.</i> , 2013)
2000s	European Phenology Network	(van Vliet <i>et al.</i> , 2003)
	USA National Phenology Network	(Geoffrey & Jake, 2015)
	Pan European Phenology project	(Templ <i>et al.</i> , 2018)
	COST Action 725	(Nekovář <i>et al.</i> , 2008)
	Remote sensing: MODIS	(Zhang <i>et al.</i> , 2003)
	Dendrometers, microcores, eddy covariance flux towers	(Gu <i>et al.</i> , 2003; Rossi <i>et al.</i> , 2006)
2007	Phenological monitoring IPCC	(Rosenzweig <i>et al.</i> , 2007)
2010s	Unmanned Aerial Vehicle (UAV)	(Berra <i>et al.</i> , 2016)
	Drones in ecological studies	(Anderson & Gaston, 2013)
2016	High resolution satellites	(Zhang <i>et al.</i> , 2016)
2020s	Multispectral and hyperspectral sensors	(Jeong <i>et al.</i> , 2017; Lu <i>et al.</i> , 2018)

0.8.1 References Table S 1.1

- Anderson, K.; Gaston, K.J. (2013) Lightweight unmanned aerial vehicles will revolutionize spatial ecology. *Front. Ecol. Environ.*, 11, 138–146.
- Aono Y, Kazui K (2008) Phenological data series of cherry tree flowering in Kyoto, Japan, and its application to reconstruction of springtime temperatures since the 9th century. *International Journal of Climatology: A Journal of the Royal Meteorological Society*, 28, 905-914.
- Berra EF, Gaulton R, Barr S (2016) Use of a digital camera onboard a UAV to monitor spring phenology at individual tree level. In: *2016 IEEE International Geoscience and Remote Sensing Symposium (IGARSS)*. pp 3496-3499.
- Chmielewski F.M, Heider S, Moryson S, E B (2013) International Phenological Observation Networks - Concept of IPG and GPM (Chapter 8). In: *Phenology: An Integrative Environmental Science*. (ed M.D. S) pp 137-153. Dordrecht, Springer Science+Business Media B.V.
- Chuine I, Yiou P, Viovy N, Seguin B, Daux V, Ladurie ELR (2004) Historical phenology: grape ripening as a past climate indicator. *Nature*, 432, 289-290.
- Clark, J.E. (1936) The History of British phenology. *Q. J. R. Meteorol. Soc.*, 62, 19–24.
- Demarée, G.R.; Rutishauser, T. (2009) Origins of the word “phenology”. *Eos Trans. Am. Geophys. Union*, 90, 291.
- Dethier B, Ashley M, Blair B, Hopp R (1973) Phenology satellite experiment. In: *Symposium on significant results obtained from the Earth Resources Technology Satellite-1, vol I. Technical presentations, section A*. (eds Freden S, Mercanti E, Becker M). Washington, DC, NASA.
- Geoffrey MH, Jake FW (2015) Review of the USA National Phenology Network. In: *Circular*. (eds Glynn PD, Owen TW) pp 36, Reston, VA.
- Gu L, Post WM, Baldocchi D, Black TA, Verma SB, Vesala T, Wofsy SC (2003) Phenology of vegetation photosynthesis. In: *Phenology: An integrative environmental science*. pp 467-485. Springer.
- Jeffrey, E. (1960) Some long-term means from The Phenological Reports (1891–1948) of the Royal Meteorological Society. *Q. J. R. Meteorol. Soc.*, 86, 95–103.
- Jackson, M.T. (1966) Effects of microclimate on spring flowering phenology. *Ecology*, 47, 407–415.

- Jeong SJ, Schimel D, Frankenberg C, Drewry DT, Fisher JB, Verma M, . . . Joiner J (2017) Application of satellite solar-induced chlorophyll fluorescence to understanding large-scale variations in vegetation phenology and function over northern high latitude forests. *Remote Sensing of Environment*, 190, 178-187.
- Koch E, Lipa W, Neumcke R, Zach S (2008) The history and current status of the Austrian phenology network. In: *COST Action 725: The history and current status of plant phenology in Europe*. (eds Nekovář J, Koch E, Kubin E, Nejedlik P, Sparks T, Wielgolaski FE). COST office.
- Lu X, Liu Z, Zhou Y, Liu Y, An S, Tang J (2018) Comparison of Phenology Estimated from Reflectance-Based Indices and Solar-Induced Chlorophyll Fluorescence (SIF) Observations in a Temperate Forest Using GPP-Based Phenology as the Standard. *Remote Sensing*, 10, 932; <https://doi.org/10.3390/rs10060932>.
- McMillan, C. (1957) Nature of the plant community. IV. Phenological variation within five woodland communities under controlled temperatures. *Am. J. Bot.*, 44, 154–163.
- Nekovář J, Koch E, Kubin E, Nejedlik P, Sparks T, Wielgolaski F (2008) *COST Action 725-the history and current status of plant phenology in Europe*, Brussels, COST Office.
- Newman, J.E.; Beard, J.B. (1962) Phenological Observations: The Dependent Variable in Bioclimatic and Agrometeorological Studies. *Agron. J.*, 54, 399–403.
- Reaumur RD (1735) Observation du thermometer, faites à Paris pendant l'année 1735, compares avec celles qui ont été faites sous la ligne, à l'Isle de France, à Alger et en quelques-unes de nos isles de l'Amérique. Paris: Mémoires de l'Académie des Sciences.
- Rosenzweig, C.; Casassa, G.; Karoly, D.J.; Imeson, A.; Liu, C.; Menzel, A.; Rawlins, S.; Root, T.L.; Seguin, B.; Tryjanowski, P. (2007) Assessment of observed changes and responses in natural and managed systems. In *Climate Change 2007: Impacts, Adaptation and Vulnerability, Contribution of Working Group II to the Fourth Assessment Report of the Intergovernmental Panel on Climate Change*; Parry, M., Canziani, O.F., Palutikof, J., van der Linden, P., Hanson, C., Eds.; Cambridge University Press: Cambridge, UK; New York, NY, USA; Volume 2007, p. 79.
- Rossi, S; Deslauriers, A.; Anfodillo, T. (2006). Assessment of cambial activity and xylogenesis by microsampling tree species: An example at the Alpine timberline. *IAWA Journal*, 27(4), 383-394.
- Schnelle F, Volkert E (1974) International Phenological Gardens in Europe The Basic Network for International Phenological Observations. In: *Phenology and Seasonality Modeling*. (ed Lieth H) pp 383-387. Berlin, Heidelberg, Springer Berlin Heidelberg.

- Sparks T, Carey P (1995) The responses of species to climate over two centuries: an analysis of the Marsham phenological record, 1736-1947. *Journal of Ecology*, 83, 321-329.
- Templ B, Koch E, Bolmgren K, Ungersböck M, Paul A, Scheifinger H, . . . Hodzić S (2018) Pan European Phenological database (PEP725): a single point of access for European data. *International Journal of Biometeorology*, 62, 1-5.
- Van Vliet AJ, De Groot RS, Bellens Y, Braun P, Bruegger R, Bruns E, . . . Sparks T (2003) The European phenology network. *Int J Biometeorol*, 47, 202-212.
- Zhang, J.; Hu, J.; Lian, J.; Fan, Z.; Ouyang, X.; Ye, W. (2016) Seeing the forest from drones: Testing the potential of lightweight drones as a tool for long-term forest monitoring. *Biol. Conserv.*, 198, 60–69.
- Zhang X, Friedl MA, Schaaf CB, Strahler AH, Hodges JC, Gao F, . . . Huete A (2003) Monitoring vegetation phenology using MODIS. *Remote Sensing of Environment*, 84, 471-475.

0.9 References

- Aitken, S. N., Yeaman, S., Holliday, J. A., Wang, T., & Curtis-McLane, S. (2008). Adaptation, migration or extirpation: climate change outcomes for tree populations. *Evolutionary Applications*, *1*(1), 95-111. <https://doi.org/10.1111/j.1752-4571.2007.00013.x>
- Allstadt, A. J., Vavrus, S. J., Heglund, P. J., Pidgeon, A. M., Thogmartin, W. E., & Radeloff, V. C. (2015). Spring plant phenology and false springs in the conterminous US during the 21st century. *Environmental Research Letters*, *10*(10), 104008.
- Balducci, L., Deslauriers, A., Giovannelli, A., Rossi, S., & Rathgeber, C. B. K. (2013). Effects of temperature and water deficit on cambial activity and woody ring features in *Picea mariana* saplings. *Tree Physiology*, *33*(10), 1006-1017. <https://doi.org/10.1093/treephys/tpt073>
- Begum, S., Nakaba, S., Yamagishi, Y., Oribe, Y., & Funada, R. (2013). Regulation of cambial activity in relation to environmental conditions: Understanding the role of temperature in wood formation of trees. *Physiologia Plantarum*, *147*(1), 46-54. <https://doi.org/10.1111/j.1399-3054.2012.01663.x>
- Buttò, V., Deslauriers, A., Rossi, S., Rozenberg, P., Shishov, V., & Morin, H. (2020). The role of plant hormones in tree-ring formation. *Trees - Structure and Function*, *34*(2), 315-335. <https://doi.org/10.1007/s00468-019-01940-4>
- Cook, B. I., Wolkovich, E. M., & Parmesan, C. (2012). Divergent responses to spring and winter warming drive community level flowering trends. *Proceedings of the National Academy of Sciences*, *109*(23), 9000-9005.
- Cuny, H. E., Rathgeber, C. B. K., Lebourgeois, F., Fortin, M., & Fournier, M. (2012). Life strategies in intra-annual dynamics of wood formation: Example of three conifer species in a temperate forest in north-east France. *Tree Physiology*, *32*(5), 612-625. <https://doi.org/10.1093/treephys/tps039>
- De Frenne, P., Graae, B. J., Brunet, J., Shevtsova, A., De Schrijver, A., Chabrerie, O., Cousins, S. A., Decocq, G., Diekmann, M., & Hermy, M. (2012). The response of forest plant regeneration to temperature variation along a latitudinal gradient. *Annals of Botany*, *109*(5), 1037-1046.
- Delpierre, N., Vitasse, Y., Chuine, I., Guillemot, J., Bazot, S., Rutishauser, T., & Rathgeber, C. B. K. (2016). Temperate and boreal forest tree phenology: from organ-scale processes to terrestrial ecosystem models. *Annals of Forest Science*, *73*(1), 5-25. <https://doi.org/10.1007/s13595-015-0477-6>
- Deslauriers, A., Huang, J. G., Balducci, L., Beaulieu, M., & Rossi, S. (2016). The contribution of carbon and water in modulating wood formation in black spruce

saplings. *Plant Physiology*, 170(4), 2072-2084.
<https://doi.org/10.1104/pp.15.01525>

- Deslauriers, A., Morin, H., & Begin, Y. (2003). Cellular phenology of annual ring formation of *Abies balsamea* in the Quebec boreal forest (Canada). *Canadian Journal of Forest Research*, 33(2), 190-200.
<https://doi.org/10.1139/x02-178>
- Dhont, P., Sylvestre, P., Gros-Louis, M. C., & Isabel, N. (2010). *Field Guide for Identifying Apical Bud Break and Bud Formation Stages in White Spruce*.
- Fitter, A., & Fitter, R. (2002). Rapid changes in flowering time in British plants. *Science*, 296(5573), 1689-1691.
- Flynn, D. F. B., & Wolkovich, E. M. (2018). Temperature and photoperiod drive spring phenology across all species in a temperate forest community. *New Phytologist*, 219(4), 1353-1362. <https://doi.org/10.1111/nph.15232>
- Fu, Y. S. H., Campioli, M., Vitasse, Y., De Boeck, H. J., Van Den Berge, J., Abdelgawad, H., Asard, H., Piao, S., Deckmyn, G., & Janssens, I. A. (2014). Variation in leaf flushing date influences autumnal senescence and next year's flushing date in two temperate tree species. *Proceedings of the National Academy of Sciences*, 111(20), 7355-7360. <https://doi.org/10.1073/pnas.1321727111>
- Gray, R. E. J., & Ewers, R. M. (2021). Monitoring Forest Phenology in a Changing World. *Forests*, 12(3), 297. <https://doi.org/10.3390/f12030297>
- Gričar, J., Krže, L., & Čufar, K. (2009). Number of cells in xylem, phloem and dormant cambium in silver fir (*Abies alba*), in trees of different vitality. *IAWA Journal*, 30(2), 121-133. <https://doi.org/10.1163/22941932-90000208>
- Hänninen, H., & Kramer, K. (2007). A framework for modelling the annual cycle of trees in boreal and temperate regions. *Silva Fennica*, 41(1), 167-205.
<https://edepot.wur.nl/41205>
- Huang, J. G., Ma, Q., Rossi, S., Biondi, F., Deslauriers, A., Fonti, P., Liang, E., Mäkinen, H., Oberhuber, W., Rathgeber, C. B. K., Tognetti, R., Treml, V., Yang, B., Zhang, J. L., Antonucci, S., Bergeron, Y., Julio Camarero, J., Campelo, F., Cufar, K., . . . Ziaco, E. (2020). Photoperiod and temperature as dominant environmental drivers triggering secondary growth resumption in Northern Hemisphere conifers. *Proceedings of the National Academy of Sciences of the United States of America*, 117(34), 20645-20652. <https://doi.org/10.1073/pnas.2007058117>
- Jeong, S. J., HO, C. H., GIM, H. J., & Brown, M. E. (2011). Phenology shifts at start vs. end of growing season in temperate vegetation over the Northern Hemisphere for the period 1982–2008. *Global Change Biology*, 17(7), 2385-2399.

- Körner, C., & Basler, D. (2010). Phenology under global warming. *Science*, 327(5972), 1461-1462. <https://doi.org/10.1126/science.1186473>
- Larson, P. R. (1994). *The vascular cambium : development and structure*. https://books.google.ca/books?hl=it&lr=&id=7mLwCAAQBAJ&oi=fnd&pg=PA2&ots=7bxBRh1rxu&sig=IPYJhviM7U5gehvzX_y7d5O-0as&redir_esc=y#v=onepage&q&f=false
- Lupi, C., Morin, H., Deslauriers, A., & Rossi, S. (2010). Xylem phenology and wood production: Resolving the chicken-or-egg dilemma. *Plant, Cell and Environment*, 33(10), 1721-1730. <https://doi.org/10.1111/j.1365-3040.2010.02176.x>
- Lupi, C., Rossi, S., Vieira, J., Morin, H., & Deslauriers, A. (2013). Assessment of xylem phenology: A first attempt to verify its accuracy and precision. *Tree Physiology*, 34(1), 87-93. <https://doi.org/10.1093/treephys/tpt108>
- Menzel, A., Sparks, T. H., Estrella, N., Koch, E., Aaasa, A., Ahas, R., Alm-Kübler, K., Bissolli, P., Braslavská, O. g., Briede, A., Chmielewski, F. M., Crepinsek, Z., Curnel, Y., Dahl, Å., Defila, C., Donnelly, A., Filella, Y., Jactzak, K., Måge, F., . . . Züst, A. (2006). European phenological response to climate change matches the warming pattern. *Global Change Biology*, 12(10), 1969-1976. <https://doi.org/10.1111/j.1365-2486.2006.01193.x>
- Milbau, A., Graae, B. J., Shevtsova, A., & Nijs, I. (2009). Effects of a warmer climate on seed germination in the subarctic. *Annals of Botany*, 104(2), 287-296.
- Parnesan, C. (2006). Ecological and evolutionary responses to recent climate change. *Annual Review of Ecology, Evolution, and Systematics*, 37(1), 637-669. <https://doi.org/10.1146/annurev.ecolsys.37.091305.110100>
- Parnesan, C., & Hanley, M. E. (2015). Plants and climate change: complexities and surprises. *Annals of Botany*, 116(6), 849-864. <https://doi.org/10.1093/aob/mcv169>
- Pelletier, E., & De Lafontaine, G. (2023). Jack pine of all trades: Deciphering intraspecific variability of a key adaptive trait at the rear edge of a widespread fire-embracing North American conifer. *American Journal of Botany*, 110(2). <https://doi.org/10.1002/ajb2.16111>
- Peñuelas, J., Rutishauser, T., & Filella, I. (2009). Phenology Feedbacks on Climate Change. *Science*, 324(5929), 887-888. <https://doi.org/doi:10.1126/science.1173004>
- Piao, S., Liu, Q., Chen, A., Janssens, I. A., Fu, Y., Dai, J., Liu, L., Lian, X., Shen, M., & Zhu, X. (2019). Plant phenology and global climate change: Current progresses and challenges. *Global Change Biology*, 25(6), 1922-1940. <https://doi.org/10.1111/gcb.14619>

- Piao, S., Liu, Z., Wang, T., Peng, S., Ciais, P., Huang, M., Ahlstrom, A., Burkhardt, J. F., Chevallier, F., Janssens, I. A., Jeong, S.-J., Lin, X., Mao, J., Miller, J., Mohammat, A., Myneni, R. B., Peñuelas, J., Shi, X., Stohl, A., . . . Tans, P. P. (2017). Weakening temperature control on the interannual variations of spring carbon uptake across northern lands. *Nature Climate Change*, 7(5), 359-363. <https://doi.org/10.1038/nclimate3277>
- Piao, S., Tan, J., Chen, A., Fu, Y. H., Ciais, P., Liu, Q., Janssens, I. A., Vicca, S., Zeng, Z., Jeong, S.-J., Li, Y., Myneni, R. B., Peng, S., Shen, M., & Peñuelas, J. (2015). Leaf onset in the northern hemisphere triggered by daytime temperature. *Nature Communications*, 6(1), 6911. <https://doi.org/10.1038/ncomms7911>
- Polgar, C. A., & Primack, R. B. (2011). Leaf-out phenology of temperate woody plants: from trees to ecosystems. *New Phytologist*, 191(4), 926-941. <https://doi.org/10.1111/j.1469-8137.2011.03803.x>
- Rathgeber, C. B. K., Rossi, S., & Bontemps, J. D. (2011). Cambial activity related to tree size in a mature silver-fir plantation. *Annals of Botany*, 108(3), 429-438. <https://doi.org/10.1093/aob/mcr168>
- Richardson, A. D., Keenan, T. F., Migliavacca, M., Ryu, Y., Sonnentag, O., & Toomey, M. (2013). Climate change, phenology, and phenological control of vegetation feedbacks to the climate system. *Agricultural and Forest Meteorology*, 169, 156-173. <https://doi.org/https://doi.org/10.1016/j.agrformet.2012.09.012>
- Rossi, S., Anfodillo, T., Čufar, K., Cuny, H. E., Deslauriers, A., Fonti, P., Frank, D., Gričar, J., Gruber, A., Huang, J. G., Jyske, T., Kašpar, J., King, G., Krause, C., Liang, E., Mäkinen, H., Morin, H., Nöjd, P., Oberhuber, W., . . . Treml, V. (2016). Pattern of xylem phenology in conifers of cold ecosystems at the Northern Hemisphere. *Global Change Biology*, 22(11), 3804-3813. <https://doi.org/10.1111/gcb.13317>
- Rossi, S., Anfodillo, T., & Menardi, R. (2006). Trephor: A new tool for sampling microcores from tree stems. *IAWA Journal*, 27(1), 89-97. <https://doi.org/10.1163/22941932-90000139>
- Rossi, S., Deslauriers, A., & Anfodillo, T. (2006). Assessment of cambial activity and xylogenesis by microsampling tree species: An example at the Alpine timberline. *IAWA Journal*, 27(4), 383-394. <https://doi.org/10.1163/22941932-90000161>
- Rossi, S., Deslauriers, A., Anfodillo, T., & Carrer, M. (2008). Age-dependent xylogenesis in timberline conifers. *New Phytologist*, 177(1), 199-208. <https://doi.org/10.1111/j.1469-8137.2007.02235.x>
- Rossi, S., Deslauriers, A., Anfodillo, T., Morin, H., Saracino, A., Motta, R., & Borghetti, M. (2006). Conifers in cold environments synchronize maximum growth rate of

tree-ring formation with day length. *New Phytologist*, 170(2), 301-310. <https://doi.org/10.1111/j.1469-8137.2006.01660.x>

- Rossi, S., Deslauriers, A., Gričar, J., Seo, J. W., Rathgeber, C. B. K., Anfodillo, T., Morin, H., Levanic, T., Oven, P., & Jalkanen, R. (2008). Critical temperatures for xylogenesis in conifers of cold climates. *Global Ecology and Biogeography*, 17(6), 696-707. <https://doi.org/10.1111/j.1466-8238.2008.00417.x>
- Rossi, S., Morin, H., & Deslauriers, A. (2012). Causes and correlations in cambium phenology: towards an integrated framework of xylogenesis. *Journal of Experimental Botany*, 63(5), 2117-2126. <https://doi.org/10.1093/jxb/err423>
- Savolainen, O., Pyhäjärvi, T., & Knürr, T. (2007). Gene flow and local adaptation in trees. *Annual Review of Ecology, Evolution, and Systematics*, 38(1), 595-619. <https://doi.org/10.1146/annurev.ecolsys.38.091206.095646>
- Schrader, J., Baba, K., May, S. T., Palme, K., Bennett, M., Bhalerao, R. P., & Sandberg, G. (2003). Polar auxin transport in the wood-forming tissues of hybrid aspen is under simultaneous control of developmental and environmental signals. *Proceedings of the National Academy of Sciences of the United States of America*, 100(17), 10096-10101. <https://doi.org/10.1073/pnas.1633693100>
- Schwartz, M. D., & Hanes, J. M. (2010). Continental-scale phenology: warming and chilling. *International Journal of Climatology*, 30(11), 1595-1598.
- Shen, M., Piao, S., Cong, N., Zhang, G., & Jassens, I. A. (2015). Precipitation impacts on vegetation spring phenology on the Tibetan Plateau. *Global Change Biology*, 21(10), 3647-3656.
- Slayback, D. A., Pinzon, J. E., Los, S. O., & Tucker, C. J. (2003). Northern hemisphere photosynthetic trends 1982–99. *Global Change Biology*, 9(1), 1-15.
- Steltzer, H., & Post, E. (2009). Seasons and life cycles. *Science*, 324(5929), 886-887.
- Suttle, K. B., Thomsen, M. A., & Power, M. E. (2007). Species Interactions Reverse Grassland Responses to Changing Climate. *Science*, 315(5812), 640-642. <https://doi.org/10.1126/science.1136401>
- Tang, J., Körner, C., Muraoka, H., Piao, S., Shen, M., Thackeray, S. J., & Yang, X. (2016). Emerging opportunities and challenges in phenology: a review. *Ecosphere*, 7(8), e01436.
- Vieira, J., Rossi, S., Campelo, F., Freitas, H., & Nabais, C. (2014). Xylogenesis of *Pinus pinaster* under a Mediterranean climate. *Annals of Forest Science*, 71(1), 71-80. <https://doi.org/10.1007/s13595-013-0341-5>

- Wodzicki, T. J., & Zajaczkowski, S. (1970). Methodical problems in studies on seasonal production of cambial xylem derivatives. *Acta Societatis Botanicorum Poloniae*, 39(3), 519-520. <https://doi.org/10.5586/asbp.1970.040>
- Wolkovich, E. M., Cook, B. I., & Davies, T. J. (2014). Progress towards an interdisciplinary science of plant phenology: building predictions across space, time and species diversity. *New Phytologist*, 201(4), 1156-1162.
- Xia, J., & Wan, S. (2013). Independent effects of warming and nitrogen addition on plant phenology in the Inner Mongolian steppe. *Annals of Botany*, 111(6), 1207-1217.
- Yang, L. H., & Rudolf, V. H. W. (2010). Phenology, ontogeny and the effects of climate change on the timing of species interactions. *Ecology Letters*, 13(1), 1-10. <https://doi.org/https://doi.org/10.1111/j.1461-0248.2009.01402.x>

CHAPTER I

BIOCLIMATIC DISTANCE AND PERFORMANCE OF APICAL SHOOT EXTENSION: DISENTANGLING THE ROLE OF GROWTH RATE AND DURATION IN ECOTYPIC DIFFERENTIATION

Published in Forest Ecology and Management

Citation:

Silvestro, R., Brasseur, S., Klisz, M., Mencuccini, M., & Rossi, S. (2020). Bioclimatic distance and performance of apical shoot extension: disentangling the role of growth rate and duration in ecotypic differentiation. *Forest Ecology and Management*, 477, 118483.

RESEARCH ARTICLE

Title

Bioclimatic distance and performance of apical shoot extension: disentangling the role of growth rate and duration in ecotypic differentiation

Authors:

Roberto Silvestro^{1, *}, Solène Brasseur², Marcin Klisz³, Maurizio Mencuccini^{4,5}, Sergio Rossi^{1,6}

Affiliations:

1 Département des Sciences Fondamentales, Université du Québec à Chicoutimi, 555 boulevard de l'Université, Chicoutimi (QC) G7H2B1, Canada.

2 Université de Technologie de Compiègne, Rue du Docteur Schweitzer CS 60319, 60203, Compiègne, Cedex, France.

3 Department of Silviculture and Genetics, Forest Research Institute, Braci Lesnej Street No 3, Sekocin Stary, PL-05-090, Raszyn, Poland.

4 Centre de Recerca Ecològica i Aplicacions Forestals (CREAF), Bellaterra, 08193, Barcelona, Spain.

5 Institució Catalana de Recerca i Estudis Avançats (ICREA), Passeig de Lluís Companys 23, 08010, Barcelona, Spain.

6 Key laboratory of vegetation restoration and management of degraded ecosystems, Guangdong provincial key laboratory of applied botany, South China Botanical Garden, Chinese Academy of Sciences, Guangzhou, China.

* Corresponding author: roberto.silvestro1@uqac.ca

1.1 Abstract

Under the same environmental conditions, southern and northern populations of temperate and boreal ecosystems exhibit different growth performance. However, which growth trait drives this difference is still unresolved. This study aimed to disentangle the effect of duration and rate of growth on shoot extension of five black spruce [*Picea mariana* (Mill.)] populations originating from a latitudinal gradient in Quebec, Canada, and growing in a common garden at the southern border of the boreal forest to simulate warming conditions. Bud phenology was monitored weekly during the growing seasons 2017-2019, and shoot length was recorded in autumn, representing annual growth of the primary meristem. Populations originating from the colder sites showed a lower annual shoot increment compared to those originating from the warmer sites. Despite similar durations of bud phenology, the period of shoot extension occurred between the beginning of June and the beginning of July and was longer in the provenances originating from the colder sites. The period of shoot extension, on average, was shortened by 0.9 days for each degree Celsius of increase in annual mean temperature of the site of origin. Moreover, the populations originating from warmer sites showed higher growth rates, which increased by 0.1 cm day⁻¹ for each degree Celsius of increase in the annual mean temperature of the site of origin. Our results confirmed ecotypic variation in growth performance among black spruce populations and demonstrated that differences in shoot length are related to both rate and duration of growth. In the context of a warming climate, northern populations may be unable to reach the current growth performance of southern ones because of their adaptations to harsh local conditions and low intrinsic growth rates.

Keywords

Boreal forest; bud phenology; bud burst; common garden; phenotypic plasticity; *Picea mariana*.

1.2 Introduction

Under the projection of a 4 °C warming by the end of the 21st century, an increase of 0.85 °C in mean annual temperature has already been documented over the 1983 – 2012 period (IPCC, 2014). Boreal ecosystems are expected to experience the greatest increase in temperature among terrestrial biomes (IPCC, 2014). Increasing rates of climate change and related disturbances could overwhelm the resilience of tree species and forest ecosystems, possibly leading to changes in both structure and species composition of stands (Reyer et al., 2015).

Boreal forests have evolved under the constraints imposed by a short growing season and severe winters with temperatures < 0 °C lasting up to 8 months per year. Tree growth in the boreal biome is thus intimately related to frost hardiness (Hannerz et al., 1999). If the adaptation strategy to tolerate cold climates interferes with growth, a trade-off may develop between growth and frost hardiness (Loehle, 1998). Three main aspects of cold tolerance can affect growth, namely structural investments (Körner & Larcher, 1988), physiological responses such as the accumulation of cryoprotectants (Woodward, 1987), and conservative growth strategies (Loehle, 1998). Conservative strategies adopted by cold tolerant species may consist of the adaptation of phenological timings to match the most suitable conditions for growth (Körner & Basler, 2010; Rossi, 2015) and use of the assimilated carbon. The latter reflects the priority of carbon storage over growth, because survival ultimately depends on carbon demand for metabolism (Sala et al., 2012).

In the last decades, scientific interest has been concentrated on tree growth and phenological responses to climate change (Körner & Basler, 2010). Phenological traits, the determinants of plant adaptation, define the seasonal timings of biological events, thereby safeguarding growth while minimizing the risk of damage in response to climate

variations. Populations may respond to warming by shifting their distribution to match the environmental conditions they are adapted to, through phenotypic plasticity or by genetically adapting to the new conditions (Aitken et al., 2008). However, most concerns focus on shifts in the distribution range of species (Chen et al., 2011; Parmesan, 2006), often assuming erroneously that species are genetically homogenous (Alberto et al., 2013). Moreover, climatic boundaries in boreal forests are moving northwards ten times faster than the ability of tree species to migrate (Pedlar & McKenney, 2017). Therefore, if populations are not able to adapt to the new local conditions, growth performance and the fitness of some species might be dramatically affected.

Species with wide geographical distributions may be composed of populations with specific adaptations to local climate conditions, which are the result of a tight interaction between environment and genotype (Klisz et al., 2019; Silvestro et al., 2019). The presence of such population differences can indicate functional variation across the species range, hypothetically leading to diverging responses to weather, and subsequently, to a changing climate (Rossi & Isabel, 2017; Savolainen et al., 2007).

Phenological adjustments and height growth are key adaptive variables that may be strongly associated with local climate (Frank et al., 2017). Under the same growing conditions (i.e., common gardens), ecotypic variations emerge in the form of divergent timings of bud phenology (Rossi, 2015; Silvestro et al., 2019; Usmani et al., 2020). Moreover, among different populations, these divergences in bud phenology may also reflect different cambial activity dynamics and, in turn, wood growth (Perrin et al., 2017; Puchałka et al., 2017). As a reliable indicator of fitness and productivity (Savolainen et al., 2007), tree height at a fixed age has been already used to describe ecotypic variation in many conifers, such as *Picea Abies* (Frank et al., 2017; Kapeller et al., 2012), *Pinus sylvestris* (Rehfeldt et al., 2002), *Pinus contorta* (Rehfeldt et al.,

1999) and *Pseudotsuga menziesii* (St Clair et al., 2005). According to the results of these studies, tree species can be classified as specialists or generalists, showing strong or weak associations between environmental gradients and adaptive traits, respectively. New insights into the adaptive strategies of species are not only interesting per se, but have the potential to be used to infer the consequences of climate change (e.g., assessing the risk of future maladaptation) and develop new proactive management strategies to adapt forests for climate-smart forestry (Nabuurs et al., 2018).

Forest management of the boreal forest has a marked latitudinal gradient in Canada due to the inaccessibility and remoteness of the northern stands and has historically focussed on the southern part, close to the most densely inhabited part of the country (Rossi, 2015). The remoteness and the low productivity of northern stands have led to a more extensive study of the boreal forest within the 48th and 51st parallels (Lussier et al., 2002), the main managed area, and consequently a more limited knowledge on the dynamics and productivity of the remote northern stands, making difficult the predictions for these regions under future climatic scenarios.

In the boreal biomes of the northern hemisphere, northern populations are sometimes transferred to southern sites to simulate warming conditions and predict responses of trees to climate change (Rehfeldt et al., 2002; Wang et al., 2010). When moved south, northern populations can improve growth compared to their sites of origin (Savolainen et al., 2007; Suvanto et al., 2016), which suggests that environmental conditions may strongly control growth. However, even if submitted to more favourable climates, the growth performance of northern populations remains lower than that of southern ones (Savolainen et al., 2007), suggesting that growth traits may also be determined genetically. Growth traits can also be controlled by an interaction between genotype and environment, with complex patterns being distinguished, especially when multiple

traits are analyzed (Li et al., 2017). Divergences in long-term growth performance among different tree populations subject to the same environmental conditions have already been reported. However, which growth trait drives divergences when comparing growth performance among different tree populations is still not clear. Some studies have focused on the duration of the growing period, a variable often recognized as a crucial factor for growth, because of its influence on cell size during xylogenesis (Buttò et al., 2019; Cuny et al., 2014). Others have focused on the growth rate achieved in terms of the trade-off in investments of the available resources between potential growth rates and survival (Endara & Coley, 2011). Lastly, major questions remain concerning how duration and rate of growth change with environment, what are the climatic variables driving these changes and how these two factors explain the differences in growth performance.

This study was performed in a common garden located at the southern limit of the closed boreal forest to test the potential effect of provenance on height growth among five black spruce [*Picea mariana* (Mill.) B.S.P] populations originating from a latitudinal gradient in Quebec (Canada). The main goal was to assess how duration and rate of growth explain the difference in height growth among populations. Three hypotheses were formulated (Figure 1.1), according to whether the difference in final height growth depends (A) on the growth rate only. Accordingly, we expected to find higher growth rates in the southern populations; (B) on the duration of growth only. Accordingly, we expected to find longer periods of shoot extension in southern populations; (C) on both duration and rate of growth.

1.3 Materials and methods

1.3.1 Provenances selection

The black spruce populations originated from five permanent plots along a latitudinal gradient ranging from the 48th to 53rd parallels in the boreal coniferous forest of Quebec, Canada [Simoncouche (abbreviated as SIM), Bernatchez (BER), Mistassibi (MIS), Camp Daniel (DAN) and Mirage (MIR)] (Figure 1.2). The climate of the area is characteristically boreal. Therefore, it is characterized by very cold winters (absolute minimum temperatures reaching -45 °C) and short and cool summers (absolute maximum temperatures rarely exceeding 30 °C). Temperatures change according to latitude and altitude, with the stands located at higher latitudes being the coldest in winter, and the least warm in summer (Figure. S1.1). The number of months with a mean daily minimum temperature below 0 °C ranges between 6 and 8 also according to the latitude. Precipitation in the form of rain is mostly concentrated during summer, culminating in the warmest month (July) (Figure S1.1).

1.3.2 Bud phenology and height growth

A common garden was established in 2014 with 457 one-year-old seedlings planted in a 2 x 2 m grid, with the position of the seedlings from each provenance randomly chosen in the grid. The resulting common garden covers an area of 0.5 ha in SIM, the southernmost provenance. In order to avoid edge effects, on each side of the plantation were planted two rows of non-experimental black spruce seedlings.

Bud burst and bud set were recorded weekly from the beginning of May to the end of October 2017-2019. According to (Dhont et al., 2010), we used the apical buds to discriminate the different phenological phases of bud burst during spring, and bud set between summer and autumn. Specifically, we considered six bud burst phases: (1) open

bud, with a pale spot at the bud tip; (2) elongated bud, with lengthening brown scales; (3) swollen bud, with smooth and pale-coloured scales but no visible needles; (4) translucent bud, with needles visible through the scales; (5) split bud, with open scales but needles still clustered; and (6) exposed shoot, with needles totally emerged from the surrounding scales and spreading outwards. Therefore, we defined five phases of bud set as follow: (1) white bud, presence of a white bud; (2) beige bud, with beige color scale around the bud; (3) brownish bud, with a substantial increase in volume; (4) brown bud, with the beginning of needles spread outwards; and (5) spread needles, with the needles in the whorl spreading outwards.

We defined bud phenology as the period ranging from the first phase of bud burst (i.e. open bud) to the last phase of bud set (i.e. spread needles). The period of shoot extension ranged from the last phase of bud burst (i.e. exposed shoot) to the first phase of bud set (i.e. white bud), corresponding to the period of annual growth of the apical arrow. Shoot extension during 2019 was recorded on the internodes on the main stem using a measuring tape to the nearest 2 mm, representing the annual growth of the primary meristem. The growth rate (i.e. mean daily growth during shoot extension) was calculated as a ratio between internode length and the period of shoot extension.

1.3.3 Statistical analyses

The climatic parameters at the sites of origin of the populations for the period 1979-2013 were extracted from the CHELSA Bioclim database (Karger et al., 2017) at a spatial resolution of 30 arcsec (Table S2.1). To describe the climatic distance between sites, we performed a Principal Component Analysis (PCA) using the 19 bioclimatic parameters proposed by O'Donnell and Ignizio (2012). We identified the variables with the strongest impact on the distribution of black spruce populations on PCA based on Pearson's correlation coefficients.

We assessed the effect of annual mean temperature at the provenance origin (Table S1.1) on the duration and rate of height growth by performing an Analysis of Covariance (ANCOVA) and by using Ordinary Least Squares (OLS) regression including the sampling year as a categorical variable. ANCOVA was performed also using the principal components estimated by the PCA as independent variables and testing their effect on the duration and rate of height growth. We therefore validated the model fitting on distribution and normality of the residuals. We applied a bootstrap test to disentangle the results from the sample size and improve their robustness. Bootstrapping was performed 10,000 times, during which P-values were repetitively calculated by randomly resampling the original dataset and estimating the 95% confidence intervals of the resulting distributions. Statistics were performed by using R version 3.5.2 (R Development Core Team, 2015).

1.4 Results

1.4.1 Climate-shift effect

The bioclimatic parameters of population origins reduced to two principal components allowed the relative climatic distances between sites to be detected (Figure 1.3). The first principal component (PC1) described the main pattern of the sites, represented by latitudinal gradient, with SIM and MIR being located at the boundary of the biplot, which indicated their distinct position in relation to the bioclimatic parameters (Figure 1.3). PC1 explained 77.31% of the overall variance and was negatively correlated with all bioclimatic parameters except for temperature seasonality (bio4), temperature annual range (bio7) and precipitation seasonality (bio15) (Table 1.1; Figure 1.3). PC2 explained 16.45% of the variance and was positively correlated with the parameters related to temperature (bio 1-11), and negatively correlated with the parameters related to precipitation (bio 12-19; Table 1.1; Figure 1.3). The southern site (SIM) and MIS were positively correlated with temperature related parameters such as annual mean temperature (bio1) and mean temperature during the warmest and coldest quarters (bio10 and bio 11 respectively). BER was the most positively correlated to the precipitations, such as annual precipitation (bio12) and that of the wettest and driest quarters (bio16 and bio17 respectively; Table 1.1). MIR was the site with the largest annual range in temperature (bio7) and highest precipitation seasonality (bio15; Table 2.1).

1.4.2 ANCOVA models

All models including the mean annual temperature of the sites of origin were highly significant, with F-values ranging between 17.73 and 88.04 ($P < 0.001$), resulting in R^2 of 0.10-0.39 (Table 1.2). The studentized residuals of the regressions were uniformly

distributed around zero, suggesting that the analyses could be considered trustworthy (Figure S1.2). Generally, the studentized residuals exceeding the range between -2 and 2 (i.e., the 95% confidence interval) were < 5% (Figure S2.2). All populations showed a high dispersion of residuals, which was confirmed by the low R-square (Table 1.2). Details for each model and their factors are reported in the next sections.

1.4.3 Phenological periods

On average, bud burst occurred from mid-May to mid-June while bud set from the end of June to the end of September, according to the study year and provenance. Northern and southern provenances showed similar periods of bud phenology (i.e., period when the bud is active) (Figure 1.4). Indeed, no significant effect of temperature of the site of origin was detected (Table 1.2). The period of bud phenology differed between years ($F = 217.79$, $P < 0.05$) (Table 1.2). On average, the period of bud phenology lasted 110 days, with a difference of 30 days between the shortest (98 days) and longest (128 days) period in 2018 and 2017, respectively (Figure 1.4). The interaction temperature \times year was not significant ($P > 0.05$) (Table 1.2).

The process of shoot extension (i.e., period when the shoot was formed) occurred from the beginning of June and the beginning of July. The effect of temperature at the site of origin was significant ($F = 15.04$, $P < 0.05$) (Table 1.2). Specifically, the duration of shoot extension was longer in the populations originating from colder sites for each study year (Figure 1.5). On average, the period of shoot extension was shorter by 0.10 – 1.77 days for each degree Celsius of increase in the annual mean temperature of the original site. The effect of year was significant, with an F-value of 44.31 ($P < 0.05$) (Table 1.2). The interaction temperature \times year was not significant ($F = 0.86$, $P > 0.05$) (Table 1.2).

1.4.4 Height growth

The populations originating from colder sites showed less height growth than those originating from warmer sites (Figure 1.5). The effect of temperature was significant in the model with an F-value of 72.19 ($P < 0.05$) (Table 1.2). Height growth increased by 0.75 – 1.32 cm for each degree Celsius increase in the mean annual temperature at the original site. The effects of year and the interaction (T x Y) were not significant, with F-values of 3.46 and 4.76, respectively ($P > 0.05$) (Table 1.2).

Growth rate

The populations originating from the colder sites showed a lower growth rate (Figure 2.5). The effect of temperature at the site of origin was significant with F-value of 121.29 ($P < 0.05$) (Table 1.2). On average, growth rate ranged between 1.17 and 1.38 cm day⁻¹, according to the study year, and increased by 0.09 – 0.11 cm day⁻¹ for each degree Celsius of increase in the mean annual temperature at the original site. No differences were observed between years ($F = 2.72$, $P > 0.05$) (Table 1.2). The interaction temperature × year was not significant ($F = 0.15$, $P > 0.05$) (Table 1.2).

1.4.5 ANCOVA models and PCA scores

The effect of provenance was also confirmed for the models performed on PC1 (Figure S1.3). All models were highly significant, with F-values ranging between 13.21 and 88.23 ($P < 0.001$), and R^2 up to 0.41 (Table S1.2). These findings mirrored the results obtained using temperature. For PC2, only the model including the duration of bud phenology resulted significant ($F = 86.54$, $P < 0.001$) (Figure S1.3, Table S1.2). The other variables were not significant ($P > 0.05$) (Table S1.2).

1.5 Discussion

This study investigated the functional responses in height growth of five populations of black spruce originating from a latitudinal range and moved south to a common garden at the lower boundary of the coniferous boreal forest of Quebec, Canada. The main goal was to assess if populations experiencing different thermal conditions evolved specific durations and rates of growth, and how these two factors could explain the difference in height growth performance. Our findings demonstrated that, growing under the same environmental conditions, i.e. in a common garden, ecotypes exhibited differences in both duration of shoot extension and growth rate (Figure 1.5), but not in total duration of bud phenology (i.e. bud burst and bud set duration) (Figure 1.4). Specifically, populations from colder sites resumed growth earlier and had a longer duration of shoot extension than those from warmer sites. However, in northern populations the growth rate during the shoot extension period was lower, resulting in a smaller increment of height growth. Overall, our results confirm the third hypothesis that the differences in height growth among populations depend on both growth rate and duration.

Northern ecotypes showed a lower height increment than southern ones (Figure 1.5). Our result is in agreement with what was observed in central Europe for *Picea abies* (Frank et al., 2017) and in North America for *Pinus contorta* (Rehfeldt et al., 1999). Rehfeldt et al. (1999) also stated that mean annual temperature at the ecotypes site of origin is an effective climatic variable to predict the performance in height growth of populations. Moreover, in a common garden experiment, Wei et al. (2004) already pointed out that black spruce populations originating from colder sites showed less height growth. The shoot extension is regulated by both predetermined and free growth. Shoot extension is predetermined since, within the bud, the growth units are already formed and closely depend on the environmental conditions occurring during the previous growing season

(Salminen & Jalkanen, 2005). However, an additional free growth has been described in fir and spruce in which new needles are initiated and expand while the shoot is flushing (Logan & Pollard, 1975).

Our study demonstrates that shoot extension lasted longer in northern populations (Figure 1.5). This provenance-related variation in the duration of shoot extension could result from the interaction of internal and external cues that determine growth. Ecotypes of northern latitudes, or colder sites, generally require less heat to resume growth in spring (Blum, 1988). The earlier breaking of dormancy allows the period of growth to be lengthened as much as possible where the duration of growing season is a limiting factor (Rossi et al., 2016). The ecotypes originating from colder sites preserve this adaptive trait when the offspring are moved to warmer environments (Silvestro et al., 2019). Comparing the timing and the duration of shoot extension among ecotypes growing under the same climatic condition still remain an important indication to make prediction on the response of populations to a future warming condition at their origin site. For example, compared with southern populations, the earlier growth resumption and the longer shoot extension of northern populations may expose the developing shoot to higher risks of frost damage (Marquis et al., 2020; Silvestro et al., 2019) or promote herbivore-plant phenological synchronisms (Ren et al., 2020). These findings should also be considered taking into account the demonstrated ontogenetic differences between young and mature trees (Wei et al., 2004), and the relative importance of changes in predetermined and free growth with age (Logan & Pollard, 1975).

We observed that the growth rate changed according to the mean annual temperature recorded at the sites of origin. Specifically, a lower growth rate was detected in northern ecotypes (Figure 1.5). Consequently, despite a longer duration of shoot extension, the lower growth rate resulted in less annual height growth. Our findings are in agreement

with the results on *Picea abies* in populations originated along an altitudinal range (Oleksyn et al., 1998), and on *Pinus sibirica* in populations originated along a latitudinal range (Zhuk & Goroshkevich, 2018). Both studies highlighted the provenance-specific variation of growth rate and height growth in common garden experiments. However, previous studies did not conclude that growth rate is likely the main characteristic determining height growth differences among ecotypes, probably because mostly focused on resources allocation. Populations originated from colder sites show a predisposition to high rates of photosynthesis and respiration and reduced growth rate (Oleksyn et al., 1998), a genetically controlled adaptive trait common to plants originating from cold environments (Reich et al., 1996). Despite the enhanced metabolic activity, the lower annual growth of northern populations is a conservative strategy triggered by the need to increase frost hardiness that prioritises an extensive production of fine roots and high partitioning of biomass to roots (Oleksyn et al., 1998). Moreover, the newly assimilated carbon serves as a defence compound in trees, and under severe low-temperature stress at high latitude or altitude, trees need to invest more resources in defence and protection of newly formed leaf tissue to ensure long-term photosynthesis (Massad et al., 2014).

This work demonstrated that populations growing under different thermal conditions evolved specific durations and rates of growth, the two important component explaining height growth performance. However, our experimental design based on a single common garden prevents to quantify the interaction between genotype and environment, and consequently, the site-related phenotypic plasticity. Such information could also result crucial to maximise genetic gain in forest tree breeding and for the selection of optimal genotypes for assisted migration.

Despite the phenological mismatch in timing between populations, our results show that the duration of all bud phenological stages is similar between ecotypes (Figure 1.4). In

the northern areas, spring warming occurs late, in June, when day length is longer and nights are shorter. Under these conditions, frosts are unlikely, and trees can start bud reactivation without exposing the new developing tissues to the risk of frost damage (Rossi & Bousquet, 2014). Subsequently, height growth takes place when the conditions are most suitable. Lastly, trees start bud set in a period calibrated to minimize the risk derived from early frosts at the end of the growing season. Indeed, shoots are particularly susceptible to frost damage before autumnal hardening, and even a slight frost can represent a potential cause of significant damages (Charrier et al., 2015). Therefore, lengthening the duration of bud burst or bud set phenological stages would result disadvantageous by increasing the risk of spring or autumnal frost damage.

The ecotypic variation in height growth between populations is accompanied by a high variability within them. This variability in both the duration of shoot extension and growth rate in individuals with the same provenance is also revealed by the wide dispersions of the residuals of our models. This heterogeneity represents a natural variability in the functional traits, allowing at least a part of the population to endure adverse and unpredictable climatic events, thus guaranteeing the survival of some individuals under changing environmental conditions (Hurme et al., 1997). In addition to black spruce (Perrin et al., 2017; Rossi & Bousquet, 2014; Silvestro et al., 2019), wide variability in both phenology and height growth within populations was observed in other species, such as *Pinus sylvestris* for phenological timing (Hurme et al., 1997), *Pinus sibirica* and *Abies alba* for growth traits (Klisz et al., 2018; Zhuk & Goroshkevich, 2018), *Fagus sylvatica* and *Picea abies* for both phenological and growth traits (Frank et al., 2017; Jastrzębowski et al., 2018; Kramer et al., 2017; Oleksyn et al., 1998).

Both within- and among-population genetic variation define evolutionary potential of a species. High within-population variation promotes population resilience, whereas high

among-population variation provides a pool of diverse genotypes and alleles available via gene flow (Frank et al., 2017). Through gene flow, pre-adapted alleles from other populations can maximize fitness-related traits and increase local adaptation (Frank et al., 2017). However, gene flow may also oppose adaptation, promoting the immigration of alleles that are less fit than existing ones (Fréjaville et al., 2019; Klisz et al., 2019). Therefore, detailed information about both within- and among-population variation is also fundamental for a better understanding of climate change adaptation.

1.6 Conclusion

The objective of this work was to assess if populations growing under different thermal conditions evolved a long-lasting adaptation regarding durations and rates of growth, and how these two factors could explain the difference in height growth performance. Our results confirmed the ecotypic variation between black spruce populations and demonstrated a trade-off between long-lasting adaptations and phenotypic plasticity. In this study, we found that populations originating from a latitudinal gradient and growing under the same environmental conditions exhibited differences in shoot length. Populations from colder sites had both a longer duration of shoot extension and a lower growth rate, resulting in less growth in height than those originated from warmer sites. Our findings demonstrated the long-term adaptation of populations evolved under different environmental conditions. These growth traits are maintained when populations are exposed to different conditions. This long-term adaptation of populations leading to differences in phenology and growth performances between ecotypes is a crucial aspect in forest management. Exploring the dynamics and growth performances of remote northern populations assume a relevant meaning given that in the last years logging activities are gradually moving towards more remote areas at higher latitudes. In a context of climate change, forest management aims to enhance the role of carbon sequestration of forest ecosystems while meeting the need for high timber production. According to our results, if exposed to warming conditions, northern populations could not reach in a short time the current growth performance of southern populations due to the long-lasting local adaptation in which growth rate remains lower. Compared with southern populations, the longer shoot extension of northern populations exposes the developing shoot to higher risks of damage by frost or pests.

1.6.1 Acknowledgements

This work was funded by the Direction général du secteur nord-est, région du Saguenay–Lac-St-Jean, Ministère des Forêts, de la Faune et des Parcs du Québec, Forêt d'Enseignement et de Recherche Simoncouche, and the Fondation de l'Université du Québec à Chicoutimi. The authors thank L. Balducci, I. Allie, V. Néron, I. Froment, T. Ziegler for technical support, A. Garside for editing the English text and the two anonymous reviewers for providing suggestions which helped to improve our manuscript.

1.6.2 Author contribution statement

SR: experimental design; RS and SB: data collection; RS, MK and SB: data analysis; RS: drafted the initial manuscript; all authors: revised and completed the manuscript.

1.6.3 Conflict of interest

The authors declare that this work has no potential conflict of interest.

1.7 Figures

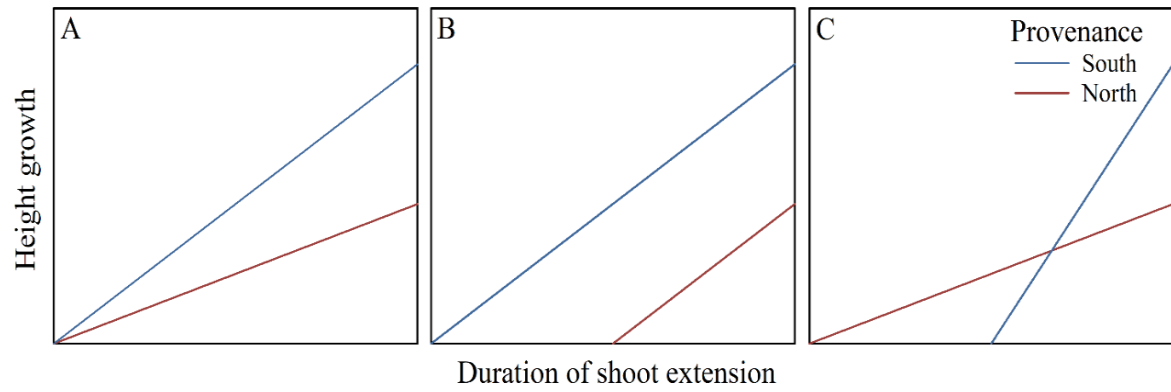


Figure 1.1 The three hypotheses testing the relationship between duration and rate of growth vs height growth in black spruce populations originating from a latitudinal gradient.

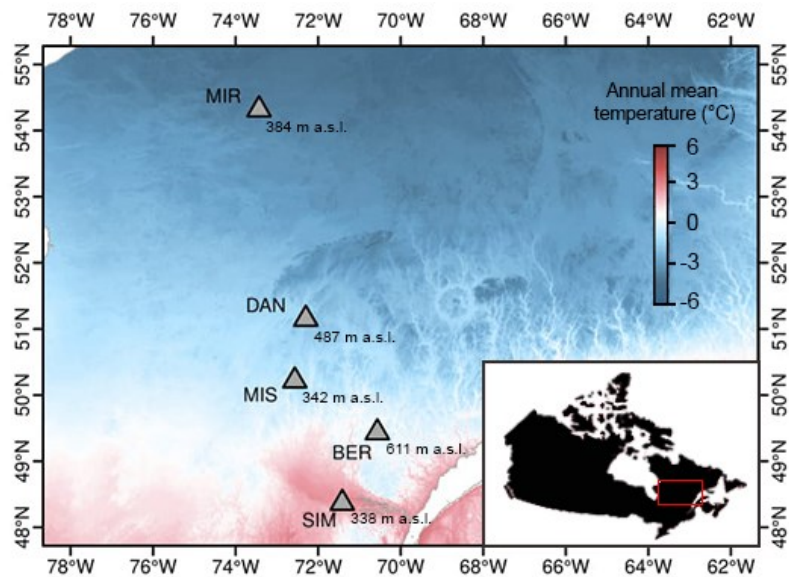


Figure 1.2 Sites of origin of the five black spruce provenances [Simoncouche (abbreviated as SIM), Bernatchez (BER), Mistassibi (MIS), Camp Daniel (DAN) and Mirage (MIR)] in the coniferous boreal forest of Québec (Canada) and annual mean temperature of the region.

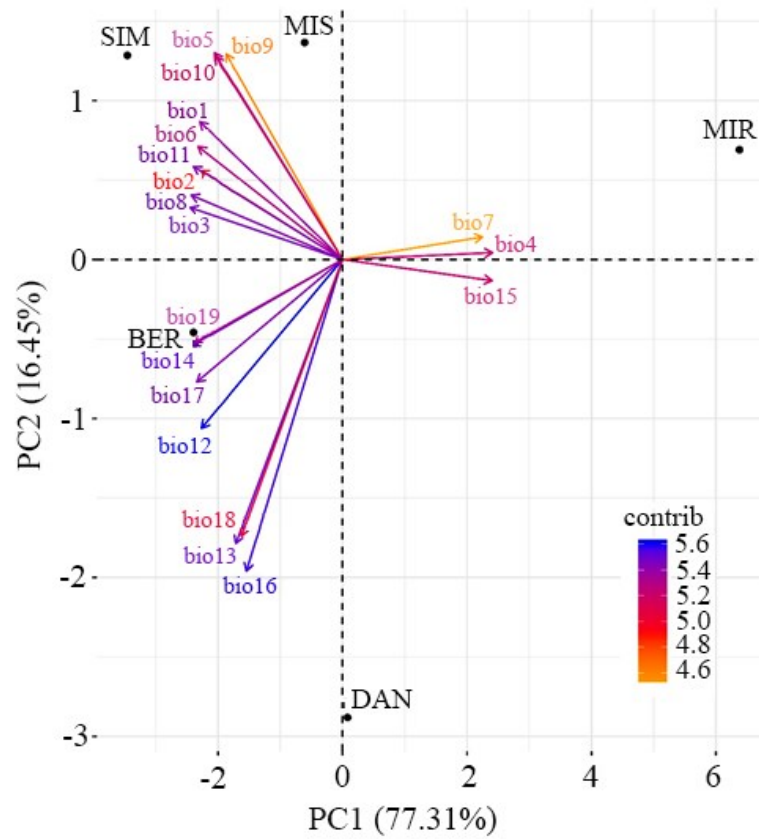


Figure 1.3 Climate-related variability between sites of origin [Simoncouche (SIM), Bernatchez (BER), Mistassibi (MIS), Camp Daniel (DAN) and Mirage (MIR)] based on 19 bioclimatic variables (refer to Table 1 for bioclimatic variables abbreviations). Variables vector are colour-coded according to their contribution to total variance.

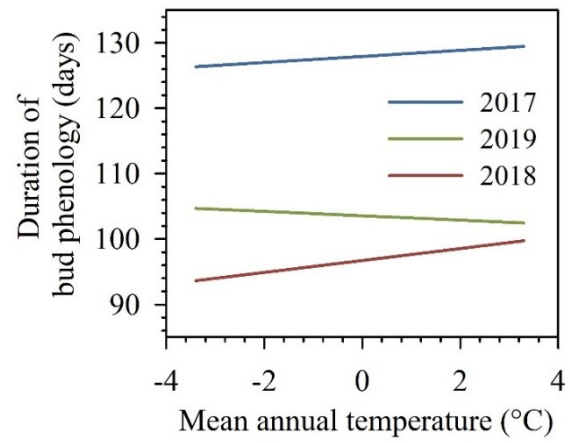


Figure 1.4 Duration of bud phenology predicted by Ordinary Least Squares (OLS) models in black spruce populations according to mean annual temperature at the site of origin.

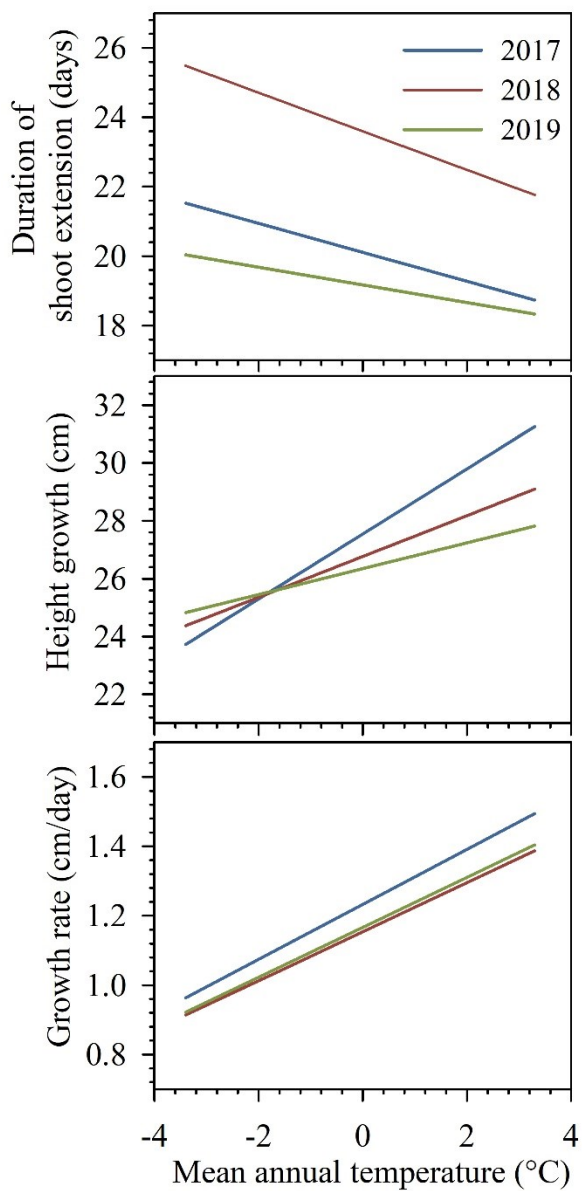


Figure 1.5 Duration of shoot extension, growth rate and height growth predicted by Ordinary Least Squares (OLS) models in black spruce populations according to the mean annual temperature at the site of origin.

1.8 Tables

Table 1.1 Pearson's correlation coefficients between the 19 bioclimatic variables proposed by O'Donnell & Ignizio (2012) and the first two

Bioclimatic variables	Abbreviation	Pearson's correlation		Contribution in PCs (%)		
		PC1	PC2	PC1	PC2	
Annual Mean Temperature	(°C)	bio1	-0.92	0.35	5.71	3.84
Mean Monthly Temperature Range	(°C)	bio2	-0.91	0.22	5.61	1.60
Isothermality (bio2/bio7) (* 100)	(°C)	bio3	-0.98	0.13	6.51	0.55
Temperature Seasonality (STD * 100)	(°C)	bio4	0.96	0.02	6.31	0.01
Max Temperature of Warmest Month	(°C)	bio5	-0.82	0.52	4.58	8.65
Min Temperature of Coldest Month	(°C)	bio6	-0.93	0.28	5.86	2.58
Temperature Annual Range (bio5-bio6)	(°C)	bio7	0.90	0.06	5.50	0.10
Mean Temperature of Wettest Quarter	(°C)	bio8	-0.97	0.16	6.42	0.84
Mean Temperature of Driest Quarter	(°C)	bio9	-0.75	0.52	3.79	8.54
Mean Temperature of Warmest Quarter	(°C)	bio10	-0.81	0.51	4.51	8.36
Mean Temperature of Coldest Quarter	(°C)	bio11	-0.96	0.23	6.23	1.75
Annual Precipitation	(mm)	bio12	-0.91	-0.42	5.58	5.76
Precipitation of Wettest Month	(mm)	bio13	-0.68	-0.71	3.19	16.3
Precipitation of Driest Month	(mm)	bio14	-0.97	-0.22	6.35	1.52
Precipitation Seasonality (CV)	(mm)	bio15	0.96	-0.05	6.28	0.09
Precipitation of Wettest Quarter	(mm)	bio16	-0.62	-0.78	2.59	19.62
Precipitation of Driest Quarter	(mm)	bio17	-0.94	-0.31	5.95	3.03
Precipitation of Warmest Quarter	(mm)	bio18	-0.65	-0.70	2.86	15.46
Precipitation of Coldest Quarter	(mm)	bio19	-0.95	-0.21	6.16	1.41

principal components (PC1 and PC2) and their contribution to explaining the climatic space across the study sites.

Table 1.2 Effects of mean annual temperature of the sites of origin (T), year (Y) and their interaction (T × Y) on bud phenology and components of height growth (shoot extension, height growth, height growth rate) evaluated by ANCOVA models. All models were significant at $P < 0.001$. The significance of the effect of the factors was obtained by bootstrapping 10,000 times by randomly resampling the original dataset and estimating the 95% confidence intervals of the resulting distributions. Asterisks indicate at least $P < 0.05$.

	Model		Effect		
	F - value	R ²	T	Y	T × Y
Bud phenology	88.04	0.39	4.11	217.79*	1.14
Shoot extension	21.08	0.15	15.04*	44.31*	0.86
Height growth	17.73	0.10	72.19*	3.46	4.76
Growth rate	25.40	0.17	121.29*	2.72	0.15

1.9 Annexes

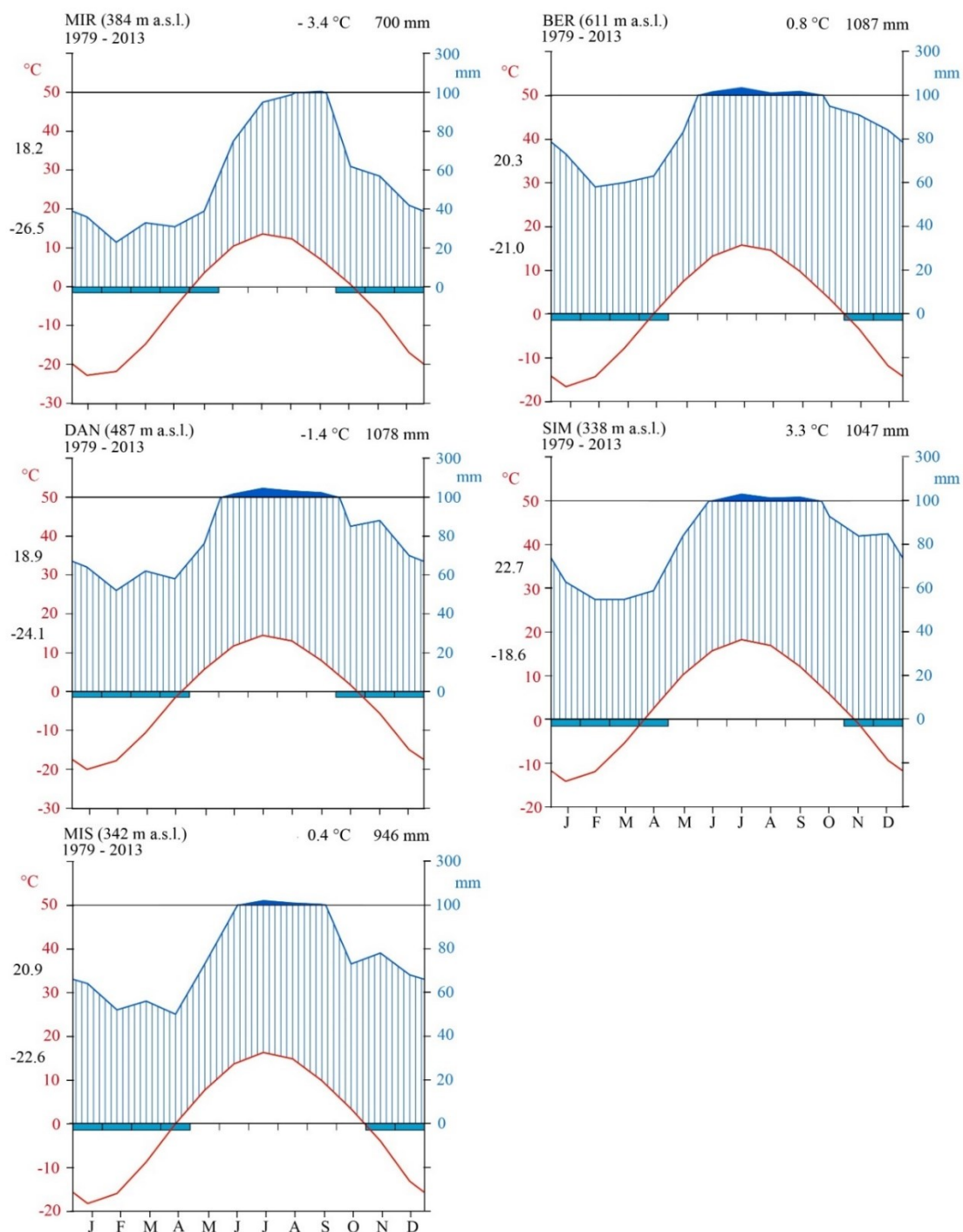


Figure S 1.1 Walter and Lieth climatic diagrams of the five black spruce sites of origin (BER, DAN, MIR, MIS and SIM) from the boreal coniferous forest of Quebec, Canada.

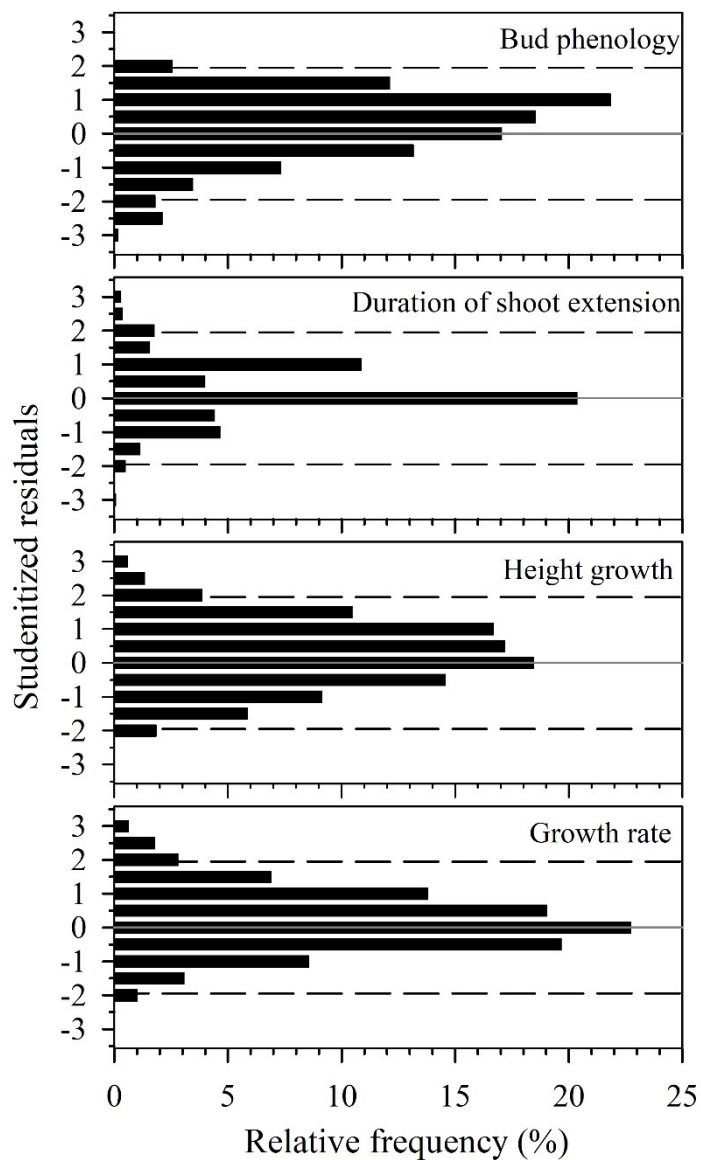


Figure S 1.2 Distribution of Studentized residuals of the Ordinary Least Squares (OLS) models. The studentized residuals were uniformly distributed around zero and, generally, residuals exceeding the range between -2 and 2 (i.e., the 95% confidence interval) were < 5.0%.

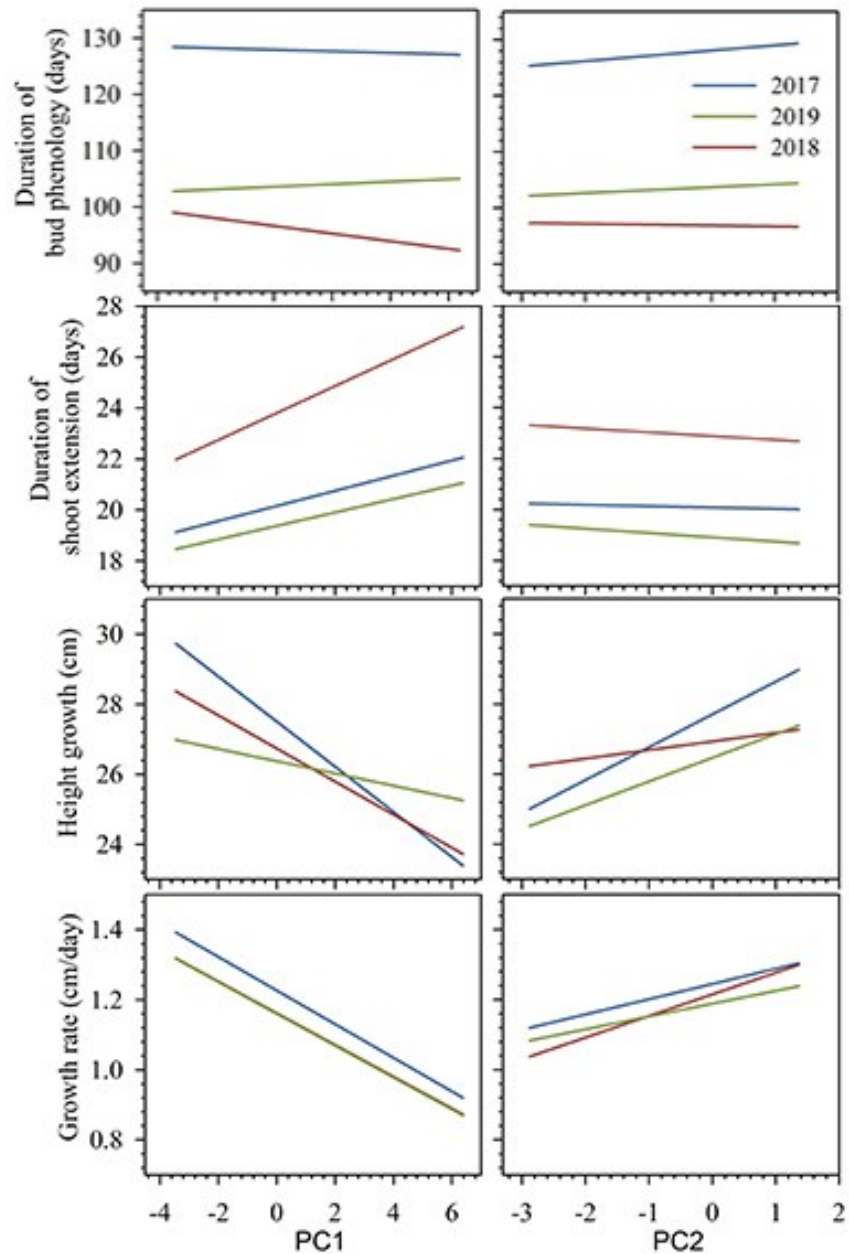


Figure S 1.3 Duration of bud phenology, duration of shoot extension, growth rate and height growth predicted by Ordinary Least Squares (OLS) models in black spruce populations according to the Principal Component Analysis (PCA) scores of the five black spruce sites of origin (BER, DAN, MIR, MIS and SIM).

Table S 1.1 The 19 bioclimatic variables proposed by O'Donnell & Ignizio (2012) of the five sites in the boreal forest of Quebec, Canada, where the studied populations come from. The climatic parameters at the sites of origin for the period 1979-2013 were extracted using CHELSA Bioclim (Karger et al., 2017) at a spatial resolution of 30 arcsec.

Variables	SIM	BER	MIS	DAN	MIR
bio1	3.3	0.8	0.4	-1.4	-3.4
bio2	8.0	8.0	8.1	7.7	7.3
bio3	1.9	1.9	1.9	1.8	1.6
bio4	1114.1	1110.8	1187.4	1184.3	1271.3
bio5	22.7	20.3	20.9	18.9	18.2
bio6	-18.6	-21.0	-22.6	-24.1	-26.5
bio7	41.3	41.3	43.6	43.0	44.7
bio8	17.5	14.9	15.3	13.5	8.8
bio9	-7.6	-10.0	-29.0	-18.5	-22.1
bio10	17.5	14.9	15.4	13.5	12.8
bio11	-12.6	-15.2	-16.8	-18.5	-22.1
bio12	1047	1087	946	1078	700
bio13	133	135	121	147	108
bio14	55	58	50	52	23
bio15	29	27	29	35	48
bio16	368	386	341	413	315
bio17	165	178	156	168	82
bio18	368	357	339	412	293
bio19	173	189	168	168	82

Table S 1.2 Effects of PCA axes (PC1 and PC2), year (Y) and their interaction on duration of bud phenology and components of height growth (duration of shoot extension, annual height growth increment, height growth rate) evaluated by ANCOVA models. All models including PC1 scores were significant at $P < 0.001$, whereas including PC2 scores only the model referring to the duration of bud phenology resulted significant at $P < 0.001$. The significance of the effect of the factors was obtained by bootstrapping 10,000 times by randomly resampling the original dataset and estimating the 95% confidence intervals of the resulting distributions. Asterisks indicate at least $P < 0.05$.

	Model		Effect		
	F - value	R ²	PC1	Y	PC1 × Y
Bud phenology	88.23	0.41	3.83	217.01*	1.67
Shoot extension	22.1	0.16	22.39*	43.09*	0.97
Height growth	13.21	0.08	49.86*	3.29	4.79
Growth rate	19.14	0.13	91.28*	2.17	0.03
	F - value	R ²	PC2	Y	PC2 × Y
Bud phenology	86.54	0.39	0.47	215.49*	0.64
Shoot extension	15.22	0.12	0.05	37.90*	0.13
Height growth	6.13	0.04	20.54*	2.76	2.3
Growth rate	4.57	0.03	19.56*	1.19	0.45

1.10 References

- Aitken, S. N., Yeaman, S., Holliday, J. A., Wang, T., & Curtis-McLane, S. (2008). Adaptation, migration or extirpation: climate change outcomes for tree populations. *Evolutionary Applications*, 1(1), 95-111. <https://doi.org/10.1111/j.1752-4571.2007.00013.x>
- Alberto, F. J., Aitken, S. N., Alía, R., González-Martínez, S. C., Hänninen, H., Kremer, A., Lefèvre, F., Lenormand, T., Yeaman, S., Whetten, R., & Savolainen, O. (2013). Potential for evolutionary responses to climate change - evidence from tree populations. *Global Change Biology*, 19(6), 1645-1661. <https://doi.org/10.1111/gcb.12181>
- Blum, B. M. (1988). Variation in the phenology of bud flushing in white and red spruce. *Canadian Journal of Forest Research*, 18(3), 315-319. <https://doi.org/10.1139/x88-048>
- Buttò, V., Rossi, S., Deslauriers, A., & Morin, H. (2019). Is size an issue of time? Relationship between the duration of xylem development and cell traits. *Annals of Botany*, 123(7), 1257-1265. <https://doi.org/10.1093/aob/mcz032>
- Charrier, G., Ngao, J., Saudreau, M., & Améglio, T. (2015). Effects of environmental factors and management practices on microclimate, winter physiology, and frost resistance in trees. *Frontiers in Plant Science*, 6(APR), 259-259. <https://doi.org/10.3389/fpls.2015.00259>
- Chen, I. C., Hill, J. K., Ohlemüller, R., Roy, D. B., & Thomas, C. D. (2011). Rapid range shifts of species associated with high levels of climate warming. *Science*, 333(6045), 1024-1026. <https://doi.org/10.1126/science.1206432>
- Cuny, H. E., Rathgeber, C. B. K., Frank, D., Fonti, P., & Fournier, M. (2014). Kinetics of tracheid development explain conifer tree-ring structure. *New Phytologist*, 203(4), 1231-1241. <https://doi.org/10.1111/nph.12871>
- Dhont, P., Sylvestre, P., Gros-Louis, M. C., & Isabel, N. (2010). *Field Guide for Identifying Apical Bud Break and Bud Formation Stages in White Spruce*.
- Endara, M. J., & Coley, P. D. (2011). The resource availability hypothesis revisited: A meta-analysis. *Functional Ecology*, 25(2), 389-398. <https://doi.org/10.1111/j.1365-2435.2010.01803.x>
- Frank, A., Sperisen, C., Howe, G. T., Brang, P., Walthert, L., Clair, J. B. S., & Heiri, C. (2017). Distinct genecological patterns in seedlings of Norway spruce and silver fir from a mountainous landscape. *Ecology*, 98(1), 211-227. <https://doi.org/10.1002/ecy.1632>

- Fréjaville, T., Vizcaíno-Palomar, N., Fady, B., Kremer, A., & Benito Garzón, M. (2019). Range margin populations show high climate adaptation lags in European trees. *Global Change Biology*, 26(2), 484-495. <https://doi.org/10.1111/gcb.14881>
- Hannerz, M., Aitken, S. N., King, J. N., & Budge, S. (1999). Effects of genetic selection for growth on frost hardiness in western hemlock. *Canadian Journal of Forest Research*, 29(4), 509-516. <https://doi.org/10.1139/x99-019>
- Hurme, P., Repo, T., Savolainen, O., & Pääkkönen, T. (1997). Climatic adaptation of bud set and frost hardiness in Scots pine (*Pinus sylvestris*). *Canadian Journal of Forest Research*, 27(5), 716-723. <https://doi.org/10.1139/x97-052>
- Jastrzębowski, S., Ukalski, K., Klisz, M., Ukalska, J., Przybylski, P., Matras, J., Barzdaj, W., & Kowalkowski, W. (2018). Assessment of the height stability in progeny of *Fagus sylvatica* L. Populations using the GGE biplot method. *Dendrobiology*, 79, 34-46. <https://doi.org/10.12657/denbio.079.004>
- Kapeller, S., Lexer, M. J., Geburek, T., Hiebl, J., & Schueler, S. (2012). Intraspecific variation in climate response of Norway spruce in the eastern Alpine range: Selecting appropriate provenances for future climate. *Forest Ecology and Management*, 271, 46-57. <https://doi.org/10.1016/j.foreco.2012.01.039>
- Karger, D. N., Conrad, O., Böhrer, J., Kawohl, T., Kreft, H., Soria-Auza, R. W., Zimmermann, N. E., Linder, H. P., & Kessler, M. (2017). Climatologies at high resolution for the earth's land surface areas. *Scientific Data*, 4. <https://doi.org/10.1038/sdata.2017.122>
- Klisz, M., Ukalska, J., Koprowski, M., Tereba, A., Puchałka, R., Przybylski, P., Jastrzębowski, S., & Nabais, C. (2019). Effect of provenance and climate on intra-annual density fluctuations of Norway spruce *Picea abies* (L.) Karst. in Poland. *Agricultural and Forest Meteorology*, 269-270, 145-156. <https://doi.org/10.1016/j.agrformet.2019.02.013>
- Klisz, M., Ukalski, K., Ukalska, J., Jastrzębowski, S., Puchałka, R., Przybylski, P., Mionskowski, M., & Matras, J. (2018). What can we learn from an early test on the adaptation of silver fir populations to marginal environments? *Forests*, 9(7), 441-441. <https://doi.org/10.3390/f9070441>
- Körner, C., & Basler, D. (2010). Phenology under global warming. *Science*, 327(5972), 1461-1462. <https://doi.org/10.1126/science.1186473>
- Körner, C., & Larcher, W. (1988). Plant life in cold climates. *Symposia of the Society for Experimental Biology*, 42, 25-57.

- Kramer, K., Ducouso, A., Gömöry, D., Hansen, J. K., Ionita, L., Liesebach, M., Lorent, A., Schöler, S., Sulkowska, M., de Vries, S., & von Wühlisch, G. (2017). Chilling and forcing requirements for foliage bud burst of European beech (*Fagus sylvatica* L.) differ between provenances and are phenotypically plastic. *Agricultural and Forest Meteorology*, 234-235, 172-181. <https://doi.org/10.1016/j.agrformet.2016.12.002>
- Li, Y., Suontama, M., Burdon, R. D., & Dungey, H. S. (2017). Genotype by environment interactions in forest tree breeding: review of methodology and perspectives on research and application. *Tree Genetics and Genomes*, 13(3), 1-18. <https://doi.org/10.1007/s11295-017-1144-x>
- Loehle, C. (1998). Height growth rate tradeoffs determine northern and southern range limits for trees. *Journal of Biogeography*, 25(4), 735-742. <https://doi.org/10.1046/j.1365-2699.1998.2540735.x>
- Logan, K. T., & Pollard, D. F. W. (1975). Mode of shoot growth in 12-year-old black spruce provenances. *Canadian Journal of Forest Research*, 5(4), 539-540. <https://doi.org/10.1139/x75-078>
- Lussier, J. M., Morin, H., & Gagnon, R. (2002). Mortality in black spruce stands of fire or clear-cut origin. *Canadian Journal of Forest Research*, 32(3), 539-547. <https://doi.org/10.1139/x01-201>
- Marquis, B., Bergeron, Y., Simard, M., & Tremblay, F. (2020). Probability of Spring Frosts, Not Growing Degree-Days, Drives Onset of Spruce Bud Burst in Plantations at the Boreal-Temperate Forest Ecotone. *Frontiers in Plant Science*, 11, Article 1031. <https://doi.org/10.3389/fpls.2020.01031>
- Massad, T. J., Trumbore, S. E., Ganbat, G., Reichelt, M., Unsicker, S., Boeckler, A., Gleixner, G., Gershenson, J., & Ruehlow, S. (2014). An optimal defense strategy for phenolic glycoside production in *Populus trichocarpa* - isotope labeling demonstrates secondary metabolite production in growing leaves. *New Phytologist*, 203(2), 607-619. <https://doi.org/10.1111/nph.12811>
- Nabuurs, G. J., Verkerk, P. J. S. M.-J., González Olabarria, J. R. T. A., & Cienciala, E. (2018). *Climate-Smart Forestry: mitigation impacts in three European regions* (9789525980530). https://www.efi.int/sites/default/files/files/publication-bank/2018/efi_fstp_6_2018.pdf
- O'Donnell, M. S., & Ignizio, D. A. (2012). *Bioclimatic predictors for supporting ecological applications in the conterminous United States: U.S. Geological Survey Data Series 691*. <https://pubs.usgs.gov/ds/691/>

- Oleksyn, J., Modrzyński, J., Tjoelker, M. G., Zytkowski, R., Reich, P. B., & Karolewski, P. (1998). Growth and physiology of *Picea abies* populations from elevational transects: common garden evidence for altitudinal ecotypes and cold adaptation. *Functional Ecology*, 12(4), 573-590. <https://doi.org/10.1046/j.1365-2435.1998.00236.x>
- Parnesan, C. (2006). Ecological and evolutionary responses to recent climate change. *Annual Review of Ecology, Evolution, and Systematics*, 37(1), 637-669. <https://doi.org/10.1146/annurev.ecolsys.37.091305.110100>
- Pedlar, J. H., & McKenney, D. W. (2017). Assessing the anticipated growth response of northern conifer populations to a warming climate. *Scientific Reports*, 7. <https://doi.org/10.1038/srep43881>
- Perrin, M., Rossi, S., & Isabel, N. (2017). Synchronisms between bud and cambium phenology in black spruce: Early-flushing provenances exhibit early xylem formation. *Tree Physiology*, 37(5), 593-603. <https://doi.org/10.1093/treephys/tpx019>
- Puchalka, R., Koprowski, M., Gričar, J., & Przybylak, R. (2017). Does tree-ring formation follow leaf phenology in Pedunculate oak (*Quercus robur* L.)? *European Journal of Forest Research*, 136(2), 259-268. <https://doi.org/10.1007/s10342-017-1026-7>
- Rehfeldt, G. E., Tchebakova, N. M., Parfenova, Y. I., Wykoff, W. R., Kuzmina, N. A., & Milyutin, L. I. (2002). Intraspecific responses to climate in *Pinus sylvestris*. *Global Change Biology*, 8(9), 912-929. <https://doi.org/10.1046/j.1365-2486.2002.00516.x>
- Rehfeldt, G. E., Ying, C. C., Spittlehouse, D. L., & Hamilton, D. A. (1999). Genetic responses to climate in *Pinus contorta*: Niche breadth, climate change, and reforestation. *Ecological Monographs*, 69(3), 375-407. <https://doi.org/10.2307/2657162>
- Reich, P. B., Oleksyn, J., Modrzyński, J., & Tjoelker, M. G. (1996). Evidence that longer needle retention of spruce and pine populations at high elevations and high latitudes is largely a phenotypic response. *Tree Physiology*, 16(7), 643-647. <https://doi.org/10.1093/treephys/16.7.643>
- Ren, P., Néron, V., Rossi, S., Liang, E., Bouchard, M., & Deslauriers, A. (2020). Warming counteracts defoliation-induced mismatch by increasing herbivore-plant phenological synchrony. *Global Change Biology*, 26(4), 2072-2080. <https://doi.org/10.1111/gcb.14991>

- Reyer, C. P. O., Brouwers, N., Rammig, A., Brook, B. W., Epila, J., Grant, R. F., Holmgren, M., Langerwisch, F., Leuzinger, S., Lucht, W., Medlyn, B., Pfeifer, M., Steinkamp, J., Vanderwel, M. C., Verbeeck, H., & Vilella, D. M. (2015). Forest resilience and tipping points at different spatio-temporal scales: Approaches and challenges. *Journal of Ecology*, *103*(1), 5-15. <https://doi.org/10.1111/1365-2745.12337>
- Rossi, S. (2015). Local adaptations and climate change: converging sensitivity of bud break in black spruce provenances. *International Journal of Biometeorology*, *59*(7), 827-835. <https://doi.org/10.1007/s00484-014-0900-y>
- Rossi, S., Anfodillo, T., Čufar, K., Cuny, H. E., Deslauriers, A., Fonti, P., Frank, D., Gričar, J., Gruber, A., Huang, J. G., Jyske, T., Kašpar, J., King, G., Krause, C., Liang, E., Mäkinen, H., Morin, H., Nöjd, P., Oberhuber, W., . . . Treml, V. (2016). Pattern of xylem phenology in conifers of cold ecosystems at the Northern Hemisphere. *Global Change Biology*, *22*(11), 3804-3813. <https://doi.org/10.1111/gcb.13317>
- Rossi, S., & Bousquet, J. (2014). The bud break process and its variation among local populations of boreal black spruce. *Frontiers in Plant Science*, *5*(October), 574-574. <https://doi.org/10.3389/fpls.2014.00574>
- Rossi, S., & Isabel, N. (2017). Bud break responds more strongly to daytime than nighttime temperature under asymmetric experimental warming. *Global Change Biology*, *23*(1), 446-454. <https://doi.org/10.1111/gcb.13360>
- Sala, A., Woodruff, D. R., & Meinzer, F. C. (2012). Carbon dynamics in trees: feast or famine? *Tree Physiology*, *32*(6), 764-775. <https://doi.org/10.1093/treephys/tpr143>
- Salminen, H., & Jalkanen, R. (2005). Modelling the effect of temperature on height increment of Scots pine at high latitudes. *Silva Fennica*, *39*(4), 497-508. <https://doi.org/10.14214/sf.362>
- Savolainen, O., Bokma, F., Knürr, T., Kärkkäinen, K., Pyhäjärvi, T., & Wachowiak, W. (2007). *Adaptation of forest trees to climate change* EUFORGEN Climate Change and Forest Genetic Diversity: implications for sustainable forest management in Europe, Paris, France, 15-16 March 2006, 19-30., Rome, Italy.
- Silvestro, R., Rossi, S., Zhang, S., Froment, I., Huang, J. G., & Saracino, A. (2019). From phenology to forest management: Ecotypes selection can avoid early or late frosts, but not both. *Forest Ecology and Management*, *436*, 21-26. <https://doi.org/10.1016/j.foreco.2019.01.005>

- St Clair, J. B., Mandel, N. L., & Vance-Borland, K. W. (2005). Genecology of Douglas fir in Western Oregon and Washington. *Annals of Botany*, 96(7), 1199-1214. <https://doi.org/10.1093/aob/mci278>
- Suvanto, S., Nöjd, P., Henttonen, H. M., Beuker, E., & Mäkinen, H. (2016). Geographical patterns in the radial growth response of Norway spruce provenances to climatic variation. *Agricultural and Forest Meteorology*, 222, 10-20. <https://doi.org/10.1016/j.agrformet.2016.03.003>
- Usmani, A., Silvestro, R., Zhang, S., Huang, J. G., Saracino, A., & Rossi, S. (2020). Ecotypic differentiation of black spruce populations: temperature triggers bud burst but not bud set. *Trees - Structure and Function*. <https://doi.org/10.1007/s00468-020-01999-4>
- Wang, T., O'Neill, G. A., & Aitken, S. N. (2010). Integrating environmental and genetic effects to predict responses of tree populations to climate. *Ecological Applications*, 20(1), 153-163. <https://doi.org/10.1890/08-2257.1>
- Wei, R. P., Sang, D. H., Dhir, N. K., & Yeh, F. C. (2004). Population variation in growth and 15-year-old shoot elongation along geographic and climatic gradients in black spruce in Alberta. *Canadian Journal of Forest Research*, 34(8), 1691-1702. <https://doi.org/10.1139/X04-050>
- Woodward, F. I. (1987). *Climate and Plant Distribution*. Cambridge University Press. <https://doi.org/10.2307/633873>
- Zhuk, E., & Goroshkevich, S. (2018). Growth and reproduction in *Pinus sibirica* ecotypes from Western Siberia in a common garden experiment. *New Forests*, 49(2), 159-172. <https://doi.org/10.1007/s11056-017-9611-7>

CHAPTER II

LOCAL ADAPTATION SHAPES FUNCTIONAL TRAITS AND RESOURCE ALLOCATION IN BLACK SPUCE

Published in Scientific Reports

Citation:

Silvestro, R., Mura, C., Alano Bonacini, D., de Lafontaine, G., Faubert, P., Mencuccini, M., & Rossi, S. (2023). Local adaptation shapes functional traits and resource allocation in black spruce. *Scientific Reports*, 13(1), 21257.

RESEARCH ARTICLE

Title:

Local adaptation in the boreal forest, a blessing in disguise or a curse in hiding?

Authors

Silvestro, R.^{1, *}, Mura, C.¹, Alano Bonacini, D.¹, de Lafontaine, G.², Faubert, P.^{1,3}, Mencuccini, M.^{4,5}, Rossi, S¹.

Affiliations

¹ Laboratoire sur les écosystèmes terrestres boréaux, Département des Sciences Fondamentales, Université du Québec à Chicoutimi, 555 boulevard de l'Université, Chicoutimi, QC G7H2B1, Canada.

² Canada Research Chair in Integrative Biology of the Northern Flora, Département de biologie, chimie et géographie, Centre for Northern Studies, Centre for Forest Research, Université du Québec à Rimouski, Rimouski, Québec, Canada.

³ Carbone boréal, Département des Sciences Fondamentales, Université du Québec à Chicoutimi, 555 boulevard de l'Université, Chicoutimi, QC G7H 2B1, Canada.

⁴ Centre de Recerca Ecològica i Aplicacions Forestals (CREAF), 08193 Bellaterra, Barcelona, Spain.

⁵ Institució Catalana de Recerca i Estudis Avançats (ICREA), Passeig de Lluís Companys 23, 08010 Barcelona, Spain.

* Corresponding author: roberto.silvestro1@uqac.ca (RS)

2.1 Abstract

Climate change is rapidly altering weather patterns, resulting in shifts in climatic zones. The survival of trees in specific locations depends on their functional traits. Local populations exhibit trait adaptations that ensure their survival and accomplishment of growth and reproduction processes during the growing season. Studying these traits offers valuable insights into species responses to present and future environmental conditions, aiding the implementation of measures to ensure forest resilience and productivity. This study investigates the variability in functional traits among five black spruce (*Picea mariana* (Mill.) B.S.P.) provenances originating from a latitudinal gradient along the boreal forest, and planted in a common garden in Quebec, Canada. We examined differences in bud phenology, growth performance, lifetime first reproduction, and the impact of a late-frost event on tree growth and phenological adjustments. The findings revealed that trees from northern sites exhibit earlier budbreak, lower growth increments, and reach reproductive maturity earlier than those from southern sites. Late-frost damage affected growth performance, but no phenological adjustment was observed in the successive year. Local adaptation in the functional traits may lead to maladaptation of black spruce under future climate conditions or serve as a potent evolutionary force promoting rapid adaptation under changing environmental conditions.

2.2 Introduction

Climate change affects the weather by raising temperatures, shifting precipitation regimes, and producing more frequent and intense extreme events (IPCC, 2022; Reichstein et al., 2013; Stott, 2016). These changes are expected to shift the climatic zones (McKenney et al., 2011) at a magnitude that exceeds the natural rate of vegetation migration (Sittaro et al., 2017). Such a shift of climatic niches challenges one of the fundamental assumptions underlying past and present forest management, which affirms that native seed sources must be preferred to those from other regions because they have a better adaptation to the local conditions (Boshier et al., 2015). The ongoing geographical shifts in climate can mismatch the trees from their optimal niche, causing maladaptation (Park & Talbot, 2018). For this reason, the current challenge for forest managers is predicting climate change impacts on the vegetation and implementing measures to sustain resilience, functionality and productivity of forest ecosystems. However, such an aim requires a deep understanding of the complex relationships between climate and the eco-physiological processes of trees (Maynard et al., 2022), which are still partially lacking for many species.

The survival of trees in a specific location relies on functional traits, which encompass the morphological, physiological and phenological attributes governing their interactions and responses to the environment (Aubin et al., 2016; Maynard et al., 2022; O'Brien et al., 2007). Within certain species, local populations exhibit divergent phenology, as well as growth and reproductive performances that are adapted to optimize survival and reproductive success in their specific local conditions (Savolainen, Pyhäjärvi, et al., 2007). The intraspecific variation of functional traits reflects differences in genotype and phenotypic plasticity across environments (Aitken et al., 2008). Local adaptation to

contrasting environments driven by natural selection leads to an increased genetic divergence over time (Aitken et al., 2008). Plasticity enables individuals to quickly adjust their phenotypes in response to local conditions, thereby mitigating selective pressures (Pelletier & De Lafontaine, 2023). Genetic variation and plasticity also play crucial roles in determining the ability of populations to adapt to climate change (de Lafontaine et al., 2018), including the opportunity of moving genotypes or provenances for restoration and reforestation practices.

In recent decades, scientists have focussed on the intraspecific variability of phenological and growth traits (Körner & Basler, 2010). Phenological traits determine the seasonal timings of biological events, ensuring growth and reproduction, while minimizing the risks due to climate hazards (Chuine, 2010). Tree size, particularly total height at a specific age, is commonly used in forestry as an indicator of fitness and productivity (Savolainen, Bokma, et al., 2007). These traits can offer valuable insights into species responses to current and future environmental conditions. In addition, adaptations in phenology and growth performance can reflect intraspecific differences in life history and resource allocation strategies, potentially encompassing other key functional traits. However, while it is important to recognize that some traits could be correlated with each other, the sensitivity and responsiveness to climate factors could vary between co-evolved traits (Aubin et al., 2016; Mlambo, 2014). Therefore, we stress the importance of assessing multiple traits when quantifying biological and ecological variations within a species.

Compared to other functional traits, very little is known about the response of plant reproduction to climate change (Parmesan & Hanley, 2015). There is a lack in the literature on lifetime first reproduction, although such a trait is closely related to plant

demography (Harper & White, 1974). The generation time is a demographic parameter that can influence the rate at which species or populations evolve. The earlier the beginning of reproduction, the higher the ability of populations to respond to a changing environment (Rice & Emery, 2003). Lifetime first reproduction is intimately linked to growth performances. Indeed, it is widely acknowledged that trees need to reach a certain age or size to produce flowers and seeds (Owens, 1995). As different provenances can show different growth performances (Frank et al., 2017; Silvestro et al., 2020; St Clair et al., 2005), we raise the hypothesis that lifetime first reproduction, or the size to initiate cone production, changes with provenance.

Frost hardiness is an important trait influenced by phenology and affecting fitness and growth performance (Charrier et al., 2011; Montwé et al., 2018; Vitasse, Lenz, & Körner, 2014). Frost hardiness changes during the year, being at a minimum during the growing season and reaching its maximum during dormancy, when temperatures are lower (Liu et al., 2018). Budbreak is a transition between dormancy and growth, and needs to be synchronized with environmental conditions in order to avoid the risk of frost damage on vulnerable new tissues (Liu et al., 2018). Under climate change, warmer spring temperatures cause an advance in spring phenology, increasing the risk of exposing the young shoots to damaging late-spring frost events (Liu et al., 2018; Marquis et al., 2022). Late-spring frost damage can occur when below-freezing temperatures hit after budbreak or the first leaf-out. Exposure to frost during the initial stages of leaf emergence can have dramatic effects on growth and reproduction by affecting individual resource acquisition (Vitasse, Lenz, Hoch, et al., 2014; Vitasse, Lenz, & Körner, 2014; Vitasse et al., 2018). Plants experiencing a non-lethal stress can respond with a phenological shift in the subsequent year (Deslauriers et al., 2018; Falk et al., 2020; Ren et al., 2020). This shift

typically involves a sugar-mediated response, manifested by earlier starch breakdown (Deslauriers et al., 2018). The higher sugar availability for shoot growth explains the phenological shift of budburst in defoliated individuals. Since frost damage primarily affects crown development, a similar phenological shift may occur in individuals with a significant degree of damaged buds, potentially increasing or decreasing frost hardiness.

This study relies on a common garden experiment to investigate the variation in adaptive traits of five black spruce [*Picea mariana* (Mill.) B.S.P.] provenances originating from a latitudinal gradient in the coniferous boreal forest in Quebec, Canada. Specifically, we assess the differences among provenances in: (i) bud phenology and growth performance, (ii) timings of lifetime first reproduction, and (iii) the consequences of the late-frost event in 2021 on the growth performance and phenological adjustments of trees. According to previous studies (Silvestro et al., 2020; Silvestro et al., 2019), the provenance differs in bud phenology and growth performance. We test the common assumption that the provenances with faster growth start reproduction at younger ages (Stearns, 2015). Lastly, we expect that the trees experiencing damage from frost show an annual growth decline but adjust their phenology to mitigate exposure to late frost events during the successive years.

2.3 Materials and methods

2.3.1 Provenances and common garden

The spruce provenances originated from five natural stands located along a latitudinal gradient that ranges from the 48th to 53rd parallels in the boreal coniferous forest of Quebec, Canada (Figure 2.1). These provenances are Simoncouche (abbreviated as SIM), Bernatchez (BER), Mistassibi (MIS), Camp Daniel (DAN), and Mirage (MIR). The site origins represent natural black spruce stands lacking in anthropogenic disturbances or forest cuttings. The climate of the area is typically boreal, with long, cold winters and short, cool and wet summers. Temperatures decrease with increasing latitude and elevation, with the stands located at higher latitudes being the coldest in winter and least warm in summer. The annual temperature at the provenance origins range from -3.4 °C to 1.2 °C.

In June 2012, we conducted sampling by randomly selecting 5-10 dominant trees in each stand and collecting 2-10 cones per tree, based on availability and accessibility of the canopy. On average, we collected 75-145 cones from each stand. In July 2014, we established the common garden by planting a total of 371 seedlings in a forest gap of 0.5 ha in SIM (48°21'29" N; 71°23'59" W) subjected to a clear-cut. We randomly planted the seedlings at a distance of 2 m × 2 m. We planted two rows of non-experimental spruces on each side of the plantation to avoid edge effects. The soil in the common garden is classified as podzolic, with a superficial organic layer reaching a depth of 10 cm. Based on the meteorological data collected from the weather station located at 500 m from the plantation, the average mean temperature during the study period (2015-2022) ranged from 1.55 to 3.29 °C. The year 2019 and 2021 were the coldest and the warmest years,

respectively (Figure S2.4). Throughout the study period, the number of months with a mean daily minimum temperature < 0 °C ranged from 6 to 8, with 2021 presenting freezing temperatures also in June (Figure S2.4). Precipitation, in the form of rain, occurs mostly between late May and early October (Figure S2.4).

For further details regarding the selection of provenances and the experimental design in the common garden see Silvestro et al. (2019).

2.3.2 Data collection

We recorded bud break and bud set on a weekly basis from the beginning of May to the end of October during 2017-2022. To distinguish between the different phenological phases of the apical bud, we followed the procedure described by Dhont et al. (2010). We recorded (1) the onset of bud break, indicated by an open bud with a pale spot at the bud tip; (2) the end of bud break, indicated by an exposed shoot with needles fully emerged from the surrounding scales and spreading outwards; (3) the onset of bud set, indicated by the presence of a white bud; and (4) the end of bud set, indicated by a fully formed bud with the needles in the whorl spreading outwards. Shoot extension corresponds to the period of annual growth of the apical arrow, occurring between the end of bud burst and the onset of bud set (Silvestro et al., 2020).

At the end of the growing season 2022, we recorded the total height and stem diameter at the collar of each tree. To track annual growth of the primary meristem, we measured shoot extension during 2017-2022 on the internodes of the main stem using a measuring tape, with a precision of 2 mm. We also identified the trees reaching reproductive maturity, based on the presence of cones, from 2020 (the first year in which cones were observed on the trees) to 2022.

2.3.3 Late frost damage assessment

We conducted a visual assessment of damage after a late frost occurring in June 2021 using the protocol on browning for conifers (Burr et al., 2001). We estimated the proportion of damaged brown buds out of the total buds on each tree and defined three damage levels based on the classes: (0) no damaged bud; (1) low, <15% of buds damaged; (2) high, >15% of buds damaged. Additional details regarding the late frost in 2021, the assessment of frost damage at the study site, and the amount of damaged trees are available in Mura et al. (2022).

2.3.4 Statistical analyses

We evaluated the effect of annual temperature at the provenance site on the timings of each phenological phase and their durations by performing an Analysis of Covariance (ANCOVA) using Ordinary Least Squares (OLS) regressions. We compared tree height and diameter among provenances using a one-way analysis of variance (ANOVA), and Tukey's HSD tests for multiple comparisons. We assessed the relationships between reproductive stage and both total height and basal diameter using a two-way ANOVA, including the origin site and reproductive stage as categorical variables.

We investigated the effect of frost damage on bud phenology and shoot growth with a two-way ANOVA. Origin site and frost damage level were included as categorical variables.

We quantified the impact of high-intensity frost damage on growth performance and bud phenology on the two provenances showing the highest level of damage (i.e., > 15% of damaged buds), DAN and MIR. For each of these two provenances, we compared growth and phenology between damaged and undamaged trees during 2017-2022 by using a two-

way ANOVA. To assess the effect of frost on the timings of bud phenology, we performed a two-way ANOVA for each phenological stage. Statistics were performed in R version 4.2.2.

2.4 Results

In this study, we assessed the timings of bud development, apical growth, reproductive maturity, and the damage caused by late-spring frost in five provenances of black spruce in a common garden experiment. These provenances originated from natural stands located along a latitudinal gradient ranging from the 48th to 53rd parallels in Quebec (Figure 2.1).

2.4.1 Phenological timings and growth performances

Bud break occurred from the beginning of May to mid-June, while bud set from the end of June to the end of September, depending on the study year and provenance (Figure S2.1; Table S2.1). On average, the period of bud break lasted 36 days, with a difference of 16 days between the shortest (28 days) and longest (44 days) period in 2020 and 2022, respectively (Figure S2.2). The duration of bud set was more variable among years. On average, bud set lasted 74 days, with a difference of 42 days between the shortest (53 days) and longest (95 days) period in 2019 and 2021, respectively (Figure S2.2). The phenological stages were delayed by 1.5–2.1 days for each degree Celsius of increase in mean annual temperature of the origin site.

The duration of growth (i.e., of the period required for apical shoot extension) occurred from the beginning of June to the beginning of July and was longer in the provenances originating from the coldest sites (Figure S2.2). On average, the period of shoot extension was shorter by 0.18–1.77 days for each degree Celsius of increase in mean annual temperature of the original site.

The annual height increment varied according to provenance, with provenances from the northern sites exhibiting lower shoot extension compared to provenances from the

southern sites (Figure S2.3). The effect of provenance was also confirmed on the total height in 2022 ($F = 4.83$, $P < 0.001$). On average, individuals from the northernmost provenance (MIR) were 40 cm shorter than those from the southernmost provenance (SIM), with an average height of 212 and 252 cm, respectively (Figure 2.2).

The effect of provenance was also confirmed on the basal diameter in 2022 ($F = 9.13$, $P < 0.001$). On average, the basal diameter of individuals from MIR was 10 mm smaller than those from SIM, with an average basal diameter of 40 and 50 mm, respectively (Figure 2.2).

2.4.2 Lifetime first reproduction

Provenances from the northern sites reached reproductive maturity earlier than those from the southern sites (Figure 2.3). In 2020, the first year in which cones were observed in the studied trees, 26% of individuals from the northernmost provenance (MIR) had cones on the crown. By 2022, 52% of trees from MIR showed cones, while only 38% of trees from the southernmost provenance SIM had started reproduction (Figure 2.3). We also found that reproducing trees were taller ($F = 56.07$, $P = 0.001$) and had a larger basal diameter ($F = 35.70$, $P = 0.001$) (Figure 3.3, Table S3.2). On average, reproductive trees were 55 cm taller and 9 mm larger in diameter than non-reproducing trees from the same provenance (Figure 2.3).

2.4.3 Late frost event and frost damages

The late frost event took place on 28 and 29 May, 2021 (DOY 148-149), when nighttime temperatures at the common garden in SIM dropped sharply, reaching -1.1 and -1.9 °C, respectively. The percentage of damaged trees followed the temperature gradient, ranging from 60.7 to 100% for the southernmost (i.e., SIM) and northernmost (i.e., MIR) sites,

respectively ($\chi^2 = 58.98$, $P < .0001$). Overall, low levels of damage (i.e., $< 15\%$ of damaged buds) were more common, accounting for 75.7% of all observations. Only 15.6% of trees showed no damage, 79.3% of which belonged to the two southernmost provenances (i.e., SIM and MIS). Provenances from the northernmost sites exhibited higher levels of damage (i.e., $> 15\%$ of damaged buds), with the two northernmost provenances (i.e., MIR and DAN) accounting for 71.8% of all trees with highly damaged trees.

2.4.4 Frost damage and bud phenology

Compared to the other study years, the onset and ending of budbreak occurred earlier in 2021, while development of the winter bud took longer, with an earlier onset and delayed ending of bud set (Figure S2.1, S2.2). In 2021, the onset of budbreak in the two northernmost provenances (i.e., MIR and DAN) occurred on average on DOY 135, 13 days before the late frost event.

For the two provenances most damaged by the frost (i.e., MIR and DAN), the timings of budbreak and bud set varied between years (Figure 2.4, Table S2.3), with significant differences observed for all phases, (F -values ranging between 44.67 and 352.58, $P < 0.001$) (Table S2.3). However, no effect of the damage level or the interaction between damage level and year was observed (Table S2.3). Therefore, we found no significant differences in phenology between damaged and undamaged trees (Figure 2.4).

2.4.5 Frost damage and height growth performances

The effects of provenance, damage level, and their interaction on apical shoot growth were significant ($P < 0.01$) (Table S2.4). In particular, provenances with a higher level of

damage (i.e., > 15% of damaged buds) exhibited a lower apical shoot growth (26 cm) compared with provenances with low or no damage (42 cm) (Figure 2.5).

The growth in height in the two provenances most damaged (MIR and DAN), varied between years (Fig. 2.6, Table S2.5). This difference was significant (F -value in MIR = 18.99, F -value in DAN = 28.32, $P < 0.001$ for both provenances) (Table S2.5). However, the growth between highly damaged trees and those with low or no damage was similar across all study years, except for 2022, when a significant difference was observed (Figure 2.6).

2.5 Discussion

This study relies on a common garden experiment to test differences in functional traits among five black spruce provenances originating from a latitudinal gradient along the boreal forest of Quebec, Canada. We profit from the late frost event occurring in 2021 to assess differences in frost tolerance and investigate the successive growth performance and phenological adjustment in trees. The results reveal significant variations in all observed traits among the provenances. Trees from the northern sites have earlier bud development, lower growth increments, and reached reproductive maturity earlier than those from southern sites. The late frost in 2021 affected growth performance, but no phenological adjustment was observed.

2.5.1 Tree size and reproductive maturity

Northern provenances exhibited an earlier reproductive maturity than those from southern regions. Trees need to reach a specific age or size before initiating cone production, which aligns with existing knowledge (Owens, 1995), although cone production does not automatically imply that the seeds are viable and fertile. However, our findings reveal

that the size for reproductive maturity varies among provenances. Northern provenances attain reproductive maturity at smaller dimensions than those originating from the southern sites. In particular, northern provenances exhibit cones at a smaller height than southern provenances.

In trees, the size for reproduction reflects the necessity to allocate the resources to growth during the early developmental stages to successively maximize reproductive success (Thomas et al., 2011). For certain coniferous species, tree size has proven to be a better indicator of cone production than tree age (Andrus et al., 2020; Viglas et al., 2013). This relationship is likely explained by the fact that tree size strongly reflects the access to resources (Davi et al., 2016). Consequently, within a provenance, the correlation between total height and reproductive maturity might be attributed to intra-provenance variability in growth performance and individual fitness (Santos-Del-Blanco et al., 2012).

Among provenances, the variability in the threshold size to reach reproductive maturity probably reflects a divergent life history strategy and resource allocation. Generally, the risk of mortality and its predictability influence the timing of first reproduction within species (Kozlowski, 1992). For example, an early high fecundity in fire-prone ecosystems is an advantageous trait (Johnstone & Chapin, 2006). In such ecosystems, the persistence of a species after recurrent wildfires (i.e., stand self-replacement) is usually contingent on immediate and vigorous post-fire tree recruitment (Dawe et al., 2022; Johnstone & Chapin, 2006). Post-fire seeding species, such as black spruce, rely on the ability to quickly establish a persistent seed bank before the subsequent wildfire event (Pausas & Keeley, 2014). In this context, the higher wildfire frequency at higher latitudes in Eastern Canada (Oris et al., 2014) likely represents a selective force advancing the reproductive maturity of northern provenances, as highlighted in our study.

Differentiation between provenances in reproductive allocation and growth performances can therefore be regarded as a fingerprint of different selection processes acting in their respective native environment. It is well known that, when moved south, growth performance of northern provenances remains lower than that of southern ones (Savolainen, Bokma, et al., 2007; Silvestro et al., 2020). In this context, the variability in certain functional traits within a species may reflect some more conservative and precautionary strategies, whereby northern provenances invest more resources during their life cycle to ensure individual survival (e.g., maintaining higher levels of frost hardiness during the dormant season) and enhance reproductive success.

2.5.2 Phenology and frost tolerance

Late frost affected the growth performance but did not trigger a phenological adjustment. As emphasized in a previous study, northern provenances were more exposed to the late frost due to their earlier growth reactivation and budbreak (Mura et al., 2022). Accordingly, the extent of damage in northern provenances exceeded that observed in provenances from the southern sites (Mura et al., 2022). Our findings highlight the existence of a threshold level of damage that results in a decline in height growth. In particular, individuals from the two northern provenances (i.e., MIR and DAN), which had a higher proportion of buds damaged, experienced the larger contraction in height growth in the following year.

The impact of a frost on growth performance has primarily been studied in terms of radial growth. Late frosts occur at the onset of the growing season, and often lead to reductions in tree ring width comparable to, or greater than, those caused by extreme summer droughts (Rubio-Cuadrado et al., 2021; Vitasse et al., 2019). However, no carry-over

effects are reported in the subsequent years (Principe et al., 2017). In this study, we observe that the effects of the late frost on height growth appears only in the subsequent growing season. There are several explanations for this delayed impact on height growth. Previous research has demonstrated that the canopy recovers in two months from a late frost event (Baumgarten et al., 2023; D'Andrea et al., 2019), suggesting a potential recovery through exact compensation (Vander Mijnsbrugge et al., 2021). Still, canopy recovery comes at a cost in terms of resource allocation. Several studies that have manipulated growth conditions have shown that non-structural carbohydrate (NSC) reserves are restored rapidly after a disturbance, at the expense of growth activity (Schönbeck et al., 2018; Weber et al., 2018). This supports the empirical evidence that carbon storage takes priority over growth (Sala et al., 2012), and trees maintain a safety margin in terms of carbohydrate reserves to cope with injuries caused by biotic or climatic events, including frost (Klein et al., 2016). Moreover, shoot increment is primarily determined by the growth units already formed within the bud, which are influenced by the environmental conditions occurring during the preceding summer (Salminen & Jalkanen, 2005). Considering that (i) frost damage negatively impacts individual resource acquisition (Vitasse, Lenz, Hoch, et al., 2014; Vitasse, Lenz, & Körner, 2014; Vitasse et al., 2018), (ii) canopy recovery and restoration of NSC reserves have priority following a frost event, and (iii) height growth is largely predetermined by the previous year's environmental conditions, it is more likely to observe a decline in height growth in the year following the frost event and in individuals with a higher degree of damages, as highlighted in our study.

The damage caused by the late frost did not induce a phenological adjustment in our trees. Indeed, the timing of budbreak for the subsequent year remained similar between

individuals of the same provenance, regardless of the frost damage levels. Bud phenology in black spruce provenances represents a local adaptation to the climatic conditions at the origin sites. Provenances from northern and colder sites exhibit an earlier budbreak than provenances from southern and warmer sites (Guo et al., 2021; Silvestro et al., 2019), due to lower forcing requirements (Mura et al., 2022). For this reason, our results indicate a maladaptive phenological plasticity and, even after a frost event, highly damaged trees do not adjust their phenology. In this context, provenances or individuals that are more susceptible to late frost damage also remain prone to suffer from similar events in the future.

Our results differ from observations of other non-lethal stresses, which resulted in phenological shifts in the following year (Deslauriers et al., 2018; Falk et al., 2020; Ren et al., 2020). This difference may be due to the degree of damage, which may not have been sufficient to alter sugar mobilization in the subsequent year. The limited number of buds produced in our damaged trees may not have created enough competition for sugars (Barbier et al., 2015). Although the trees may compensate for the damage at the expense of radial growth in the same year and height growth in the subsequent year, a prolonged carry-over effect on growth performance seems, to our knowledge, unlikely.

2.5.3 A blessing in disguise or a curse in hiding?

Our results indicate that the functional traits studied in black spruce are related to the provenances, and thus probably affected by a local adaptation to the origin sites. When considering the phenological traits and the associated risk of late-spring frost exposure, northern provenances may be maladapted to future climatic conditions. However, assuming a certain degree of genetic variation within natural populations, this

maladaptation could potentially serve as an evolutionary force that promotes a rapid local adaptation to the new environment. Given the magnitude of the ongoing climate change, adaptation would need to occur swiftly, which is a challenge for long-living organisms. Our results suggest that northern populations may have a faster generation turnover, which should foster a quicker evolutionary response to selective pressures compared with southern populations. A deeper assessment of reproductive traits such as seed production and germination rate is necessary to validate our hypothesis.

Similar considerations arise when contemplating the potential of moving species or provenances. The timing of first reproduction and generation turnover are vital traits to take into account in these practices. While further research is needed to evaluate variations in reproductive traits, migrating southern provenances to northern regions could potentially disrupt the long-standing adaptations to cope with recurring disturbances, such as wildfires. According to our results, southern provenances must reach an older age or larger size to reach reproductive maturity, which could impact the resilience of certain species in locations with more frequent and intense wildfires, like the northern latitudes of Quebec. So far, reproduction has received much less attention compared to growth-related traits, although it plays a critical role in ensuring the persistence of trees in specific locations and, consequently, the long-term success of the practices of forest management in a context of climate change.

2.5.4 Acknowledgements

This work was funded by the Fonds de Recherche du Québec - Nature et Technologies FRQNT (project AccFor #309064), the Fondation de l'Université du Québec à Chicoutimi, and the Forêt d'Enseignement et de Recherche Simoncouche. R. Silvestro

received the Merit scholarship for foreign students (PBEEE) by the FRQNT. The authors thank A. Garside for editing the English text.

2.5.5 Author contribution

RS and SR conceived the ideas and designed the study; RS, CM and DAB collected data; RS analysed the data and led the writing of the manuscript; CM, GdL, PF, MM and SR contributed critically to the drafts; All authors gave final approval for publication.

2.5.6 Competing interests

The authors declare no competing interests.

2.5.7 Data availability

Once accepted for publication, data associated with this paper will be available in Borealis, the Canadian Dataverse Repository.

2.6 Figures

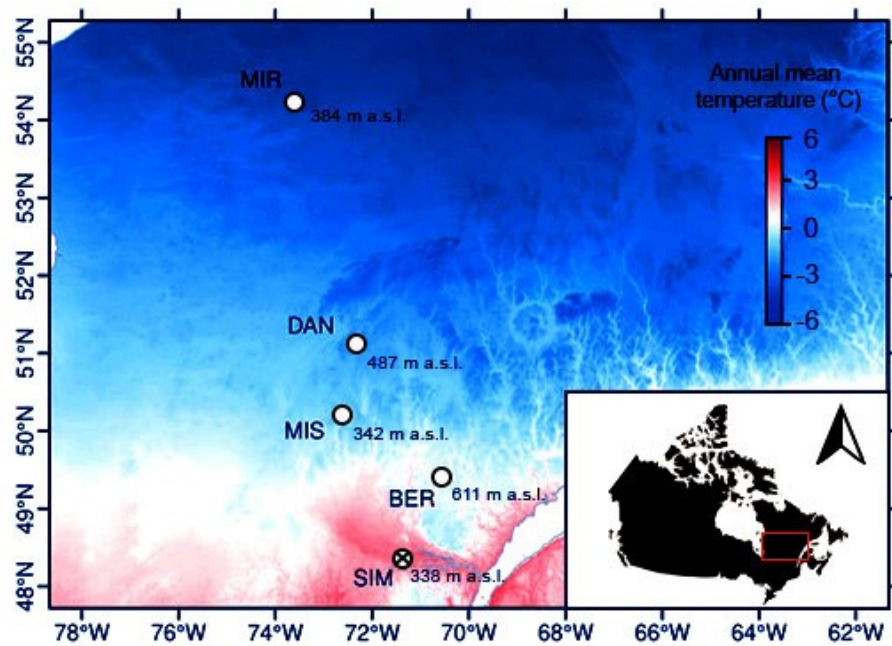


Figure 2.1 Origin sites of the five black spruce provenances [Simoncouche (abbreviated as SIM), Bernatchez (BER), Mistassibi (MIS), Camp Daniel (DAN) and Mirage (MIR)] in Quebec, Canada, and annual temperature across the study region. All provenances were planted in a common garden located in SIM (crossed circle).

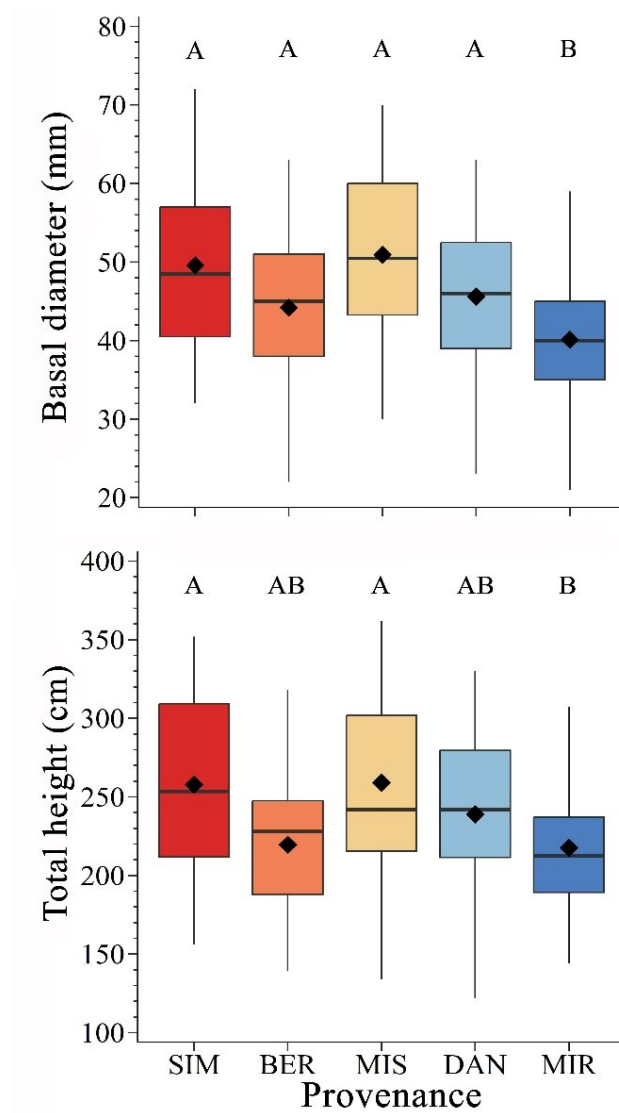


Figure 2.2 Comparison of basal diameter and total height across the five black spruce provenances [Simoncouche (abbreviated as SIM), Bernatchez (BER), Mistassibi (MIS), Camp Daniel (DAN) and Mirage (MIR)]. Boxplots represent upper and lower quartiles; whiskers achieve the 10th and 90th percentiles; the median and mean values are drawn as horizontal black lines and black diamond, respectively.

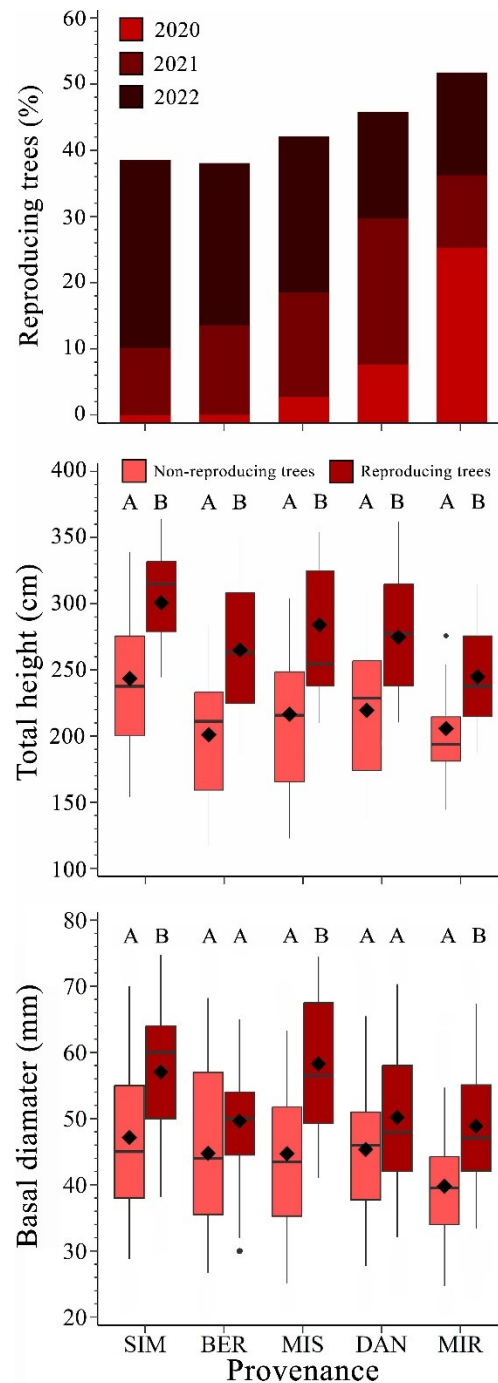


Figure 2.3 Number of trees in reproduction and tree growth in the five black spruce provenances [Simoncouche (abbreviated as SIM), Bernatchez (BER), Mistassibi (MIS), Camp Daniel (DAN) and Mirage (MIR)]. The boxplots illustrate the upper and lower quartiles, with whiskers indicating the 10th and 90th percentiles. The median and the mean are represented by horizontal black lines and a black diamond, respectively.

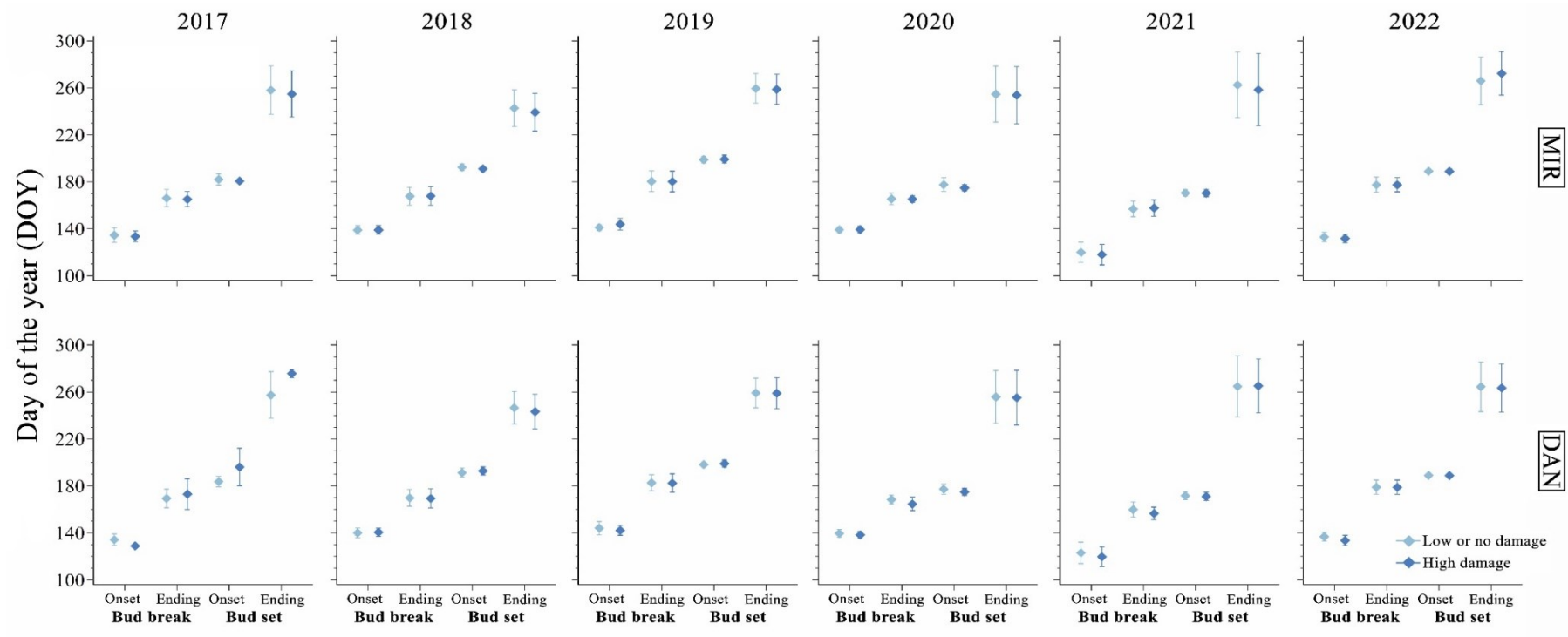


Figure 2.4 Bud phenology in trees according to their visible damage by the late frost in 2021. Mean values are denoted by dots, while vertical lines indicate the standard deviations.

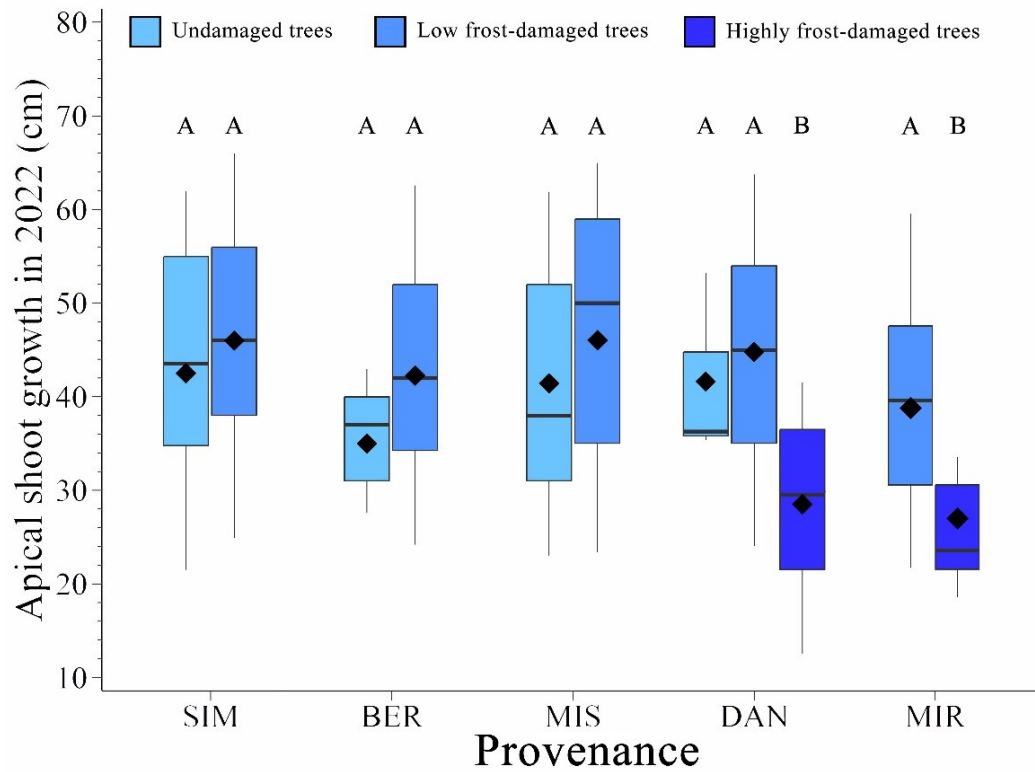


Figure 2.5 Apical shoot extension in 2022 in trees with different damage by the late frost in 2021. The boxplots illustrate the upper and lower quartiles, with whiskers indicating the 10th and 90th percentiles. The median and the mean are represented by horizontal black lines and a black diamond, respectively.

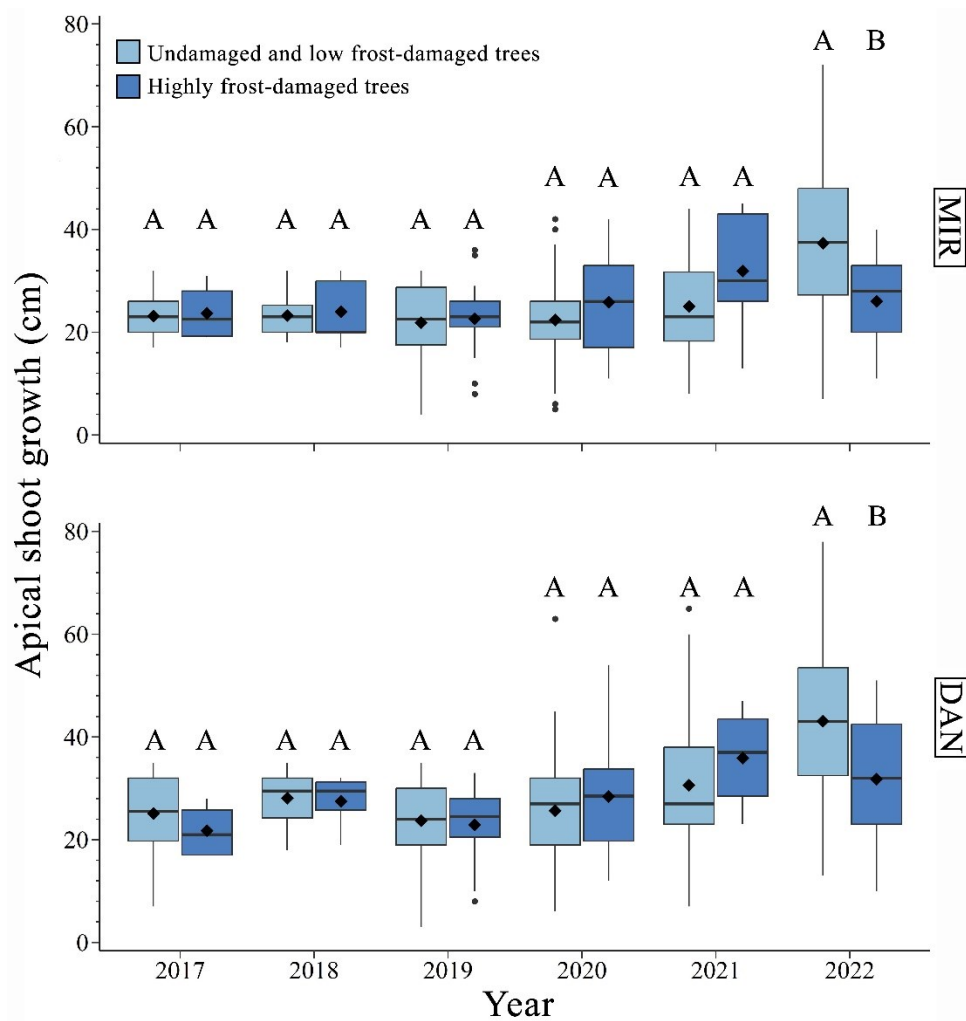


Figure 2.6 Apical shoot extension in trees with different damage by the late frost in 2021 for the study years 2017-2022. The boxplots illustrate the upper and lower quartiles, with whiskers indicating the 10th and 90th percentiles. The median and the mean are represented by horizontal black lines and a black diamond, respectively.

2.7 Annexes

Table S 2.1 Effects of mean annual temperature of the provenance (Temp), Year and their interaction (Temp×Year) on the phenological phases evaluated by ANCOVA models.

	Phase	R ²	Effects		
			Temp	Year	Temp x Year
Bud break	Onset	0.63	302.70***	978.28***	2.45**
	Ending	0.51	492.35***	1182.11***	3.27*
	Duration	0.19	28.95***	342.17***	10.01*
Growing season	Duration	0.14	29.31***	136.82***	16.88**
Bud set	Onset	0.73	116.41***	954.77***	9.92**
	Ending	0.20	97.04***	276.88***	13.67*
	Duration	0.30	30.89***	546.35***	4.52*

* $P < 0.05$; ** $P < 0.01$; *** $P < 0.001$.

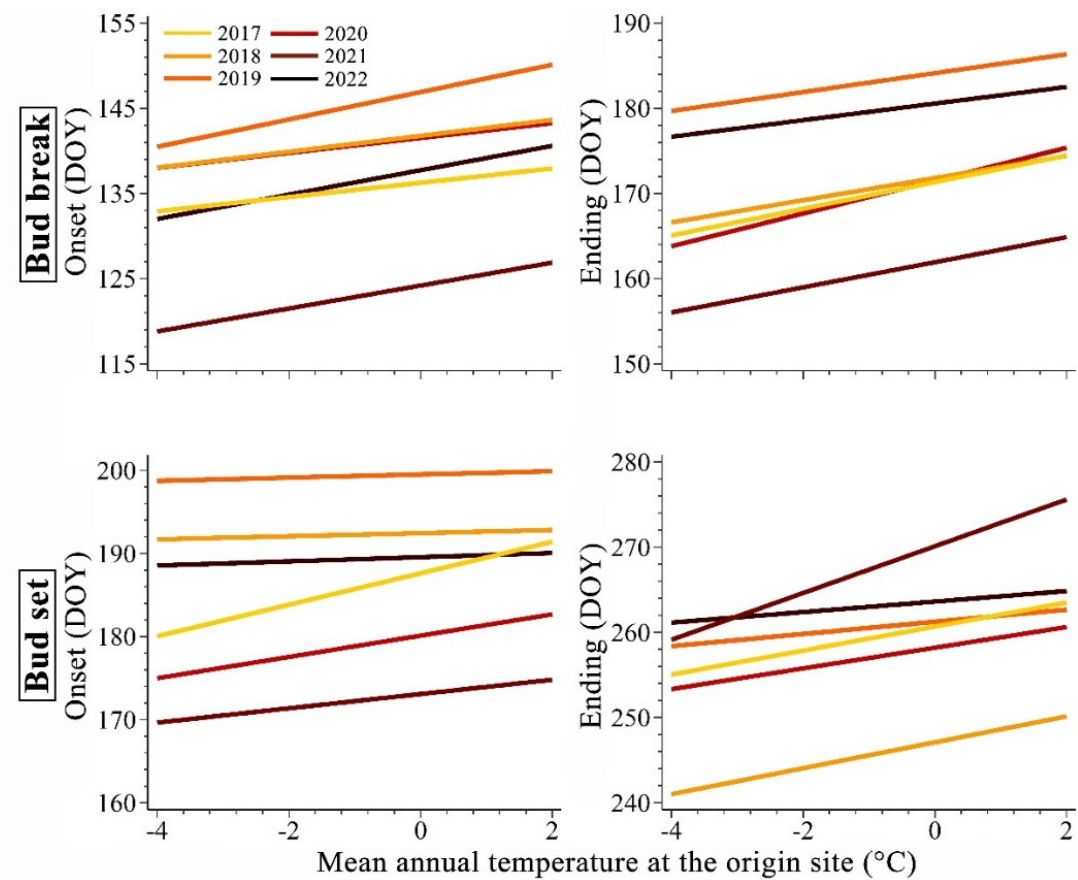


Figure S 2.1 Days of occurrence of the onset and the ending for both budbreak and bud set for each black spruce provenance predicted by the Ordinary Least Squares (OLS) models.

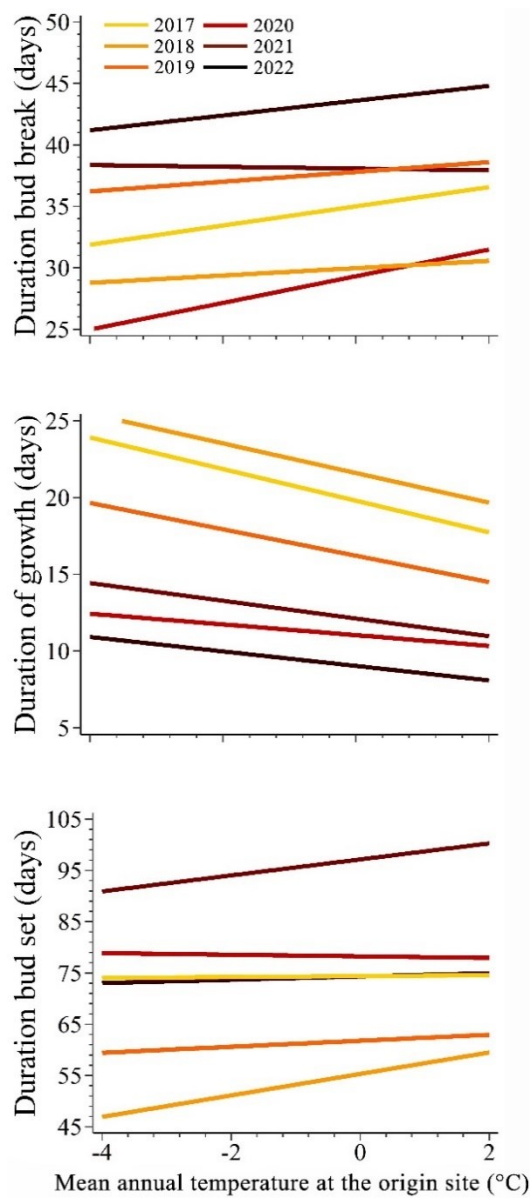


Figure S 2.2 Duration of budbreak, shoot extension, and bud set for each black spruce provenance predicted by the Ordinary Least Squares (OLS) models.

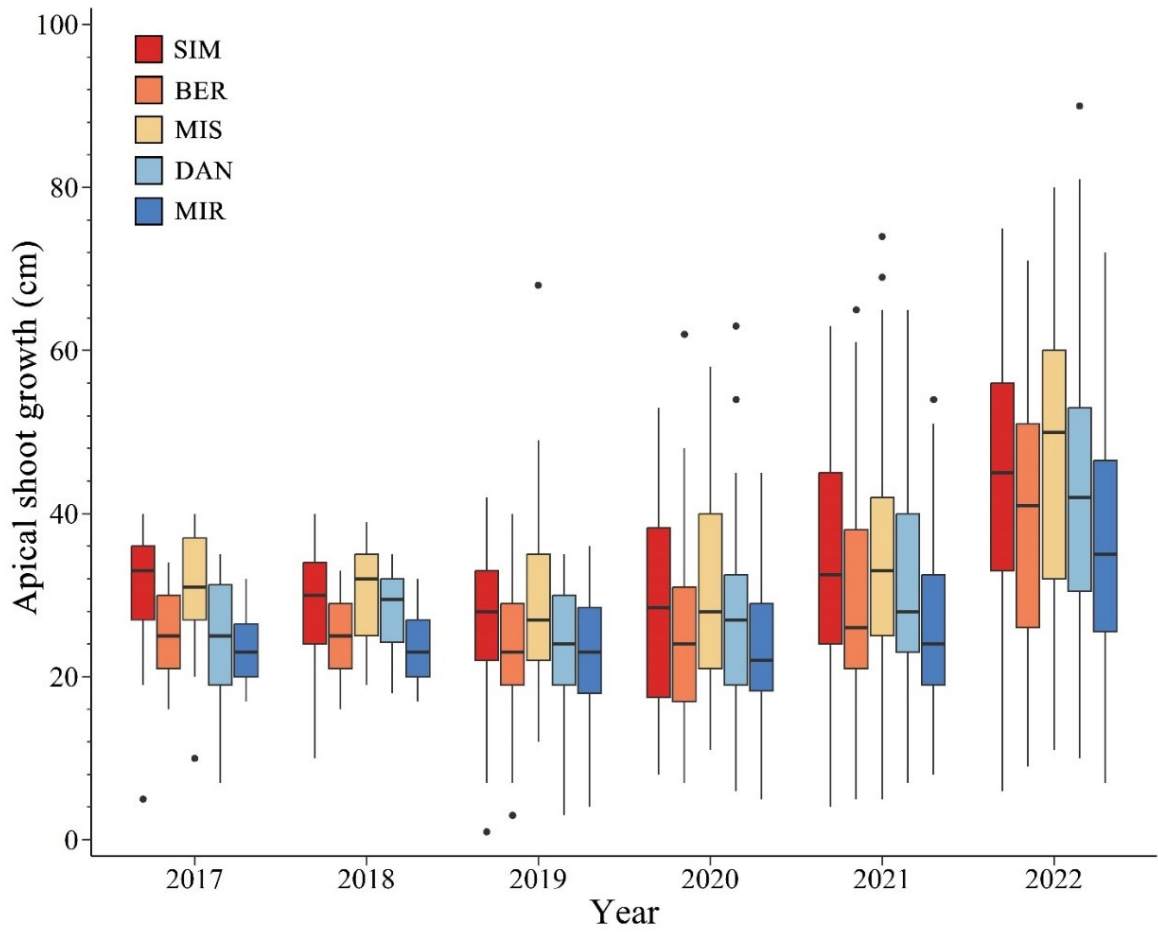


Figure S 2.3 Apical shoot growth for each black spruce provenance during the study years 2017-2022.

Table S 2.2 Effects of the provenance (Prov), reproductive maturity (Repr) and their interaction (Prov \times Repr) on basal diameter and total height evaluated by ANCOVA models.

	R ²	Effects		
		Prov	Repr	Prov x Repr
Diameter	0.17	6.77***	35.68***	2.96*
Height	0.19	6.11***	56.07***	3.74*

* $P < 0.05$; ** $P < 0.01$; *** $P < 0.001$.

Table S 2.3 Effects of the Year, damage level (Damage) and their interaction (Year x Damage) on the timing of onset and ending for both bud break and bud set evaluated by ANOVA models.

		Phase	R ²	Effects		
				Year	Damage	Year x Damage
MIR	Bud break	Onset	0.70	246.34***	0.96	1.18
		Ending	0.53	312.93***	0.01	0.19
	Bud set	Onset	0.80	337.50***	2.73	0.68
		Ending	0.15	65.57***	1.58	1.58
DAN	Bud break	Onset	0.63	192.76***	7.22	0.83
		Ending	0.52	256.75***	0.04	3.18
	Bud set	Onset	0.85	352.58***	5.73	9.75
		Ending	0.11	44.67***	0.14	1.17

* $P < 0.05$; ** $P < 0.01$; *** $P < 0.001$.

Table S 2.4 Effects of the provenance (Prov), damage level (Damage) and their interaction (Prov x Damage) on growth performances evaluated by ANOVA model.

R ²	Effects		
	Prov	Damage	Prov x Damage
0.21	4.73**	5.85**	2.01**

* $P < 0.05$; ** $P < 0.01$; *** $P < 0.001$.

Table S 2.5 Effects of the year, damage level (Damage) and their interaction (Year x Damage) on growth performances for Mirage (MIR) and Camp Daniel (DAN) provenances evaluated by ANOVA models.

Provenance	Phase	R ²	Effects		
			Year	Damage	Year x Damage
MIR	Onset	0.26	18.99***	0.01	4.80***
DAN	Ending	0.30	28.32***	0.75	3.72**

* $P < 0.05$; ** $P < 0.01$; *** $P < 0.001$.

2.8 References

- Aitken, S. N., Yeaman, S., Holliday, J. A., Wang, T., & Curtis-McLane, S. (2008). Adaptation, migration or extirpation: climate change outcomes for tree populations. *Evolutionary Applications*, 1(1), 95-111. <https://doi.org/10.1111/j.1752-4571.2007.00013.x>
- Andrus, R. A., Harvey, B. J., Hoffman, A., & Veblen, T. T. (2020). Reproductive maturity and cone abundance vary with tree size and stand basal area for two widely distributed conifers. *Ecosphere*, 11(5). <https://doi.org/10.1002/ecs2.3092>
- Aubin, I., Munson, A. D., Cardou, F., Burton, P. J., Isabel, N., Pedlar, J. H., Paquette, A., Taylor, A. R., Delagrangé, S., Kebli, H., Messier, C., Shipley, B., Valladares, F., Kattge, J., Boisvert-Marsh, L., & McKenney, D. (2016). Traits to stay, traits to move: a review of functional traits to assess sensitivity and adaptive capacity of temperate and boreal trees to climate change. *Environmental Reviews*, 24(2), 164-186. <https://doi.org/10.1139/er-2015-0072>
- Barbier, F. F., Lunn, J. E., & Beveridge, C. A. (2015). Ready, steady, go! A sugar hit starts the race to shoot branching. *Current Opinion in Plant Biology*, 25, 39-45. <https://doi.org/https://doi.org/10.1016/j.pbi.2015.04.004>
- Baumgarten, F., Gessler, A., & Vitasse, Y. (2023). No risk—no fun: Penalty and recovery from spring frost damage in deciduous temperate trees. *Functional Ecology*, 37(3), 648-663. <https://doi.org/10.1111/1365-2435.14243>
- Boshier, D., Broadhurst, L., Cornelius, J., Gallo, L., Koskela, J., Loo, J., Petrokofsky, G., & St Clair, B. (2015). Is local best? Examining the evidence for local adaptation in trees and its scale. *Environmental Evidence*, 4(1). <https://doi.org/10.1186/s13750-015-0046-3>
- Burr, K. E., Hawkins, C. D. B., L'Hirondelle, S. J., Binder, W. D., George, M. F., & Repo, T. (2001). Methods for Measuring Cold Hardiness of Conifers. In *Conifer Cold Hardiness* (pp. 369-401). Springer, Dordrecht. https://doi.org/10.1007/978-94-015-9650-3_14
- Charrier, G., Bonhomme, M., Lacoïnte, A., & Améglio, T. (2011). Are budburst dates, dormancy and cold acclimation in walnut trees (*Juglans regia* L.) under mainly genotypic or environmental control? *International Journal of Biometeorology*, 55(6), 763-774. <https://doi.org/10.1007/s00484-011-0470-1>
- Chuine, I. (2010). Why does phenology drive species distribution? *Philosophical Transactions of the Royal Society B: Biological Sciences*, 365(1555), 3149-3160. <https://doi.org/10.1098/rstb.2010.0142>

- D'Andrea, E., Rezaie, N., Battistelli, A., Gavrichkova, O., Kuhlmann, I., Matteucci, G., Moscatello, S., Proietti, S., Scartazza, A., Trumbore, S., & Muhr, J. (2019). Winter's bite: beech trees survive complete defoliation due to spring late-frost damage by mobilizing old C reserves. *New Phytologist*, 224(2), 625-631. <https://doi.org/10.1111/nph.16047>
- Davi, H., Cailleret, M., Restoux, G., Amm, A., Pichot, C., & Fady, B. (2016). Disentangling the factors driving tree reproduction. *Ecosphere*, 7(9), e01389. <https://doi.org/10.1002/ecs2.1389>
- Dawe, D. A., Parisien, M.-A., Van Dongen, A., & Whitman, E. (2022). Initial succession after wildfire in dry boreal forests of northwestern North America. *Plant Ecology*, 223(7), 789-809. <https://doi.org/10.1007/s11258-022-01237-6>
- de Lafontaine, G., Napier, J. D., Petit, R. J., & Hu, F. S. (2018). Invoking adaptation to decipher the genetic legacy of past climate change. *Ecology*, 99(7), 1530-1546. <https://www.jstor.org/stable/26625766>
- Deslauriers, A., Fournier, M.-P., Carteni, F., & Mackay, J. (2018). Phenological shifts in conifer species stressed by spruce budworm defoliation. *Tree Physiology*, 39(4), 590-605. <https://doi.org/10.1093/treephys/tpy135>
- Dhont, P., Sylvestre, P., Gros-Louis, M. C., & Isabel, N. (2010). *Field Guide for Identifying Apical Bud Break and Bud Formation Stages in White Spruce*.
- Falk, M. A., Donaldson, J. R., Stevens, M. T., Raffa, K. F., & Lindroth, R. L. (2020). Phenological responses to prior-season defoliation and soil-nutrient availability vary among early- and late-flushing aspen (*Populus tremuloides* Michx.) genotypes. *Forest Ecology and Management*, 458, 117771. <https://doi.org/https://doi.org/10.1016/j.foreco.2019.117771>
- Frank, A., Sperisen, C., Howe, G. T., Brang, P., Walthert, L., Clair, J. B. S., & Heiri, C. (2017). Distinct genecological patterns in seedlings of Norway spruce and silver fir from a mountainous landscape. *Ecology*, 98(1), 211-227. <https://doi.org/10.1002/ecy.1632>
- Guo, X., Klisz, M., Puchałka, R., Silvestro, R., Faubert, P., Belien, E., Huang, J., & Rossi, S. (2021). Common-garden experiment reveals clinal trends of bud phenology in black spruce populations from a latitudinal gradient in the boreal forest. *Journal of Ecology*, 1365-2745.13582. <https://doi.org/10.1111/1365-2745.13582>
- Harper, J., & White, J. (1974). The demography of plants. *Annual Review of Ecology and Systematics*, 5(1), 419-463.
- IPCC. (2022). *Climate change 2022: Impacts, adaptation and vulnerability*.

- Johnstone, J. F., & Chapin, F. S. (2006). Fire Interval Effects on Successional Trajectory in Boreal Forests of Northwest Canada. *Ecosystems*, 9(2), 268-277. <https://doi.org/10.1007/s10021-005-0061-2>
- Klein, T., Vitasse, Y., & Hoch, G. (2016). Coordination between growth, phenology and carbon storage in three coexisting deciduous tree species in a temperate forest. *Tree Physiology*, 36(7), 847-855. <https://doi.org/10.1093/treephys/tpw030>
- Körner, C., & Basler, D. (2010). Phenology under global warming. *Science*, 327(5972), 1461-1462. <https://doi.org/10.1126/science.1186473>
- Kozłowski, T. T. (1992). Carbohydrate sources and sinks in woody plants. *The Botanical Review*, 58(2), 107-222. <https://doi.org/10.1007/BF02858600>
- Liu, Q., Piao, S., Janssens, I. A., Fu, Y., Peng, S., Lian, X., Ciais, P., Myneni, R. B., Peñuelas, J., & Wang, T. (2018). Extension of the growing season increases vegetation exposure to frost. *Nature Communications*, 9(1). <https://doi.org/10.1038/s41467-017-02690-y>
- Marquis, B., Bergeron, Y., Houle, D., Leduc, M., & Rossi, S. (2022). Variability in frost occurrence under climate change and consequent risk of damage to trees of western Quebec, Canada. *Scientific Reports*, 12(1). <https://doi.org/10.1038/s41598-022-11105-y>
- Maynard, D. S., Bialic-Murphy, L., Zohner, C. M., Averill, C., Van Den Hoogen, J., Ma, H., Mo, L., Smith, G. R., Acosta, A. T. R., Aubin, I., Berenguer, E., Boonman, C. C. F., Catford, J. A., Cerabolini, B. E. L., Dias, A. S., González-Melo, A., Hietz, P., Lusk, C. H., Mori, A. S., . . . Crowther, T. W. (2022). Global relationships in tree functional traits. *Nature Communications*, 13(1). <https://doi.org/10.1038/s41467-022-30888-2>
- McKenney, D. W., Pedlar, J. H., Rood, R. B., & Price, D. (2011). Revisiting projected shifts in the climate envelopes of North American trees using updated general circulation models. *Global Change Biology*, 17(8), 2720-2730. <https://doi.org/10.1111/j.1365-2486.2011.02413.x>
- Mlambo, M. C. (2014). Not all traits are 'functional': insights from taxonomy and biodiversity-ecosystem functioning research. *Biodiversity and Conservation*, 23(3), 781-790. <https://doi.org/10.1007/s10531-014-0618-5>
- Montwé, D., Isaac-Renton, M., Hamann, A., & Spiecker, H. (2018). Cold adaptation recorded in tree rings highlights risks associated with climate change and assisted migration. *Nature Communications*, 9(1). <https://doi.org/10.1038/s41467-018-04039-5>

- Mura, C., Buttò, V., Silvestro, R., Deslauriers, A., Charrier, G., Raymond, P., & Rossi, S. (2022). The early bud gets the cold: Diverging spring phenology drives exposure to late frost in a *Picea mariana* [(Mill.) BSP] common garden. *Physiologia Plantarum*, 174(6), e13798-e13798. <https://doi.org/10.1111/ppl.13798>
- O'Brien, E. K., Mazanec, R. A., & Krauss, S. L. (2007). Provenance variation of ecologically important traits of forest trees: implications for restoration. *Journal of Applied Ecology*, 44(3), 583-593. <https://doi.org/10.1111/j.1365-2664.2007.01313.x>
- Oris, F., Asselin, H., Finsinger, W., Hély, C., Blarquez, O., Ferland, M.-E., Bergeron, Y., & Ali, A. A. (2014). Long-term fire history in northern Quebec: implications for the northern limit of commercial forests. *Journal of Applied Ecology*, 51(3), 675-683. <https://doi.org/10.1111/1365-2664.12240>
- Owens, J. N. (1995). Constraints to seed production: temperate and tropical forest trees. *Tree Physiology*, 15(7-8), 477-484. <https://doi.org/10.1093/treephys/15.7-8.477>
- Park, A., & Talbot, C. (2018). Information Underload: Ecological Complexity, Incomplete Knowledge, and Data Deficits Create Challenges for the Assisted Migration of Forest Trees. *BioScience*, 68(4), 251-263. <https://doi.org/10.1093/biosci/biy001>
- Parnesan, C., & Hanley, M. E. (2015). Plants and climate change: complexities and surprises. *Annals of Botany*, 116(6), 849-864. <https://doi.org/10.1093/aob/mcv169>
- Pausas, J. G., & Keeley, J. E. (2014). Evolutionary ecology of resprouting and seeding in fire-prone ecosystems. *New Phytologist*, 204(1), 55-65. <https://doi.org/10.1111/nph.12921>
- Pelletier, E., & De Lafontaine, G. (2023). Jack pine of all trades: Deciphering intraspecific variability of a key adaptive trait at the rear edge of a widespread fire-embracing North American conifer. *American Journal of Botany*, 110(2). <https://doi.org/10.1002/ajb2.16111>
- Príncipe, A., Van Der Maaten, E., Van Der Maaten-Theunissen, M., Struwe, T., Wilmking, M., & Kreyling, J. (2017). Low resistance but high resilience in growth of a major deciduous forest tree (*Fagus sylvatica* L.) in response to late spring frost in southern Germany. *Trees*, 31(2), 743-751. <https://doi.org/10.1007/s00468-016-1505-3>
- Reichstein, M., Bahn, M., Ciais, P., Frank, D., Mahecha, M. D., Seneviratne, S. I., Zscheischler, J., Beer, C., Buchmann, N., Frank, D. C., Papale, D., Rammig, A.,

- Smith, P., Thonicke, K., Van Der Velde, M., Vicca, S., Walz, A., & Wattenbach, M. (2013). Climate extremes and the carbon cycle. *Nature*, *500*(7462), 287-295. <https://doi.org/10.1038/nature12350>
- Ren, P., Néron, V., Rossi, S., Liang, E., Bouchard, M., & Deslauriers, A. (2020). Warming counteracts defoliation-induced mismatch by increasing herbivore-plant phenological synchrony. *Global Change Biology*, *26*(4), 2072-2080. <https://doi.org/10.1111/gcb.14991>
- Rice, K. J., & Emery, N. C. (2003). Managing microevolution: restoration in the face of global change. *Frontiers in Ecology and the Environment*, *1*(9), 469-478. [https://doi.org/10.1890/1540-9295\(2003\)001\[0469:mmritf\]2.0.co;2](https://doi.org/10.1890/1540-9295(2003)001[0469:mmritf]2.0.co;2)
- Rubio-Cuadrado, Á., Camarero, J. J., Rodríguez-Calcerrada, J., Perea, R., Gómez, C., Montes, F., & Gil, L. (2021). Impact of successive spring frosts on leaf phenology and radial growth in three deciduous tree species with contrasting climate requirements in central Spain. *Tree Physiology*, *41*(12), 2279-2292. <https://doi.org/10.1093/treephys/tpab076>
- Sala, A., Woodruff, D. R., & Meinzer, F. C. (2012). Carbon dynamics in trees: feast or famine? *Tree Physiology*, *32*(6), 764-775. <https://doi.org/10.1093/treephys/tpr143>
- Salminen, H., & Jalkanen, R. (2005). Modelling the effect of temperature on height increment of Scots pine at high latitudes. *Silva Fennica*, *39*(4), 497-508. <https://doi.org/10.14214/sf.362>
- Santos-Del-Blanco, L., Climent, J., González-Martínez, S. C., & Pannell, J. R. (2012). Genetic differentiation for size at first reproduction through male versus female functions in the widespread Mediterranean tree *Pinus pinaster*. *Annals of Botany*, *110*(7), 1449-1460. <https://doi.org/10.1093/aob/mcs210>
- Savolainen, O., Bokma, F., Knürr, T., Kärkkäinen, K., Pyhäjärvi, T., & Wachowiak, W. (2007). *Adaptation of forest trees to climate change* EUFORGEN Climate Change and Forest Genetic Diversity: implications for sustainable forest management in Europe, Paris, France, 15-16 March 2006, 19-30., Rome, Italy.
- Savolainen, O., Pyhäjärvi, T., & Knürr, T. (2007). Gene flow and local adaptation in trees. *Annual Review of Ecology, Evolution, and Systematics*, *38*(1), 595-619. <https://doi.org/10.1146/annurev.ecolsys.38.091206.095646>
- Schönbeck, L., Gessler, A., Hoch, G., McDowell, N. G., Rigling, A., Schaub, M., & Li, M. H. (2018). Homeostatic levels of nonstructural carbohydrates after 13 yr of drought and irrigation in *Pinus sylvestris*. *New Phytologist*, *219*(4), 1314-1324. <https://doi.org/10.1111/nph.15224>

- Silvestro, R., Brasseur, S., Klisz, M., Mencuccini, M., & Rossi, S. (2020). Bioclimatic distance and performance of apical shoot extension: Disentangling the role of growth rate and duration in ecotypic differentiation. *Forest Ecology and Management*, 477. <https://doi.org/10.1016/j.foreco.2020.118483>
- Silvestro, R., Rossi, S., Zhang, S., Froment, I., Huang, J. G., & Saracino, A. (2019). From phenology to forest management: Ecotypes selection can avoid early or late frosts, but not both. *Forest Ecology and Management*, 436, 21-26. <https://doi.org/10.1016/j.foreco.2019.01.005>
- Sittaro, F., Paquette, A., Messier, C., & Nock, C. A. (2017). Tree range expansion in eastern North America fails to keep pace with climate warming at northern range limits. *Global Change Biology*, 23(8), 3292-3301. <https://doi.org/10.1111/gcb.13622>
- St Clair, J. B., Mandel, N. L., & Vance-Borland, K. W. (2005). Genecology of Douglas fir in Western Oregon and Washington. *Annals of Botany*, 96(7), 1199-1214. <https://doi.org/10.1093/aob/mci278>
- Stearns, S. C. (2015). The Concept of Phenotypic Plasticity and the Evolution of Phenotypic Plasticity in Life History Traits. In A. C. Love (Ed.), *Conceptual Change in Biology: Scientific and Philosophical Perspectives on Evolution and Development* (pp. 131-146). Springer Netherlands. https://doi.org/10.1007/978-94-017-9412-1_6
- Stott, P. (2016). How climate change affects extreme weather events. *Science*, 352(6293), 1517-1518. <https://doi.org/10.1126/science.aaf7271>
- Thomas, S., Meinzer, F., Lachenbruch, B., & Dawson, T. (2011). Size-and age-related changes in tree structure and function. *Size-and Age-Related Changes in Tree Structure and Function*. Springer Science+ Business Media BV, Dordrecht, 33-64.
- Vander Mijnsbrugge, K., Malanguis, J. M., Moreels, S., Lauwers, A., Thomaes, A., De Keersmaeker, L., & Vandekerckhove, K. (2021). Growth Recovery and Phenological Responses of Juvenile Beech (*Fagus sylvatica* L.) Exposed to Spring Warming and Late Spring Frost. *Forests*, 12(11), 1604. <https://doi.org/10.3390/f12111604>
- Viglas, J. N., Brown, C. D., & Johnstone, J. F. (2013). Age and size effects on seed productivity of northern black spruce. *Canadian Journal of Forest Research*, 43(6), 534-543. <https://doi.org/10.1139/cjfr-2013-0022>
- Vitasse, Y., Bottero, A., Cailleret, M., Bigler, C., Fonti, P., Gessler, A., Lévesque, M., Rohner, B., Weber, P., Rigling, A., & Wohlgemuth, T. (2019). Contrasting

- resistance and resilience to extreme drought and late spring frost in five major European tree species. *Global Change Biology*, 25(11), 3781-3792. <https://doi.org/10.1111/gcb.14803>
- Vitasse, Y., Lenz, A., Hoch, G., & Körner, C. (2014). Earlier leaf-out rather than difference in freezing resistance puts juvenile trees at greater risk of damage than adult trees. *Journal of Ecology*, 102(4), 981-988. <https://doi.org/10.1111/1365-2745.12251>
- Vitasse, Y., Lenz, A., & Körner, C. (2014). The interaction between freezing tolerance and phenology in temperate deciduous trees [Review]. *Frontiers in Plant Science*, 5. <https://doi.org/10.3389/fpls.2014.00541>
- Vitasse, Y., Schneider, L., Rixen, C., Christen, D., & Rebetez, M. (2018). Increase in the risk of exposure of forest and fruit trees to spring frosts at higher elevations in Switzerland over the last four decades. *Agricultural and Forest Meteorology*, 248, 60-69. <https://doi.org/https://doi.org/10.1016/j.agrformet.2017.09.005>
- Weber, R., Schwendener, A., Schmid, S., Lambert, S., Wiley, E., Landhäusser, S. M., Hartmann, H., & Hoch, G. (2018). Living on next to nothing: tree seedlings can survive weeks with very low carbohydrate concentrations. *New Phytologist*, 218(1), 107-118. <https://doi.org/10.1111/nph.14987>

CHAPTER III

UPSCALING XYLEM PHENOLOGY: SAMPLE SIZE MATTERS

Published in Annals of Botany

Citation:

Silvestro, R., Sylvain, J. D., Drolet, G., Buttò, V., Auger, I., Mencuccini, M., & Rossi, S. (2022). Upscaling xylem phenology: sample size matters. *Annals of Botany*, 130(6), 811-824.

RESEARCH ARTICLE**Title:**

Upscaling xylem phenology: Sample size matters

Authors:

Roberto Silvestro^{1, *}, Jean-Daniel Sylvain², Guillaume Drolet², Valentina Buttò^{1, 3},
Isabelle Auger², Maurizio Mencuccini^{4, 5}, Sergio Rossi¹.

Affiliation:

¹ Laboratoire sur les écosystèmes terrestres boréaux, Département des Sciences Fondamentales, Université du Québec à Chicoutimi, 555 boulevard de l'Université, Chicoutimi (QC) G7H2B1, Canada.

² Direction de la recherche forestière Ministère des Forêts, de la Faune et des Parcs, Québec, QC G1P3W8, Canada.

³ Current Affiliation: Forest Research Institute, Université du Québec en Abitibi-Témiscamingue, Rouyn-Noranda, QC, Canada

⁴ Centre de Recerca Ecològica i Aplicacions Forestals (CREAF), Bellaterra, 08193, Barcelona, Spain

⁵ Institució Catalana de Recerca i Estudis Avançats (ICREA), Passeig de Lluís Companys 23, 08010, Barcelona, Spain

* Corresponding author: roberto.silvestro1@uqac.ca (RS)

3.1 Abstract

Background and Aims: Upscaling carbon allocation requires knowledge of the variability at the scales at which data are collected and applied. Trees exhibit different growth rates and timings of wood formation. However, the factors explaining these differences remain undetermined, making samplings and estimations of the growth dynamics a complicated task, habitually based on technical rather than statistical reasons. This study explored the variability in xylem phenology among 159 balsam firs (*Abies balsamea* (L.) Mill.).

Methods: Wood microcores were collected weekly from April to October 2018 in a natural stand in Quebec, Canada, to detect cambial activity and wood formation timings. We tested spatial autocorrelation, tree size, and cell production rates as explanatory variables of xylem phenology. We assessed sample size and margin of error for wood phenology assessment at different confidence levels.

Key Results: Xylem formation lasted between 40 and 110 days, producing between 12 and 93 cells. No effect of spatial proximity or size of individuals was detected on the timings of xylem phenology. Trees with larger cell production rates showed a longer growing season, starting xylem differentiation earlier and ending later. A sample size of 23 trees produced estimates of xylem phenology at a confidence level of 95% with a margin of error of one week.

Conclusions: This study highlighted the high variability in the timings of wood formation among trees within an area of 1 km². The correlation between the number of new xylem cells and the growing season length suggests a close connection between the processes of

wood formation and carbon sequestration. However, the causes of the observed differences in xylem phenology remain partially unresolved. We point out the need to carefully consider sample size while assessing xylem phenology to explore the reasons underlying this variability and to allow reliable upscaling of carbon allocation in forests.

Keywords

Boreal forest; Carbon allocation; Cell production; *Abies balsamea*; Tree growth; Tree size; Wood formation; Xylem development; Xylem differentiation, Xylogenesis.

3.2 Introduction

The Intergovernmental Panel on Climate Change and the United Nations through the Paris Agreement recognize the role played by forest ecosystems in achieving climate change mitigation goals (IPCC, 2019; United Nations). By covering 31% of the total land surface (FAO & UNEP, 2020), the forests store 861 ± 66 GtC (Pan et al., 2011) and represent a net carbon sink of 2.1 ± 13 GtC per year (Harris et al., 2021). Plants use most of the assimilated carbon for metabolism and structural biomass (Hartmann et al., 2015). In trees, the largest part of the biomass accumulated is the result of carbon allocation during wood formation (Deslauriers et al., 2016). Considering the crucial role of wood in tackling climate change, it is surprising to see that our understanding of its formation is still largely incomplete.

The need to assess climate-biosphere relationships has led to the development of vegetation models that use physiological and ecological principles to predict changes in the distribution of plant functional types or forest productivity over time (Prentice et al., 2007). Models challenge our understanding of the factors influencing plant distribution or tree growth at regional to global scales (Prentice et al., 2007). Several currently available models still lack an explicit representation of tree-level growth processes (Friend et al., 2019). Plant growth is generally represented as the Net Primary Production (NPP) and determined as the difference between the Gross Primary Production (GPP) and the maintenance respiration. The main limitation of this approach is that NPP lacks a direct quantification of the timings of carbon allocation into the wood and its physiological processes (Cuny et al., 2015). At the intra-annual scale, biomass accumulation in wood occurs after the increase in stem size (Cuny et al., 2015). This lag helps to explain the differences observed between net ecosystem productivity and

changes in tree size at short time scales (Zweifel et al., 2010). But more accurately, this approach to modelling growth has not been perceived as a problem until recently (Friend et al., 2019), given the widespread understanding that plant productivity is limited by the input of C through photosynthesis (i.e., growth is C source-limited). However, evidence that direct restrictions on sink activities and growth processes may occur before those on photosynthesis suggests the need to build growth models in which the demand for carbon plays a leading role (i.e., sink limitation) (Körner, 2015).

At the beginning of the growing season, cambial cells divide, and the new cells undergo differentiation, finally resulting in mature xylem (Rossi et al., 2012). Cells enlarge by stretching the primary walls, then they produce, thicken and lignify secondary walls, and ultimately succumb to programmed cell death (Rossi et al., 2012). Given the importance of wood formation in the process of carbon sequestration from the atmosphere to wood biomass, it is not surprising that climate-growth relationships have gained considerable interest worldwide. Models including xylogenesis are now available and promise to incorporate the intra-annual dynamics of the sink activity of cambium (Friend et al., 2019). However, such models still lack data for their calibration and validation. Xylogenesis provides a picture of wood formation that can be directly used to test hypotheses or calibrate model parameters (Cuny et al., 2013). Modelling xylogenesis would potentially allow reliable wood formation dynamics to be upscaled from tree to stand and, potentially, to ecosystem or biome. However, such a challenge requires answering the unsolved question about the variability in xylogenesis among individuals and the drivers of xylem phenology.

3.2.1 Wood formation: standards and limits

Interest in wood formation dynamics has grown worldwide in the last decades, leading to a substantial increase of studies available in the literature (De Micco et al., 2019). Some standards have emerged, and microcoring and pinning have been adopted as sampling techniques (Gričar et al., 2007; Rossi, Deslauriers, et al., 2006). Most research groups use the same criteria to discriminate between phenological phases of the developing xylem and count cell numbers in conifers or measure the width of the differentiation zones in broadleaves (Martinez del Castillo et al., 2016; Rossi, Deslauriers, et al., 2006). Thanks to these common standards, scientists can obtain comparable data (Rathgeber et al., 2016), thus encouraging global studies to identify general patterns (e.g., Cuny et al., 2015; Huang et al., 2020; Rossi et al., 2016).

Logistical and technical difficulties related to repeated sampling constrain the number of trees under investigation. As a result, the sample size for wood formation is based on a pragmatic decision involving a trade-off among cost, time and convenience (Buttò et al., 2020) rather than assuring an accurate representation of the process. The variability in wood phenology among individuals has been well known since the first pioneer studies (Wodzicki & Zajaczkowski, 1970) and demonstrated in many species (Gričar et al., 2009; Linares et al., 2009; Lupi et al., 2010; Rathgeber et al., 2011; Rossi et al., 2008; Vieira et al., 2014). In some cases, this variability has affected the success of some investigations (e.g., Lupi et al., 2012). Although part of this variability can be related to the genetic differences among individuals, other factors such as tree size and age, and microsite conditions might influence xylem phenology (Lupi et al., 2013). This methodological problem could finally raise doubts over the consistency of the results.

A preliminary assessment of sample size is a crucial step in statistics. Nowadays, most of the studies on wood formation use samples from five individuals (De Micco et al., 2019), although the overall range is usually comprised between one and ten (Deslauriers et al., 2015). To our knowledge, no paper on wood formation in the literature involves sample-size assessment, thus preventing an accurate generalization of the statistical estimations.

Power analysis is a tool for sample-size assessment based on the standard deviation of the population. If the standard deviation is unknown, researchers can estimate it or rely on comparable values available in the literature. As an example, according to the results reported in the literature (Lupi et al., 2010; Rathgeber et al., 2011), we run a power analysis with standard deviations of between 3 and 12 days for the estimated day of the year of the occurrence of cell differentiation. To obtain a margin of error of ± 1 day with a standard deviation of 3, the sample size is estimated to be 37 trees (Figure S3.1). A standard deviation of 12 requires 200 trees to obtain the same margin of error (Figure S3.1). These results are surprisingly high when compared to the sample sizes used in the literature.

This study explores the variability in xylem phenology among 159 trees of balsam fir (*Abies balsamea* (L.) Mill.) sampled weekly in 2018 in natural stands in boreal forest. We assess the variability in wood phenology among trees in an even-aged population by testing the spatial distribution of individuals, their size, and the annual xylem production as explanatory variables for the timings of xylem phenology. We raise the hypothesis that xylem phenology is (1) affected by tree size; (2) spatially heterogeneous within a population; and (3) related to the rate of annual cell production. Once variability is assessed and explained, we quantify the thresholds of sample sizes that can be used as a

guideline for sampling during the assessment of wood phenology in the field, and for building and calibrating intra-annual growth models.

3.3 Materials and methods

3.3.1 Study area

The study area is located at the Forêt Montmorency in Quebec, Canada (47°16'20'' N, 71°08'20'' W), within the balsam fir-white birch bioclimatic domain (Figure 3.1). According to the Köppen Classification System, the climate type is continental, with a short growing season characterized by cool temperatures and high humidity. Mean annual temperature is 0.4 °C. January is the coldest month with a mean temperature of -15.9 °C. July is the warmest month with a mean temperature of 14.6 °C. Mean annual precipitation is 1422 mm, of which 465 mm falls in the form of snow. Overall, the stands are composed of 80% balsam fir (*Abies balsamea* (L.) Mill.), 10% white birch (*Betula papyrifera* Marsh.), and 10% spruce (*Picea glauca* (Moench) Voss and *Picea mariana* (Mill.) B.S.P.). The study area covers 218 ha that was submitted to clear cuts during 1993-1994. The actual age of the dominant and co-dominant balsam fir stands in this study ranges between 25 and 30 years.

3.3.2 Sampling and data collection

We selected 33 permanent plots of 20 m × 20 m (Figure 3.1). In each plot, we chose 4 to 5 dominant balsam firs with upright stems for a total sampling of 159 trees. Trees with polycormic stems, partially dead crowns, reaction wood or evident damage due to parasites were avoided. For each tree, we recorded height and diameter at breast height (i.e., 1.3 m above the ground).

Wood microcores were collected weekly from April to October 2018 on every tree using a Trephor (Rossi, Anfodillo, et al., 2006). The samples included mature and developing xylem of the current year, the cambial zone and adjacent phloem, and at least one previous

complete tree ring. The microcores were dehydrated through successive immersions in ethanol and d-limonene, embedded in paraffin, cut into 8 μm cross-sections, and stained with cresyl violet acetate (0.16 % in water) (Rossi, Deslauriers, et al., 2006). We discriminated between developing and mature tracheids under visible and polarized light at magnifications of $\times 400$. Cells were counted across three radial rows and classified as (1) cambium, (2) enlarging, (3) wall-thickening and lignifying, or (4) mature (Deslauriers et al., 2003) (Figure 3.2). Cambial cells were characterized by thin cell walls and small radial diameters. The enlargement zone was represented by the absence of glistening under polarized light, which indicates the presence of only primary cell walls. Cells undergoing secondary cell wall formation glistened under polarized light. Cresyl violet acetate reacts with lignin, turning from violet to blue in mature cells. Maturation was reached when the cell walls were entirely blue (Rossi, Deslauriers, et al., 2006) (Figure 3.2).

3.3.3 Variability in xylem phenology

The onset and ending of the developmental phases were calculated and analysed for each tree. The onset and the ending of each cell developmental phase were determined as the date, expressed as the day of the year (DOY) calculated by interpolating two consecutive observations (Deslauriers et al., 2018). Specifically, for each phenological phase, we defined the onset when the first cell was observed, and the ending when we observed the last cell. The duration of the growing season was calculated as the period between the onset of enlargement and ending of wall thickening and lignification. Cell production, i.e., the total number of cells in the tree ring at the end of the growing period, was computed with Gompertz functions using the equation (Rossi et al., 2003):

$$[1] \quad y = \alpha e^{-e^{\beta - \kappa t}}$$

where y represents the number of weekly cumulative cells (enlarging, thickening and lignifying, mature at the time t , represented by a specific day of the year (DOY), α is the upper asymptote representing the final cell production, β the x-axis placement parameter, κ is the growth rate. The relationship between duration and timings of xylem formation and cell production was tested using standardized major axis (SMA) regressions. We used SMA regression as we cannot state which one of the variables is independent. Therefore, the aim is to test the relationship between the variables and estimate the line best describing the scatter.

The relationship between xylem phenology and tree size (i.e., tree height and diameter at breast height) was tested using linear regressions. We measured the distance among experimental plots and individual trees and calculated Moran's index using the inverse of the distance to test for the spatial autocorrelation of xylem phenology and tree size at both plot and tree levels.

3.3.4 The margin of error and minimum sample size

Bootstrapping was performed 10,000 times, during which the mean and standard deviation of each phenological phase were repetitively calculated by randomly resampling the original dataset for sample sizes ranging from 2 to 300 trees. We calculated the Margin of Error (ME), i.e., the degree of error in results obtained by random sampling, on the outputs at different confidence levels (CL) according to

$$[2] \quad ME = t * SD$$

Where t (critical value) represents the two-tailed t-value for a given confidence level (i.e., from 70 to 99%) at a degree of freedom of $n-1$, and SD represents the standard deviation of the bootstrapped mean values (Moore et al., 2012).

The margin of error for a given parameter expresses the maximum expected difference between the true population and the sample estimate. We obtained the minimum sample size for each phenological phase for a desired margin of error of $\pm 1 - 5$ days at 70 - 99% confidence levels. We defined the minimum sample size as the minimum number of sample trees to meet an expected confidence level and margin of error for each phenological phase. All statistics were performed with R version 3.6.1 (R Developmental Core Team 2015).

3.4 Results

3.4.1 Timings of xylogenesis

The dormant cambium was composed of 3-5 narrow cells (Figure 3.3). Only cell division occurred at the onset of the growing season (i.e., beginning of May), and the cambial zone rapidly increased. The cells produced by the cambium moved into the phase of cell enlargement at the beginning of June. When the division rate slowed down (i.e., mid-June), the cambial zone began to narrow as the rate of cell differentiation was faster than cell division, and the number of enlarging cells increased to 7.5 ± 3.7 on June 26th (Figure 3.3). The first wall-thickening cells were observed in mid-June, reaching 10.4 ± 4.8 on July 10th (Figure 3.3). The first mature cells were observed at the beginning of July, reaching 42.4 ± 25.8 mature cells in mid-September.

Overall, xylem phenology described the annual pattern represented by three delayed bell-shaped curves (i.e., cambial, enlarging, and wall thickening cells) and a growing S-shaped curve (i.e., mature cells) (Figure 3.3). These patterns result from the variation in time of the number of xylem cells passing through each differentiation phase. In contrast, the S-shaped curve is related to the gradual accumulation of mature cells in the tree ring.

3.4.2 Variability in xylem phenology

The onset of enlargement occurred from DOY 133 to 184, with 38% of trees showing at least one enlarging cell between DOY 160 and 165 (Figure 3.4). The onset of wall thickening and lignification occurred from DOY 158 to 193. However, 82% of trees showed at least one cell in secondary wall formation between DOY 160 and 175. The first mature cells were observed from DOY 165 to 198, 74% occurring between DOY 175 and 185. Compared to the onset, the ending of cell differentiation exhibited a higher

variability. The enlargement phase ended from DOY 191 to 244, whereas the end of wall thickening and lignification phase was observed between DOY 205 and 266 (Figure 3.4).

The length of the growing season ranged between 40 and 110 days. Cell production, i.e., total number of cells in the tree ring, varied between 12 and 93 cells. The relationships between cell production and the onset and ending of xylem formation were highly significant ($P < 0.001$), with an R^2 of 0.26 and 0.22, respectively (Figure 3.5). The relationship between cell production and both duration of cell enlargement and cell wall thickening and lignification produced significant regressions ($P < 0.001$), with an R^2 of 0.29 and 0.41, respectively (Figure 3.6).

3.4.3 Tree size and spatial variability

Stem diameter at breast height ranged between 58 and 194 mm among the 159 sampled trees (Figure S3.2). Height varied between 4 and 13 m. Both variables had a bell-shaped distribution (Figure S3.2). A total of 61% of trees showed a diameter ranging from 75 to 135 mm, and 68% of trees showed a height ranging from 8 to 12 m (Figure S3.1). Moran's index indicated no spatial autocorrelation among experimental plots for either stem diameter or tree height, while it was significant for cell production (Table S3.1). The Moran's index was significant ($P < 0.001$) among individual trees, producing negative coefficients for stem diameter, tree height and cell production (Table S3.1, Figure S3.3).

No significant relationships were detected between stem diameter and xylem phenology. R^2 of the regressions were low, between 0.002 and 0.0055 ($P > 0.05$) (Table 3.1, Figure S3.4, Figure S3.5). Also, the regressions between height and xylem phenology were non-significant, with R^2 ranging between 0.001 and 0.027 ($P > 0.05$) (Table 3.1, Figure S3.4, Figure S3.5).

The Moran's index calculated for each phenological phase and for either plots or trees was not significant, which indicated the absence of spatial autocorrelation in the timings of the phenological phases (Table 3.2, Figure S3.5). When testing for the autocorrelation among plots, coefficients ranged between -0.043 and -0.014 ($P > 0.05$). The onset of all developmental phases had coefficients ranging between 0.014 and 0.057 ($P > 0.05$). When testing for the autocorrelation among trees, the coefficients ranged between 0.071 and 0.128 ($P > 0.05$, Table 3.2).

3.4.4 The margin of error and sample size

Sample size required to estimate parameters of the population increased at higher confidence levels and lower margins of error (Figure 3.7, Figure 3.8, Table 3.3), allowing reliable parameters of the population to be estimated. The confidence level refers to the percentage of samples expected to include the true population parameter. In this study, considering average values, the sample size ranged from a minimum of 4 trees for a margin of error of ± 5 days at a 70% CL to ~ 300 trees for a margin of error of ± 1 days at a 99% CL (Table 3.3).

Considering average values for each margin of error among phases at a confidence level of 95%, the minimum sample size ranged from 11 (margin of error ± 5 days) to more than 220 (margin of error ± 1 day) trees, with 29 trees being the suitable sample to obtain an estimation of the population at an accuracy of ± 3 days (Figure 3.7 and 3.8, Table 3.3). A sample of 23 trees reaches a confidence interval of 95% and a margin of error of one week (margin of error ranging between ± 3 and ± 4 days).

The sample size required to assess the endings of both enlargement and lignification is bigger than that to determine the beginning of the phenological phases (Table 3.3). This

reflects the abovementioned larger considerable variability among trees observed for the end of cell enlargement and cell-wall thickening.

3.5 Discussion

This study investigated the timings of wood formation in 159 balsam firs from 33 permanent plots in Quebec, Canada. We used a large sample size from even-aged stands to assess the variability among individuals and the factors that could explain this variability. The dynamics of xylem formation have already been described in trees growing under different climatic conditions or characterized by different ages, sizes, and vitalities (Gričar et al., 2009; Linares et al., 2009; Lupi et al., 2010; Rathgeber et al., 2011; Rossi et al., 2008; Vieira et al., 2014). Despite such a vast literature, the causes of the observed differences in xylem phenology and length of the growing season remain partially unresolved. Our findings confirmed that trees of the same age exhibited a wide variation in the xylem formation timings and growing season duration. We confirmed the hypothesis that in boreal forest cell production is a main factor involved in such differences.

3.5.1 Does tree size shape tree growth dynamics?

In this study, the relationships between tree size (i.e., diameter or height) and the timings and duration of xylem formation were not significant. The question of whether size influences xylem development is a long-standing issue. As age and size are intrinsically coupled during tree lifespan, the main problem has historically been how to uncouple these two factors. An attempt to disentangle the effect of size from that of age was realized using grafting techniques (Abdul-Hamid & Mencuccini, 2009; Mencuccini et al., 2007; Mencuccini et al., 2005) or reducing population density by thinning (Martínez-Vilalta et al., 2007). These manipulations demonstrated that photosynthesis and tree growth decline at increasing tree size (Abdul-Hamid & Mencuccini, 2009; Martínez-Vilalta et al., 2007).

However, while there is a general agreement that tree size, and in particular tree height, drives variation of xylem traits (Kašpar et al., 2019; Rosell et al., 2017), its role on xylem phenology remained uncertain (Li et al., 2019; Rossi et al., 2008).

Rossi et al. (2008) observed that xylem phenology is not constant throughout the tree lifespan. Older trees showed shorter periods of cambial activity and xylem cell differentiation. Nevertheless, the older trees considered in that study were also taller and larger; thus, the effect of age was not finally disentangled from tree size. Rathgeber et al. (2011) investigated xylogenesis in trees with the same age and similar height but belonging to different social classes. Wood formation started earlier, stopped later, lasted longer, and resulted in higher cell productivity in dominant individuals. However, since dominant trees also showed larger stem diameters and greater annual radial increments, the question of whether either or both factors affected xylem phenology remained unanswered. Li et al. (2013) monitored xylem phenology in two age classes and showed that xylem differentiation started earlier in young trees, resulting in a longer growing season. However, older trees were still also taller and larger. Zeng et al. (2018) selected trees according to their size and age, observing that small-young pines exhibited earlier cambial reactivation and later end of cell differentiation compared to big-old pines. However, these differences were not confirmed in junipers of different sizes but similar ages. The hypothesis that xylem phenology is size-dependent could not be entirely rejected. Still, results suggested that age plays an important role in the timings and duration of xylem formation.

Our sample is represented by an even-aged population with individuals of different sizes. No significant effect of stem size was observed on the timings of xylem formation, suggesting that the differences in dynamics of xylem formation detected in the previous

studies resulted from an age effect or other factors (e.g., genetics, microsite, competition) not explicitly considered. Our results suggest that tree selection for tree growth dynamics may ignore the factor size when individuals have the same age and dominance. Senescence, the progressive loss of function accompanied by decreasing fertility and increasing mortality with advancing age (Kirkwood & Austad, 2000), in the previous studies emerged as an important factor in xylem phenology. This loss of function would also affect carbon sequestration at the stand level, which is a complex function of tree age (Kowalski et al., 2004). This forest ecosystem effect results from a less efficient metabolism in old trees that leads to reduced growth (Bond-Lamberty et al., 2004; Campbell et al., 2004). Assuming that the differences in dynamics of xylem formation detected in the previous studies result from senescence, likely a function of a less efficient metabolism, it seems worthwhile to further explore the question to solve the chicken-egg dilemma in the relationship between phenological timing and C demand.

3.5.2 Should we sample closely located trees?

Xylem phenology is spatially heterogeneous. The variability has a similar magnitude within and between plots. Consequently, no spatial autocorrelation was detected by our analyses. Similar results were observed by Liang and Schwartz (2009) on the timings of bud phenology in a similar experimental design. Therefore, our results are not surprising given the synchronism between primary and secondary growth (Buttó et al., 2021; Klein et al., 2016). The spatial variability could reflect genetic differences within a population. The natural variation in phenology allows a part of the population to endure unfavourable climatic events and increases survival under changing conditions (Guo et al., 2021; Silvestro et al., 2019). However, variability in phenology is also reported among clones, i.e., individuals with the same genotype (Deslauriers et al., 2009). Moreover, a part of the

observed variation is the consequence of heterogeneous growth along the circumference of the stem (Lupi et al., 2013).

Contrary to phenological timings, we highlighted a significant spatial autocorrelation in the annual cell production. This result suggests that growth rates, and consequently cell production, are not exclusively dependent on the corresponding wood phenology and growing season length. Indeed, other studies have pointed out the plasticity and the complex interactions underlying the dynamic of wood formation in response to temperature (Cuny et al., 2019) and water availability (Pasho et al., 2012), factors that could likely play a role also at microsite scale.

The variation among trees is a scale issue in ecology, related to landscape and ecosystem patterns over time and space (Levin, 1992; Wu & Li, 2006). Our results show that while studying xylem formation dynamics of a population, the variability among trees assumes a leading role and should be carefully considered. At large scales (e.g., at ecosystem level or along environmental gradients), the variability within the stand seems to be usually lower than those among stands (Buttò et al., 2019; Guo et al., 2021). Nevertheless, at smaller scales (i.e., at population or community level) the variability in phenology among trees assumes a greater relevance even if it lacks spatial autocorrelation. These scale-dependent phenological behaviours therefore need to be considered when setting up an experimental design. Our results suggest that sampling for the determination of xylem formation dynamics may favour trees located in the same plot, given that the variability among individuals has a similar magnitude when compared within and among plots.

3.5.3 Is phenology an issue of carbon sink?

Our results showed that cell production is related to the period of xylogenesis. Trees with higher cell production start xylem differentiation earlier and end later, thus resulting in a longer growing season. Moreover, durations of cell enlargement and cell wall thickening and lignification correlate with cell production. Several authors observed that the larger the amount of xylem produced, the longer the period of wood formation (Gričar et al., 2009; Rathgeber et al., 2011; Thibeault-Martel et al., 2008; Vieira et al., 2014). Cell production is composed of successive phases representing longitudinal data, i.e., a chain of consecutive events (Rossi et al., 2012). Specifically, the timing of onset and the rate of cambial division affect the number of cells in the cambial zone which, in turn, influences the timing of cell differentiation (Lupi et al., 2010; Rossi et al., 2012). In the case of the occurrence of water deficit during the growing season, individual growth rate assumes a leading control on the annual cell production (Ren et al., 2019). However, if water availability does not represent a constraint, the larger the number of xylem cells in differentiation the longer the time needed to complete their maturation.

Xylogenesis is a crucial component of plant metabolism, and it is likely affected by carbon dynamics at both plant and ecosystem scale. Wall thickening and lignification is the largest carbon sink in trees (Cuny et al., 2015). Thus, if the number of cells produced during cambial activity affects the duration of each cell differentiation phenological phase, carbon availability could also potentially play a role in defining the duration of maturation of cell walls. Xylem cells start differentiation by stretching their thin primary walls (Cuny et al., 2015). Most carbon is allocated during cell-wall thickening (Cuny et al., 2015). The high carbon demand required during formation of the cell walls can

explain the strong correlation between cell production and the duration of this phase during cell differentiation.

3.5.4 Xylogenesis: sample size matters

Our results showed that estimates of xylem phenology at a confidence level of 95% with a margin of error of ± 1 day require samples larger than 100 trees, an excessive effort for a lab. Most studies on wood formation use samples with five individuals (De Micco et al., 2019), with a broad range of between one and ten (Deslauriers et al., 2015). The sample size for xylogenesis is closely related to the scaling, i.e., data collected at one scale and applied at another one (Seidl et al., 2013). Data collection requires resources, and our analyses offer an accurate baseline for upscaling by linking local (i.e., at tree level) with population scale information (i.e., at the stand level). According to our results, the range in sample size reported in the literature (i.e., from 5 to 12 individuals) can reach, at best, a confidence level of 95% with a margin of error of ± 5 days. It is well known that precision and accuracy are, in part, a function of sample size, but cost and time to collect, prepare and analyse wood samples remain a severe constraint in studying wood formation. Therefore, the question defines a trade-off between accuracy (i.e., sample size) and resource investment (i.e., time and costs). According to our results, a sample size of 29 trees may increase the confidence interval substantially at 95% and maintain a low margin of error of ± 3 days. However, a more reasonable sample size in terms of efforts and benefits is a sample of 23 trees reaching a confidence interval of 95% and a margin of error a week (margin of error ranging between ± 4 and ± 3 days), the common sample time span used for sampling in xylem differentiation assessment.

Our estimates on the timings of phenological phases demonstrated that the sample size for spring events is defined by the beginning of cell enlargement, the spring phenological phase with the widest among-trees variability. And, above all, autumnal events require larger samples than spring events for a given accuracy level. This means that using a single sample size that results from averaged value among phenological phases, we can estimate their beginning and the ending with different levels of accuracy (i.e., different margins of error at different confidence levels). In temperate and boreal regions, growth resumption is closely driven by environmental factors, mainly temperature and photoperiod (Linares et al., 2009; Rossi et al., 2012). On the contrary, internal factors, such as the timings of growth reactivation and amount of cell production, are involved in the duration of the growing season and the ending of wood formation, as shown by our findings and previous studies (Li et al., 2013; Rathgeber et al., 2011). The larger the number of xylem cells produced, the longer the time needed to complete cell differentiation. When precise estimates at tree level have marginal importance, a practical solution could be that investigation on xylem formation should consider larger sample sizes for assessing autumnal phenology or gradually increasing the number of samples during the growing season. Even though further exploration is required to confirm this proposal, according to our results, it would allow maintaining a comparable margin of error among the phenological phases.

Estimates of xylem phenology obviously improve with larger sample sizes, as also demonstrated by our results. The literature indicates that experimental designs with more modest sample sizes were able to detect differences among ecosystems or species or along climatic gradients (Antonucci et al., 2017; Antonucci et al., 2019; Buttò et al., 2019; Prislán et al., 2016; Rossi et al., 2016; Zhang et al., 2018). However, some manipulative

experiments on xylogenesis failed to find conclusive relationships between wood formation dynamics and the environmental factors under investigation. Manipulations involved rain exclusion (Belien et al., 2012; Loïc D'Orangeville et al., 2013), soil warming and acceleration of snow melting (Lupi et al., 2012; Repo et al., 2011), nitrogen fertilization (Camargo et al., 2014; L. D'Orangeville et al., 2013; Lupi et al., 2012) or thinning (Lemay et al., 2017; Primicia et al., 2013). These studies used between 3 and 10 trees per group. The lack of significant results could be caused by the small sample size accompanied by the high among-trees variability in xylem phenology and the conservative behavior of wood formation. The variability among trees (i.e., within a population) can vary according to a number of factors (e.g., species, tree age, the social status of the trees). For this reason, a preliminary assessment of the variability among trees can help in improving the accuracy of the results and deepening the knowledge on the factors driving the growth dynamics of a population.

This study highlighted the existence of a high variability in the timings of wood formation among trees within an area of 1 km², although the causes of the observed differences in xylem phenology still remain partially unresolved. The correlation between the growing season length and xylem cell production suggests a close connection between the processes of wood formation and carbon uptake. A deeper analysis of the relationships between carbon source and sink processes could provide new insights to explain the variability in growth dynamics among trees and understanding of the physiological processes driving wood production. This work points out the need to consider sample size while assessing xylem phenology. Considering the huge variability within a population, increasing the sample size is a crucial step to further explore the reasons underlying this variability. Moreover, there is an ever-increasing interest in simulation models, developed

mainly for research purposes in the past, and now applied in forest management planning and decision support. In this context, finding better ways to incorporate variability in growth dynamics and performance among individuals can help to improve the analysis of forest productivity and its changes under a warming climate.

3.5.5 Acknowledgements

This work was conducted and funded as part of the Evap-for project of Ministère des Forêts, de la Faune et des Parcs (Quebec, Canada) (project #142332139). R. Silvestro received the Merit scholarship for international PhD students (PBEEE) assigned by the Fonds de Recherche du Québec - Nature et Technologies (FRQNT). The authors thank L. Papillon, F. Wiseman, J. Monffette, P.-L. Déchêne, M. Rhéaume and V. Néron for technical support, and A. Garside for editing the English text.

3.5.6 Authors contribution

RS, VB, and SR conceived the ideas and designed methodology; JDS and GD administrated the project and the data collection; RS and VB analysed the data; JDS, GD, and IA validate the results, RS led the writing of the manuscript. All authors contributed critically to the drafts and gave final approval for publication.

3.6 Figures

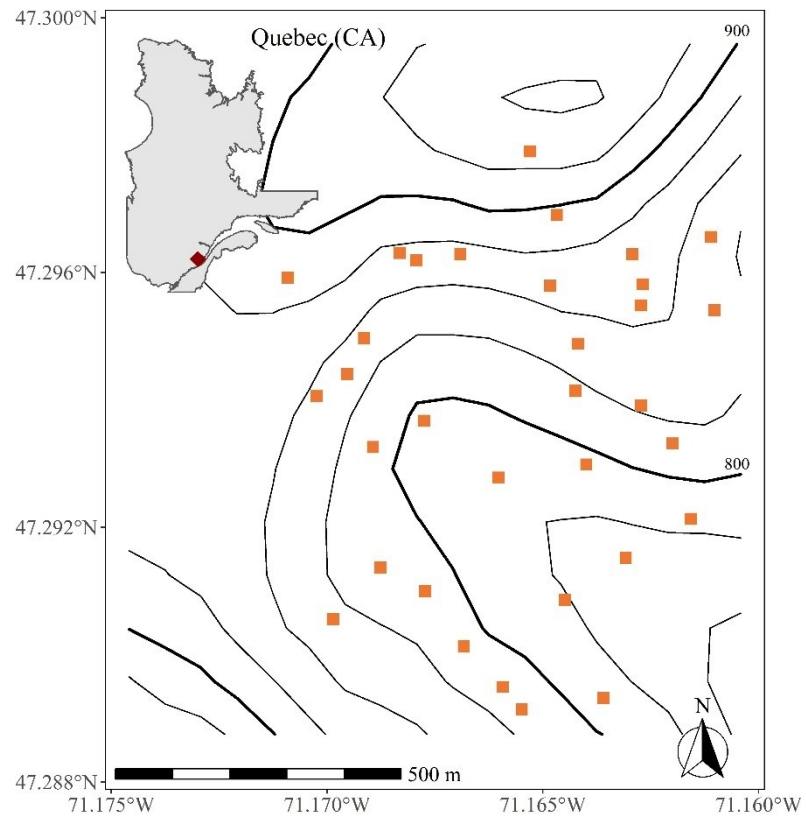


Figure 3.1 Location of the experimental plots in the Montmorency Forest (QC, Canada).

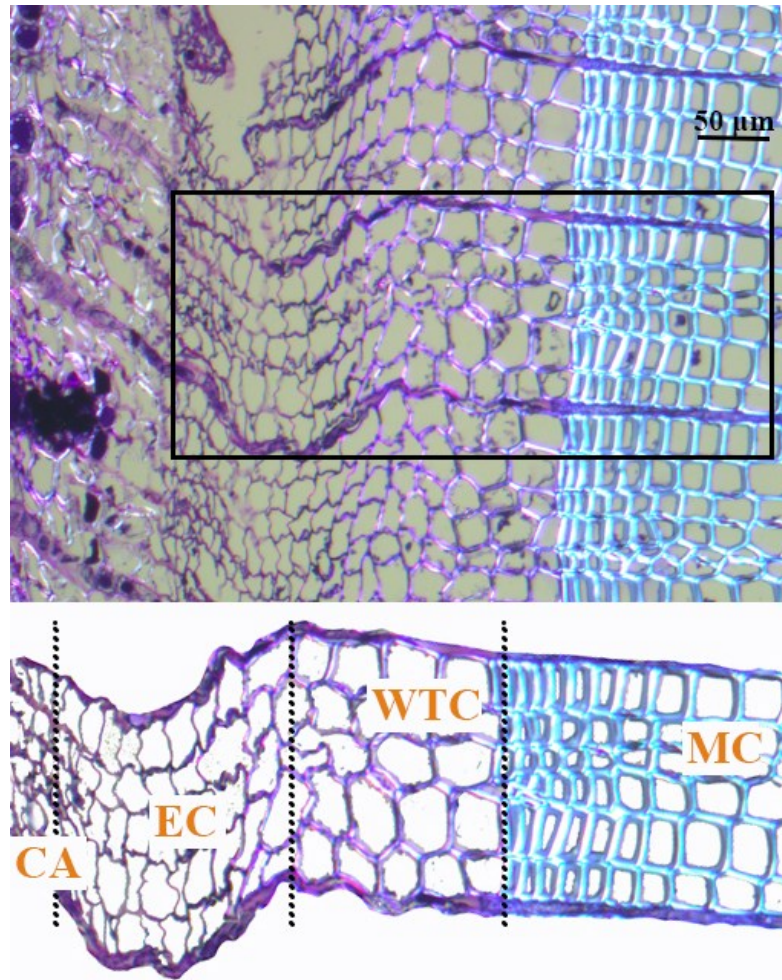


Figure 3.2 Transverse section of a weekly sampled microcore, observed at $\times 400$ magnification, for counting the developing tracheids, and classified as (CA) cambium, (EC) enlarging cells, (WTC) wall-thickening and lignifying cells, and (MC) mature cells of the previous year.

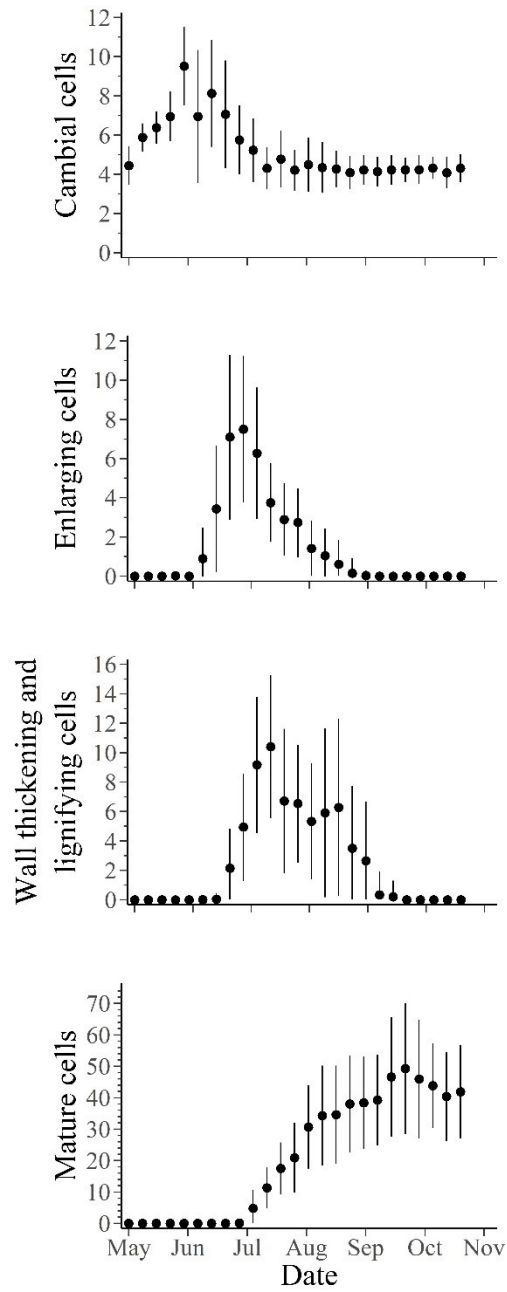


Figure 3.3 Number of cambial, enlarging, wall thickening and lignifying, and mature cells observed in 159 balsam firs during 2018. Dots and bars represent average and standard deviation, respectively.

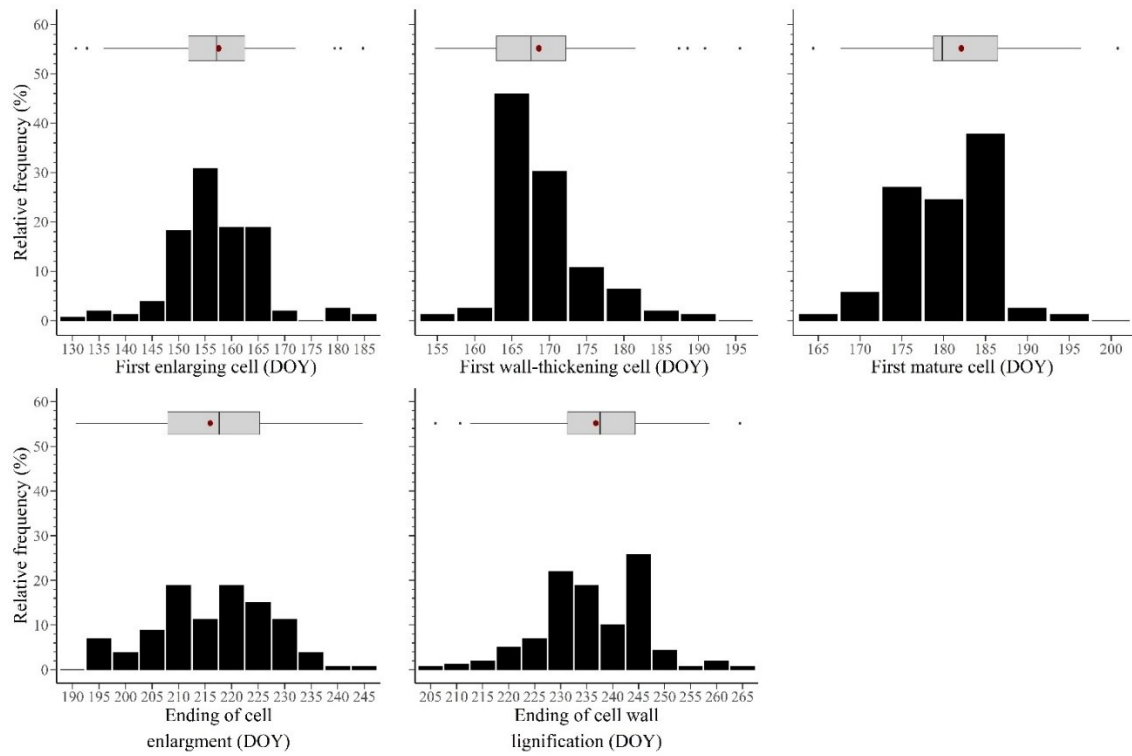


Figure 3.4 Frequency distributions of the phenological dates determined in 159 balsam firs during 2018. Horizontal boxplots represent upper and lower quartiles, and the mean and median are drawn as orange dots and vertical black lines, respectively.

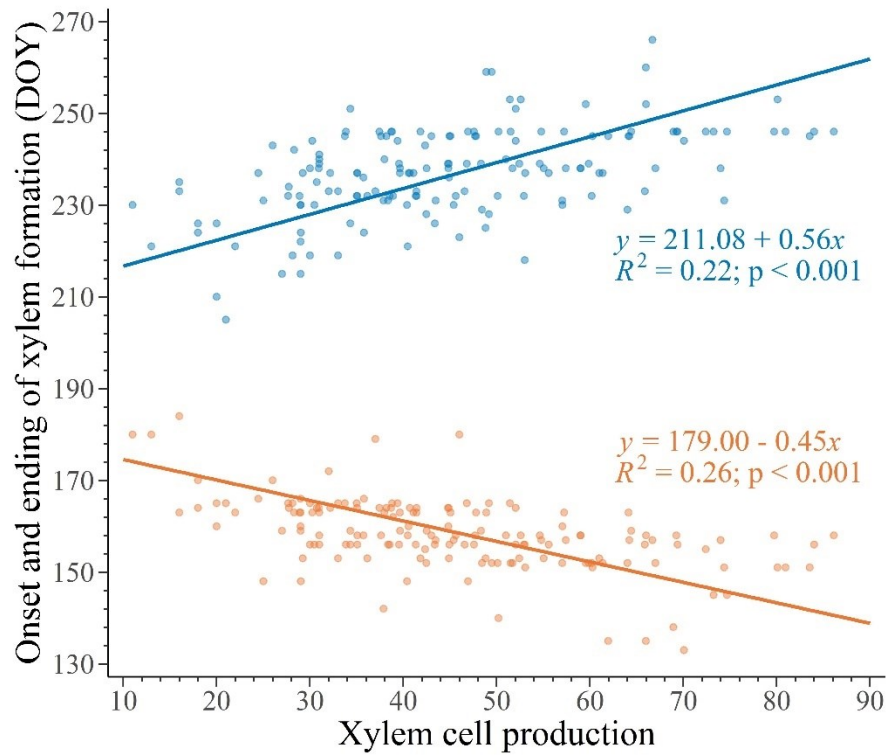


Figure 3.5 Standardized major axis (SMA) regressions among timings of onset (orange dots) and ending (blue dots) of xylem phenology and total number of cells in the tree ring at the end of the growing season in 159 balsam firs at Montmorency forest.

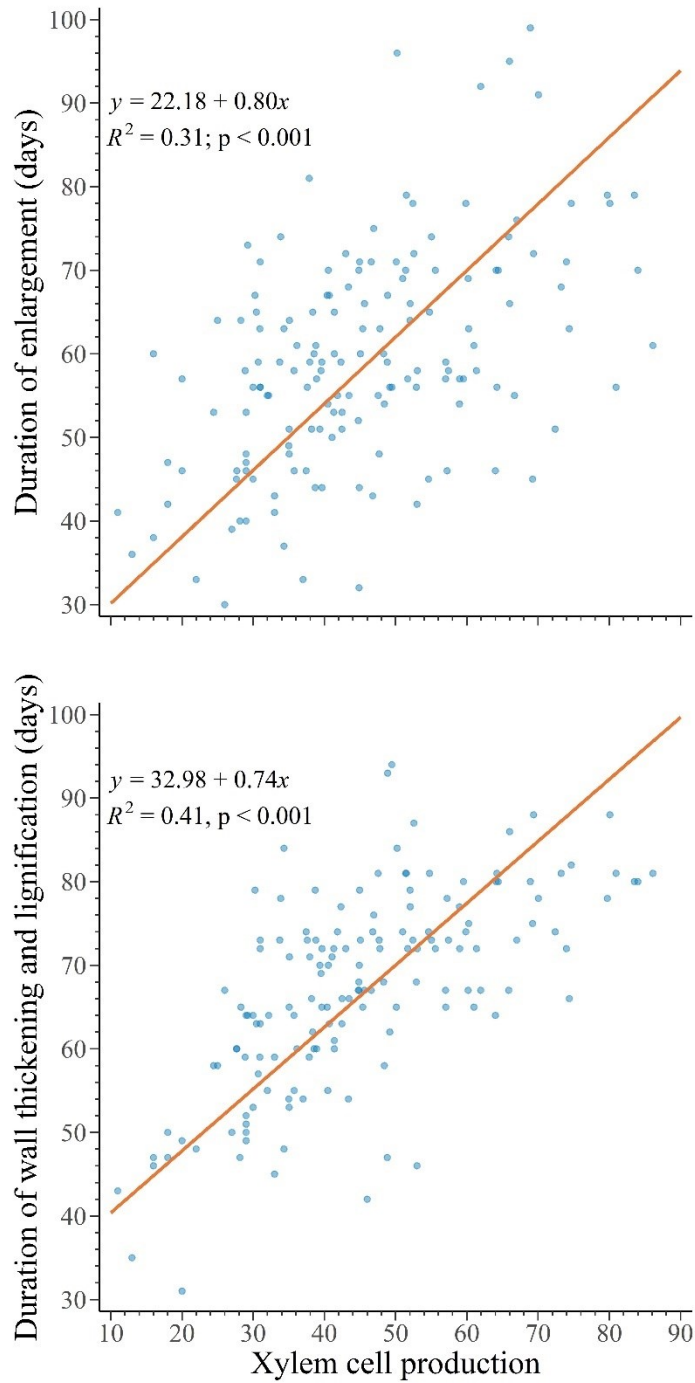


Figure 3.6 Standardized major axis (SMA) regressions among total duration of cell enlargement and cell wall thickening and lignification, and total number of cells in the tree ring at the end of the growing season in 159 balsam firs at Montmorency forest.

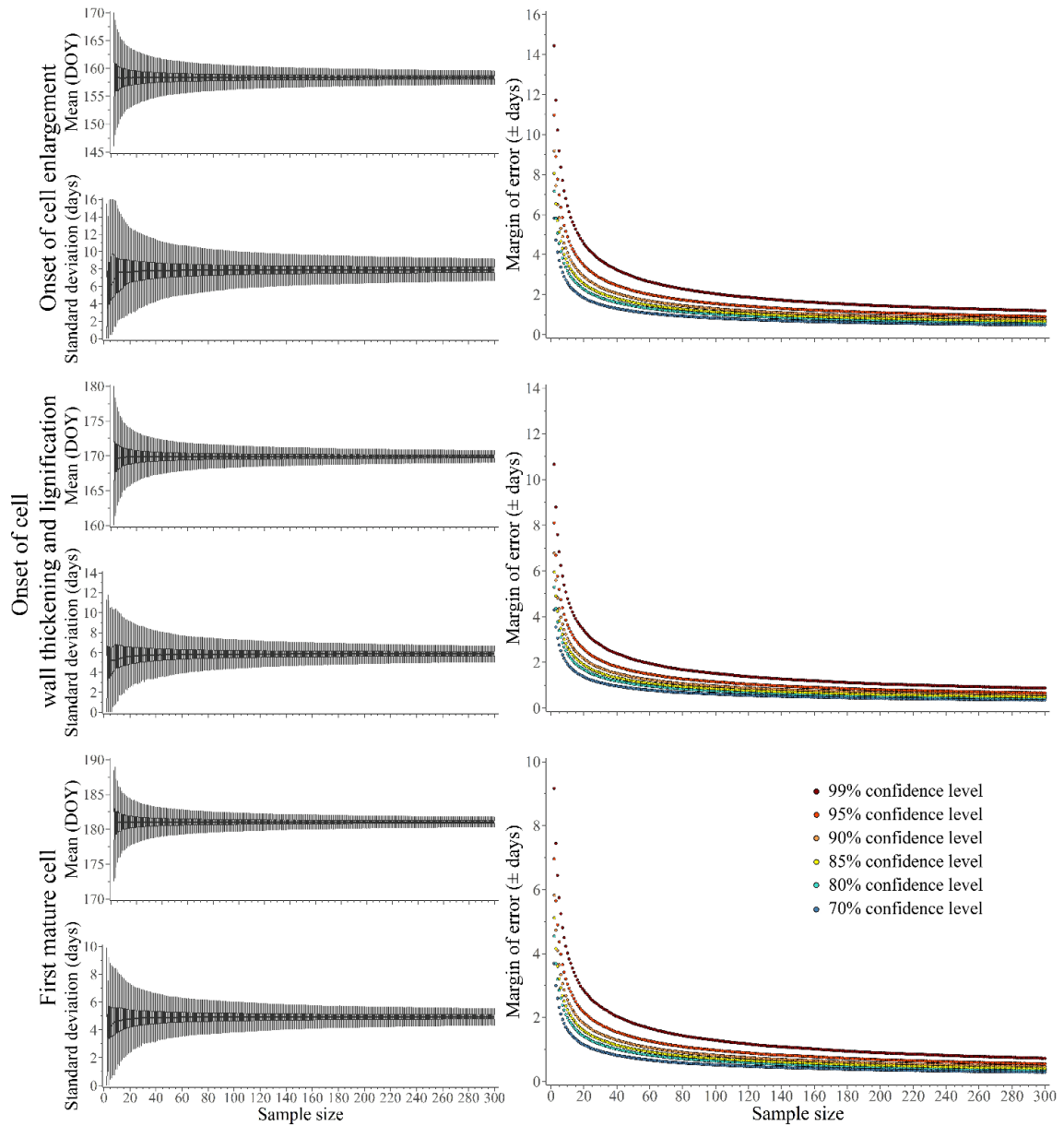


Figure 3.7 Sample size for the onset of xylem formation. Boxplots represent upper and lower quartiles of bootstrapped mean and standard deviation outputs for the onset of enlargement, wall-thickening and first mature cell. The minimum sample size is calculated at different confidence levels and margins of error.

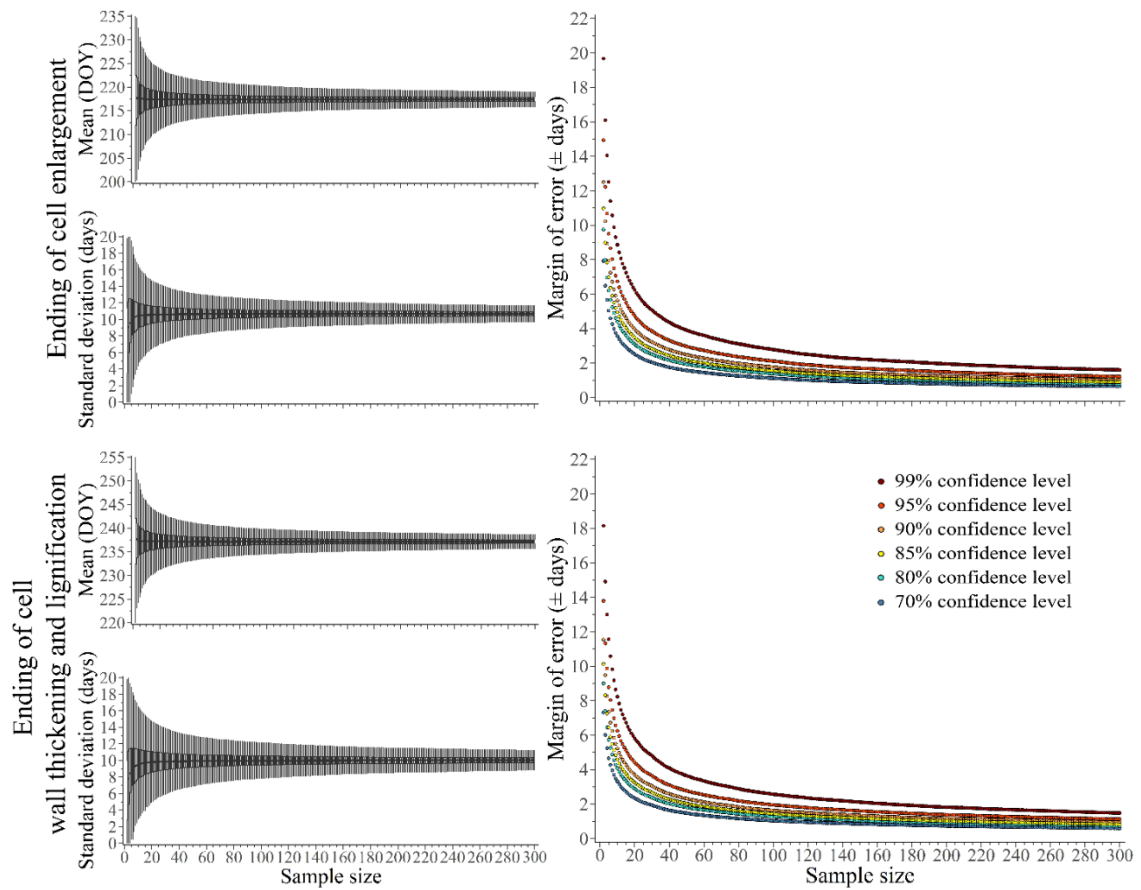


Figure 3.8 Sample size for the ending of xylem formation. Boxplots represent upper and lower quartiles of bootstrapped mean and standard deviation outputs for the ending of enlargement and wall thickening and lignification. The minimum sample size is calculated at different confidence levels and margins of error.

3.7 Tables

Table 3.1 Linear regression between xylem phenology and stem diameter (DHB) and height. The “q” represents the slope, SE the standard error. No significant results were observed.

Phenological phases	DBH		Height	
	R ²	q ± SE	R ²	q ± SE
Onset of enlargement	0.002	-0.011 ± 0.02	0.001	-0.116 ± 0.34
Onset of wall thickening and lignification	0.002	-0.008 ± 0.01	0.011	-0.326 ± 0.25
First mature cell	0.006	-0.011 ± 0.01	0.027	-0.413 ± 0.21
Ending of enlargement	0.055	0.006 ± 0.03	0.009	0.548 ± 0.46
Ending of wall thickening and lignification	0.009	0.028 ± 0.02	0.019	0.715 ± 0.42

Table 3.2 Moran's correlation coefficients testing for the spatial autocorrelation of xylem phenology for experimental plots and individual trees. No significant results were observed ($p < 0.05$). Values indicated as Moran's coefficient and standard deviation.

Phenological phases	Plots	Trees
Onset of enlargement	0.054 ± 0.035	0.099 ± 0.028
Onset of wall thickening and lignification	0.057 ± 0.035	0.109 ± 0.029
Mature cells	0.014 ± 0.035	0.071 ± 0.029
Ending of enlargement	-0.039 ± 0.035	0.071 ± 0.029
End of wall thickening and lignification	-0.030 ± 0.034	0.128 ± 0.029

Table 3.3 Minimum sample size for each phenological phase (both onset and end of enlargement, both onset and end of wall thickening and lignification, and onset of maturation) for each confidence level (CL, 70, 80, 85, 90, 95, and 99%) and each desired margin of error (± 1 , ± 2 , ± 3 , ± 4 , ± 5 days). For average assessment, we used 300 when the value was > 300 .

Phenological phases	Margin of error (\pm days)														
	1	2	3	4	5	1	2	3	4	5	1	2	3	4	5
	CL 70%					CL 80%					CL 85%				
Onset of enlargement	69	18	8	5	3	103	26	12	7	5	130	33	15	9	6
Onset of wall thickening and lignification	37	10	5	3	2	56	15	7	4	3	71	18	9	5	3
First mature cell	27	7	3	2	2	42	10	5	3	2	52	13	6	4	3
Ending of enlargement	122	32	15	8	8	189	47	22	13	8	239	61	27	16	10
Ending of wall thickening and lignification	109	29	13	7	5	165	42	19	11	7	209	52	24	14	9
Average among phases	73	19	9	5	4	111	28	13	8	5	141	35	16	29	6
	CL 90%					CL 95%					CL 99%				
Onset of enlargement	169	43	19	11	7	243	61	27	16	10	>30 0	10 4	47	27	17
Onset of wall thickening and lignification	93	24	11	6	4	132	33	15	9	6	227	57	26	15	10
First mature cell	67	17	8	5	3	96	24	11	6	4	165	42	18	11	7
Ending of enlargement	>30 0	79	33	20	13	>30 0	11 0	49	28	19	>30 0	19 2	87	48	31
Ending of wall thickening and lignification	268	68	30	18	11	>30 0	96	43	25	16	>30 0	16 7	75	42	28
Average among phases	179	46	20	12	8	214	65	29	17	11	258	112	50	29	19

3.8 Annexes

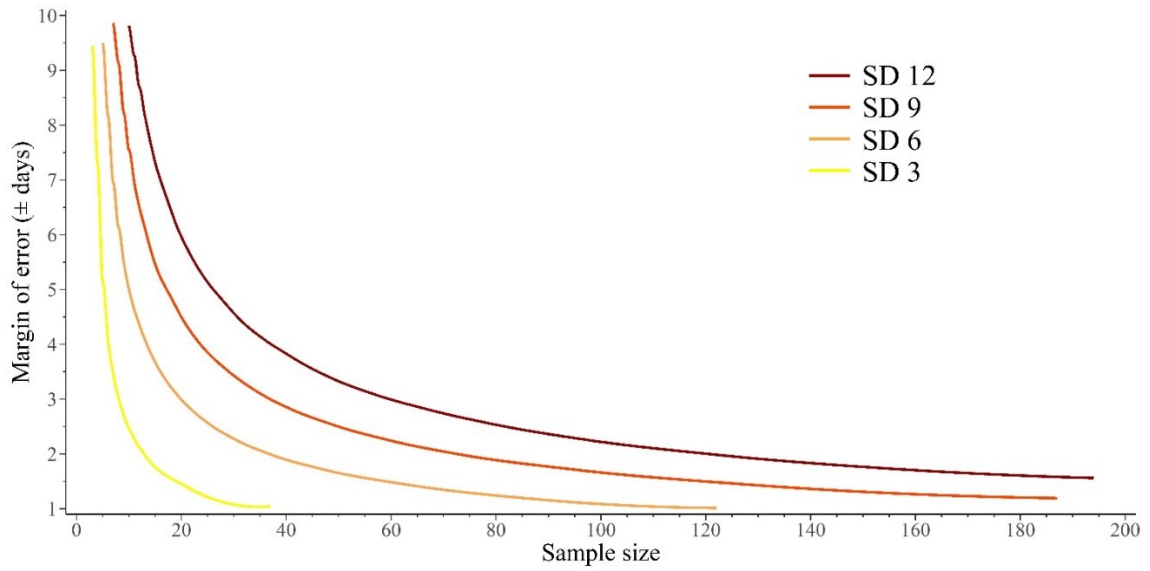


Figure S 3.1 Sample size related to the margin of error according to a range of different standard deviations.

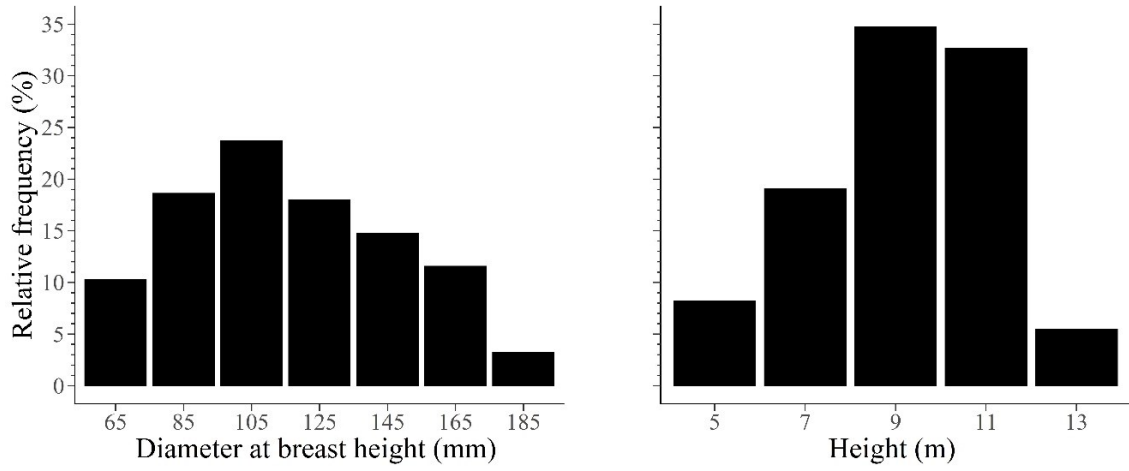


Figure S 3.2 Relative frequency of diameter classes (left) and height classes (right) among the 159 individual trees sampled in Montmorency forest, Quebec, Canada.

Table S 3.1 Moran's correlation coefficients tested for the spatial autocorrelation of diameter at breast height, tree height and xylem cell production for experimental plots and individual trees. Values indicated as Moran's coefficient and standard deviation. * Indicated significant results.

Variables	Plots	Trees
DBH	-0.031 ± 0.035	$-0.006 \pm 0.029^*$
Height	-0.031 ± 0.044	$-0.007 \pm 0.031^*$
Xylem cell production	$-0.032 \pm 0.035^*$	$-0.007 \pm 0.029^*$

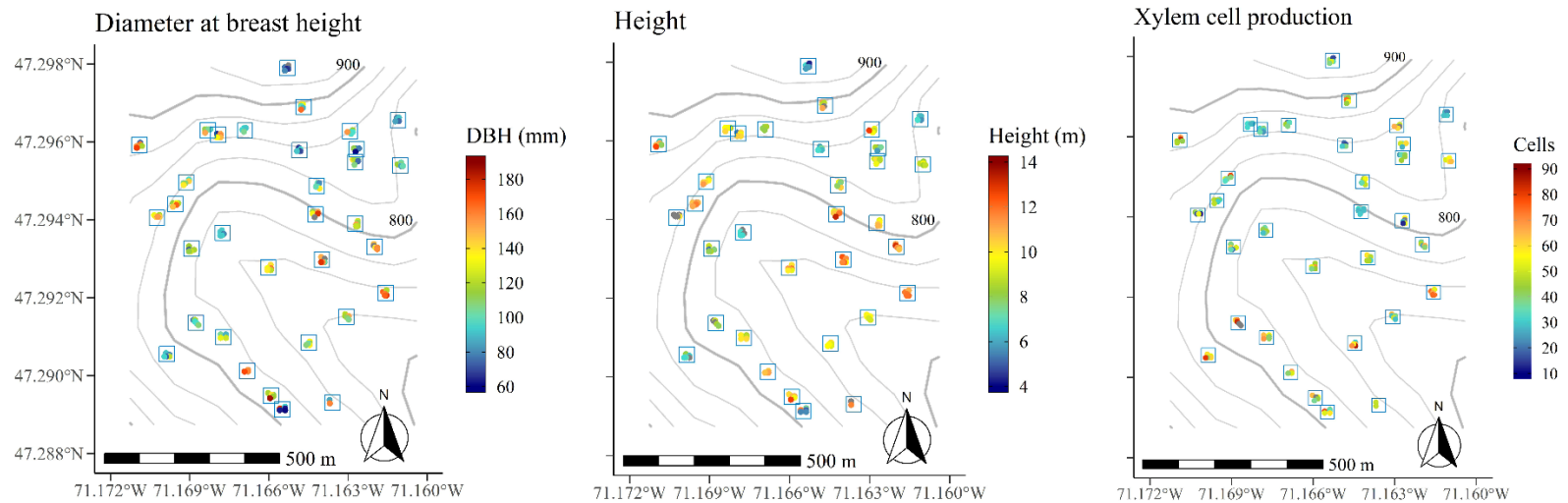


Figure S 3.3 Diameter at breast height, tree height and cell production in 159 trees at Montmorency Forest.

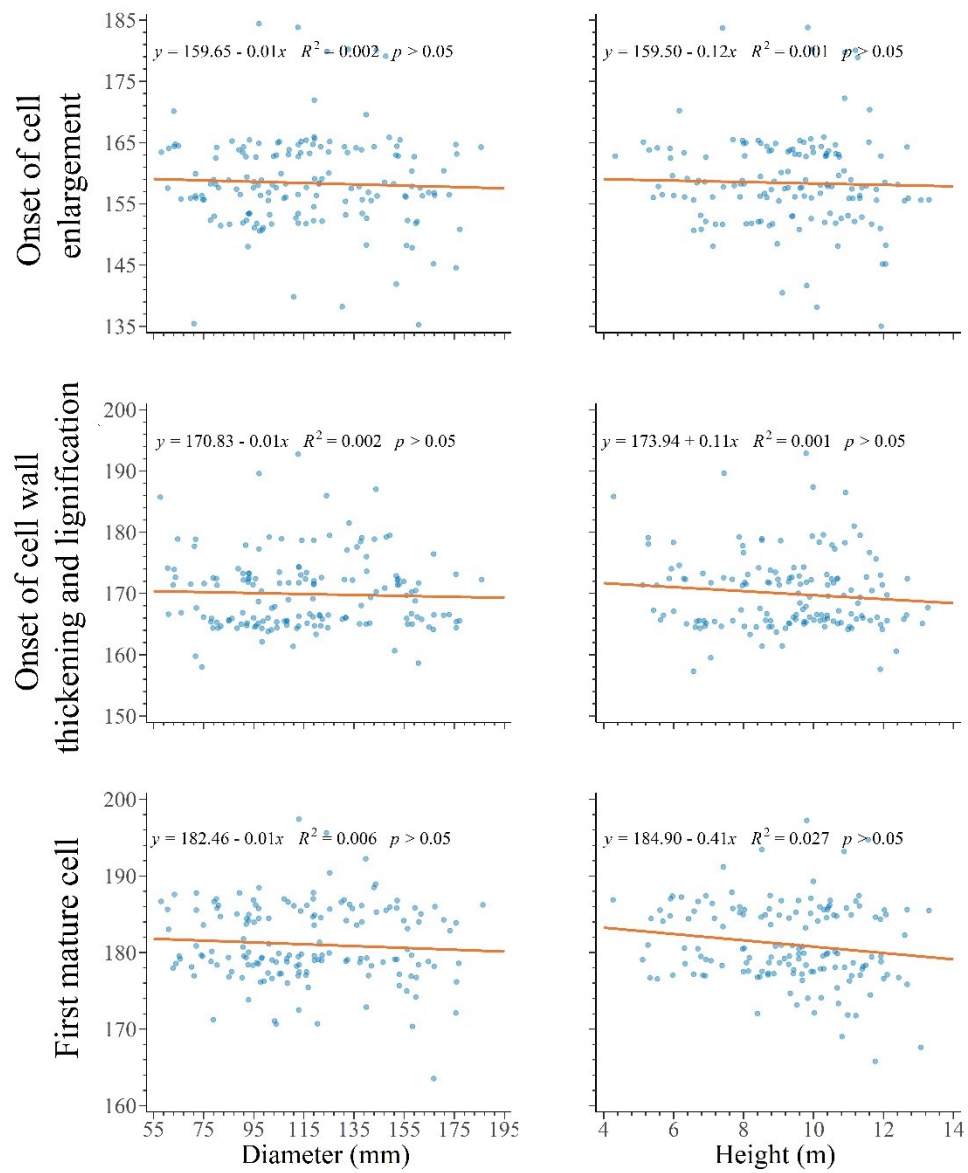


Figure S 3.4 Linear regressions among timings of the onset of xylem developmental phases and stem diameter and tree height in 159 balsam fir at Montmorency forest (QC, Canada).

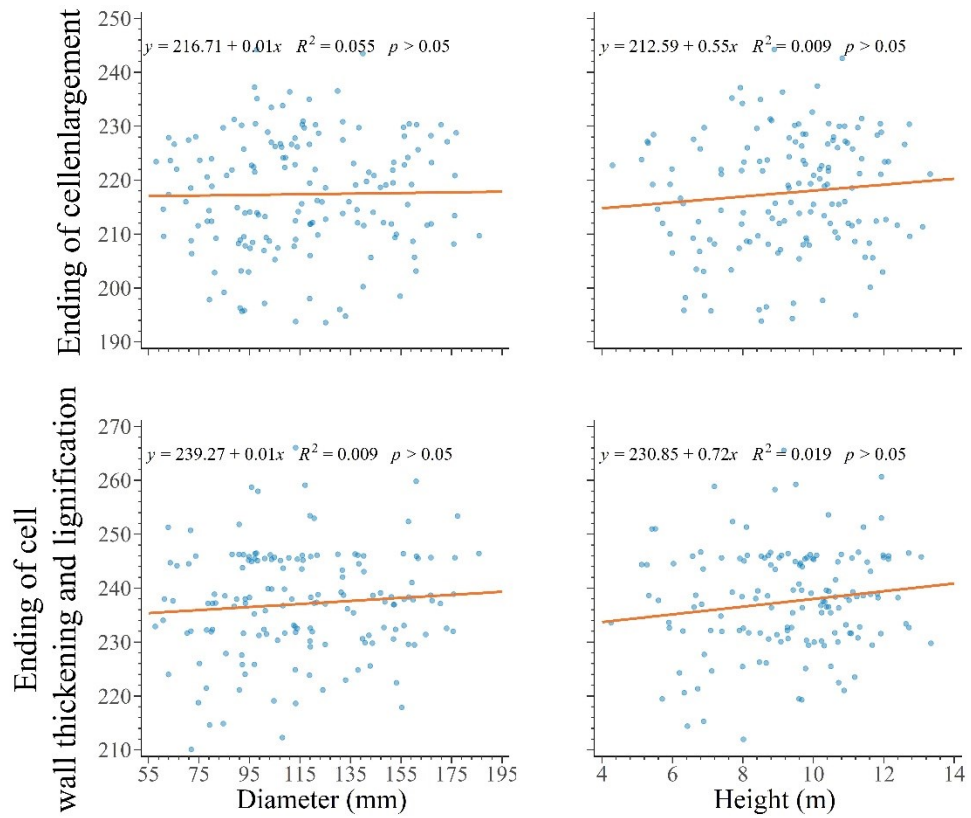


Figure S 3.5 Linear regressions among timings of the ending of xylem developmental phases and stem diameter and tree height in 159 balsam firs at Montmorency forest (QC, Canada).

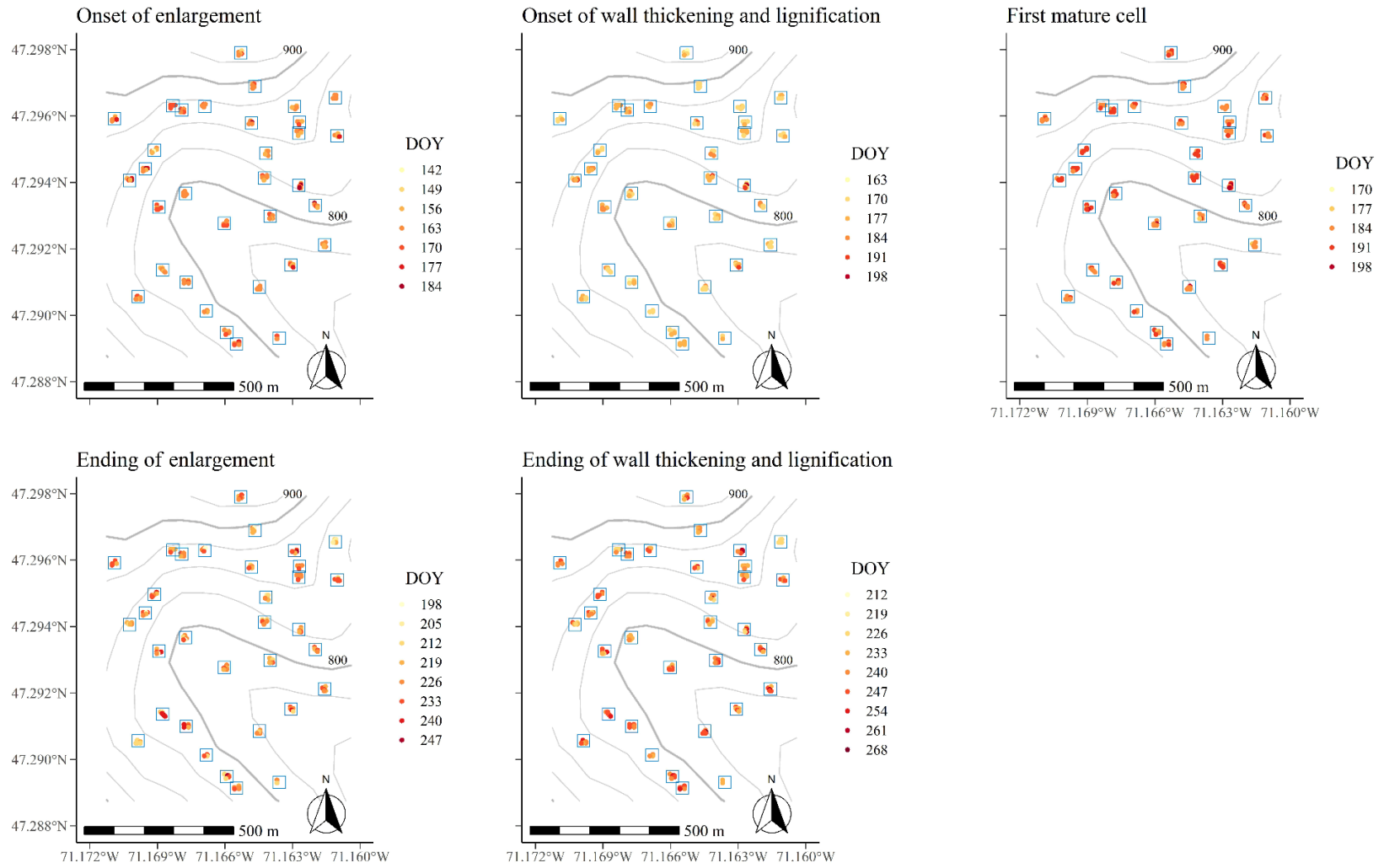


Figure S 3.6 Timings of xylem phenology in 159 trees at Montmorency forest.

3.9 References

- Abdul-Hamid, H., & Mencuccini, M. (2009). Age- and size-related changes in physiological characteristics and chemical composition of *Acer pseudoplatanus* and *Fraxinus excelsior* trees. *Tree Physiology*, 29(1), 27-38. <https://doi.org/10.1093/treephys/tpn001>
- Antonucci, S., Rossi, S., Deslauriers, A., Morin, H., Lombardi, F., Marchetti, M., & Tognetti, R. (2017). Large-scale estimation of xylem phenology in black spruce through remote sensing. *Agricultural and Forest Meteorology*, 233, 92-100. <https://doi.org/10.1016/j.agrformet.2016.11.011>
- Antonucci, S., Rossi, S., Lombardi, F., Marchetti, M., & Tognetti, R. (2019). Influence of climatic factors on silver fir xylogenesis along the Italian Peninsula. *IAWA Journal*, 40(2), 259-275. <https://doi.org/10.1163/22941932-40190222>
- Belien, E., Rossi, S., Morin, H., & Deslauriers, A. (2012). Xylogenesis in black spruce subjected to rain exclusion in the field. *Canadian Journal of Forest Research*, 42(7), 1306-1315. <https://doi.org/10.1139/X2012-095>
- Bond-Lamberty, B., Wang, C., & Gower, S. T. (2004). Net primary production and net ecosystem production of a boreal black spruce wildfire chronosequence. *Global Change Biology*, 10(4), 473-487. <https://doi.org/10.1111/j.1529-8817.2003.0742.x>
- Buttò, V., Khare, S., Drolet, G., Sylvain, J. D., Gennaretti, F., Deslaruiers, A., Morin, H., & Rossi, S. (2021). Regionwide temporal gradients of carbon allocation allow for shoot growth and latewood formation in boreal black spruce. *Global Ecology and Biogeography*, 30(8), 1657-1670. <https://doi.org/10.1111/geb.13340>
- Buttò, V., Rossi, S., Deslauriers, A., & Morin, H. (2019). Is size an issue of time? Relationship between the duration of xylem development and cell traits. *Annals of Botany*, 123(7), 1257-1265. <https://doi.org/10.1093/aob/mcz032>
- Buttò, V., Shishov, V., Tychkov, I., Popkova, M., He, M., Rossi, S., Deslauriers, A., & Morin, H. (2020). Comparing the Cell Dynamics of Tree-Ring Formation Observed in Microcores and as Predicted by the Vaganov–Shashkin Model. *Frontiers in Plant Science*, 11, 1268-1268. <https://doi.org/10.3389/fpls.2020.01268>
- Camargo, E. L. O., Nascimento, L. C., Soler, M., Salazar, M. M., Lepikson-Neto, J., Marques, W. L., Alves, A., Teixeira, P. J. P. L., Mieczkowski, P., Carazzolle, M. F., Martinez, Y., Deckmann, A. C., Rodrigues, J. C., Grima-Pettenati, J., & Pereira, G. A. G. (2014). Contrasting nitrogen fertilization treatments impact xylem gene expression and secondary cell wall lignification in *Eucalyptus*. *BMC Plant Biology*, 14(1), 1-17. <https://doi.org/10.1186/s12870-014-0256-9>

- Campbell, J. L., Sun, O. J., & Law, B. E. (2004). Disturbance and net ecosystem production across three climatically distinct forest landscapes. *Global Biogeochemical Cycles*, 18(4), 1-11. <https://doi.org/10.1029/2004GB002236>
- Cuny, H. E., Fonti, P., Rathgeber, C. B. K., von Arx, G., Peters, R. L., & Frank, D. C. (2019). Couplings in cell differentiation kinetics mitigate air temperature influence on conifer wood anatomy. *Plant Cell and Environment*, 42(4), 1222-1232. <https://doi.org/10.1111/pce.13464>
- Cuny, H. E., Rathgeber, C. B. K., Frank, D., Fonti, P., Makinen, H., Prislan, P., Rossi, S., Del Castillo, E. M., Campelo, F., Vavřčík, H., Camarero, J. J., Bryukhanova, M. V., Jyske, T., Gricar, J., Gryc, V., De Luis, M., Vieira, J., Cufar, K., Kirilyanov, A. V., . . . Fournier, M. (2015). Woody biomass production lags stem-girth increase by over one month in coniferous forests. *Nature Plants*, 1(11), 1-6. <https://doi.org/10.1038/nplants.2015.160>
- Cuny, H. E., Rathgeber, C. B. K., Kiessé, T. S., Hartmann, F. P., Barbeito, I., & Fournier, M. (2013). Generalized additive models reveal the intrinsic complexity of wood formation dynamics. *Journal of Experimental Botany*, 64(7), 1983-1994. <https://doi.org/10.1093/jxb/ert057>
- D'Orangeville, L., Côté, B., Houle, D., & Morin, H. (2013). The effects of throughfall exclusion on xylogenesis of balsam fir. *Tree Physiology*, 33(5), 516-526. <https://doi.org/10.1093/treephys/tpt027>
- D'Orangeville, L., Houle, D., Côté, B., Duchesne, L., & Morin, H. (2013). Increased soil temperature and atmospheric N deposition have no effect on the N status and growth of a mature balsam fir forest. *Biogeosciences*, 10(7), 4627-4639. <https://doi.org/10.5194/bg-10-4627-2013>
- De Micco, V., Carrer, M., Rathgeber, C. B. K., Julio Camarero, J., Voltas, J., Cherubini, P., & Battipaglia, G. (2019). From xylogenesis to tree rings: Wood traits to investigate tree response to environmental changes. *IAWA Journal*, 40(2), 155-182. <https://doi.org/10.1163/22941932-40190246>
- Deslauriers, A., Giovannelli, A., Rossi, S., Castro, G., Fragnelli, G., & Traversi, L. (2009). Intra-annual cambial activity and carbon availability in stem of poplar. *Tree Physiology*, 29(10), 1223-1235. <https://doi.org/10.1093/treephys/tpp061>
- Deslauriers, A., Huang, J. G., Balducci, L., Beaulieu, M., & Rossi, S. (2016). The contribution of carbon and water in modulating wood formation in black spruce saplings. *Plant Physiology*, 170(4), 2072-2084. <https://doi.org/10.1104/pp.15.01525>

- Deslauriers, A., Morin, H., & Begin, Y. (2003). Cellular phenology of annual ring formation of *Abies balsamea* in the Quebec boreal forest (Canada). *Canadian Journal of Forest Research*, 33(2), 190-200. <https://doi.org/10.1139/x02-178>
- Deslauriers, A., Rossi, S., & Liang, E. (2015). Collecting and processing wood microcores for monitoring xylogenesis. In (pp. 417-429). Springer International Publishing. https://doi.org/10.1007/978-3-319-19944-3_23
- Deslauriers, A., Rossi, S., Morin, H., & Krause, C. (2018). Analyse du développement intraannuel des cernes de croissance. In S. Payette & L. Filion (Eds.), (pp. 772-772). Presses de l'Université Laval.
- FAO, & UNEP. (2020). *The State of the World's Forests 2020. Forests, biodiversity and people* (978-92-5-132419-6). <http://www.fao.org/documents/card/en/c/ca8642en>
- Friend, A. D., Eckes-Shephard, A. H., Fonti, P., Rademacher, T. T., Rathgeber, C. B. K., Richardson, A. D., & Turton, R. H. (2019). On the need to consider wood formation processes in global vegetation models and a suggested approach. *Annals of Forest Science*, 76(2), 49-49. <https://doi.org/10.1007/s13595-019-0819-x>
- Gričar, J., Krže, L., & Čufar, K. (2009). Number of cells in xylem, phloem and dormant cambium in silver fir (*Abies alba*), in trees of different vitality. *IAWA Journal*, 30(2), 121-133. <https://doi.org/10.1163/22941932-90000208>
- Gričar, J., Zupančič, M., Čufar, K., & Oven, P. (2007). Wood formation in Norway spruce (*Picea abies*) studied by pinning and intact tissue sampling method. *Wood Research*, 52(2), 1-10.
- Guo, X., Klisz, M., Puchałka, R., Silvestro, R., Faubert, P., Belien, E., Huang, J., & Rossi, S. (2021). Common-garden experiment reveals clinal trends of bud phenology in black spruce populations from a latitudinal gradient in the boreal forest. *Journal of Ecology*, 1365-2745.13582. <https://doi.org/10.1111/1365-2745.13582>
- Harris, N. L., Gibbs, D. A., Baccini, A., Birdsey, R. A., de Bruin, S., Farina, M., Fatoyinbo, L., Hansen, M. C., Herold, M., Houghton, R. A., Potapov, P. V., Suarez, D. R., Roman-Cuesta, R. M., Saatchi, S. S., Slay, C. M., Turubanova, S. A., & Tyukavina, A. (2021). Global maps of twenty-first century forest carbon fluxes. *Nature Climate Change*, 11(3), 234-240. <https://doi.org/10.1038/s41558-020-00976-6>
- Hartmann, H., McDowell, N. G., & Trumbore, S. (2015). Allocation to carbon storage pools in Norway spruce saplings under drought and low CO₂. *Tree Physiology*, 35(3), 243-252. <https://doi.org/10.1093/treephys/tpv019>

- Huang, J. G., Ma, Q., Rossi, S., Biondi, F., Deslauriers, A., Fonti, P., Liang, E., Mäkinen, H., Oberhuber, W., Rathgeber, C. B. K., Tognetti, R., Treml, V., Yang, B., Zhang, J. L., Antonucci, S., Bergeron, Y., Julio Camarero, J., Campelo, F., Cufar, K., . . . Ziaco, E. (2020). Photoperiod and temperature as dominant environmental drivers triggering secondary growth resumption in Northern Hemisphere conifers. *Proceedings of the National Academy of Sciences of the United States of America*, 117(34), 20645-20652. <https://doi.org/10.1073/pnas.2007058117>
- IPCC. (2019). *Climate Change and Land: an IPCC special report on climate change, desertification, land degradation, sustainable land management, food security, and greenhouse gas fluxes in terrestrial ecosystems*. [P.R. Shukla, J. Skea, E. Calvo Buendia, V. Masson-Delmo.
- Kašpar, J., Anfodillo, T., & Treml, V. (2019). Tree size mostly drives the variation of xylem traits at the treeline ecotone. *Trees - Structure and Function*, 33(6), 1657-1665. <https://doi.org/10.1007/s00468-019-01887-6>
- Kirkwood, T. B. L., & Austad, S. N. (2000). Why do we age? *Nature*, 408(6809), 233-238. <https://doi.org/10.1038/35041682>
- Klein, T., Vitasse, Y., & Hoch, G. (2016). Coordination between growth, phenology and carbon storage in three coexisting deciduous tree species in a temperate forest. *Tree Physiology*, 36(7), 847-855. <https://doi.org/10.1093/treephys/tpw030>
- Körner, C. (2015). Paradigm shift in plant growth control. *Current Opinion in Plant Biology*, 25, 107-114. <https://doi.org/10.1016/J.PBI.2015.05.003>
- Kowalski, A. S., Loustau, D., Berbigier, P., Manca, G., Tedeschi, V., Borghetti, M., Valentini, R., Kolari, P., Berninger, F., Rannik, Ü., Hari, P., Rayment, M., Mencuccini, M., Moncrieff, J., & Grace, J. (2004). Paired comparisons of carbon exchange between undisturbed and regenerating stands in four managed forest in Europe. *Global Change Biology*, 10(10), 1707-1723. <https://doi.org/10.1111/j.1365-2486.2004.00846.x>
- Lemay, A., Krause, C., Rossi, S., & Achim, A. (2017). Xylogenesis in stems and roots after thinning in the boreal forest of Quebec, Canada. *Tree Physiology*, 37(11), 1554-1563. <https://doi.org/10.1093/treephys/tpx082>
- Levin, S. A. (1992). The problem of pattern and scale in ecology. *Ecology*, 73(6), 1943-1967. <https://doi.org/10.2307/1941447>
- Li, X., Liang, E., Gričar, J., Prislan, P., Rossi, S., & Čufar, K. (2013). Age dependence of xylogenesis and its climatic sensitivity in Smith fir on the south-eastern Tibetan Plateau. *Tree Physiology*, 33(1), 48-56. <https://doi.org/10.1093/treephys/tps113>

- Li, X., Rossi, S., & Liang, E. (2019). The onset of xylogenesis in Smith fir is not related to outer bark thickness. *American Journal of Botany*, *106*(10), 1386-1391. <https://doi.org/10.1002/ajb2.1360>
- Liang, L., & Schwartz, M. D. (2009). Landscape phenology: An integrative approach to seasonal vegetation dynamics. *Landscape Ecology*, *24*(4), 465-472. <https://doi.org/10.1007/s10980-009-9328-x>
- Linares, J. C., Camarero, J. J., & Carreira, J. A. (2009). Plastic responses of *Abies pinsapo* xylogenesis to drought and competition. *Tree Physiology*, *29*(12), 1525-1536. <https://doi.org/10.1093/treephys/tpp084>
- Lupi, C., Morin, H., Deslauriers, A., & Rossi, S. (2010). Xylem phenology and wood production: Resolving the chicken-or-egg dilemma. *Plant, Cell and Environment*, *33*(10), 1721-1730. <https://doi.org/10.1111/j.1365-3040.2010.02176.x>
- Lupi, C., Morin, H., Deslauriers, A., Rossi, S., & Houle, D. (2012). Increasing nitrogen availability and soil temperature: Effects on xylem phenology and anatomy of mature black spruce. *Canadian Journal of Forest Research*, *42*(7), 1277-1288. <https://doi.org/10.1139/X2012-055>
- Lupi, C., Rossi, S., Vieira, J., Morin, H., & Deslauriers, A. (2013). Assessment of xylem phenology: A first attempt to verify its accuracy and precision. *Tree Physiology*, *34*(1), 87-93. <https://doi.org/10.1093/treephys/tpt108>
- Martínez-Vilalta, J., Vanderklein, D., & Mencuccini, M. (2007). Tree height and age-related decline in growth in Scots pine (*Pinus sylvestris* L.). *Oecologia*, *150*(4), 529-544. <https://doi.org/10.1007/s00442-006-0552-7>
- Martinez del Castillo, E., Longares, L. A., Gričar, J., Prislan, P., Gil-Pelegrín, E., Čufar, K., & de Luis, M. (2016). Living on the edge: Contrasted wood-formation dynamics in *Fagus sylvatica* and *Pinus sylvestris* under mediterranean conditions. *Frontiers in Plant Science*, *7*(MAR2016), 370-370. <https://doi.org/10.3389/fpls.2016.00370>
- Mencuccini, M., Martínez-Vilalta, J., Hamid, H. A., Korakaki, E., & Vanderklein, D. (2007). Evidence for age- And size-mediated controls of tree growth from grafting studies. *Tree Physiology*, *27*(3), 463-473. <https://doi.org/10.1093/treephys/27.3.463>
- Mencuccini, M., Martínez-Vilalta, J., Vanderklein, D., Hamid, H. A., Korakaki, E., Lee, S., & Michiels, B. (2005). Size-mediated ageing reduces vigour in trees. *Ecology Letters*, *8*(11), 1183-1190. <https://doi.org/10.1111/j.1461-0248.2005.00819.x>

- Moore, D. S., McCabe, G. P., & Craig, B. A. (2012). *Introduction to the Practice of Statistics* (Seventh ed.). W.H. Freeman and Company.
- Pan, Y., Birdsey, R. A., Fang, J., Houghton, R., Kauppi, P. E., Kurz, W. A., Phillips, O. L., Shvidenko, A., Lewis, S. L., Canadell, J. G., Ciais, P., Jackson, R. B., Pacala, S. W., McGuire, A. D., Piao, S., Rautiainen, A., Sitch, S., & Hayes, D. (2011). A large and persistent carbon sink in the world's forests. *Science*, 333(6045), 988-993. <https://doi.org/10.1126/science.1201609>
- Pasho, E., Camarero, J. J., & Vicente-Serrano, S. M. (2012). Climatic impacts and drought control of radial growth and seasonal wood formation in *Pinus halepensis*. *Trees - Structure and Function*, 26(6), 1875-1886. <https://doi.org/10.1007/s00468-012-0756-x>
- Prentice, I. C., Bondeau, A., Cramer, W., Harrison, S. P., Hickler, T., Lucht, W., Sitch, S., Smith, B., & Sykes, M. T. (2007). Dynamic Global Vegetation Modeling: Quantifying Terrestrial Ecosystem Responses to Large-Scale Environmental Change. In (pp. 175-192). https://doi.org/10.1007/978-3-540-32730-1_15
- Primicia, I., Camarero, J. J., Imbert, J. B., & Castillo, F. J. (2013). Effects of thinning and canopy type on growth dynamics of *Pinus sylvestris*: Inter-annual variations and intra-annual interactions with microclimate. *European Journal of Forest Research*, 132(1), 121-135. <https://doi.org/10.1007/s10342-012-0662-1>
- Prislan, P., Gričar, J., de Luis, M., Novak, K., Del Castillo, E. M., Schmitt, U., Koch, G., Štrus, J., Mrak, P., Žnidarič, M. T., & Čufar, K. (2016). Annual cambial rhythm in *Pinus halepensis* and *Pinus sylvestris* as indicator for climate adaptation. *Frontiers in Plant Science*, 7(DECEMBER2016). <https://doi.org/10.3389/fpls.2016.01923>
- Rathgeber, C. B. K., Cuny, H. E., & Fonti, P. (2016). Biological basis of tree-ring formation: A crash course. *Frontiers in Plant Science*, 7(MAY2016), 734-734. <https://doi.org/10.3389/fpls.2016.00734>
- Rathgeber, C. B. K., Rossi, S., & Bontemps, J. D. (2011). Cambial activity related to tree size in a mature silver-fir plantation. *Annals of Botany*, 108(3), 429-438. <https://doi.org/10.1093/aob/mcr168>
- Ren, P., Ziaco, E., Rossi, S., Biondi, F., Prislan, P., & Liang, E. (2019). Growth rate rather than growing season length determines wood biomass in dry environments. *Agricultural and Forest Meteorology*, 271, 46-53. <https://doi.org/10.1016/j.agrformet.2019.02.031>
- Repo, T., Roitto, M., & Sutinen, S. (2011). Does the removal of snowpack and the consequent changes in soil frost affect the physiology of Norway spruce needles?

Environmental and Experimental Botany, 72(3), 387-396.
<https://doi.org/10.1016/j.envexpbot.2011.04.014>

- Rosell, J. A., Olson, M. E., & Anfodillo, T. (2017). Scaling of Xylem Vessel Diameter with Plant Size: Causes, Predictions, and Outstanding Questions. *Current Forestry Reports*, 3(1), 46-59. <https://doi.org/10.1007/s40725-017-0049-0>
- Rossi, S., Anfodillo, T., Čufar, K., Cuny, H. E., Deslauriers, A., Fonti, P., Frank, D., Gričar, J., Gruber, A., Huang, J. G., Jyske, T., Kašpar, J., King, G., Krause, C., Liang, E., Mäkinen, H., Morin, H., Nöjd, P., Oberhuber, W., . . . Treml, V. (2016). Pattern of xylem phenology in conifers of cold ecosystems at the Northern Hemisphere. *Global Change Biology*, 22(11), 3804-3813. <https://doi.org/10.1111/gcb.13317>
- Rossi, S., Anfodillo, T., & Menardi, R. (2006). Trephor: A new tool for sampling microcores from tree stems. *IAWA Journal*, 27(1), 89-97. <https://doi.org/10.1163/22941932-90000139>
- Rossi, S., Deslauriers, A., & Anfodillo, T. (2006). Assessment of cambial activity and xylogenesis by microsampling tree species: An example at the Alpine timberline. *IAWA Journal*, 27(4), 383-394. <https://doi.org/10.1163/22941932-90000161>
- Rossi, S., Deslauriers, A., Anfodillo, T., & Carrer, M. (2008). Age-dependent xylogenesis in timberline conifers. *New Phytologist*, 177(1), 199-208. <https://doi.org/10.1111/j.1469-8137.2007.02235.x>
- Rossi, S., Deslauriers, A., & Morin, H. (2003). Application of the Gompertz equation for the study of xylem cell development. *Dendrochronologia*, 21(1), 33-39. <https://doi.org/10.1078/1125-7865-00034>
- Rossi, S., Morin, H., & Deslauriers, A. (2012). Causes and correlations in cambium phenology: towards an integrated framework of xylogenesis. *Journal of Experimental Botany*, 63(5), 2117-2126. <https://doi.org/10.1093/jxb/err423>
- Seidl, R., Eastaugh, C. S., Kramer, K., Maroschek, M., Reyer, C., Socha, J., Vacchiano, G., Zlatanov, T., & Hasenauer, H. (2013). Scaling issues in forest ecosystem management and how to address them with models. *European Journal of Forest Research*, 132(5-6), 653-666. <https://doi.org/10.1007/s10342-013-0725-y>
- Silvestro, R., Rossi, S., Zhang, S., Froment, I., Huang, J. G., & Saracino, A. (2019). From phenology to forest management: Ecotypes selection can avoid early or late frosts, but not both. *Forest Ecology and Management*, 436, 21-26. <https://doi.org/10.1016/j.foreco.2019.01.005>

- Thibeault-Martel, M., Krause, C., Morin, H., & Rossi, S. (2008). Cambial activity and intra-annual xylem formation in roots and stems of *Abies balsamea* and *Picea mariana*. *Annals of Botany*, 102(5), 667-674. <https://doi.org/10.1093/aob/mcn146>
- United Nations. FCCC/CP/2015/10/Add.1: Paris Agreement.
- Vieira, J., Rossi, S., Campelo, F., & Nabais, C. (2014). Are neighboring trees in tune? Wood formation in *Pinus pinaster*. *European Journal of Forest Research*, 133(1), 41-50. <https://doi.org/10.1007/s10342-013-0734-x>
- Wodzicki, T. J., & Zajaczkowski, S. (1970). Methodical problems in studies on seasonal production of cambial xylem derivatives. *Acta Societatis Botanicorum Poloniae*, 39(3), 519-520. <https://doi.org/10.5586/asbp.1970.040>
- Wu, J., & Li, H. (2006). Concepts of scale and scaling. In (pp. 3-15). Springer Netherlands. https://doi.org/10.1007/1-4020-4663-4_1
- Zeng, Q., Rossi, S., & Yang, B. (2018). Effects of age and size on xylem phenology in two conifers of northwestern China. *Frontiers in Plant Science*, 8. <https://doi.org/10.3389/fpls.2017.02264>
- Zhang, J., Gou, X., Manzanedo, R. D., Zhang, F., & Pederson, N. (2018). Cambial phenology and xylogenesis of *Juniperus przewalskii* over a climatic gradient is influenced by both temperature and drought. *Agricultural and Forest Meteorology*, 260-261, 165-175. <https://doi.org/10.1016/j.agrformet.2018.06.011>
- Zweifel, R., Eugster, W., Etzold, S., Dobbertin, M., Buchmann, N., & Häsler, R. (2010). Link between continuous stem radius changes and net ecosystem productivity of a subalpine Norway spruce forest in the Swiss Alps. *New Phytologist*, 187(3), 819-830. <https://doi.org/10.1111/j.1469-8137.2010.03301.x>

CHAPTER IV

A LONGER WOOD GROWING SEASON DOES NOT LEAD TO HIGHER CARBON SEQUESTRATION

Published in Scientific Reports

Citation:

Silvestro, R., Zeng, Q., Buttò, V., Sylvain, J. D., Drolet, G., Mencuccini, M., Thiffault, N., Yuan, S., & Rossi, S. (2023). A longer wood growing season does not lead to higher carbon sequestration. *Scientific reports*, 13(1), 4059.

RESEARCH ARTICLE**Title:**

A longer wood growing season does not lead to higher carbon sequestration

Authors:

Roberto Silvestro^{1, *}, Qiao Zeng², Valentina Buttò³, Jean-Daniel Sylvain⁴, Guillaume Drolet⁴, Maurizio Mencuccini^{5, 6}, Nelson Thiffault^{7, 8}, Shaoxiong Yuan², Sergio Rossi¹.

Affiliation:

¹ Laboratoire sur les écosystèmes terrestres boréaux, Département des Sciences Fondamentales, Université du Québec à Chicoutimi, 555 boulevard de l'Université, Chicoutimi (QC) G7H2B1, Canada.

² Guangdong Open Laboratory of Geospatial Information Technology and Application, Guangzhou Institute of Geography, Guangdong Academy of Sciences, Guangzhou, PR China, 510070.

³ Forest Research Institute, Université du Québec en Abitibi-Témiscamingue, Rouyn-Noranda, QC, Canada.

⁴ Direction de la recherche forestière Ministère des Forêts, de la Faune et des Parcs, Québec, QC G1P3W8, Canada.

⁵ Centre de Recerca Ecològica i Aplicacions Forestals (CREAF), Bellaterra, 08193, Barcelona, Spain.

⁶ Institució Catalana de Recerca i Estudis Avançats (ICREA), Passeig de Lluís Companys 23, 08010, Barcelona, Spain.

⁷ Canadian Wood Fibre Centre, Canadian Forest Service, Natural Resources Canada, 1055, du P.E.P.S., P.O. Box 10380, Sainte-Foy Stn., Quebec, QC G1V 4C7, Canada

⁸ Centre for Forest Research, Faculty of Forestry, Geography and Geomatics, Université Laval, 2405 rue de la Terrasse, Quebec, QC G1V 0A6, Canada

* Corresponding author: roberto.silvestro1@uqac.ca (RS)

4.1 Abstract

A reliable assessment of forest carbon sequestration depends on our understanding of wood ecophysiology. Within a forest, trees exhibit different timings and rates of growth during wood formation. However, their relationships with wood anatomical traits remain partially unresolved. This study evaluated the intra-annual individual variability in growth traits in balsam fir [*Abies balsamea* (L.) Mill.]. We collected wood microcores weekly from April to October 2018 from 27 individuals in Quebec (Canada) and prepared anatomical sections to assess wood formation dynamics and their relationships with the anatomical traits of the wood cells. Xylem developed in a time window ranging from 44 to 118 days, producing between 8 and 79 cells. Trees with larger cell production experienced a longer growing season, with an earlier onset and later ending of wood formation. On average, each additional xylem cell lengthened the growing season by 1 day. Earlywood production explained 95% of the variability in xylem production. More productive individuals generated a higher proportion of earlywood and cells with larger sizes. Trees with a longer growing season produced more cells but not more biomass in the wood. Lengthening the growing season driven by climate change may not lead to enhanced carbon sequestration from wood production.

4.2 Introduction

Wood is one of the largest terrestrial carbon pools on Earth and a natural and renewable resource. Over the last decades, there has been growing interest in applied wood science. Firstly, as a raw material and all its derived products, wood is of crucial importance in the global bioeconomy and world trade (Verkerk et al., 2022). Several research teams are exploring the possibility that wood can substitute fossil fuels and non-biomass materials (Chen et al., 2018; Howard et al., 2021), especially in the construction industry (Eriksson et al., 2012; Howard et al., 2021). In addition, wood growth counteracts global warming by carbon sequestration (Pan et al., 2011). However, despite the economic and ecological roles that wood plays, our understanding of its formation and the factors influencing the resulting tree-ring structure remains incomplete.

Phenology is a crucial driver of tree fitness and species distribution (Chuine, 2010). Outside the tropics, meristems follow alternating periods of activity and dormancy according to the annual cycle of the seasons. Plants use environmental triggers (e.g., temperature, water, solar radiation) to synchronize the timings of growth and reproduction with favorable conditions during the year. The timing of phenological events is thus calibrated to ensure the optimal conditions to complete all stages of the annual life cycle while minimizing the risk of damage (Silvestro et al., 2019).

Wood formation dynamics are key drivers of the variation in wood features across the growth ring (Buttò et al., 2019). The ratio between cell diameter and cell wall thickness discriminates between earlywood and latewood cells, which result from different temporal dynamics of their cellular trait formation. Earlywood cells undergo a longer duration of enlargement than latewood cells, forming bigger cells with lower cell wall thickness (Buttò et al., 2019). Latewood cells are subjected to a longer duration of

secondary wall deposition, leading to smaller cells with thicker cell walls. These changes in the temporal dynamics of earlywood-latewood formation lead to different sensitivities of wood formation to endogenous and environmental factors during the growing season. In conifers, earlywood is more dependent on soil water content to sustain a greater cell extension, and latewood depends more often on temperature and sugar availability. The availability of this last resource increases when shoot elongation ends (Buttò, Khare, et al., 2021; Buttò, Rozenberg, et al., 2021; Carteni et al., 2018).

Variability within xylem anatomical traits, i.e., tracheid diameter and wall thickness, reflects structural and physiological trade-offs at the base of tree functioning and performance (Rathgeber et al., 2022). Indeed, wider tracheids are more efficient in transporting water but possibly more susceptible to cavitation (Dória et al., 2022). In contrast, narrower thick-walled tracheids afford most of the mechanical support and hydraulic safety but are less conductive (Dória et al., 2022). Anatomical traits and tracheid morphology also drive many fundamental wood properties and play a crucial role in determining the quality of forest-derived products (Rossi et al., 2015). Among all wood traits, density has a major impact on wood quality and the value of resulting wood products and composites (Shi et al., 2007). Wood density is the measure of the total amount of cell wall material available per volume unit. Tissue properties such as earlywood tracheid diameter, the proportion of latewood and, specifically, cell-wall thickness are major factors explaining variation in the intra-ring wood density (Rathgeber et al., 2006; Rossi et al., 2015). Therefore, geometric models based on cell anatomical features have been used to calculate the so-called morphometric density (Cuny et al., 2014), which represents an acceptable simplification, even if only partially explaining the density variation along the growth ring (Rathgeber et al., 2016).

Wood formation dynamics and the duration of differentiation stages influence cell traits (Buttò et al., 2019). However, wood phenology can vary significantly among individuals (Silvestro et al., 2022; Wodzicki & Zajaczkowski, 1970). For this reason, it is worth exploring the consequences of this variability on the relationship between the phenology of wood formation and anatomical characteristics and the resulting effects on wood density. This study evaluates the variability among individuals in xylem developmental dynamics and the related anatomical traits during the growing season 2018 in a balsam fir [*Abies balsamea* (L.) Mill.] stand.

The study aims to explore the relationships and trade-offs among wood formation temporal dynamics, annual productivity, and wood anatomical traits. Based on an intra-annual scale, we will first quantify the inter-individual variability in wood phenology (Silvestro et al., 2022) and then test whether a longer duration of the growing season corresponds to a greater cell production (Rossi et al., 2014; Silvestro et al., 2022). Subsequently, we test three alternative hypotheses related to the anatomical traits of xylem. A longer growing season leads to a greater annual tracheid production in which: (1) Earlywood and latewood productions increase proportionally, no differences in morphometric density can be highlighted; (2) A longer growing season increases carbon assimilation in wood (Gonsamo et al., 2018), latewood production augments and thus increases carbon sequestration and morphometric density; or (3) An earlier onset of the growing season does not result in extra carbon sequestration from wood production (Dow et al., 2022), earlywood production increases, resulting in a lower morphometric wood density.

4.3 Materials and methods

4.3.1 Study area

We conducted our study in the balsam fir–white birch bioclimatic domain at the Montmorency Forest (47°16'20'' N, 71°08'20'' W), Quebec, Canada. The study area has a typical continental climate with cool and humid summers and cold and long winters. The annual temperature is 0.5 °C during 1981-2010. July is the warmest month with a mean temperature of 14.6 °C. January is the coldest, with a mean temperature of -15.9 °C. Annual precipitation is 1583 mm, of which a third falls in the form of snow.

The study area covers 218 ha and was submitted to a clear cut during 1993-1994. The dominant species is balsam fir, presenting pure and mixed stands with a current age ranging between 25 and 30 years. The soil type is classified as Ferro-Humic Podzol and Humic Podzol (Soil Classification Working, 1998), covered by a 4.6 MOR humus layer.

4.3.2 Xylem phenology

We selected 27 dominant balsam firs from permanent plots with healthy crowns and upright stems to assess wood formation from April to October 2018. The sampled trees were of the same age but different in height and diameter at breast height (DBH; 1.3 m). Microcores were collected weekly from each sampled tree using a Trephor (Rossi, Anfodillo, et al., 2006). To avoid the development of resin ducts, samples were collected 10 cm apart (Deslauriers et al., 2003).

The samples were dehydrated through successive immersion in ethanol and D-limonene, then embedded in paraffin (Rossi, Deslauriers, et al., 2006). Transverse sections of wood tissue 8 µm in thickness were cut with a rotary microtome and stained with cresyl violet acetate (0.16% in water) (Rossi, Deslauriers, et al., 2006). We discriminated between

developing and mature tracheids under visible and polarised light at magnifications of $\times 400$ – $\times 500$. The number of cambial, enlarging, cell wall thickening and lignifying and mature cells was counted along three radial rows. Specifically, cambial and enlarging cells remained dark under polarised light, indicating only primary cell walls. During the cell wall thickening and lignification phase, cells glistened under polarized light. Cell maturation was reached when they were completely blue (Rossi, Deslauriers, et al., 2006).

4.3.3 Xylem cell anatomy

Two additional microcores per tree were collected at the end of summer 2018. We prepared the samples according to the abovementioned experimental protocol. Wood sections were stained in safranin (1% water) and stored on micro slides with a Permount™ mounting medium. We collected digital images of wood transversal sections with a camera fixed on an optical microscope at magnifications of $\times 20$. We measured the lumen radial diameter, lumen tangential diameter, wall radial thickness, and lumen area for all the transversal sections using WinCELL™ (Regent Instruments, Canada).

Since cell size increases in the radial rather than the tangential direction during the enlarging phase, we used cell radial diameter to show the variation of the cell enlarging phase (Cuny et al., 2014). We calculated cell radial diameter as the sum of the lumen radial diameter and the two wall radial thicknesses. As wall tangential thickness was estimated to be 1.2 times wall radial thickness, we defined cell tangential diameter as the sum of lumen tangential diameter and 2 times wall tangential thickness (or 2.4 times wall radial thickness) (Cuny et al., 2014). As the shape of a cell in the transversal section was approximate to a rectangle, we computed cell area as the product of cell radial diameter

and tangential diameter, and wall area was defined as the difference between cell and lumen area.

According to Mork's criterion, latewood cells were defined as the tracheids showing a wall radial thickness four times larger than the lumen radial diameter (Filion & Cournoyer, 1995). We determined the percentage of latewood cells as the ratio of latewood cells to the total number of xylem cells at the end of the growing season (Filion & Cournoyer, 1995). The morphometric density was calculated as a function of the wall cross-sectional area, cell radial diameter and cell tangential diameter according to Cuny et al. (2014).

4.3.4 Statistical Analyses

Based on the raw data of the number of cells counted at each sampling date, generalized additive models (GAMs) were performed for each sampled tree to evaluate the annual cell production and both the timings and duration of each xylogenesis phenological phase (Cuny et al., 2014) and to generate the tracheidograms following Buttò et al. (2019). Accordingly, the duration of cell enlargement was defined as the difference between the onset of cell wall thickening and lignification and onset of cell enlargement. The duration of the cell wall thickening and lignification phase was defined as the difference between the date of mature cell and the onset of cell wall thickening and lignification, and the duration of xylogenesis was calculated as the period between the first mature cell and first enlarging cell (Buttò et al., 2019).

For each individual, we obtained the tracheidograms of cell diameter, cell area, wall thickness, wall area and morphometric density according to the percentile position of cells across the growth ring (Buttò et al., 2019). For each tree, we applied GAMs to fit the

variations of these wood anatomical traits along with the relative tree-ring positions (Buttò et al., 2019). Loess function was performed to obtain the general patterns of the duration of wood formation and wood anatomical traits across the growth ring. We validated the reliability of fitting by performing the distribution of studentized residuals. Linear regressions were used to assess the relationship between cell production, anatomical traits and timings of xylogenesis. We used standardised major axis (SMA) linear regressions to test the relationship between the timings of xylem formation and cell production (Silvestro et al., 2019). We used SMA regression as we could not state which one of the variables was independent. Therefore, the aim was to test the relationship between the variables and estimate the line best describing the scatter. All statistics were performed in R 3.6.1.

4.4 Results

4.4.1 Wood formation dynamics

The first enlarging cells of earlywood, corresponding to the onset of wood formation, were observed from mid-May to late June between the day of the year (DOY) 136 and 178. More than 58% of the trees started cell differentiation between DOY 149 and 157 (Figure S4.1). On average, cell wall thickening and lignification started 13 days after the onset of cell enlargement, between early June and early July (DOY 158–184), with 71% of the trees beginning between DOY 163 and 170 (Figure S4.1). The first mature cells of earlywood were detected 10 days after the onset of cell wall thickening and lignification, between late June and early July (DOY 171–191), with 79% of the trees starting between DOY 173 and 182 (Figure S4.1).

The first enlarging cells of latewood were observed 53 days after the onset of earlywood differentiation, between DOY 190 and 243, corresponding to the period between early July and late August (Figure S4.1). The onset of cell wall thickening and lignification of latewood occurred 33 days later than the onset of cell enlargement of latewood. About 63% of the sampled trees started cell wall thickening and lignification of latewood between mid and late July (DOY 194–207) (Figure S4.1). The first mature latewood cell was observed 14 days after the onset of cell-wall thickening and lignification of latewood. The first mature latewood cell was observed between late July and early September (DOY 200–251), occurring in late August (DOY 233–242) in more than 40% of the trees (Figure S4.1).

On average, 93% of the studentized residuals of the duration of wood formation obtained by the fitting of the loess function ranged between -1.96 and 1.96, demonstrating that the

model adequately represented the average pattern of the duration of wood formation (Figure S4.2). On average, the duration of cell enlargement of a tracheid lasted 5 days. The longest duration (12 days) of cell enlargement was observed for the first xylem cells, while the development of enlarging cells lasted only 3 days at the end of the growth ring (Figure 4.1). On average, earlywood cell enlargement duration (6 days) was higher than that of latewood (3 days). Overall, cell wall thickening and lignification duration showed a higher variation in latewood, lasting 9 and 17 days in earlywood and latewood, respectively. At the first percentile of the growth ring, xylem cells required 11 days to complete cell-wall thickening and gradually decreased to 7 days at 50% of the growth ring, then increased to 23 days at its end. Compared to earlywood, latewood showed higher variability in the duration of xylogenesis. On average, earlywood and latewood cells required 15 and 20 days to complete xylogenesis, respectively. According to loess function, the duration of xylogenesis was 24 days for the first earlywood cell and decreased to 11 days at 60% of the growth ring, while it increased to 26 days for the last latewood cell (Figure 4.1).

4.4.2 Cell production and anatomical traits

Xylem cell production varied highly among trees, resulting in a range of between 8 and 79 cells observed at the end of the growing season (Figure 4.2). Latewood cells varied from 6 to 40%. 60% of trees showing 12–24% of latewood (Figure 4.2).

The studentised residuals of the wood anatomical traits resulting from the fitting of the loess function exhibited no trend, with random distribution around zero (Figure S4.3). On average, 94% of the studentised residuals showed an absolute value of ± 1.96 , indicating that the model appropriately represented the trends of wood anatomical traits (Figure

S4.3). In general, cell diameter ranged from 13.1 to 34.2 μm , with a mean of 28.8 μm . Cell radial diameter decreased gradually during earlywood production (average value of 31.2 μm) but sharply declined during latewood formation (average value of 19.7 μm). The largest standard deviations ($\pm 4.3 \mu\text{m}$) were observed at the beginning of wood formation, decreasing towards the end of the growth ring ($\pm 2.5 \mu\text{m}$) (Figure 4.3). The variation of cell area had a similar pattern to cell radial diameter (Figure 4.3). The largest cell area (958.0 μm^2) was observed from the first earlywood cells, decreasing to 305.3 μm^2 at the end of the growth ring. Wall radial thickness gradually increased from 1.9 to 4.2 μm during the tree-ring formation, with an average of 2.7 μm across the growth ring. Cell wall area slowly increased from 295.3 μm^2 at the first percentile of the growth ring, culminated at 369.1 μm^2 at 73% of the growth ring, and reduced during latewood production. The standard deviation of the cell wall area was relatively constant ($\pm 67.4 \mu\text{m}^2$ on average) across the growth ring (Figure 4.3). The values of morphometric density ranged from 307.9 to 791.0 kg m^{-3} , with an average of 449.5 kg m^{-3} (Figure 4.3). The morphometric density was lower across the earlywood and higher in latewood, which matched the pattern of cell wall thickness.

4.4.3 Wood formation dynamics, production and cell traits

Cell production exhibited a positive linear relationship with cell-wall area ($P < 0.05$, $R^2 = 0.18$, Figure 4.4). The linear relationship between cell production and cell wall area was also positive but not statistically significant ($P > 0.05$, $R^2 = 0.04$, Figure 4.4). We observed a negative relationship between cell production and average morphometric density ($p < 0.001$, $R^2 = 0.33$, Figure 4.4), indicating that the morphometric density progressively declines as cell production increases.

The relationships between cell production and the onset, ending, and duration of xylem formation were highly significant ($P < 0.001$, R^2 of 0.40, 0.55 and 0.62, respectively, Figure 4.5). These relationships indicate that an earlier growth resumption and later growth cessation, which correspond to a longer growing season, lead to greater annual cell production. This trend was maintained when the relationship between the onset, ending, and duration of earlywood formation was examined ($P < 0.001$, R^2 of 0.40, 0.55 and 0.66, respectively, Figure 4.5). Considering the relationship between latewood formation and annual cell production, both a later onset and later ending were positively correlated with a greater xylem cell production ($P < 0.001$, R^2 of 0.33 and 0.55, respectively, Figure 4.5), which led to a non-significant relationship between the length of latewood formation and annual production of xylem cells ($P > 0.05$, Figure 4.5). According to the previous results, we observed that a longer growing season, with earlier onset and later ending, increased both the number of earlywood cells and their percentage out of the total annual production ($P < 0.001$, with R^2 ranging from 0.42 to 0.60, Figure 4.6). On the contrary, the relationships ($P > 0.05$) between the number of latewood cells and the timings of onset and ending of their production were not significant (R^2 of 0.007 and 0.09, respectively, Figure 4.6). The percentage of latewood of the total cell production was correlated with both the onset and the ending of its formation ($P < 0.001$, R^2 of 0.33 and 0.51, respectively, Figure 4.6). That means that the longer latewood production is delayed during the growing season the more earlywood is produced.

The linear relationship between number of earlywood and latewood cells and total xylem cell production was significant and positive ($P < 0.001$ and 0.05, R^2 of 0.98 and 0.18, Figure 4.7), demonstrating that the production of both earlywood and latewood cells increases with greater cell production. However, the rate of increase differs between

earlywood and latewood, with earlywood cells representing 95% of all tracheids produced. This became evident when observing the ratio between earlywood and latewood cells. Indeed, while we observed an increase in the percentage of earlywood ($P < 0.001$, $R^2 = 0.62$, Figure 4.7), latewood percentage decreased with annual cell production ($P < 0.001$, $R^2 = 0.62$, Figure 4.7). Therefore, a greater cell production corresponds to a longer duration of the growing season and a greater production in earlywood compared to latewood.

4.5 Discussion

This study investigated the intra-annual dynamics of wood formation in 27 balsam firs at the Montmorency Forest, Quebec, Canada. Trees with a higher cell production experienced a longer duration of the growing season, represented by an earlier onset and a later ending of wood formation. More productive individuals also generated a higher proportion of earlywood and, at the same time, of cells with larger dimensions, resulting in a lower morphometric wood density than individuals with lower cell production. These results support the initial hypothesis that, at the intra-annual scale, individuals experiencing an earlier resumption of xylem growth increase earlywood production and decrease morphometric wood density.

4.5.1 More is less: phenology, productivity and cell traits

According to our results, the number of cells produced at the end of the growing season is related to the duration of xylogenesis. Trees starting xylem differentiation earlier and ending later, thus experiencing a longer growing season, have a higher cell production. Moreover, the number of earlywood and latewood cells increases in trees with a longer growing season. However, the production does not increase proportionally. Still, we observed a longer duration and greater production of earlywood cells and, consequently, a reduction in latewood percentage in the tree-ring in trees with a longer growing season. The disproportional augmentation in earlywood production over latewood finally results in a higher proportion of larger cell sizes and, thus, a lower morphometric density.

This relationship between wood phenology, annual cell productivity and the related cell traits may be explained by physiological processes affecting primary and secondary growth. At the beginning of the growing season, xylem development depends on the

influx of auxin from bud primordia (Oribe et al., 2003), where this hormone is primarily produced, to then be conveyed into polar auxin via phloem transport (Schrader et al., 2003). Consequently, activation of the apical meristems is essential for the onset of wood phenology, which could explain their synchronism (Buttò, Khare, et al., 2021).

Primary and secondary growth processes depend on one another, are synchronous, and unquestionably competitive (Buttò, Khare, et al., 2021; Deslauriers et al., 2016). Therefore, primary growth can potentially play a role in contributing to defining the ratio between earlywood and latewood. Once the synchronous resumption of primary and secondary meristem activity begins in the early spring, sink competition for carbon allocation is unavoidable (Carteni et al., 2018). Specifically, when shoots and needles in the canopy are actively growing, the wood formation process has a lower allocation priority of the recently assimilated C. As for secondary growth, a large variability is found in the timings and duration of primary growth phenological phases (Perrin et al., 2017; Silvestro et al., 2020; Silvestro et al., 2019). Given the synchronism between primary and secondary meristematic activity (Buttò, Khare, et al., 2021) and the influence of primary growth on sugar availability for xylogenesis (Begum et al., 2013; Carteni et al., 2018), the timing of bud break and duration of shoot extension can likely influence the timing of secondary growth resumption but also the related cell traits and the ratio between earlywood and latewood. The result of this close interaction is that an anticipated bud break and longer duration of shoot extension could drive a greater earlywood production, given that this type of xylem cells also relies on C assimilated from the previous growing seasons (Fu et al., 2017; Hansen & Beck, 1990; Kagawa et al., 2006). At the end of summer, once the shoot extension is completed, the priority in C allocation changes, and

latewood formation can finally profit from an increased and continuous carbon supply (Buttò, Khare, et al., 2021; Carteni et al., 2018).

These close interactions between primary and secondary growth can explain why the difference in the rates of increase between earlywood and latewood correlated to a longer growing season, as observed in the present study. Therefore, if our hypothesis is correct, anatomical patterns in wood formation could be directly determined by the C allocation patterns during the growing season.

4.5.2 Variability at the onset and end of the growing season

The variability among trees in the duration of wood formation increased from the onset to ending of the growing season. The source of this variability along the tree-ring lay in the larger variability in the duration of cell wall deposition during latewood formation. However, this variability in the secondary cell wall deposition duration was independent of the individual variability in anatomical traits along the growth ring.

A complex relationship exists between cell traits and the duration of their differentiation phases (Carteni et al., 2018; Rathgeber et al., 2022). In our study, the duration of cell enlargement is longer during earlywood than latewood development. This result agrees with other studies performed on several conifer species in which larger earlywood cells were coupled with a longer duration of cell enlargement (Anfodillo et al., 2012; Buttò et al., 2019; Cuny et al., 2014). Despite the difference in the duration of cell enlargement between early and latewood formation, the variability among trees remained constant during the growing season.

At the end of the growing season, the duration of cell wall thickening drives the timing of latewood formation (Buttò et al., 2019; Carteni et al., 2018; Deslauriers et al., 2016).

According to our data, the duration of cell wall thickening is characterised by a large variability among individuals. Our results agree with previous studies (Silvestro et al., 2022), in which the end of the growing season was marked by a larger among-tree variability than the onset. The difference in variability between the onset and the ending of wood phenology is likely related to a different contribution of the endogenous and environmental factors driving these phenological phases. Indeed, while environmental and overall weather conditions drive growth resumption (Linares et al., 2009; Rossi et al., 2012), internal factors, such as the timing and duration of resumption of primary growth, as well as the amount of cell production and water and sugar availability, are likely involved in defining the duration and the ending of wood formation (Buttò et al., 2020; Li et al., 2013; Rathgeber et al., 2011).

Balsam fir is known for the low quality of its wood, especially regarding its mechanical properties (Koga & Zhang, 2002). However, the same xylem anatomical features of balsam fir explain its great capacity for physiological adjustments (e.g. high light-use efficiency, a low respiration rate, and a long seasonal period of active photosynthesis) (Messier et al., 1999; Paixao et al., 2019; Pothier et al., 2012). The highlighted relationships between phenological timings, annual productivity and the resulting anatomical traits of the growth ring may also be found in other species. However, the degree of variability among individuals might differ, for example in species with a slower growth habit and a more pronounced conservative behavior in wood formation.

4.5.3 Growing season length and carbon sequestration

Our study analyzed patterns at intra-annual scale by focusing on processes occurring at a daily resolution during one growing season. However, some considerations can arise for

a picture at larger scale. Our results confirm the relationships between the reduction in wood density and enhanced growth in volume of wood observed in the last century in Central Europe (Pretzsch et al., 2018). Over the last decade, the scientific literature provided evidence of a global acceleration of forest growth dynamics due to climate change (Fang et al., 2014; Gao et al., 2022; Pretzsch et al., 2018; Pretzsch et al., 2014; Reyer et al., 2014). It has been demonstrated that an earlier onset of the growing season induced by climate change does not result in enhanced carbon sequestration from wood production in temperate deciduous trees of North America (Dow et al., 2022). Our results at the intra-annual scale confirm what was observed by Dow et al. (2022), and specifically that an increase in xylem cell production or related traits such as tree-ring width or volume of wood cannot be straightforwardly converted into sequestered carbon, neither should we look at it as a biomass harvest potential. New insights into the relationships between wood functional traits can deliver crucial knowledge to upscale carbon sequestration from tissue-to-individual scale. However, assessment at intra-annual scale lacks the resolution to estimate the effect of weather on wood formation and how growth ring width relates to wood mass. In this context, the combination of tree ring analysis, quantitative wood anatomy, and the assessment of wood formation has the potential to quantify how climatic variations affect wood functional traits and the amount of carbon annually sequestered in the tree stem. Enhancing our accuracy in linking climatic features to carbon sequestration is a crucial step for making reliable ecological predictions in a changing climate that will unavoidably impact the forestry industry and the global market related to wood production.

4.6 Conclusions

Our results show the high variability in wood phenology among trees of the same stand. A longer growing season corresponds to greater annual cell production. This interaction finally results in less dense wood due to a larger size of cells and lower proportion of latewood. Our study provides an eco-physiological explanation that reflects the interaction between the endogenous and environmental factors driving xylem phenology and wood production. We assume that temperature and precipitation play a key role in defining the timing of wood formation, while the pattern in C allocation during the growing season is involved in determining the wood anatomical traits. This interaction among multiple factors became even more complex when considering the weight of each factor and the period during the growing season.

These results about the relationships and interactions between phenological timings and the dynamics of cell trait development illustrate that our understanding of wood formation remains incomplete. Accordingly, a clear understanding of all the factors involved in the variability in wood phenology and production among trees still need further investigations.

4.6.1 Acknowledgements

This work was conducted and funded by the Ministère des Forêts, de la Faune et des Parcs of Quebec, Canada (Evap-for, project #142332139), the Fonds de Recherche du Québec - Nature et Technologies (AccFor, project #309064), the Observatoire régional de recherche en forêt boréale, the GDAS' Special Project of Science and Development (2020GDASYL-20200103001) and the National Natural Science Foundation of China (42107482). R. Silvestro received the Merit scholarship for international PhD students

(PBEEE) by the Fonds de Recherche du Québec - Nature et Technologies (FRQNT). The authors thank Brasseur, S. L. Papillon, F. Wiseman, J. Monffette, P.-L. Déchêne and M. Rhéaume for technical support, and A. Garside for editing the English text.

4.6.2 Author contribution

RS, VB, MM and SR conceived the ideas and designed methodology; JDS and GD administrated the project and data collection; JDS, GD, NT and SR conceived experimental design of at *Montmorency Forest* (Evap-For project). RS, QZ, VB and SY analysed the data; RS led the writing of the manuscript. All authors contributed critically to the drafts and gave final approval for publication.

4.6.3 Competing interests

The authors declare no competing interests.

4.6.4 Data availability

Data associated with this paper are available in Borealis:

<https://doi.org/10.5683/SP3/OTADBZ>

4.7 Figures

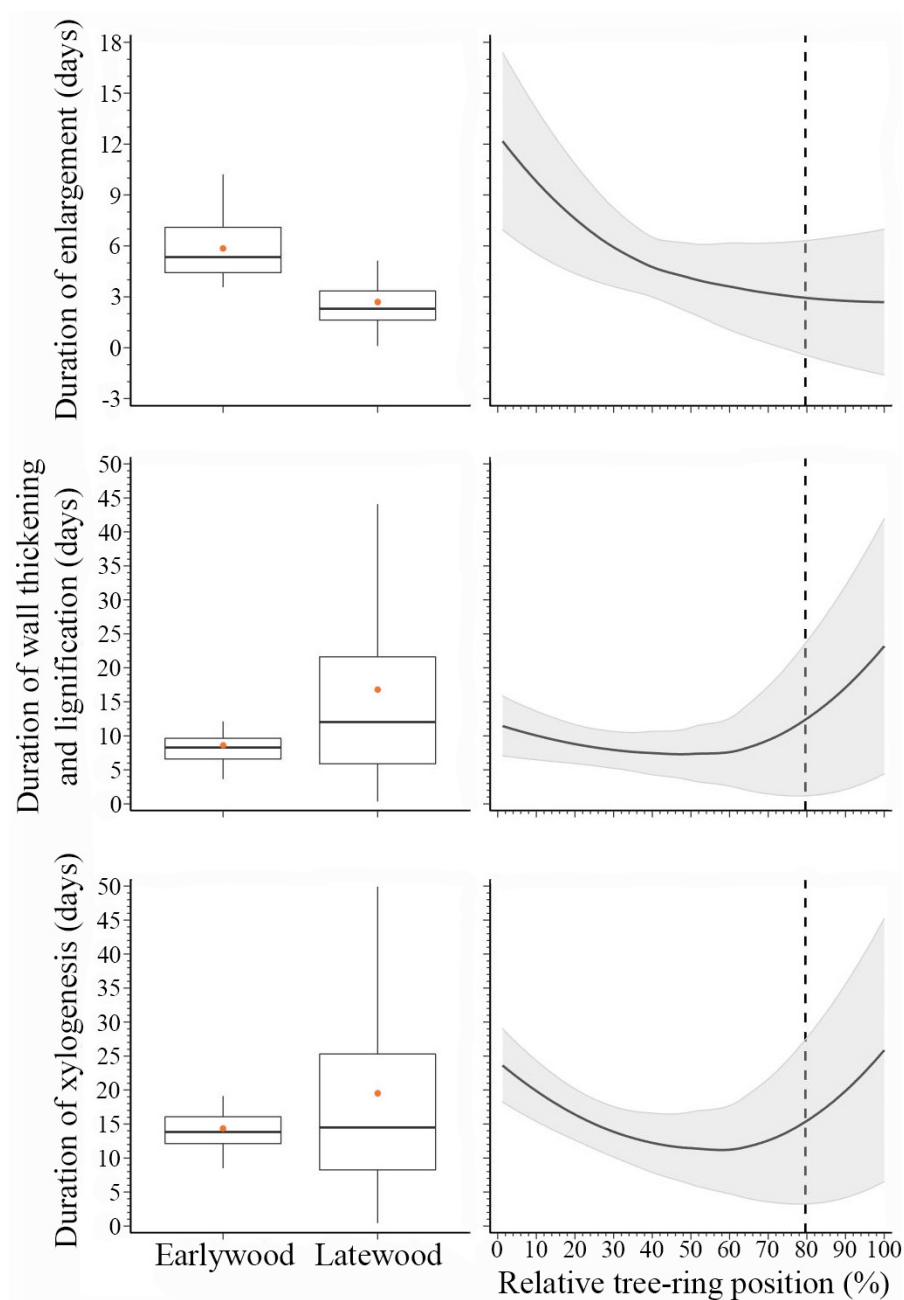


Figure 4.1 Duration of xylem formation (cell enlargement and secondary cell-wall deposition) across the growth ring in 27 balsam firs at the Montmorency Forest (QC, Canada). Boxplots represent upper and lower quartiles; whiskers achieve the 10th and 90th percentiles; the median and mean values are drawn as horizontal black lines and black dots, respectively. The trends result from loess function (span 0.9), with the grey background representing the standard deviation. The dotted line represents the boundary between earlywood and latewood.

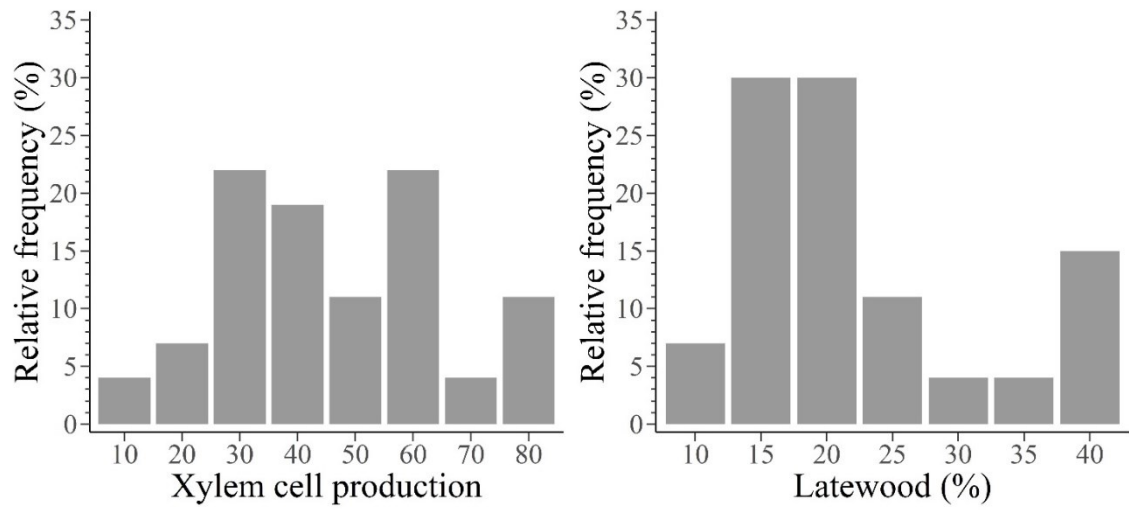


Figure 4.2 Xylem cell production and latewood cell percentage in 27 balsam firs at the Montmorency Forest (QC, Canada).

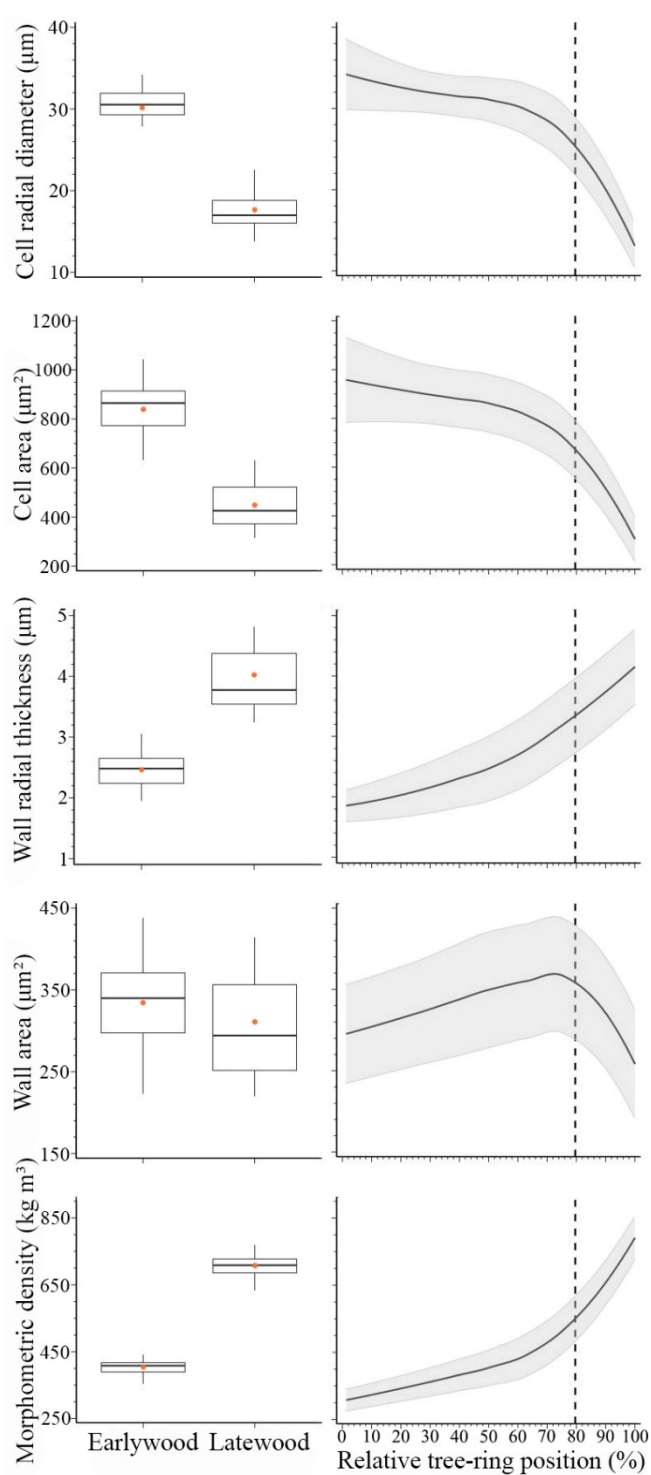


Figure 4.3 Wood anatomical traits and morphometric density across the growth ring in 27 balsam firs at the Montmorency Forest (QC, Canada). Boxplots represent upper and lower quartiles; whiskers achieve the 10th and 90th percentiles; the median and mean values are drawn as horizontal black lines and black dots, respectively. The trends result from loess function (span 0.9), with the grey background representing the standard deviation. The dotted line represents the boundary between earlywood and latewood.

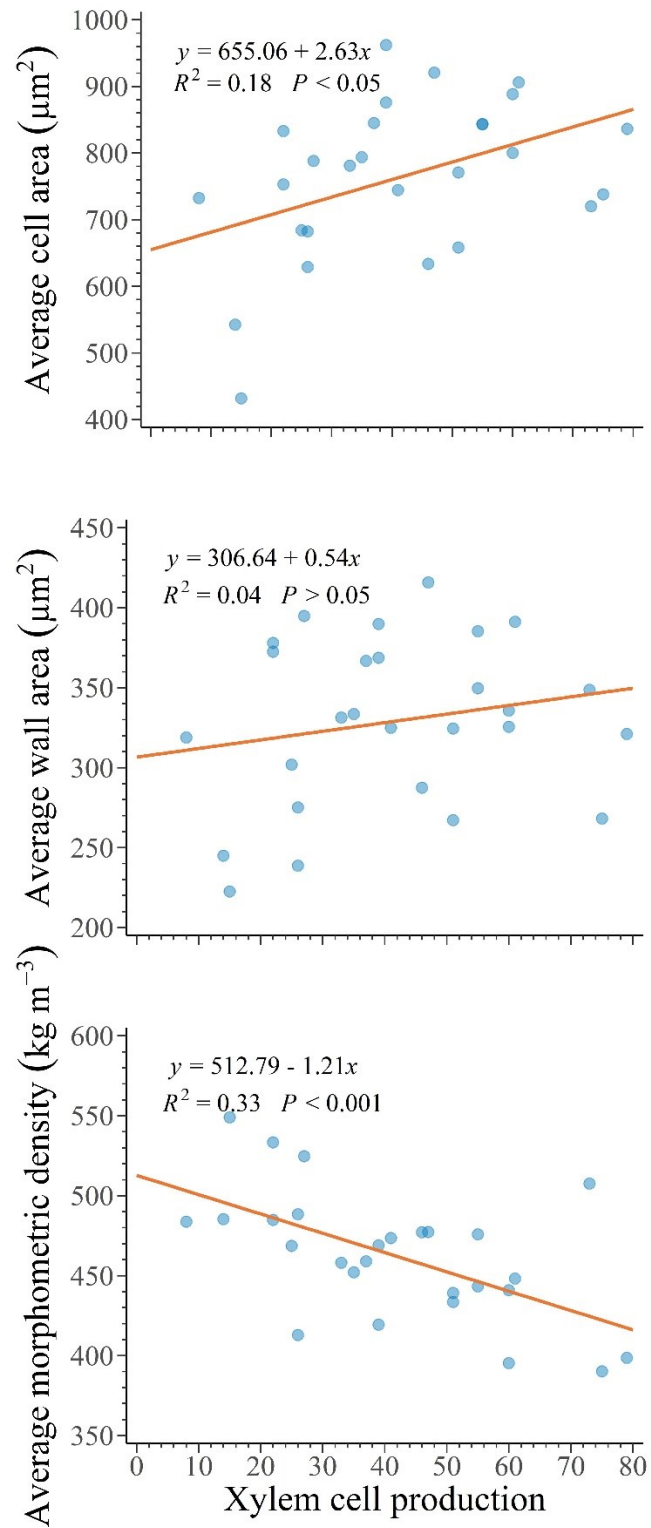


Figure 4.4 Relationships between cell production and anatomical traits in 27 balsam firs at the Montmorency forest (QC, Canada).

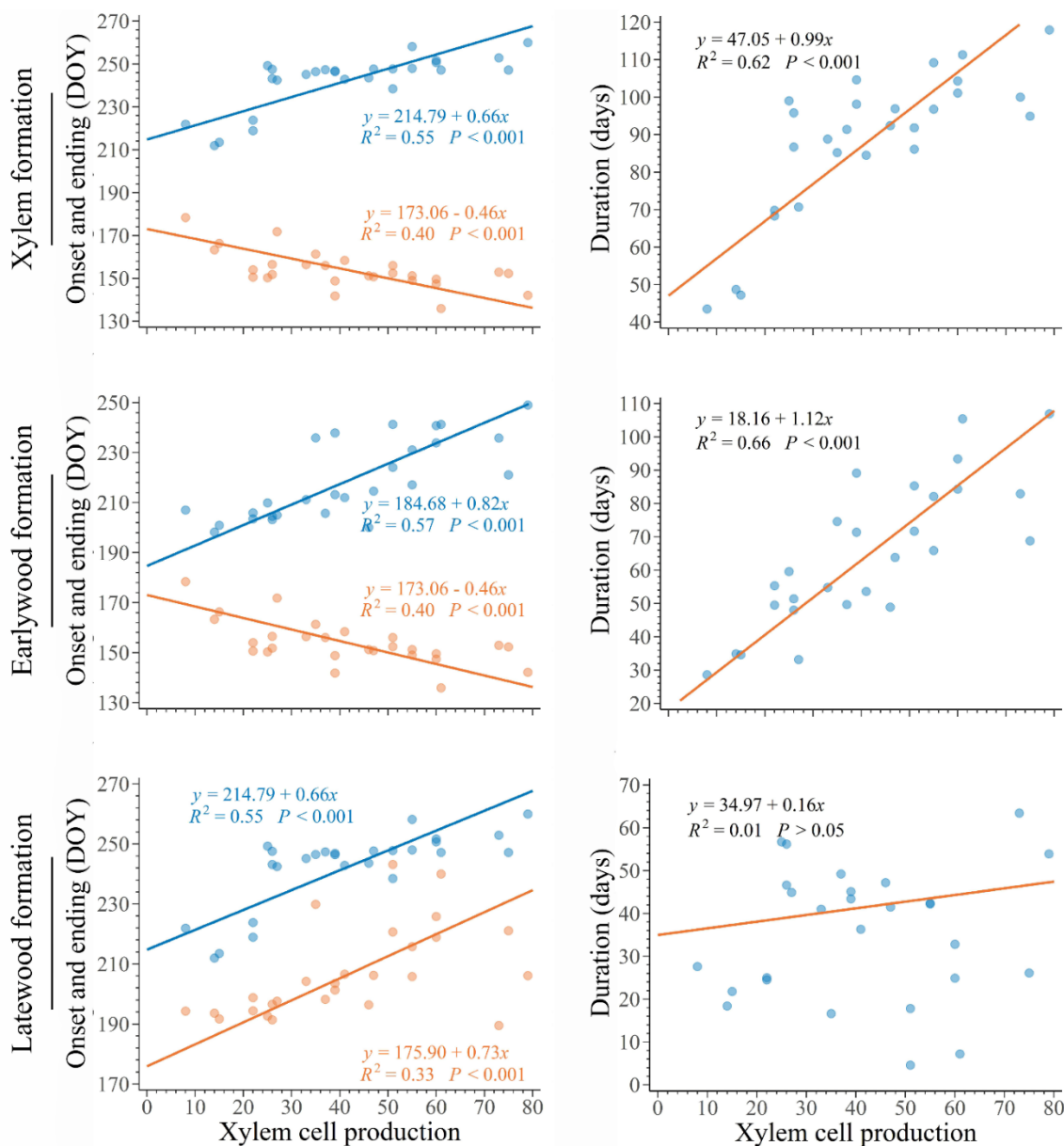


Figure 4.5 Standardized major axis (SMA) regressions among timings of onset (orange dots) and ending (blue dots) of xylem phenology, earlywood and latewood phenology as a function of the total number of cells in the growth ring at the end of the growing season in 27 balsam firs at Montmorency forest (QC, Canada).

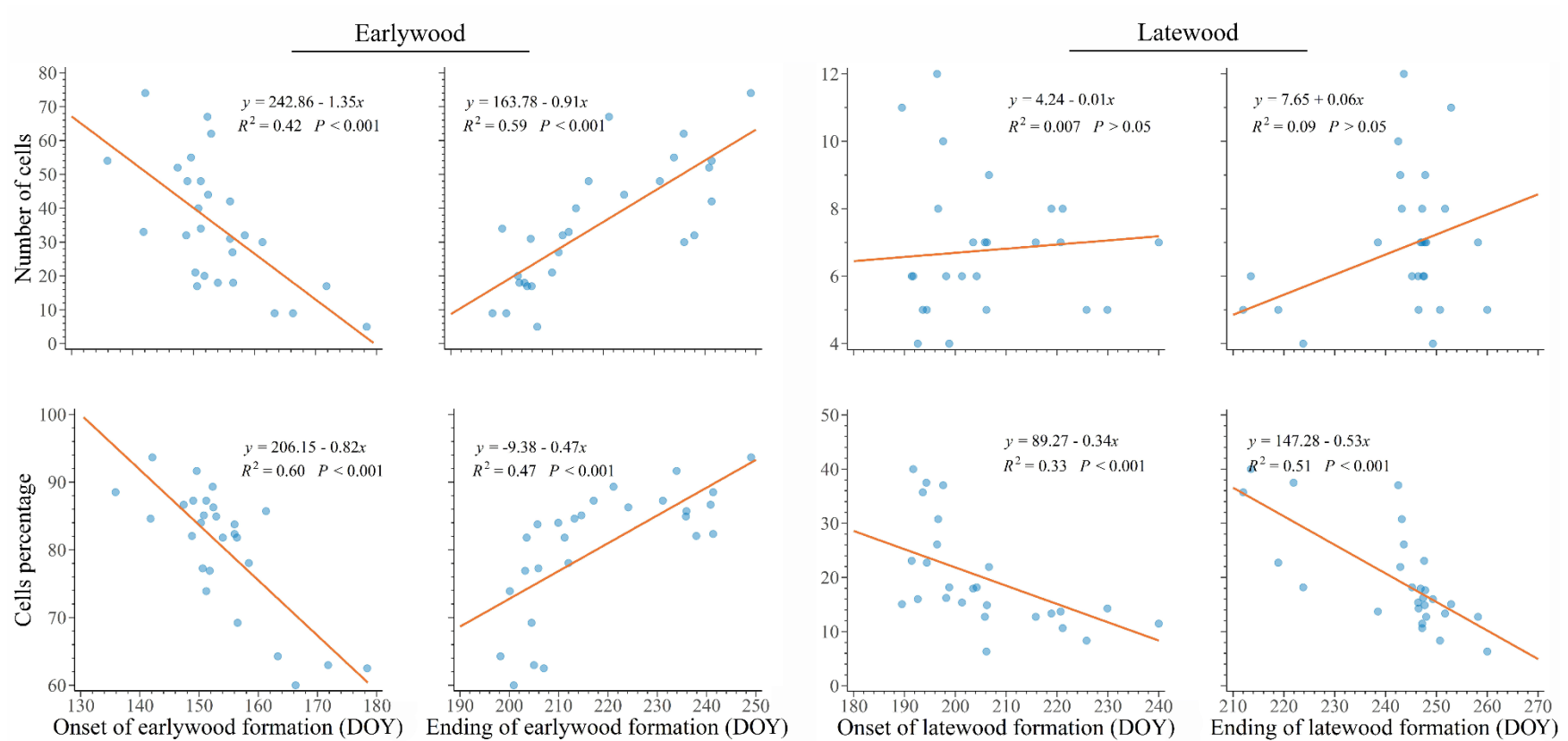


Figure 4.6 Relationships between the amount of earlywood and latewood (expressed as cell number and percentage of total cell production) and earlywood and latewood phenology in 27 balsam firs at Montmorency forest (QC, Canada).

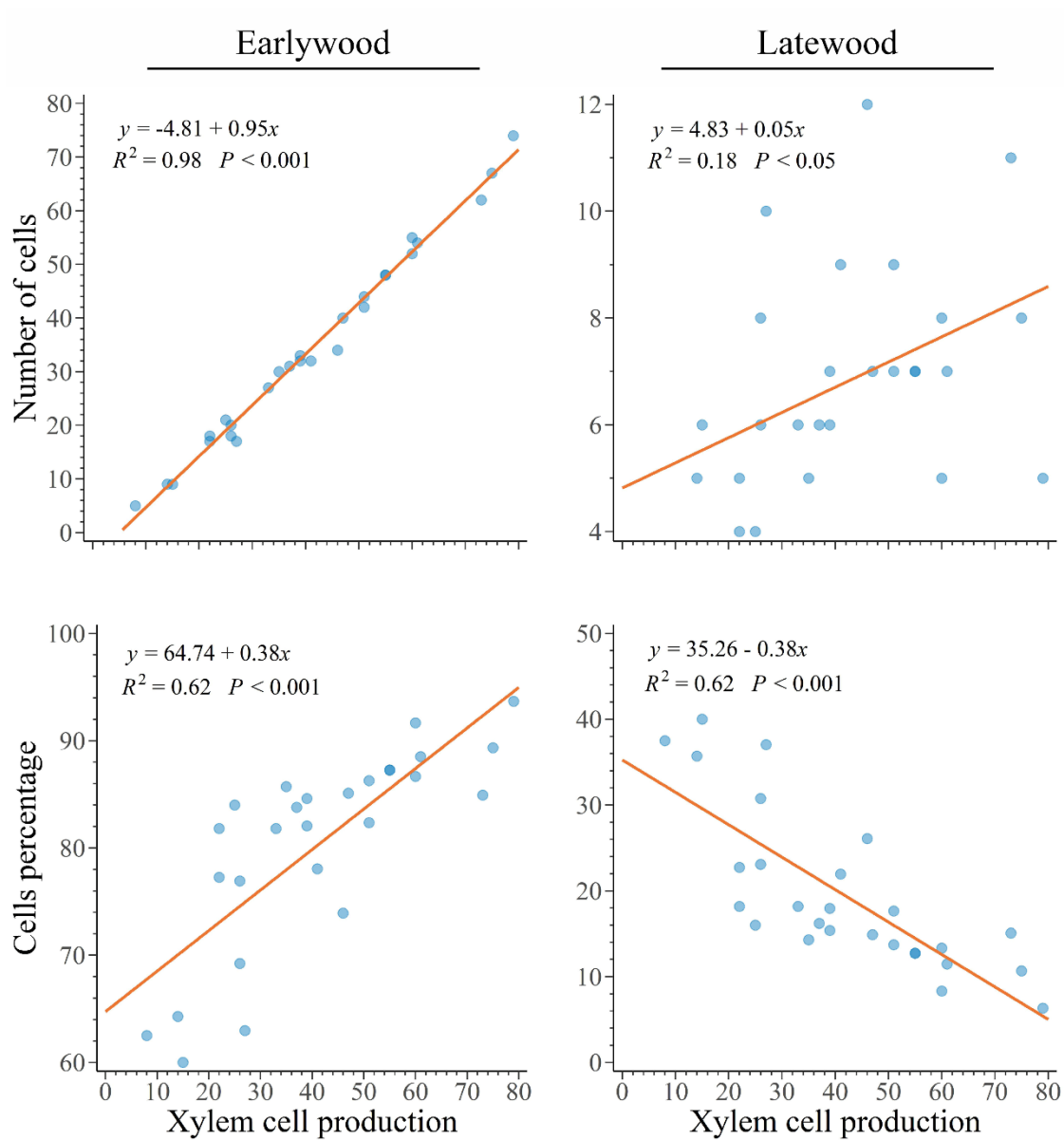


Figure 4.7 Relationships between the amount of earlywood and latewood (expressed as cell number and percentage of total cell production) and annual cell production in 27 balsam firs at Montmorency forest (QC, Canada).

4.8 Annexes

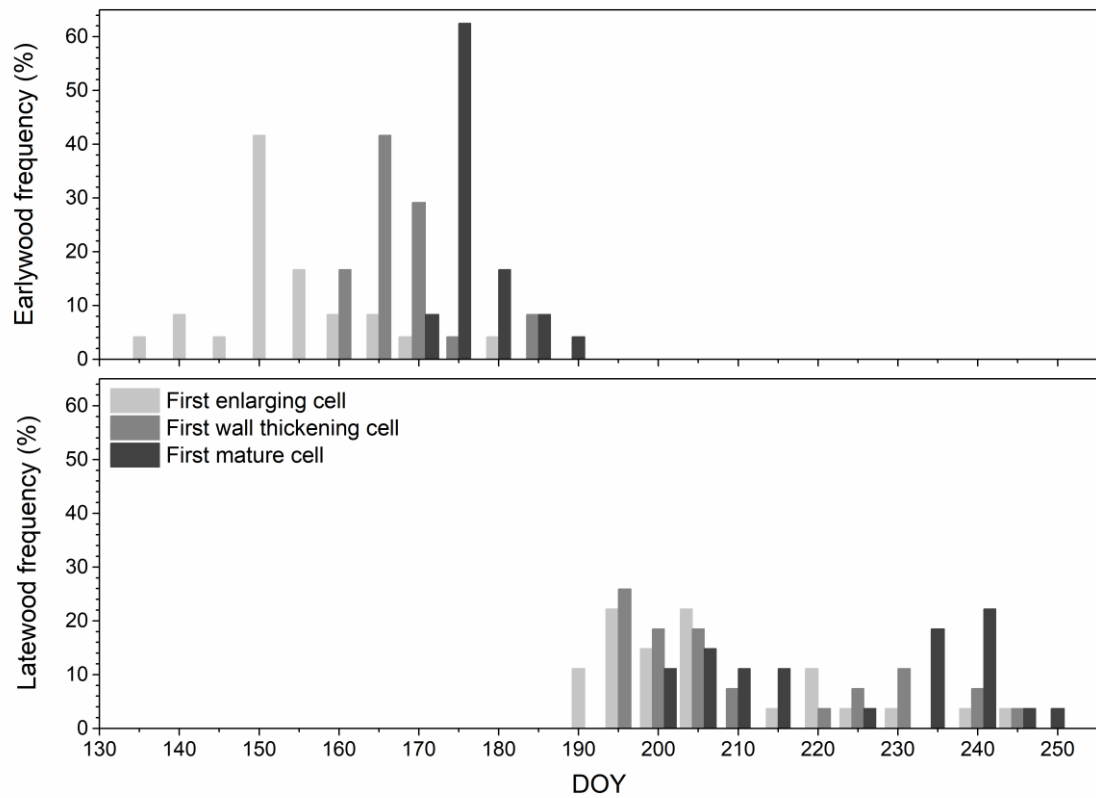


Figure S 4.1 Modelized timings of xylem phenology in earlywood and latewood of 27 balsam firs at the Montmorency Forest, QC, Canada.

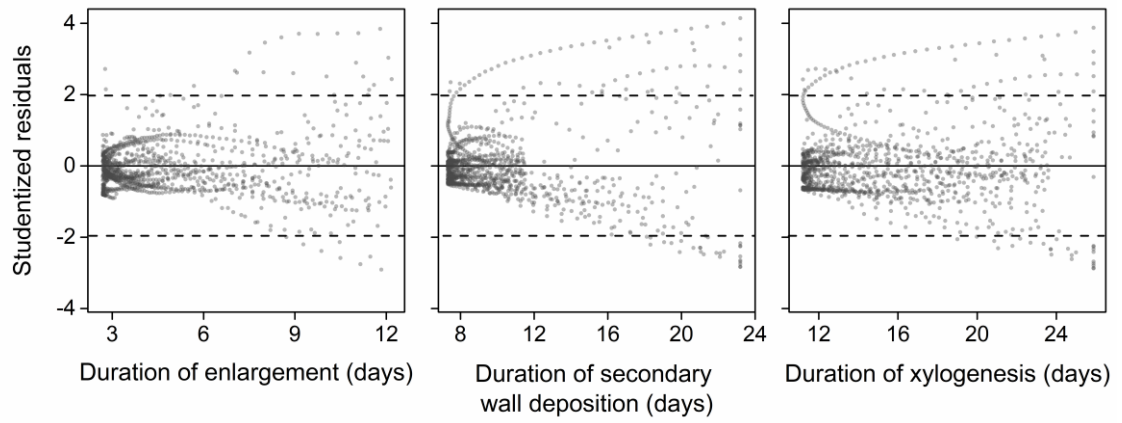


Figure S 4.2 Studentized residuals vs duration of wood formation phases resulting from the fitting of loess function. The dotted lines represent the range between -1.96 and 1.96.

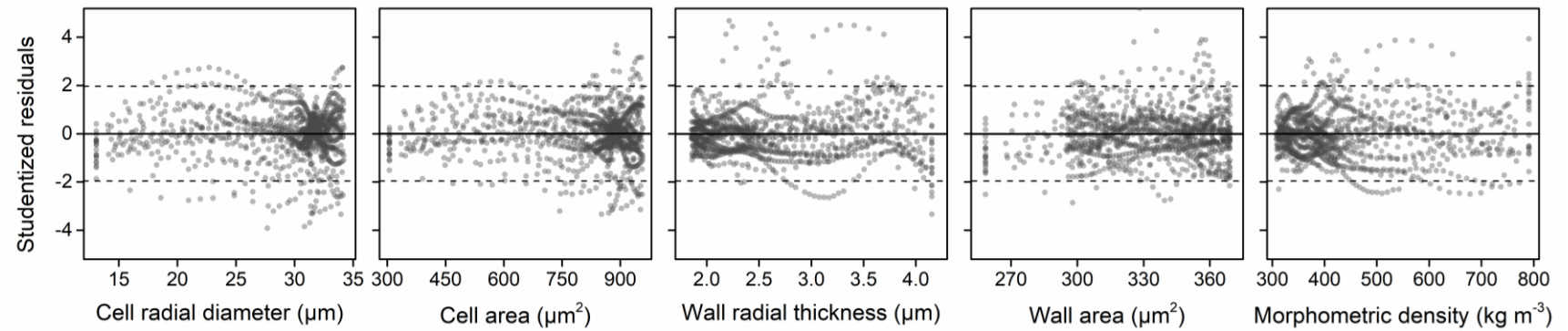


Figure S 4.3 Studentized residuals vs wood anatomical traits resulting from the fitting of loess function. The dotted lines represent the range between -1.96 and 1.96.

4.9 References

- Anfodillo, T., Deslauriers, A., Menardi, R., Tedoldi, L., Petit, G., & Rossi, S. (2012). Widening of xylem conduits in a conifer tree depends on the longer time of cell expansion downwards along the stem. *Journal of Experimental Botany*, *63*(2), 837-845. <https://doi.org/10.1093/jxb/err309>
- Begum, S., Nakaba, S., Yamagishi, Y., Oribe, Y., & Funada, R. (2013). Regulation of cambial activity in relation to environmental conditions: Understanding the role of temperature in wood formation of trees. *Physiologia Plantarum*, *147*(1), 46-54. <https://doi.org/10.1111/j.1399-3054.2012.01663.x>
- Buttò, V., Khare, S., Drolet, G., Sylvain, J. D., Gennaretti, F., Deslauriers, A., Morin, H., & Rossi, S. (2021). Regionwide temporal gradients of carbon allocation allow for shoot growth and latewood formation in boreal black spruce. *Global Ecology and Biogeography*, *30*(8), 1657-1670. <https://doi.org/10.1111/geb.13340>
- Buttò, V., Rossi, S., Deslauriers, A., & Morin, H. (2019). Is size an issue of time? Relationship between the duration of xylem development and cell traits. *Annals of Botany*, *123*(7), 1257-1265. <https://doi.org/10.1093/aob/mcz032>
- Buttò, V., Rozenberg, P., Deslauriers, A., Rossi, S., & Morin, H. (2021). Environmental and developmental factors driving xylem anatomy and micro-density in black spruce. *New Phytologist*, *230*(3), 957-971. <https://doi.org/10.1111/nph.17223>
- Buttò, V., Shishov, V., Tychkov, I., Popkova, M., He, M., Rossi, S., Deslauriers, A., & Morin, H. (2020). Comparing the Cell Dynamics of Tree-Ring Formation Observed in Microcores and as Predicted by the Vaganov–Shashkin Model. *Frontiers in Plant Science*, *11*, 1268-1268. <https://doi.org/10.3389/fpls.2020.01268>
- Carteni, F., Deslauriers, A., Rossi, S., Morin, H., De Micco, V., Mazzoleni, S., & Giannino, F. (2018). The physiological mechanisms behind the earlywood-to-latewood transition: A process-based modeling approach. *Frontiers in Plant Science*, *9*, 1053-1053. <https://doi.org/10.3389/fpls.2018.01053>
- Chen, J., Ter-Mikaelian, M. T., Ng, P. Q., & Colombo, S. J. (2018). Ontario's managed forests and harvested wood products contribute to greenhouse gas mitigation from 2020 to 2100. *Forestry Chronicle*, *43*(3), 269-282. <https://doi.org/10.5558/tfc2018-040>
- Chuine, I. (2010). Why does phenology drive species distribution? *Philosophical Transactions of the Royal Society B: Biological Sciences*, *365*(1555), 3149-3160. <https://doi.org/10.1098/rstb.2010.0142>

- Cuny, H. E., Rathgeber, C. B. K., Frank, D., Fonti, P., & Fournier, M. (2014). Kinetics of tracheid development explain conifer tree-ring structure. *New Phytologist*, 203(4), 1231-1241. <https://doi.org/10.1111/nph.12871>
- Deslauriers, A., Huang, J. G., Balducci, L., Beaulieu, M., & Rossi, S. (2016). The contribution of carbon and water in modulating wood formation in black spruce saplings. *Plant Physiology*, 170(4), 2072-2084. <https://doi.org/10.1104/pp.15.01525>
- Deslauriers, A., Morin, H., & Begin, Y. (2003). Cellular phenology of annual ring formation of *Abies balsamea* in the Quebec boreal forest (Canada). *Canadian Journal of Forest Research*, 33(2), 190-200. <https://doi.org/10.1139/x02-178>
- Dória, L. C., Sonsin-Oliveira, J., Rossi, S., & Marcati, C. R. (2022). Functional trade-offs in volume allocation to xylem cell types in 75 species from the Brazilian savanna Cerrado. *Annals of Botany*, 130(3), 445-456. <https://doi.org/10.1093/aob/mcac095>
- Dow, C., Kim, A. Y., D'Orangeville, L., Gonzalez-Akre, E. B., Helcoski, R., Herrmann, V., Harley, G. L., Maxwell, J. T., McGregor, I. R., McShea, W. J., McMahon, S. M., Pederson, N., Tepley, A. J., & Anderson-Teixeira, K. J. (2022). Warm springs alter timing but not total growth of temperate deciduous trees. *Nature*, 608(7923), 552-557. <https://doi.org/10.1038/s41586-022-05092-3>
- Eriksson, L. O., Gustavsson, L., Hänninen, R., Kallio, M., Lyhykäinen, H., Pingoud, K., Pohjola, J., Sathre, R., Solberg, B., Svanaes, J., & Valsta, L. (2012). Climate change mitigation through increased wood use in the European construction sector-towards an integrated modelling framework. *European Journal of Forest Research*, 131(1), 131-144. <https://doi.org/10.1007/s10342-010-0463-3>
- Fang, J., Kato, T., Guo, Z., Yang, Y., Hu, H., Shen, H., Zhao, X., Kishimoto-Mo, A. W., Tang, Y., & Houghton, R. A. (2014). Evidence for environmentally enhanced forest growth. *Proceedings of the National Academy of Sciences of the United States of America*, 111(26), 9527-9532. <https://doi.org/10.1073/pnas.1402333111>
- Filion, L., & Cournoyer, L. (1995). Variation in wood structure of eastern larch defoliated by the larch sawfly in subarctic Quebec, Canada. *Canadian Journal of Forest Research*, 25(8), 1263-1268. <https://doi.org/10.1139/x95-139>
- Fu, P. L., Griebinger, J., Gebrekirstos, A., Fan, Z. X., & Bräuning, A. (2017). Earlywood and latewood stable carbon and oxygen isotope variations in two pine species in Southwestern China during the recent decades. *Frontiers in Plant Science*, 7, 2050-2050. <https://doi.org/10.3389/FPLS.2016.02050/BIBTEX>

- Gao, S., Liang, E., Liu, R., Babst, F., Camarero, J. J., Fu, Y. H., Piao, S., Rossi, S., Shen, M., Wang, T., & Peñuelas, J. (2022). An earlier start of the thermal growing season enhances tree growth in cold humid areas but not in dry areas. *Nature Ecology and Evolution*, 1-8. <https://doi.org/10.1038/s41559-022-01668-4>
- Gonsamo, A., Chen, J. M., & Ooi, Y. W. (2018). Peak season plant activity shift towards spring is reflected by increasing carbon uptake by extratropical ecosystems. *Global Change Biology*, 24(5), 2117-2128. <https://doi.org/10.1111/gcb.14001>
- Hansen, J., & Beck, E. (1990). The fate and path of assimilation products in the stem of 8-year-old Scots pine (*Pinus sylvestris* L.) trees. *Trees*, 4(1), 16-21. <https://doi.org/10.1007/BF00226235>
- Howard, C., Dymond, C. C., Griess, V. C., Tolkien-Spurr, D., & van Kooten, G. C. (2021). Wood product carbon substitution benefits: a critical review of assumptions. *Carbon Balance and Management*, 16(1), 1-11. <https://doi.org/10.1186/s13021-021-00171-w>
- Kagawa, A., Sugimoto, A., & Maximov, T. C. (2006). ¹³C pulse-labelling of photoassimilates reveals carbon allocation within and between tree rings. *Plant, Cell and Environment*, 29(8), 1571-1584. <https://doi.org/10.1111/j.1365-3040.2006.01533.x>
- Koga, S., & Zhang, S. Y. (2002). Relationships between wood density and annual growth rate components in balsam fir (*Abies balsamea*). *Wood and Fiber Science*, 34(1), 146-157. <https://wfs.swst.org/index.php/wfs/article/view/127>
- Li, X., Liang, E., Gričar, J., Prislán, P., Rossi, S., & Čufar, K. (2013). Age dependence of xylogenesis and its climatic sensitivity in Smith fir on the south-eastern Tibetan Plateau. *Tree Physiology*, 33(1), 48-56. <https://doi.org/10.1093/treephys/tps113>
- Linares, J. C., Camarero, J. J., & Carreira, J. A. (2009). Plastic responses of *Abies pinsapo* xylogenesis to drought and competition. *Tree Physiology*, 29(12), 1525-1536. <https://doi.org/10.1093/treephys/tpp084>
- Messier, C., Doucet, R., Ruel, J. C., Claveau, Y., Kelly, C., & Lechowicz, M. J. (1999). Functional ecology of advance regeneration in relation to light in boreal forests. *Canadian Journal of Forest Research*, 29(6), 812-823. <https://doi.org/10.1139/x99-070>
- Oribe, Y., Funada, R., & Kubo, T. (2003). Relationships between cambial activity, cell differentiation and the localization of starch in storage tissues around the cambium in locally heated stems of *Abies sachalinensis* (Schmidt) Masters. *Trees - Structure and Function*, 17(3), 185-192. <https://doi.org/10.1007/s00468-002-0231-1>

- Paixao, C., Krause, C., Morin, H., & Achim, A. (2019). Wood quality of black spruce and balsam fir trees defoliated by spruce budworm: A case study in the boreal forest of Quebec, Canada. *Forest Ecology and Management*, 437, 201-210. <https://doi.org/10.1016/j.foreco.2019.01.032>
- Pan, Y., Birdsey, R. A., Fang, J., Houghton, R., Kauppi, P. E., Kurz, W. A., Phillips, O. L., Shvidenko, A., Lewis, S. L., Canadell, J. G., Ciais, P., Jackson, R. B., Pacala, S. W., McGuire, A. D., Piao, S., Rautiainen, A., Sitch, S., & Hayes, D. (2011). A large and persistent carbon sink in the world's forests. *Science*, 333(6045), 988-993. <https://doi.org/10.1126/science.1201609>
- Perrin, M., Rossi, S., & Isabel, N. (2017). Synchronisms between bud and cambium phenology in black spruce: Early-flushing provenances exhibit early xylem formation. *Tree Physiology*, 37(5), 593-603. <https://doi.org/10.1093/treephys/tpx019>
- Pothier, D., Elie, J. G., Auger, I., Mailly, D., & Gaudreault, M. (2012). Spruce budworm-caused mortality to balsam fir and black spruce in pure and mixed conifer stands. *Forest Science*, 58(1), 24-33. <https://doi.org/10.5849/forsci.10-110>
- Pretzsch, H., Biber, P., Schütze, G., Kemmerer, J., & Uhl, E. (2018). Wood density reduced while wood volume growth accelerated in Central European forests since 1870. *Forest Ecology and Management*, 429, 589-616. <https://doi.org/10.1016/j.foreco.2018.07.045>
- Pretzsch, H., Biber, P., Schütze, G., Uhl, E., & Rötzer, T. (2014). Forest stand growth dynamics in Central Europe have accelerated since 1870. *Nature Communications*, 5(1), 1-10. <https://doi.org/10.1038/ncomms5967>
- Rathgeber, C. B. K., Cuny, H. E., & Fonti, P. (2016). Biological basis of tree-ring formation: A crash course. *Frontiers in Plant Science*, 7(MAY2016), 734-734. <https://doi.org/10.3389/fpls.2016.00734>
- Rathgeber, C. B. K., Decoux, V., & Leban, J. M. (2006). Linking intra-tree-ring wood density variations and tracheid anatomical characteristics in Douglas fir (*Pseudotsuga menziesii* (Mirb.) Franco). *Annals of Forest Science*, 63(7), 699-706. <https://doi.org/10.1051/forest:2006050>
- Rathgeber, C. B. K., Pérez-De-Lis, G., Fernández-De-Uña, L., Fonti, P., Rossi, S., Treydte, K., Gessler, A., Deslauriers, A., Fonti, M. V., Ponton, S., Rathgeber, C. B. K., Fonti, P., Treydte, K., Gessler, A., Rossi, S., Deslauriers, A., Gessler, A., & Fonti, M. V. (2022). Anatomical, Developmental and Physiological Bases of Tree-Ring Formation in Relation to Environmental Factors. In R. T. W. Siegwolf, J. R. Brooks, J. Roden, & M. Saurer (Eds.), (Vol. 8, pp. 61-99). Springer, Cham. https://doi.org/10.1007/978-3-030-92698-4_3

- Rathgeber, C. B. K., Rossi, S., & Bontemps, J. D. (2011). Cambial activity related to tree size in a mature silver-fir plantation. *Annals of Botany*, 108(3), 429-438. <https://doi.org/10.1093/aob/mcr168>
- Reyer, C., Lasch-Born, P., Suckow, F., Gutsch, M., Murawski, A., & Pilz, T. (2014). Projections of regional changes in forest net primary productivity for different tree species in Europe driven by climate change and carbon dioxide. *Annals of Forest Science*, 71(2), 211-225. <https://doi.org/10.1007/s13595-013-0306-8>
- Rossi, S., Anfodillo, T., & Menardi, R. (2006). Trephor: A new tool for sampling microcores from tree stems. *IAWA Journal*, 27(1), 89-97. <https://doi.org/10.1163/22941932-90000139>
- Rossi, S., Cairo, E., Krause, C., & Deslauriers, A. (2015). Growth and basic wood properties of black spruce along an alti-latitudinal gradient in Quebec, Canada. *Annals of Forest Science*, 72(1), 77-87. <https://doi.org/10.1007/s13595-014-0399-8>
- Rossi, S., Deslauriers, A., & Anfodillo, T. (2006). Assessment of cambial activity and xylogenesis by microsampling tree species: An example at the Alpine timberline. *IAWA Journal*, 27(4), 383-394. <https://doi.org/10.1163/22941932-90000161>
- Rossi, S., Girard, M. J., & Morin, H. (2014). Lengthening of the duration of xylogenesis engenders disproportionate increases in xylem production. *Global Change Biology*, 20(7), 2261-2271. <https://doi.org/10.1111/gcb.12470>
- Rossi, S., Morin, H., & Deslauriers, A. (2012). Causes and correlations in cambium phenology: towards an integrated framework of xylogenesis. *Journal of Experimental Botany*, 63(5), 2117-2126. <https://doi.org/10.1093/jxb/err423>
- Schrader, J., Baba, K., May, S. T., Palme, K., Bennett, M., Bhalerao, R. P., & Sandberg, G. (2003). Polar auxin transport in the wood-forming tissues of hybrid aspen is under simultaneous control of developmental and environmental signals. *Proceedings of the National Academy of Sciences of the United States of America*, 100(17), 10096-10101. <https://doi.org/10.1073/pnas.1633693100>
- Shi, J. L., Riedl, B., Deng, J., Cloutier, A., & Zhang, S. Y. (2007). Impact of log position in the tree on mechanical and physical properties of black spruce medium-density fibreboard panels. *Canadian Journal of Forest Research*, 37(5), 866-873. <https://doi.org/10.1139/X06-268>
- Silvestro, R., Brasseur, S., Klisz, M., Mencuccini, M., & Rossi, S. (2020). Bioclimatic distance and performance of apical shoot extension: Disentangling the role of growth rate and duration in ecotypic differentiation. *Forest Ecology and Management*, 477. <https://doi.org/10.1016/j.foreco.2020.118483>

- Silvestro, R., Rossi, S., Zhang, S., Froment, I., Huang, J. G., & Saracino, A. (2019). From phenology to forest management: Ecotypes selection can avoid early or late frosts, but not both. *Forest Ecology and Management*, 436, 21-26. <https://doi.org/10.1016/j.foreco.2019.01.005>
- Silvestro, R., Sylvain, J.-D., Drolet, G., Buttò, V., Auger, I., Mencuccini, M., & Rossi, S. (2022). Upscaling xylem phenology: Sample size matters. *Annals of Botany*, 1-13. <https://doi.org/10.1093/aob/mcac110>
- Soil Classification Working, G. (1998). *The Canadian System of Soil Classification*. https://books.google.ca/books?hl=it&lr=&id=4aHVg18eDLYC&oi=fnd&pg=PR10&dq=soil+classification+working+group+1998&ots=GqFnXwNFJz&sig=_9vVicb8QVkrWpwIUf8l_jjQZg#v=onepage&q&f=false
- Verkerk, P. J., Hasegawa, M., Van Brusselen, J., Cramm, M., Chen, X., Maximo, Y. I., Koç, M., Lovrić, M., & Tegegne, Y. T. (2022). *Forest products in the global bioeconomy*.
- Wodzicki, T. J., & Zajaczkowski, S. (1970). Methodical problems in studies on seasonal production of cambial xylem derivatives. *Acta Societatis Botanicorum Poloniae*, 39(3), 519-520. <https://doi.org/10.5586/asbp.1970.040>

CHAPTER V

PARTIAL ASYNCHRONY OF FOREST CARBON SOURCES AND SINKS AT THE INTRA-ANNUAL TIME SCALE

Submitted to Nature Communications

Current status: Major revisions received

RESEARCH ARTICLE**Title**

Bridging forest carbon sources and sinks through intra-annual growth assessment.

Authors:

Silvestro, R.¹, Mencuccini, M.^{2,3}, García-Valdés, R.⁴, Antonucci, S.⁵, Arzac, A.⁶, Biondi, F.⁷, Buttò, V.^{8,1}, Camarero, J. J.⁹, Campelo, F.¹⁰, Cochard, H.¹¹, Čufar, K.¹², Cuny, H. E.¹³, De Luis, M.¹⁴, Deslauriers, A.¹, Drolet, G.¹⁵, Fonti, M. V.¹⁶, Fonti, P.¹⁶, Giovannelli, A.¹⁷, Gričar, J.¹⁸, Gruber, A.¹⁹, Gryc, V.²⁰, Guerrieri, R.^{21, 2}, Güney, A.²², Guo, X.²³, Huang, J. G.^{24,25}, Jyske, T.²⁶, Kašpar, J.²⁷, Kirilyanov, A.V.^{6,28,29}, Klein, T.³⁰, Lemay, A.¹, Li, X.³¹, Liang, E.³¹, Lintunen A. M.^{32,33}, Liu, F.³⁴, Lombardi, F.³⁵, Ma, Q.^{36,34}, Mäkinen, H.²⁶, Malik, R.A.³⁷, Martinez del Castillo, E.³⁸, Martinez-Vilalta, J.^{2,39}, Mayr, S.¹⁹, Morin, H.¹, Nabais, C.¹⁰, Nöjd, P.²⁶, Oberhuber, W.¹⁹, Olano, J. M.⁴⁰, Ouimette A. P.⁴¹, Paljakka, T. V. S.³³, Peltoniemi, M.⁴², Peters, R. L.^{16,43}, Ping, R.³⁶, Prislan, P.¹², Rathgeber, C. B. K.⁴⁴, Sala, A.⁴⁵, Saracino, A.⁴⁶, Saulino, L.⁴⁶, Schiestl-Aalto, P.⁴⁷, Shishov, V.⁶, Stokes, A.⁴⁸, Sukumar, R.³⁷, Sylvain, J. D.¹⁵, Tognetti, R.⁵, Treml, T.²⁷, Urban, J.⁴⁹, Vavrčik, H.²⁰, Vieira, J.⁵⁰, von Arx, G.^{51,52}, Wang, Y.⁴⁸, Yang, B.⁵³, Qiao, Z.⁵⁴, Zhang, S.^{36,34}, Ziaco, E.³⁸, Rossi, S.¹

Affiliations:

¹ Laboratoire sur les écosystèmes terrestres boreaux, Département des Sciences Fondamentales, Université du Québec à Chicoutimi, 555 boulevard de l'Université, Chicoutimi, QC G7H2B1, Canada.

² CREAM, E08193 Bellaterra (Cerdanyola del Vallès), Catalonia, Spain.

³ Institució Catalana de Recerca i Estudis Avançats (ICREA), Passeig de Lluís Companys 23, 08010 Barcelona, Spain.

⁴ Department of Biology and Geology, Physics and Inorganic Chemistry, Rey Juan Carlos University, c/ Tulipán s/n, 28933 Móstoles, Spain.

⁵ Dipartimento di Agricoltura, Ambiente e Alimenti, Università degli Studi del Molise, 86100 Campobasso, Italy.

⁶ Siberian Federal University, 79 Svobodny pr., 660041 Krasnoyarsk, Russia.

⁷ DendroLab, Department of Natural Resources and Environmental Science, University of Nevada, Reno, NV 89557, USA.

⁸ Forest Research Institute, Université du Québec en Abitibi-Témiscamingue, Rouyn-Noranda, QC, Canada.

⁹ Instituto Pirenaico de Ecología, Consejo Superior de Investigaciones Científicas, 50192 Zaragoza, Spain.

¹⁰ Centre for Functional Ecology, Department of Life Sciences, University of Coimbra, 3000-456 Coimbra, Portugal.

¹¹ Université Clermont Auvergne, INRAE, PIAF, 63000, Clermont-Ferrand, France.

¹² Biotechnical Faculty, University of Ljubljana, 1000 Ljubljana, Slovenia.

¹³ Institut National de Information Géographique et Forestière (IGN), 54250 Champigneulle, France.

¹⁴ Department of Geography and Regional Planning, Environmental Science Institute, University of Zaragoza, 50009 Zaragoza, Spain.

¹⁵ Direction de la Recherche Forestière, Ministère des Ressources Naturelles et des Forêts du Québec, 2700 rue Einstein, Québec, QC G1P 3W8, Canada.

¹⁶ Swiss Federal Institute for Forest, Snow and Landscape Research WSL, Zürcherstrasse 111, CH-8903 Birmensdorf, Switzerland.

¹⁷ Istituto di Ricerca sugli Ecosistemi Terrestri, Consiglio Nazionale delle Ricerche, 50019 Sesto Fiorentino, Italy.

¹⁸ Laboratory for Dendrochronology, Slovenian Forestry Institute, 1000 Ljubljana, Slovenia

¹⁹ Department of Botany, Leopold-Franzens University of Innsbruck, 6020 Innsbruck, Austria.

²⁰ Department of Wood Science and Wood Technology, Mendel University in Brno, 61300 Brno, Czech Republic.

²¹ Department of Agricultural and Food Sciences, University of Bologna, 40127, Bologna, Italy.

²² Izmir Katip Çelebi University, Faculty of Forestry, Izmir, Turkey.

²³ College of Forestry, Guangxi Key Laboratory of Forest Ecology and Conservation, Guangxi University, Daxue East Road 100, Nanning, Guangxi 530004, China.

²⁴ Key Laboratory of Desert and Desertification, Northwest Institute of Eco-Environment and Resources, Chinese Academy of Sciences, Lanzhou, China.

²⁵ College of Life Sciences, Zhejiang University, Hangzhou, China, 866 Yuhangtang Road, Xihu District, Hangzhou, China 310058.

²⁶ Natural Resources Institute Finland, Latokartanonkaari 9, 00790 Helsinki, Finland.

- ²⁷ Department of Physical Geography and Geoecology, Charles University, CZ-12843 Prague, Czech Republic.
- ²⁸ V.N. Sukachev Institute of Forest SB RAS, Federal Research Center 'Krasnoyarsk Science Center SB RAS, 660036 Krasnoyarsk, Akademgorodok, Russia.
- ²⁹ Department of Geography, University of Cambridge, Cambridge, CB2 3EN, United Kingdom.
- ³⁰ Department of Plant and Environmental Sciences, Weizmann Institute of Science, Rehovot 76100, Israel.
- ³¹ State Key Laboratory of Tibetan Plateau Earth System, Environment and Resources (TPESER), Institute of Tibetan Plateau Research, Chinese Academy of Sciences, Beijing 100101, China.
- ³² Institute for Atmospheric and Earth System Research / Physics, Faculty of Science, P.O. Box 68, FI-00014 University of Helsinki, Helsinki, Finland.
- ³³ Institute for Atmospheric and Earth System Research / Forest Sciences, Faculty of Agriculture and Forestry, P.O. Box 27, FI-00014 University of Helsinki, Helsinki, Finland.
- ³⁴ South China National Botanical Garden, Guangzhou 510650, China.
- ³⁵ Dipartimento di Agraria, Università Mediterranea di Reggio Calabria, 89122 Reggio Calabria, Italy.
- ³⁶ Key Laboratory of Vegetation Restoration and Management of Degraded Ecosystems, Guangdong Provincial Key Laboratory of Applied Botany, South China Botanical Garden, Chinese Academy of Sciences, Guangzhou 510650, China.

- ³⁷ Centre for Ecological Sciences, Indian Institute of Science (IISc), Bangalore, 560012, India.
- ³⁸ Institute of Geography, Johannes Gutenberg University Mainz, Germany.
- ³⁹ Universitat Autònoma de Barcelona, E08193 Bellaterra (Cerdanyola del Vallès), Catalonia, Spain.
- ⁴⁰ EIFAB – iuFOR. Universidad de Valladolid, Campus Duques de Soria, E-42004 Soria, Spain.
- ⁴¹ Earth Systems Research Center, Institute for the Study of Earth, Oceans, and Space, University of New Hampshire, Durham, NH, USA.
- ⁴² National Resources Institute (Luke), Helsinki, Finland.
- ⁴³ Laboratory of Plant Ecology, Department of Plants and Crops, Faculty of Bioscience Engineering, Ghent University, B-9000 Ghent, Belgium.
- ⁴⁴ Université de Lorraine, AgroParisTech, INRAE, SILVA, F-54000 Nancy, France.
- ⁴⁵ Division of Biological Sciences, University of Montana, Missoula, MT, USA.
- ⁴⁶ Department of Agricultural Sciences, University of Naples Federico II, I-80055 Portici, Napoli, Italy.
- ⁴⁷ Institute for Atmospheric and Earth System Research (INAR)/Physics, Helsinki, Finland.
- ⁴⁸ AMAP, INRAE, IRD, CIRAD, CNRS, and University of Montpellier, Montpellier, France.

⁴⁹ Department of Forest Botany, Dendrology and Geobiocenology, Faculty of Forestry and Wood Technology, Mendel University in Brno, Zemedelska 1, 61300 Brno, Czech Republic.

⁵⁰ CoLAB ForestWISE - Collaborative Laboratory for Integrated Forest & Fire Management, Quinta de Prados, 5000-801 Vila Real, Portugal.

⁵¹ Swiss Federal Institute for Forest Snow and Landscape Research WSL, Zuercherstrasse 111, CH-8903 Birmensdorf, Switzerland.

⁵² Oeschger Centre for Climate Change Research, University of Bern, Hochschulstrasse 4, CH-3012 Bern, Switzerland.

⁵³ School of Geograph and Oceanograph Sciences, Nanjing University, Nanjing 210093, China.

⁵⁴ Guangdong Open Laboratory of Geospatial Information Technology and Application, Guangzhou Institute of Geography, Guangdong Academy of Sciences, Guangzhou 510070, China.

5.1 Abstract

As major terrestrial carbon sinks, forests play an important role in mitigating climate change. Despite decades of work, the relationship between the seasonal uptake of carbon and its allocation to woody biomass remains poorly understood, leaving a significant gap in our capacity to predict carbon sequestration by forests. Here, we provide a comparative analysis of the intra-annual dynamics of carbon fluxes and wood formation across the Northern hemisphere in boreal, temperate and Mediterranean biomes, from carbon assimilation and the formation of non-structural carbon compounds to their incorporation in woody tissues of conifers. Our findings revealed temporally coupled seasonal peaks of carbon assimilation (GPP) and wood cell differentiation, while the two processes were substantially decoupled during off-peak periods. Peaks of cambial activity occurred substantially earlier compared to GPP, highlighting the buffer role of non-structural carbohydrates between the processes of carbon assimilation and allocation to wood. These results highlight the importance of examining high-resolution seasonal patterns of ecosystem carbon fluxes, wood formation and the associated physiological processes to better understand the carbon cycle in forest ecosystems. Such an assessment can help reduce uncertainties in carbon source-sink relationships at different spatial scales, from stand to ecosystem levels.

5.2 Introduction

In the Northern Hemisphere, the atmospheric CO₂ concentration undergoes a seasonal annual cycle ranging from 6 to 19 ppm, a net result of intra-annual fluxes greater than those from annual anthropogenic emissions (Graven et al., 2013). This cycle is driven by the seasonal dynamics of terrestrial plant activity, i.e., the balance between the two main processes determining net accumulation of carbon (C) in the biosphere: gross primary production (GPP) and ecosystem respiration (RECO). GPP represents the total amount of CO₂ assimilated by the ecosystem, the result of the photosynthetic process. RECO represents the release of CO₂ to the atmosphere by oxidation of C compounds in vegetation and soil.

Once absorbed by leaves, atmospheric C undergoes a set of chemical reactions that lead to the formation of C compounds (Martínez-Vilalta et al., 2016), a process known as C assimilation. The assimilated C is used as fundamental bricks to support plant growth and sustain the consequent respiratory costs. Among all plant tissues, wood is the main reservoir for long-term C sequestration, and its formation represents a highly C-demanding process (Friend et al., 2019). During wood formation, C resources supply energy for cell division, contribute to generate and maintain turgor pressure during cell expansion, and are used to build complex compounds required for cell wall thickening and lignification (Deslauriers et al., 2016). During this process, a substantial fraction of C is released again into the atmosphere through respiration (Cuny et al., 2015; Muller et al., 2011), a fraction thought to comprise up to 40% of total respiration from vegetation (Yang et al., 2016).

Historically, scientists have considered photosynthesis as a main driver of stem growth (source limitation) (Friend et al., 2019). However, in recent decades, several studies have

suggested that direct environmental and developmental constraints control wood growth (sink limitation) (Fatichi et al., 2014; Körner, 2003). Nowadays, the extent to which stem growth is linked to carbon assimilation and their respective temporal relationships are still not completely understood. The temporal relationships between C assimilation and biomass production are the key to solve one of the largest sources of uncertainty in global vegetation models because the feedbacks of processes between terrestrial ecosystems and atmosphere are at the basis of the global C cycle (Friend et al., 2019). Moreover, environmental drivers, mainly temperature and precipitations, affect C assimilation and wood formation in different ways (Balducci et al., 2016). Thus, climate change might alter the C partitioning to the stem and affect the potential of net C sequestration in wood and the productivity of forests. For this reason, improvements in understanding the chronological sequence of growth phenological events and associated processes are crucial for a better understanding of C sequestration in woody tissues.

Previous meta-analyses have shown that northern conifers synchronize the activity of meristems with local climate, concentrating the timings of wood formation within precise time windows (Rossi et al., 2016) when the environmental conditions are favourable for growth (Huang et al., 2020; Rossi et al., 2016). Similarly to wood formation, ecosystem C fluxes in forests have clear seasonal patterns according to thermal and precipitation gradients (Xu et al., 2014). Several studies have tried to disentangle the temporal and functional relationship between ecosystem productivity and forest biomass production (Vicente-Serrano et al., 2020). Nowadays, the possibility to use direct measurements and multi-year records of ecosystem C fluxes from eddy-covariance (EC) stations in forests has greatly increased the potential of assessing the association between C fluxes at ecosystem scale with wood production. However, these analyses have proposed different

or even contrasting conclusions. While some studies found strong correlations between source and sink activities (McKenzie et al., 2021; Metsaranta et al., 2021; Puchi et al., 2023; Teets et al., 2018; Tei et al., 2019; Xu et al., 2017), others lacked in significant results (Cabon et al., 2022; Delpierre et al., 2016; Krejza et al., 2022; Oddi et al., 2022; Rocha et al., 2006).

The contrasting results reported by the literature in the last decades (Cabon et al., 2022; Delpierre et al., 2016; Krejza et al., 2022; McKenzie et al., 2021; Metsaranta et al., 2021; Oddi et al., 2022; Puchi et al., 2023; Rocha et al., 2006; Teets et al., 2018; Tei et al., 2019; Xu et al., 2017) could be explained by the different approaches employed to address the complex issue of assessing temporal relationships between these processes. In this context, some studies have explored temporal relationships between source and sink activities, focusing on interannual patterns. At a global scale, in particular, eddy covariance GPP records have been shown to be largely decoupled from tree growth at the inter-annual time scale (Cabon et al., 2022). Several reasons were proposed to explain this asynchrony, e.g., stored carbohydrates may provide much of the C necessary for growth during certain growth stages, and the seasonal dynamics of GPP and wood formation may substantially differ from one another. Nevertheless, it is crucial to highlight the importance of precisely defining the temporal resolution when investigating the temporal dynamics of specific processes. Indeed, studies conducted at annual resolution cannot assess physiological processes occurring during seasonal growth and the underlying mechanisms may significantly vary within and across years. This issue should be addressed with observations performed at higher temporal resolution because intra-annual growth-related physiological processes may demonstrate a buffering effect, possibly desynchronizing source and sink activities. A detailed analysis of these processes

and the examination of their seasonal patterns at intra-annual scale may provide a more comprehensive understanding of the C cycle in forest ecosystems and quantify the degree of synchrony between C sources and sinks at different spatial scales, from stand to ecosystem.

This study aims to provide a comparative analysis of the intra-annual dynamics of C fluxes and wood formation, from C assimilation and the formation of non-structural compounds to their incorporation in woody tissues in conifers of the Northern hemisphere. Specifically, we generated a new database combining intra-annual data of 1) ecosystem-scale NEE (Net Ecosystem Exchange, the measure of net exchange of C between an ecosystem and the atmosphere per unit ground area (Waring & Running, 2007)), GPP and RECO, 2) non-structural carbohydrates (NSC) concentrations in various tissues (needles, stems, roots), and 3) observations of cambial activity (i.e. cambial cell division) and wood formation (i.e. xylem cell differentiation) of 39 conifer species in boreal, temperate and Mediterranean biomes. We use this dataset to: 1) identify and describe the seasonal patterns of these processes; 2) assess the co-occurrence of seasonal peak and off-peak periods among processes; and, specifically, 3) determine the temporal relationships between C assimilation and wood formation at intra-annual scale. Given the high C-demanding nature of wood formation, we hypothesize that a synchronization should exist between the seasonal peaks in carbon assimilation and cell differentiation during wood formation.

5.3 Materials and Methods

5.3.1 Data selection

This study used data collected in 177 sites of boreal, temperate and Mediterranean biomes across the Northern hemisphere (Figure 5.1). The sites are located in North America, Europe and Asia, and distributed over latitudes from 23 to 68 °N and elevations reaching 3,850 m a.s.l. (Figure 5.1). The sites were assigned to a specific biome based on information in the papers from which the data were extracted. The study covers 38 coniferous species belonging to eight genera (Table S5.2). The dataset consists of the temporal dynamics of wood formation, i.e. cambial activity and xylem differentiation (81 sites), non-structural carbohydrates, i.e. starch and soluble sugars in needles, stem and roots (57 sites), and C fluxes, i.e. Net Ecosystem Exchange (NEE), Ecosystem Respiration (RECO), and Gross Primary Production (GPP) (39 sites), this latter dataset extracted from the FLUXNET2015 dataset (Pastorello et al., 2020). The observations collected in the sites where wood formation was monitored were combined with estimates of gross primary production (GPP) using modelled data from FluxSat v2.0 (Joiner & Yoshida, 2021). FluxSat outputs consist of a gridded GPP product obtained by upscaling FLUXNET data using MODIS reflectance (Joiner & Yoshida, 2021). Details on site selection and assembly of the datasets can be found in supplementary material 1, while site information, coordinates, and data sources are reported in supplementary material 2.

5.3.2 Bioclimatic analyses

To assess the climatic differences among sites where wood formation has been monitored, we collected bioclimatic data from the CHELSA bioclimatic database V2.1 (Karger et al., 2017; Karger et al., 2021) with a spatial resolution of 30 arcseconds. Out of the 19

available bioclimatic parameters (Karger et al., 2017; Karger et al., 2021), we selected seven variables (Table S6.1), excluding those that provided overly general descriptions of climate (e.g., annual temperature and precipitation) and removing variables that were highly correlated with each other ($r > |0.7|$). Subsequently, to group the study sites based on their climate-related characteristics, we applied the Partitioning Around Medoids (PAM) clustering algorithm, which is an extension of the k-means clustering algorithm (Kaufman & Rousseeuw, 1987). To determine the optimal number of clusters, we utilized the Within-Sum-of-Squares method (WSS), which minimizes the distance between points within each cluster. Therefore, we determined that four clusters were the optimal choice for grouping the wood formation study sites. We then conducted a Principal Component Analysis (PCA) on the bioclimatic variables to determine the climatic classification of our 81 sites. Pearson's correlation coefficient was employed to identify the climatic factors that influenced the ordering of wood formation study sites by principal components (Table S5.1).

5.3.3 Assessment of seasonal patterns

The seasonal patterns of wood formation (i.e., cambial activity and xylem cell differentiation), NSC concentrations (i.e., starch and soluble sugars in needles, stem and roots) and C flux (i.e., NEE, GPP, RECO) for each biome were determined by performing non-linear regressions on data normalised between 0 and 1. The normalisation was performed to reduce the variability within the same range and compare the temporal dynamics among sites. We applied two non-linear parametric functions that are a generalisation of the normal distribution, skewed normal distribution (Azzalini, 2013) and the V-type exponential curve (Sit & Poulin-Costello, 1994). The former allows for non-zero skewness, the latter is a symmetric curve that describes concave, convex and

linear shapes. The skewed curve, enabling curve asymmetry, was preferred over the exponential curve, which was used only when data had a concave or linear-like shape not allowed by the first curve.

The skewed normal distribution curve (Azzalini, 2013) is given by the following formula:

$$\text{Seasonal pattern} = \frac{1}{\omega * \sqrt{2\pi}} * e^{\left(\frac{1}{2} * \left(\frac{t-\xi}{\omega}\right)^2\right) * \left(1 + \text{erf} * \left(\alpha * \left(\frac{t-\xi}{\omega * \sqrt{2}}\right)\right)\right)}$$

$$\text{erf}_z = \text{error function} = \frac{2}{\sqrt{\pi}} \int_0^z e^{-t^2} dt$$

Where ξ represents the location parameter, which determines the "location" or shift of the distribution; ω represents the scale parameter; α represents the shape or form parameter. This parameter skews the normal distribution to the left or right. The time is represented by t , included as a month for NSC seasonal pattern and DOY (day of the year) for wood formation and C fluxes.

The V-type exponential curve (Sit & Poulin-Costello, 1994) is given by the following formula:

$$\text{Seasonal pattern} = Y_{max} * \mu^{(t - X_{max})^2}$$

Where μ controls the growth rate of the curve; parameter Y_{max} controls the height (Y-value) of function maximum or minimum; parameter X_{max} controls the location (X-value) of the function maximum or minimum. The curve has a minimum for $Y_{max} > 0$ and $X_{max} > 1$, and a maximum for $Y_{max} > 0$ and $X_{max} < 1$. It is horizontal line (i.e., $Y = Y_{max}$) for $\mu = 1$. The time is represented by t , included as the month for NSC seasonal pattern and DOY (day of the year) for wood formation observations and C fluxes.

Each curve estimated the timing of the maximum value (or minimum while considering soluble sugar concentrations). In addition to this, fitted curves pertaining to the seasonal pattern of wood formation (i.e., cambial activity, cell enlargement, and cell wall thickening and lignification) and carbon fluxes derived from FluxNet data (i.e., NEE, GPP, and RECO) were utilized to estimate the timing of key percentiles, namely the 10th, 25th, 50th, 75th and 90th percentiles, for both the ascending and descending portions of the curves. We opted to use the 75th percentile as the threshold for defining the period of maximum activity. However, when the curve exhibited a minimum in soluble sugar concentrations, the period of maximum activity was determined based on the 25th percentile. We assessed the area under each curve (AUC) and assessed the AUC of the maximum activity itself by means of definite integrals by considering the period of maximum activity interval (supplementary material 3).

To assess functional scaling among biomes, we assessed the bivariate relationships between the timings of culmination of the GPP extracted from FluxSat, and wood formation using standardized major axis (SMA). Global scaling patterns (i.e., intercepts and slopes \pm 95% confidence intervals) were obtained from the fitted regressions. Slopes were compared between biomes using a likelihood ratio test (Warton et al., 2006). When the biomes had similar slopes, we tested for intercept differences using a Wald test (Warton et al., 2006).

To analyze the variability and influence of specific predictors on the timings of peaks of C fluxes and wood formation, we employed skewed normal distribution curves. These regressions delineated the seasonal patterns of cambial activity and xylem cell differentiation for each study year, species, site, and biome. The same methodology was applied to FluxNET (i.e., NEE, GPP, RECO) and FluxSat (i.e., GPP) data. For each

regression, the timings of the maximum value (i.e., peak timing) of each process was extracted. A random forest regression model was utilized to quantify the relative importance of predictors in determining the peak timing for each process.

For each process, we split the timings of the maximum values into a training set (80%) and a test set (20%) to assess the model performance. Five-fold cross-validation with five repetitions was employed as a resampling method to ensure more robust performance metrics. The goodness of fit for the regression models was evaluated using the coefficient of determination (R^2) for both the training and test sets, while the root mean squared error (RMSE) was employed to measure the accuracy of the models.

5.4 Results and discussion

5.4.1 Bioclimatic analysis

The dataset used in this work consists of observations collected at 177 sites belonging to boreal, temperate and Mediterranean biomes of the Northern hemisphere (Figure 5.1).

Bioclimatic analyses were conducted to establish a more precise climate-based classification of the study sites. However, since this bioclimatic analysis did not significantly enhance the subsequent outcomes, we have chosen to present, in this text, the results based on the classification according to the biome to which each site belongs (i.e., boreal, temperate, and Mediterranean). Detailed results of the bioclimatic classification and the subsequent analyses following this classification are provided in Supplementary Material 3.

5.4.2 Sources and sinks seasonal dynamics within and among biomes

The seasonal dynamics of wood formation (i.e., cambial activity, cell enlargement, and cell wall thickening and lignification), NSC (i.e., starch and soluble sugars in needles, stem and roots), and carbon fluxes (i.e., NEE, GPP and RECO) were fitted with skewed normal distribution or V-type exponential curves. All curves were significant (at least $p < 0.05$) with a residual standard error (RSE) ranging between 0.09 and 0.27 (Supplementary Material 3 - Table S5.3).

Seasonal peaks in C fluxes, NSC concentrations and number of cells during wood formation occur first in the Mediterranean biome, and later in the boreal biome (Figure 5.2 right-hand panel). Soluble sugars in roots represent the only exception in the Mediterranean biome, where the minimum concentration is substantially later than that in boreal and temperate biomes.

The boreal biome is characterized by very sharp peaks, concentrated in a short time window of almost 60 days in which the climatic conditions are favorable for C assimilation and the development of tissues (Rossi et al., 2016). All processes peak in the boreal biome from mid-May to mid-July (Figure 5.2). The growing season in the temperate biome last 73 days, from the beginning of May to the end of July (Figure 5.2). The Mediterranean biome has the longest growing season, from the beginning of April to the beginning of October, for a total of 170 days (Figure 5.2).

Within each biome, we observe a similar sequence of events during the growing season (Figure 5.2 left-hand panel). At the beginning of the growing season, the peaks of NEE and cambial activity are followed after 1 week by peaks of starch content in needles and stems, and often roots. The peaks in starch content are followed by peaks in cell enlargement. Subsequently, we observe in quick succession the peaks of GPP, RECO and cell wall thickening and lignification. The peak in cell enlargement precedes GPP by 13 days. The peak of GPP is followed by peaks of cell wall thickening and lignification by 9 days, and peaks of RECO by 12 days. Finally, we observe a sequential event of minimum concentrations of soluble sugars in all organs (i.e., needles, stem and roots) (Figure 5.2). Details of sampling and statistical fits are provided in Supplementary Material 3.

NEE reached a maximum 32 days before GPP, and 44 days before RECO (Figure 5.2). Our results generalize the evidence from local studies that NEE cumulates in spring, when the temperature and ecosystem respiration are still low (Falk et al., 2008). When respiration culminates in the summer, the photosynthetic rate is reduced by high vapor pressure deficit (Chen et al., 2004), which explains the short time gap between GPP and RECO. For this reason, the culmination of GPP and RECO are associated to reductions

in NEE (Falk et al., 2008). Our results suggest that NEE is unable to define the timing of long-term C storage during wood formation.

Assessment of the seasonal dynamics suggests that NSC may act as a buffer between C flux and the process of wood formation. The seasonal dynamics in NSC and their peaks in the different organs define two distinct periods of the growing season. A first period (i.e., early or late spring depending on the biome), characterized by a starch accumulation in plant organs lasting 51 days (average across biomes) (Figure 5.2). A second period (i.e., late spring or early summer depending on the biome), with low concentrations of soluble sugars, lasting 21 days (average across biomes) (Figure 5.2). Starch is a pure storage compound that may be severely depleted during tree growth, under harsh winter conditions, or after disturbance events (e.g., defoliation) (Carteni et al., 2023; Deslauriers et al., 2019). During the tree lifespan, starch plays a dual role in C allocation (MacNeill et al., 2017). Beyond its role as a long-term storage compound (especially in roots, tubers or seeds), starch can act as a sink in the form of a temporary C reserve (MacNeill et al., 2017). Starch is converted to soluble sugars in winter to promote cold tolerance (Gruber et al., 2011), and re-converted into starch at the beginning of the growing season (Carteni et al., 2023). Unlike starch, soluble sugars perform various immediate functions, including the supply for new growth, metabolism, osmoregulation, defence, and adopting the role of intermediary metabolites and substrates for transport (Hartmann & Trumbore, 2016). Soluble sugars, therefore, need to remain consistently above a physiological threshold (Dietze et al., 2014; Martínez-Vilalta et al., 2016).

5.4.3 Cambial activity and C assimilation

The peak of cambial activity in trees is uncoupled from the peaks of photosynthesis and ecosystem respiration (Figure 5.3 and 5.4). Standardized major axis (SMA) regressions

were all significant ($p < 0.05$, R^2 ranging from 0.21 to 0.81) (Table 6.1). Cambial activity peaked 30 to 60 days earlier than GPP, in the boreal and Mediterranean biome, respectively (Figure 5.4). Moreover, the slopes of these relationships differed significantly among biomes, ranging from 0.51 in the boreal biome to 0.98 in the Mediterranean biome (Table 5.1).

The highest rates of xylem cell division occur at the onset of the growing season, which explains the asynchrony between the peaks of cambial activity and GPP. The beginning of cell division corresponds with the peak of starch content (Figure 5.2) and the reactivation of primary growth, i.e. bud burst (Buttò et al., 2021). The relationship between primary and secondary growth is regulated by a physiological trade-off in which the two processes depend on one another but are also certainly in competition for the same resources (Buttò et al., 2021; Deslauriers et al., 2016). In this phase, developing buds represent a priority sink, supported mainly by new sugars produced with the photosynthesis occurring in old needles. In contrast, cambial cell division also relies on reserves stored in the stem rather than C translocated from the leaves (Begum et al., 2013; Deslauriers et al., 2019; Deslauriers et al., 2016; Fajstavr et al., 2019). During the growing season, the peak in cambial cell division represents a watershed moment in which the prioritization of resources changes to be finally committed to secondary growth. It is likely that the peak of cambial activity is reached when sufficient resources have been allocated to support cell differentiation, which may account for the coordination between peaks in cell division and accumulation in reserves (i.e. starch). Several regulation and post-translational processes are known to control the allocation to starch as well as the enzymatic hydrolysis of soluble sugars (MacNeill et al., 2017).

5.4.4 The sequence of C allocation in wood

Xylem peak of xylem cell differentiation is temporally coupled with the peak in photosynthesis and ecosystem respiration, suggesting a close relationship between C assimilation and allocation, and related respiratory costs (Figure 5.3). In all biomes, the culmination of GPP occurs 13 days later than the peak of cell enlargement, and 9 days earlier than the peak of wall thickening and lignification. The same results were obtained when the timing of cell differentiation phenological phases was compared with the estimated GPP extracted from FluxSat (Figure 5.4). The regressions comparing the timing of the peak of GPP and both cell enlargement and cell wall thickening and lignification phenological phase were all significant ($R^2=0.21-0.43$ for cell enlargement, and $R^2=0.31-0.81$ for cell wall thickening and lignification, both $p < 0.05$) (Table 5.1). In both phenological phases, the regressions presented a common slope across biomes of 0.78 for cell enlargement and 0.80 for cell wall thickening and lignification. Given that the slopes were not significantly different, we tested for differences in intercept (Table 5.1). The intercepts were statistically different across biomes, with the boreal biome showing the earliest peaks in both cell enlargement and cell wall thickening and lignification (Table 5.1 and Figure 5.4). The Mediterranean biome showed the latest peaks.

Photosynthesis and cell differentiation are synchronized across a wide spatial scale (Figure 5.3), probably because the two processes occur during the time window when environmental conditions are optimal for both. By considering the 10th percentiles of the fitted curves, the onset of photosynthesis occurs earlier (55 days, average across biomes) than the onset of cell differentiation during wood formation (i.e., onset of cell enlargement stage) (Figure 5.3, Table S5.7). Conversely, considering the 10th percentiles of the descending portions of the curve the ending of photosynthesis occurs later (33 days,

average across biomes) than the ending of cell differentiation (i.e., ending of cell wall thickening and lignification stage) (Figure 5.3, Table S5.7). As we progress towards the peaks of these processes, the time lag between GPP and wood formation gradually diminishes (Figure 5.3, Table S5.7). During the period of maximum activity (75th percentile, ascending portion of the curves), the time gap between GPP and the cell enlargement stage narrows to an average of 18 days across biomes, and 12 days across biomes between GPP and the cell wall thickening and lignification stage, in the descending portions of the curve (Figure 5.3, Table S5.7). This asynchrony for the onset and ending of these processes is linked to the different sensitivities of these processes to environmental drivers (Körner, 2003, 2012). Indeed, it is well known that growth-related processes, such as cell enlargement and the synthesis of cell wall and proteins are more sensitive to temperature and water stress than photosynthesis (Körner, 2003, 2015).

Photosynthesis is less constrained by environmental factors than meristematic activity and cell differentiation. In conifers, photosynthesis can occur as soon as leaf temperature is above freezing point, and the tree has sufficient water availability (Blechsmidt-Schneider, 1990). Moreover, photosynthesis can stop and reactivate according to changes in the weather (Lawlor & Tezara, 2009; Warren & Adams, 2004). On the contrary, the flexibility observed in C assimilation cannot be found in primary and secondary meristematic activity. These processes are triggered by a specific set of environmental cues that act as signals for reactivation during precise time windows, ensuring optimal growth while minimizing the risks of damage (Guo et al., 2021; Huang et al., 2020; Rossi et al., 2016; Silvestro et al., 2019). Unlike photosynthesis and the resulting C assimilation, the growth process cannot be completely stopped or resumed based on sudden changes in environmental factors during the growing season.

The peak of GPP falls between the preceding peak in cell enlargement (averaging 13 days across biomes) and the subsequent peak in cell wall thickening and lignification (averaging 8 days across biomes) (Figure 5.3). Cell division and cell enlargement are known to be turgor-driven processes, while secondary-wall formation is based on the supply of sugars (Carteni et al., 2018). In summer, once primary growth (i.e. shoot elongation) is completed, secondary growth (i.e. xylem formation) can benefit from a strong and continuous supply of carbohydrates (Carteni et al., 2018). At the peak of xylem development, specifically during latewood formation, the phloem pool acts as the ultimate C source for wood formation (Andreu-Hayles et al., 2022; Rinne et al., 2015). Accordingly, the growth process prevalently uses C assimilated during the current growing season (Andreu-Hayles et al., 2022; Kagawa et al., 2006; Kodama et al., 2008; Rinne et al., 2015). This synchronism between sink and source could explain the culmination of GPP between the peaks of cell enlargement and secondary wall formation: the moment the demand for C is higher, the supply is also greater.

5.4.5 Variance and predictors of phenological events

To determine whether the distribution of available data for the main processes of ecosystem fluxes and wood formation affected our conclusions, we used random forest regression models to assess the relative importance of study year, site, species and biome as predictors for the peak timing of NEE, GPP and RECO. These variables explained between 24 and 44% of the variance. Overall, the R^2 ranged between 0.72 and 0.96 for the training set and 0.49 to 0.68 for the test set (Table S5.8). Biome resulted as the most important predictor followed by site and study year across all models (Fig. S5.14). We observed the same pattern in the random forest model applied for FluxSat data (Figure 5.5), where the model explained 54.06% of the variance, showing an R^2 of 0.89 for the

training set and 0.66 for the test set (Table S6.8).

In the random forest regression models for the peak timing of cambial activity, cell enlargement, and cell wall thickening and lignification phases, the species of the monitored trees was also considered as a predictor alongside study year, site, and biome. These models explained from the 38.09 to the 43.09% of the variance, with R^2 ranging from 0.76 to 0.83 for the training set and from 0.70 to 0.83 for the test set (Table S5.8). The importance of the biome was confirmed, followed by site, species, and study year in each model (Figure 5.5). However, in the model for cambial activity, the species showed a greater importance than the site (Figure 5.5).

Biome emerged as the most influential predictor for the peak timing of both wood formation processes and ecosystem C fluxes. This result underscores the substantial role of the broader climatic context in shaping the temporal dynamics in source and sink activities. The observation that site exceeds the importance of the study year suggests a more important influence of site-specific environmental conditions in determining the temporal occurrence of seasonal peaks. This possibly implies a more conservative pattern of peak occurrences, calibrated to the local characteristics, rather than a response to annual weather variations.

A prior study focusing on conifers in cold environments showed that the rate of xylem cell production culminates around the summer solstice (Rossi et al., 2006). After that date, cell production gradually decreases until ceasing. This pattern suggests that trees would have evolved by synchronizing their growth rates with day length (Rossi et al., 2006). Conversely, growth reactivation (i.e., reactivation of secondary meristem) and onset of xylem cell differentiation, despite the variability within populations (Silvestro et al., 2022; Silvestro et al., 2023), are driven by weather conditions, mainly temperature and

water availability (Deslauriers et al., 2016; Guo et al., 2021; Huang et al., 2020; Muller et al., 2011; Rossi et al., 2016; Silvestro et al., 2019).

These insights not only clarify the outcomes of our random forest regression model but substantiate the observed synchronism of peaks in ecosystem C fluxes and cell differentiation, contrasting their asynchrony during the onset and ending of the growing season. Indeed, photosynthesis experiences fewer constraints from environmental factors compared to meristematic activity and cell differentiation (Lawlor & Tezara, 2009; Rossi et al., 2016; Warren & Adams, 2004), resulting in the desynchronization of both onset and ending of source and sinks activities. However, considering that both the rates of photosynthesis (Bamberg et al., 1967) and xylem cell production (Rossi et al., 2006) respond to day length, it is plausible that this factor predominantly governs the synchronization of source and sink peaks. Day length likely acts as a constant environmental factor over time, ensuring the convergence of a high demand with a proportionately high supply.

Finally, we emphasize the comparable significance of predictors between the site and the species. However, these conclusions are drawn from the analysis of phenological timings in conifers. Therefore, we cannot directly recognize the potential variation introduced by broadleaf species.

5.4.6 A reconciliation between C-sources and sinks

The limited availability of sites with concurrent measurements of C fluxes, NSC concentrations, and wood phenology has hindered our ability to quantitatively explore the relationships between these three categories of processes. The extent to which C sources and sinks are closely linked is fundamentally determined by the magnitude of C fluxes

between different compartments, which are exceedingly difficult to measure. However, given the ongoing debates surrounding the significance of potential drivers, temporal sequences, and the level of correlation among these processes at larger temporal and spatial scales, we believe that our temporal analysis provides a unique broad picture of the overall coordination of source and sink activities (and ultimately of C sequestration in wood) at large scales. Consequently, our study serves as a foundation to deepen our understanding of the consequences of climate changes on C sequestration in Northern hemisphere forests, along with exploring potential biome-specific responses.

The asynchrony between C assimilation and cell differentiation during the wood formation process observed in many local studies, can be largely attributed to limiting carbon sinks governed by meristem activity (i.e., C sink limitation to growth) (Faticchi et al., 2014). In isolation, the asynchrony between these two processes can be attributed to their respective different sensitivities to environmental factors and possibly to differences in biome-specific resource use strategies. At broader scale, however, our results suggest that this asynchrony may originate from the longer time window of C assimilation compared to the period of C allocation to woody tissues. This discrepancy is also evident in the periods of maximum activity of the processes, as demonstrated by the present study.

The different responses of photosynthesis and growth to the climate may also account for the asynchronies observed at local scale, e.g., under drought conditions. Water deficit can decouple growth from photosynthesis (Cabon et al., 2022; Muller et al., 2011), and likely explain the greater variability in the peaks of photosynthesis and cell differentiation observed in the Mediterranean biome in this study (Figure 5.4). As a typical response to water deficit, C allocation (i.e., growth) always decreases before C assimilation (i.e., photosynthesis) (Körner, 2003, 2015; Muller et al., 2011).

In Mediterranean regions, a potential lag between C assimilation and xylem formation can be bimodal, as tree radial growth may slow down in response to water shortage, and resume in autumn after summer suspension (Camarero et al., 2010; Muller et al., 2011). These conditions cause a rise in the concentration of C stores, resulting in the accumulation of compatible solutes (typically hexoses and polysaccharides) in sink organs (Muller et al., 2011). These compounds serve as energy sources and as sources of compatible sugars and other carbon-based solutes, protect subcellular compartments against the harmful effects of water loss, and increase drought tolerance (Muller et al., 2011). This process of C accumulation in sink organs helps to explain how water deficit uncouples growth from photosynthesis. However, in precipitation manipulation experiments an almost synchronic coupling between new assimilates and xylem formation was observed when trees were irrigated after a long drought period (Eilmann et al., 2010). This suggests that the observation of an asynchrony between photosynthetic activity and growth is primarily a response to limiting environmental conditions for growth.

Environmental constraints limit sink activity, which may be the primary cause of decoupling between the processes of C assimilation and growth. However, C-sink limitation should not be interpreted as a complete disjunction between C resources and sink activity. C is a limited resource and, in the form of soluble sugars and starch, fulfils various functional roles, such as transport, energy metabolism, osmoregulation, and provides substrates for the synthesis of defense, exchange and biomass components (Hartmann & Trumbore, 2016). While the prioritization of certain uses of newly-formed photoassimilates is not well understood, there is evidence that processes related to survival have a higher priority than increasing structural biomass, i.e., growth (Andreu-

Hayles et al., 2022). This is supported by evidence showing that trees prioritize storage even when experiencing a C shortage (Weber et al., 2018). Therefore, it is also possible that, beyond direct environmental limitations, the partial asynchrony found here between C fluxes and wood formation may reflect varying allocation priorities among different species and biomes, reflecting different functional traits and resource use strategies. In summary, direct environmental cues and biotic disturbances can limit sink activity and desynchronize C assimilation and growth. In addition, the competition among sinks for a limited resource should likely be expected to further contribute to this asynchrony.

Numerous sites are currently equipped for monitoring and measuring carbon fluxes in various forest ecosystems. However, within the last decade, only a small percentage of these sites have been monitoring wood formation on an intra-annual scale. Incorporating detailed intra-annual observations of NSC pools, which act as a buffer between atmospheric C flux measurements (e.g., eddy covariance GPP and RECO) and intra-annual assessments of forest biomass growth (i.e., wood formation monitoring and intra-ring analysis of wood anatomy), can facilitate the complex task of reconciling, and ultimately clarifying, the temporal and functional relationships between C uptake and long-term C sequestration. This, in turn, will enable the examination of the timing and magnitude of C transfer processes and C use efficiency across various spatial and temporal scales. Such an analysis is a crucial step to reduce the sources of uncertainty in global vegetation models and achieve a deeper understanding of the C cycle at global scale.

5.4.7 Acknowledgements

This work was funded by the Ministère des Forêts, de la Faune et des Parcs du Québec, Fonds de Recherche du Québec - Nature et Technologies (AccFor, project #309064), the Observatoire régional de recherche en forêt boréale and Forêt d'Enseignement et de Recherche Simoncouche. R. Silvestro received the Merit scholarship for international PhD students (PBEEE) by the Fonds de Recherche du Québec - Nature et Technologies (FRQNT) and a scholarship for an internship by the Centre d'étude de la forêt (CEF) realized at the Centre for Ecological Research and Forestry Applications (CREAF). V. Shishov is appreciated for supporting the RSF project #22-14-00048. C.B.K. Rathgeber would like to thank the Agence Nationale de la Recherche (ANR) in the framework of the Investissements d'Avenir (ANR-11-LABX-0002-01, Laboratoire d'Excellence ARBRE) for the support given to its work as well as the SILVATECH platform (Silvatech, INRAE, 2018. Structural and functional analysis of tree and wood Facility, doi: 10.15454/1.5572400113627854E12) for its contribution to the acquisition of wood formation monitoring data. The authors thank A. Garside for editing the English text.

5.4.8 Author Contributions

RS, MM, VB and SR conceived the ideas and designed methodology; SA, AA, FB, VB, JJC, FC, HC, KC, HEC, MDL, AD, GD, PF, MF, RGV, AG, JG, AG, VG, RG, AG, XG, JGH, TJ, JK, AVK, TK, AL, XL, EL, AML, FL, FL, QM, HM, RAM, EMC, JMV, SM, MM, HM, CN, PN, WO, JMO, APO, TVSP, MP, RLP, RP, PP, ZQ, CBKR, SR, AS, AS, LS, PPSA, VS, RS, AS, RS, JDS, RT, VT, JU, HV, JV, GA, YW, BY, SZ and EZ provided local wood formation and non-structural carbohydrates data; GVR downloaded and assembled FluxSat data; RS and SR assembled the final datasets; RS analysed data and led the writing of the manuscript. All authors contributed to the drafts and gave final

approval for publication.

5.4.9 Competing Interests

The authors declare no competing interests.

5.4.10 Data Availability

Once accepted for publication, data associated with this paper will be available in Borealis, the Canadian dataverse repository.

5.5 Figures

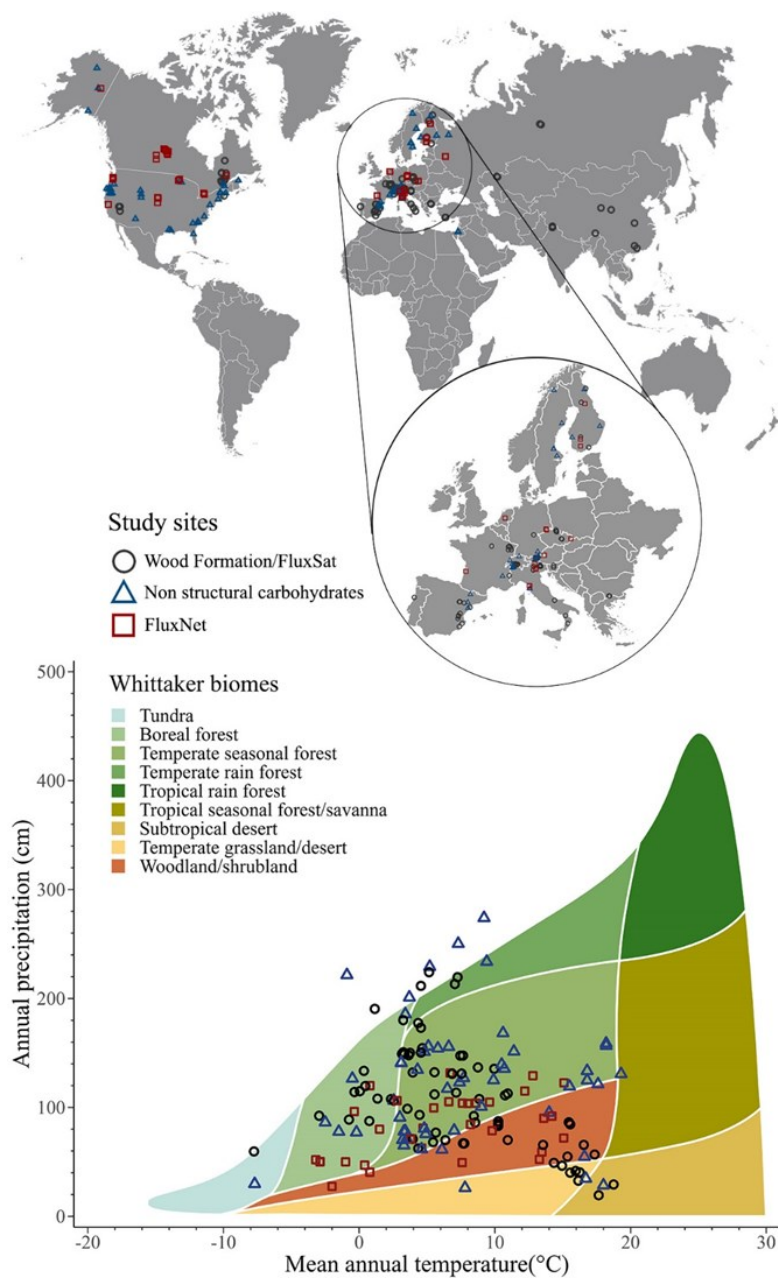


Figure 5.1 Study sites in the Northern hemisphere where the dynamics of wood formation (81 sites), non-structural carbohydrates (57 sites) and C fluxes (39 sites) were determined. C fluxes were also estimated from the FluxSat product for each pixel corresponding to the 87 sites where wood formation was determined. Below, a Whittaker biome plot illustrates the mean annual temperature ($^{\circ}\text{C}$) and mean annual precipitation (cm) for all 177 study sites.

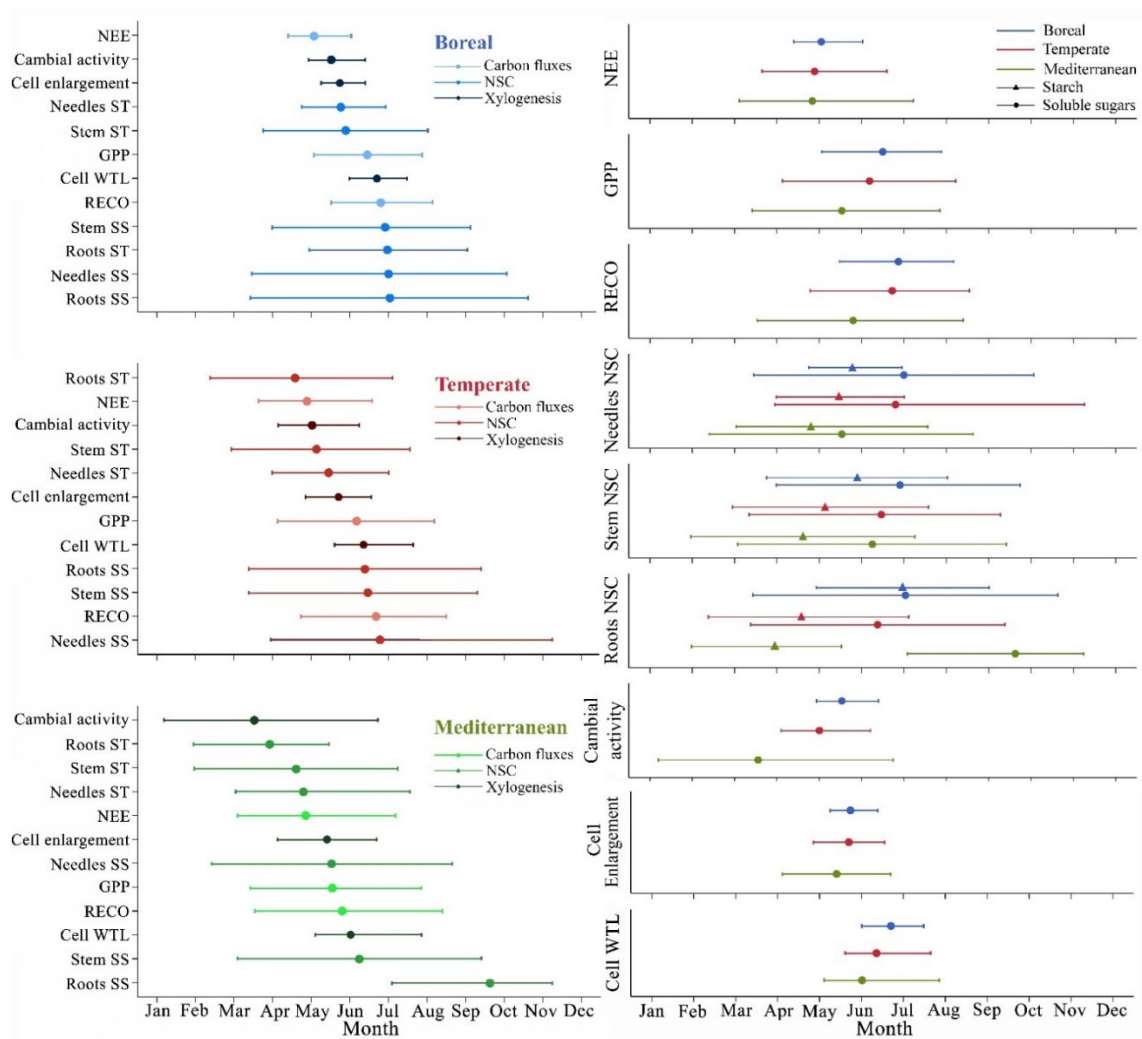


Figure 5.2 Peak (dot or triangle) and period of maximum activity (horizontal lines) for C fluxes, NSC dynamics and wood formation phenological phases. Minimum concentration is shown for soluble sugars. On the right, for each event the difference among biomes is shown. On the left, for each biome, the temporal consecutive events during the growing season are shown. NEE, GPP and RECO represent the Net Ecosystem Exchange, Gross Primary Production and Ecosystem Respiration. ST and SS represent starch and soluble sugars, respectively. Cell WTL represents the phenological stage of cell wall thickening and lignification.

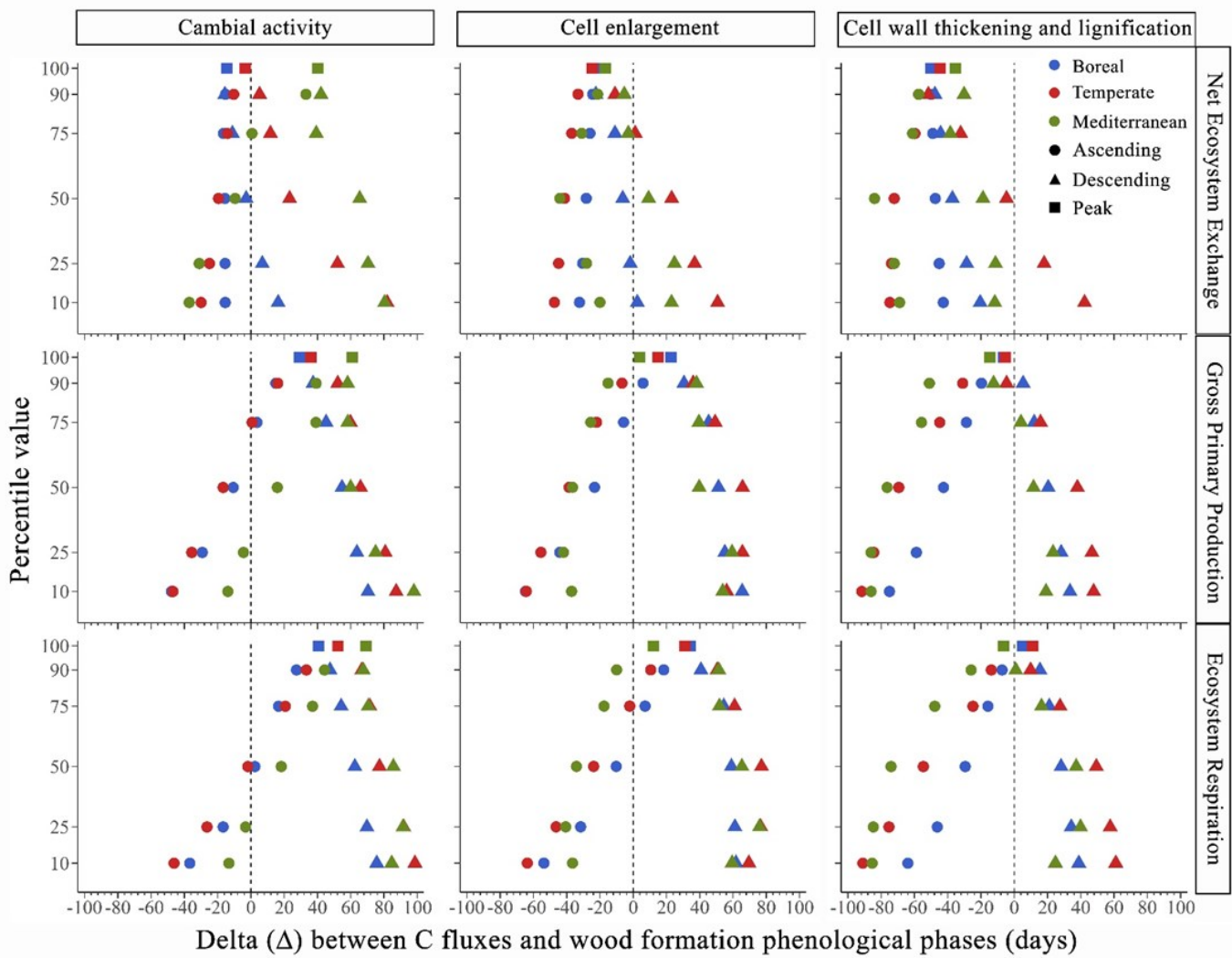


Figure 5.3 Differences (i.e., subtraction) between the timing of different percentiles and peak (i.e., 100th percentile) of C fluxes, i.e., NEE, GPP, RECO and those of phenological phases of wood formation, i.e., cambial activity, cell enlargement and cell wall thickening and lignification in boreal, temperate and Mediterranean biomes. Negative deltas indicate that C fluxes occurred earlier, while positive deltas that C fluxes occurred later, relative to wood formation, for each percentile shown in the figure.

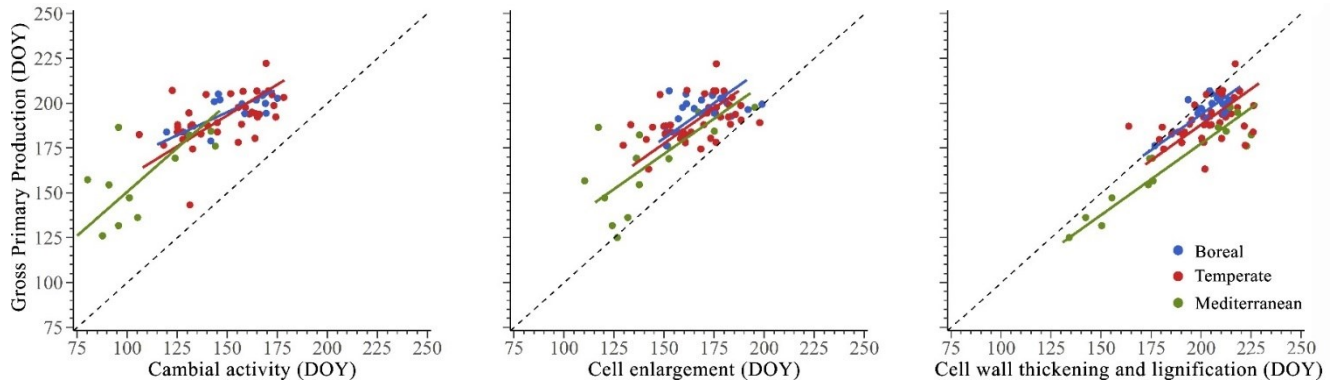


Figure 5.4 Synchronisms among the timing of peak of Gross Primary Production (GPP) and phenological phases of wood formation (i.e., cambial activity, cell enlargement, and cell wall thickening and lignification) in 87 sites across boreal, temperate and Mediterranean biomes. The dashed line represents a bisecting line (1:1).

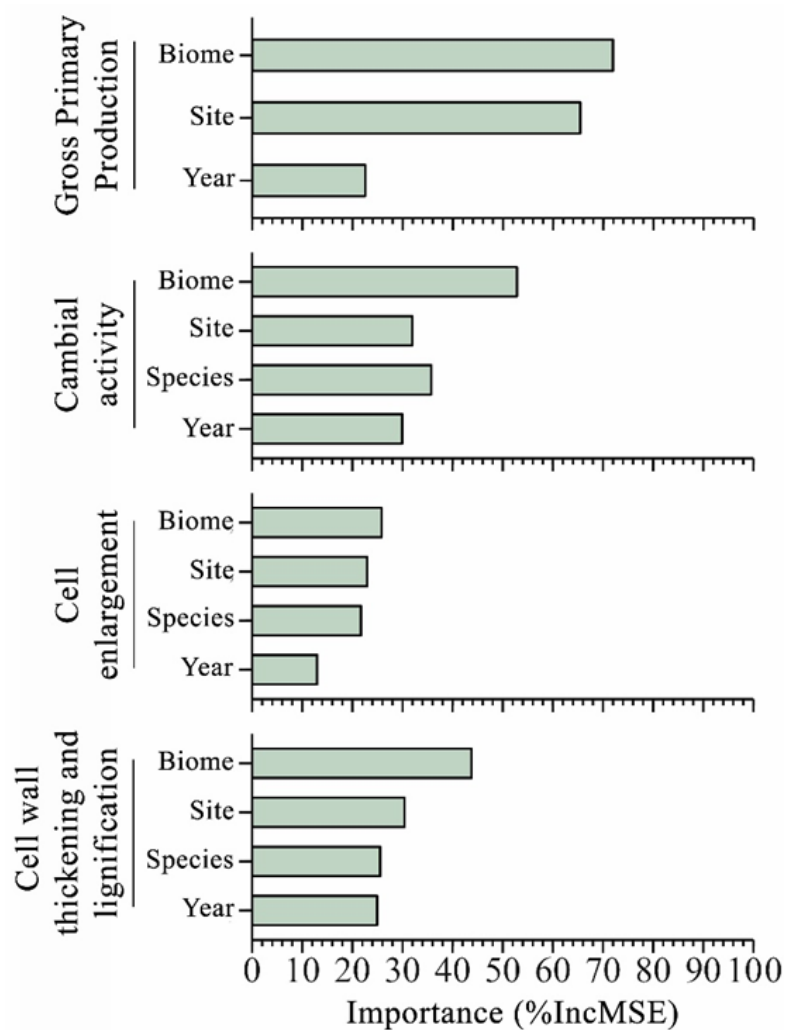


Figure 5.5 Relative importance in terms of Mean Decrease Accuracy (%IncMSE) of predictors in the random forest regression models for the timing of peak of FluxSat Gross Primary Production (GPP) and phenological phases of wood formation (i.e., cambial activity, cell wall thickening and lignification).

5.6 Tables

Table 5.1 Results of Standardized Major Axis (SMA) analyses of the bivariate relationships among timing of the peak of GPP and timing of cambial activity, cell enlargement and cell wall thickening and lignification in 87 sites across boreal, temperate and Mediterranean biomes.

Phenological		95% CI			
stage	Biome	Y-intercept	Slope	slope	R²
Cambial activity	Boreal	118.01	0.51	0.34 - 0.77	0.50
	Temperate	89.83	0.69	0.52 - 0.91	0.27
	Mediterranean	52.71	0.98	0.56 - 1.71	0.40
Cell enlargement	Boreal	62.64	0.78	0.63 - 0.96	0.26
	Temperate	59.74	0.78	0.63 - 0.96	0.43
	Mediterranean	53.93	0.78	0.63 - 0.96	0.21
Cell wall thickening and lignification	Boreal	11.16	0.80	0.69 - 0.94	0.51
	Temperate	23.73	0.80	0.69 - 0.94	0.31
	Mediterranean	28.26	0.80	0.69 - 0.94	0.81

5.7 Annexes

5.7.1 Supplementary materials 1 - Site selection and dataset assembly

Wood formation

This study uses wood formation data collected in 87 sites belonging to boreal, temperate and Mediterranean biomes. All the data followed the criteria or procedures applied either in the field or laboratory, as described below and according to the methodology described by Rossi, Anfodillo, et al. (2006); Rossi, Deslauriers, et al. (2006).

The timings of wood formation were determined by monitoring healthy dominant trees. The sample size ranged from 1 to 55 trees among all sites throughout the entire growing seasons of 1998 to 2018. Stem microcores were collected weekly, or occasionally biweekly, at breast height (i.e., 1.3 m) using surgical bone-sampling needles or a Trephor tool. The samples included mature and developing xylem of the current year, the cambial zone and adjacent phloem, and at least one previous complete tree ring. The microcores were fixed in propionic or acetic acid solutions mixed with formaldehyde and stored in ethanol-water at 5 °C. They were then dehydrated with successive immersions in ethanol and D-limonene and finally embedded in paraffin or glycol methacrylate (samples from Switzerland were not embedded). The microcores were cut with rotary or sledge microtomes to obtain 10 to 30 µm thickness transverse sections.

The sections obtained were stained with cresyl violet acetate or a mixture of safranin and astra/Alcian blue, then examined by light microscopy (bright-field and polarised light). Cambial initials of the vascular cambium, a secondary meristem, divide outward and inward to produce phloem and xylem mother cells that, in turn, form new phloem and xylem tissues. The process of tracheid formation (i.e., cell differentiation) is divided into

different phenological phases including cell enlargement, secondary cell wall thickening and lignification, and then programmed cell death, leading to the mature stage. Cambial cells are characterised by thin cell walls and small radial diameters. The enlargement zone is represented by the absence of glistening under polarised light, which indicates the presence of only primary cell walls. Cells undergoing secondary cell wall formation glistened under polarised light. In mature cells, Cresyl violet acetate reacts with lignin, turning from violet to blue. Maturation is reached when the cell walls are entirely blue.

To investigate the variations in climate among the locations where we monitored wood formation, we sourced bioclimatic data from the CHELSA bioclimatic database V2.1, offering a spatial resolution of 30 arcseconds. From the set of 19 bioclimatic parameters, we curated a selection of seven variables, as detailed in the Table S1. We excluded parameters that delivered overly broad climate descriptions, like annual temperature and precipitation, and filtered out variables that exhibited strong autocorrelations (with a correlation coefficient exceeding $|0.7|$). To categorize our study sites based on their climate-related attributes, we applied the Partitioning Around Medoids clustering algorithm (PAM), an extension of k-means clustering approach. We employed the Within-Sum-of-Squares method (WSS) to identify the optimal number of clusters. This method minimizes the internal distances between data points within each cluster. We determined that four clusters best suited the task of grouping our wood formation study sites effectively (Figure S5.1). We proceeded to perform a Principal Component Analysis (PCA) on the selected bioclimatic variables. This analytical technique allowed us to visualize and understand the climatic positioning of our 81 wood formation sites in relation to these variables. Pearson's correlation coefficient was employed to identify the

climatic factors that influenced the ordering of wood formation study sites by principal components (Table S5.1).

In this study, data referring to the phenological phases of cambial activity, cell enlargement, and cell wall thickening and lignification were grouped by biome and site and normalized (min-max normalisation) on a scale from 0 to 1.

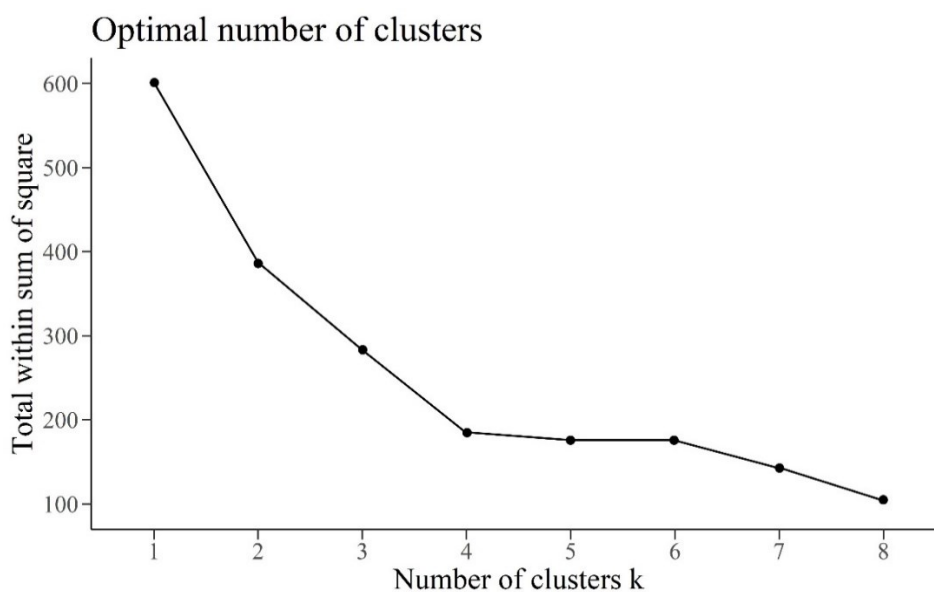


Figure S 5.1 Within Sum of Square (WSS) of the optimal number of clusters determined for climate-related wood formation sites grouping.

Table S 5.1 Pearson correlation coefficients between climatic variable and the first two principal components, eigenvalues, and variance explained.

Bioclimatic variables	Abbreviation	PC1	PC2
Temperature seasonality (STD x 100)	bio4	-0.43	-0.82
Mean temperature of the driest quarter	bio9	0.88	0.38
Mean temperature of the warmest quarter	bio10	0.84	-0.14
Mean temperature of the coldest quarter	bio11	0.82	0.54
Precipitation seasonality (CV)	bio16	-0.55	0.63
Precipitation of the driest quarter	bio17	-0.56	0.50
Precipitation of the warmest quarter	bio18	-0.72	0.53
Eigenvalue		3.49	2.08
Variance explained		49.90	29.73

In the main text of this work and for all the following analysis, data referring to the phenological phases of cambial activity, cell enlargement, and cell wall thickening and lignification were grouped by biome and site and normalized (min-max normalisation) on a scale from 0 to 1.

NSC

We assembled the NSC dataset by sub-setting the conifers section of the dataset used by Martínez-Vilalta et al. (2016) and updating it with more recent data, finally resulting in 57 sites distributed in boreal, temperate and Mediterranean biomes. The studies included seasonal NSC data on wild species measured under natural field conditions. When studies involved experimental manipulations, we only considered results from unmanipulated controls. In addition, to ensure good temporal coverage and reduce unwanted variability due to some specific characteristics of the samples, we selected only work that fulfilled the following criteria: (1) study duration was at least four months, (2) the same individuals

or populations were measured at least three times spanning the length of the study, (3) plants were mature, (4) measurements were taken on needles, main stem, fine or coarse roots (5) values reported were starch/fructans, or soluble sugars. All individual NSC data points were extracted from the text, tables, or figures of each study or by contacting authors directly, in the latter case using the software GetData Graph Digitizer (Version 2.26). Usually, NSC concentrations are expressed as % or mg/g dry mass directly, otherwise, values were converted to mg/g. Finally, NSC concentration was grouped by biome, organ, study, extraction and quantification method. These two latter grouping operations were performed given that a study on the comparability of NSC measurements across laboratories concludes that NSC estimates for woody plant tissues may not be directly comparable (Quentin et al., 2015). Ultimately, all data were normalized (min-max normalisation) on a scale from 0 to 1.

Flux data evergreen needleleaf forests (FLUXNET 2015)

We used tier-one level data from the FLUXNET2015 dataset (Pastorello et al., 2020) and extracted data at daily temporal aggregation from ENF (Evergreen Needleleaf Forests) sites. These sites consist of forest lands dominated by woody vegetation with a cover of >60% and height exceeding 2 meters. In addition, to reduce unwanted variability due to some specific characteristics of the site, we selected only data in which stands (1) belonged to boreal, temperate, or Mediterranean biomes, (2) were at least 15 years old, and (3) were not recently disturbed (e.g., burn sites). The dataset finally consisted of 39 sites. CO₂ fluxes extracted for each site were Net Ecosystem Exchange (NEE), Ecosystem Respiration (RECO), and Gross Primary Production (GPP). Specifically, for the NEE we used the variable NEE_VUT_REF since it maintains the temporal variability and

represents the ensemble (Pastorello et al., 2020). There are two main ways to estimate GPP and RECO (in units of $\text{g C m}^{-2} \text{d}^{-1}$) by partitioning of the NEE computed with the variable Ustar (u^*) threshold (VUT): (1) night-time method (GPP_NT_VUT_REF and RECO_NT_VUT_REF); and (2) day-time method (GPP_DT_VUT_REF) (Pastorello et al., 2020). All results are shown here use an average of the night- and day-time partitioning methods (RECO_NT_VUT_REF and RECO_DT_VUT_REF for RECO, GPP_NT_VUT_REF and GPP_DT_VUT_REF for GPP). Finally, C fluxes were grouped by biome, flux type (i.e., NEE, GPP, RECO), and site and normalized (min-max normalisation) on a scale from 0 to 1.

Flux data in wood formation sites (FLUXSAT V2.0)

Daily GPP data were extracted for each site and each year where the wood formation was monitored. Differently from the dataset obtained with the data from FLUXNET2015, in this case, while the samples were collected on coniferous species, the study area could consist of a mixed forest. These GPP products were extracted by FluxSat v2.0 (Joiner & Yoshida, 2021), where FluxSat refers to data derived using FLUXNET eddy covariance tower site data and the coincident satellite data. This dataset provides global gridded daily estimates of terrestrial GPP and uncertainties at 0.05° resolution for the period 01/03/2000 to the recent past (Joiner & Yoshida, 2021). The GPP was derived from the MODerate-resolution Imaging Spectroradiometer (MODIS) instruments on the NASA Terra and Aqua satellites using the Nadir Bidirectional Reflectance Distribution Function (BRDF)-Adjusted Reflectances (NBAR) product as input to neural networks that were used to globally upscale GPP estimated from selected FLUXNET 2015 eddy covariance tower

sites. GPP value (in $\text{g C m}^{-2} \text{d}^{-1}$) for each site resulted from the interpolation of GPP values of the four nearest pixels (Joiner & Yoshida, 2021).

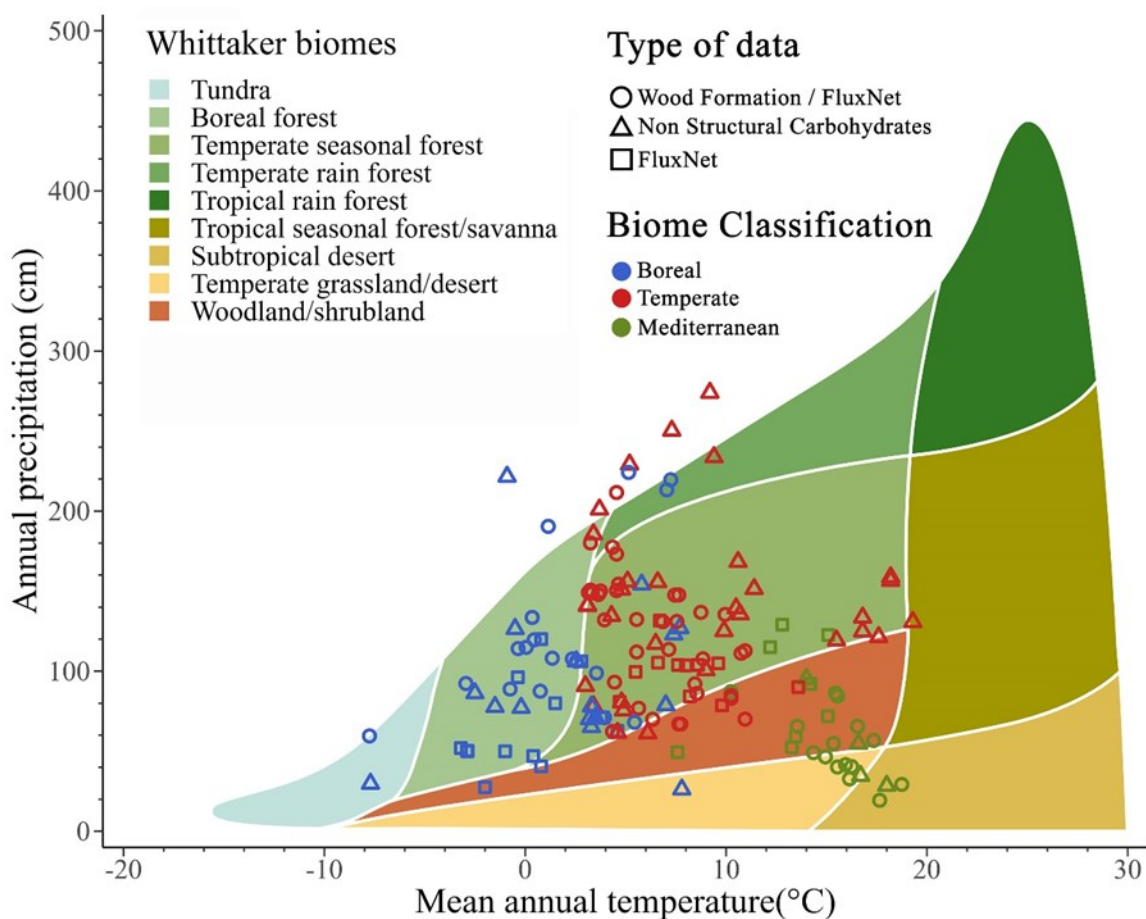


Figure S 5.2 Whittaker biome plot showing the comparison between the study site classification in the present study (i.e. boreal, temperate and Mediterranean biomes) and Whittaker biome classification according to mean annual temperature ($^{\circ}\text{C}$) and annual precipitation (cm).

Table S 5.2 Alphabetical list of all the species monitored in the study. 39 species of conifers belonging to 8 different genera were the object of the study.

Wood formation species	Non-structural carbohydrates species
<i>Abies alba</i> Mill.	<i>Abies alba</i> Mill.
<i>Abies balsamea</i> (L.) Mill.	<i>Abies lasiocarpa</i> (Hook.) Nutt.
<i>Abies georgei</i> (var. <i>smithii</i>)	<i>Juniperus occidentalis</i> Hook.
<i>Abies pindrow</i> (Royle ex D.Don) Royle	<i>Larix decidua</i> Mill.
<i>Cedrus libani</i> A. Rich	<i>Picea abies</i> L. Karst
<i>Juniperus przewalskii</i> Kom.	<i>Picea engelmannii</i> Parry ex Engelm.
<i>Juniperus thurifera</i> L.	<i>Picea glauca</i> (Moench) Voss
<i>Larix decidua</i> Mill.	<i>Picea rubens</i> Sarg.
<i>Picea abies</i> L. Karst	<i>Picea sitchensis</i> (Bongard) Carrière
<i>Picea mariana</i> (Mill.) B.S.P.	<i>Pinus banksiana</i> Lamb.
<i>Pinus cembra</i> L.	<i>Pinus cembra</i> L.
<i>Pinus flexilis</i> James.	<i>Pinus contorta</i> Douglas ex Loudon
<i>Pinus halepensis</i> Mill.	<i>Pinus elliotii</i> Engelm.
<i>Pinus heldreichii</i> Christ	<i>Pinus halepensis</i> Mill.
<i>Pinus longaeva</i> Bailey	<i>Pinus palustris</i> Mill.
<i>Pinus massoniana</i> Lamb.	<i>Pinus pinaster</i> Ait.
<i>Pinus peuce</i> Griseb.	<i>Pinus ponderosa</i> Douglas ex Lawson
<i>Pinus pinaster</i> Ait.	<i>Pinus radiata</i> D.Don
<i>Pinus ponderosa</i> Douglas ex Lawson	<i>Pinus sylvestris</i> L.
<i>Pinus strobus</i> L.	<i>Pinus taeda</i> L.
<i>Pinus sylvestris</i> L.	<i>Pseudotsuga menziesii</i> (Mirb.) Franco
<i>Pinus tabulaeformis</i> Carr.	<i>Tsuga canadensis</i> (L.) Carrière
<i>Pinus uncinata</i> Mill. Ex Mirb	<i>Tsuga heterophylla</i> (Raf.) Sarg.
	<i>Tsuga mertensiana</i> (Bong.) Carr.

5.7.2 Supplementary material 2 – Data sources and sites

Wood Formation sites

ID	latitude	longitude	altitude	Study years
5T1	46.45	12.13	2085	2001-2005
5T2	46.46	12.13	2156	2002-2005
5T3	46.45	12.13	2085	2004-2005
ABR	48.35	7.06	430	2007-2009
AMA	48.75	6.31	270	2006-2013
AMN	48.73	6.31	270	2006-2007
ARV	48.43	-71.15	80	1999-2000
BER	48.85	-70.33	611	2002-2014
BLJ	50.73	15.65	1270	2013-2014
BLS	50.73	15.65	1270	2013-2014
BOR	46.73	12.31	1150	2015
DAN	50.68	-72.18	487	2002-2014
DRY	47.23	10.83	750	2010-2011
GRA	48.46	4.13	650	2007-2008
GRD	48.48	7.15	643	2007-2009
GUA	38.01	-0.65	15	2005
HSM	37.03	104.47	2456	2013-2014
HYY	61.88	24.30	181	2008
JAN	39.31	-1.25	850	2004
JAR	39.25	-1.25	571	2005
KIV	66.20	26.38	140	2009
L23	49.97	-72.50	380	1998-2000
L24	49.97	-72.50	430	1998-2001
LAV	46.21	11.30	1776	2010
LH1	50.70	15.65	1310	2010-2012
LH2	50.71	50.67	1450	2010-2012
MAI	38.51	-0.51	845	2004-2005
MEN	46.26	14.80	1200	2009-2012
MIR	53.78	-72.86	384	2012-2014
MIS	49.71	-71.93	342	2002-2014
MYH	41.78	-1.81	1600	2011-2013
MYL	41.78	-1.81	1600	2011-2012
N08	46.38	7.75	804	2008-2010
N13d	46.38	7.75	1361	2007-2013
N13w	46.38	7.75	1321	2013
N16	46.38	7.75	1634	2007-2010
N19	46.38	7.76	1961	2007-2010

N22	46.36	7.76	2184	2007-2010
OI	49.91	11.58	355	2013
PAN	46.00	14.67	400	2009-2012
PEN	41.65	-0.97	340	2006-2010
PES	41.86	14.50	1380	2015
POL	39.90	16.20	2053	2003-2004
RAJ	49.43	16.68	620	2009-2011
RUO	60.20	25.00	60	2008-2010
S16	46.40	7.75	1670	2007-2013
S19	46.40	7.75	1928	2007-2013
S22	46.40	7.73	2104	2007-2013
SAV	45.56	11.03	677	2010
SDL	38.45	99.93	3550	2013-2014
SER	38.76	16.51	1008	2015
SHM	36.98	-115.35	2320	2015-2016
SIM	48.21	-71.25	338	2005-2014
SIM2	48.20	-71.23	350	2010-2011
SISE	50.75	15.65	1375	2014-2015
SISW	50.76	50.63	1360	2014-2015
SOB	49.48	16.36	404	2013-2014
SSM	38.88	-114.33	2810	2013-2014
SSW	38.90	-114.13	3355	2013-2014
SUS	45.05	6.67	2030	2003-2004
SVT	46.43	12.21	1000	2003
SYG	29.65	94.70	3850	2007-2009
T1	36.56	29.59	1665	2013
T2	36.56	29.59	1960	2013
T3	36.56	29.59	1355	2013
T4	36.56	29.59	1055	2013
TCH	40.36	-8.82	10	2010-2014
TDR	41.43	23.42	1780	2012-2014
VAR	67.50	29.38	390	2009
VIL	40.51	0.65	1690	2005
VRN	41.45	23.25	1850	2012-2014
WAL	48.36	7.08	370	2007-2009
ZWY	23.18	113.36	23	2015-2016
MOF	47.32	-71.15	800	2018
THF	43.06	-70.57	23.3	2015
JAS	39.16	-1.15	850	2004
PKKH	47.20	11.45	2180	2007
PKTB	47.20	11.45	1950	2007
PKTR	47.20	11.45	2110	2007
TRL	64.18	100.11	140	2012

TOR	40.20	-0.95	1600	2005
TRH	64.18	100.11	589	2013
IN1	33.67	74.72	2350	2014-2015
IN2	33.66	74.70	2650	2014-2015
IN3	33.66	74.69	2950	2014-2015

Non-structural carbohydrates sites

ID	latitude	longitude	country	reference
L1	43.45	10.43	Italy	Puri E. Hoch G. and C. Körner. 2015. Defoliation reduces growth but not carbon reserves in Mediterranean Pinus pinaster trees. <i>Trees</i> 29(4) 1187-1196.
L1	43.44	10.44	Italy	Puri E. Hoch G. and C. Körner. 2015. Defoliation reduces growth but not carbon reserves in Mediterranean Pinus pinaster trees. <i>Trees</i> 29(4) 1187-1196.
L2	61.52	21.57	Finland	Schiestl-Aalto, P., Ryhti, K., Mäkelä, A., Peltoniemi, M., Bäck, J., & Kulmala, L. (2019). Analysis of the NSC storage dynamics in tree organs reveals the allocation to belowground symbionts in the framework of whole tree carbon balance. <i>Frontiers in Forests and Global Change</i> , 2, 17.
L3	31.20	35.20	Israel	Klein, T., Hoch, G., Yakir, D., & Körner, C. (2014). Drought stress, growth and nonstructural carbohydrate dynamics of pine trees in a semi-arid forest. <i>Tree physiology</i> , 34(9), 981-992.
L4	31.20	35.20	Israel	Atzmon N.Schiller G. and Y. Riov. 2002. Survey of seasonal carbohydrate level fluctuations as a basis to understand development and growth of forest trees in Israel. KKL-JNF Report #90-3-085-02.
L5	47.24	-71.22	Canada	Deslauriers, A., Caron, L., & Rossi, S. (2015). Carbon allocation during defoliation: testing a defense-growth trade-off in balsam fir. <i>Frontiers in plant science</i> , 6, 338.
L5	48.71	-65.59	Canada	Deslauriers, A., Caron, L., & Rossi, S. (2015). Carbon allocation during defoliation: testing a defense-growth trade-off in balsam fir. <i>Frontiers in plant science</i> , 6, 338.
L5	47.24	-71.22	Canada	Deslauriers, A., Caron, L., & Rossi, S. (2015). Carbon allocation during defoliation: testing a defense-growth trade-off in balsam fir. <i>Frontiers in plant science</i> , 6, 338.
L6	43.47	-110.57	US	Bansal, S., & Germino, M. J. (2009). Temporal variation of nonstructural carbohydrates in montane conifers: similarities and differences among developmental stages, species and environmental conditions. <i>Tree Physiology</i> , 29(4), 559-568.
L7	47.83	-93.83	US	Furze, M. E. (2018). Seasonal patterns of nonstructural carbohydrate reserves in four woody boreal species1. <i>The Journal of the Torrey Botanical Society</i> , 145(4), 332-339.
L8	42.45	0.52	Spain	Camarero, J. J., Gazol, A., Sangüesa-Barreda, G., Oliva, J., & Vicente-Serrano, S. M. (2015). To die or not to die: early warnings of tree dieback in response to a severe drought. <i>Journal of Ecology</i> , 103(1), 44-57.
L8	40.26	0.58	Spain	Camarero, J. J., Gazol, A., Sangüesa-Barreda, G., Oliva, J., & Vicente-Serrano, S. M. (2015). To die or not to die: early warnings of tree dieback in response to a severe drought. <i>Journal of Ecology</i> , 103(1), 44-57.
L8	41.47	0.44	Spain	Camarero, J. J., Gazol, A., Sangüesa-Barreda, G., Oliva, J., & Vicente-Serrano, S. M. (2015). To die or not to die: early warnings of tree dieback in response to a severe drought. <i>Journal of Ecology</i> , 103(1), 44-57.
L9	47.11	11.19	Austria	Mayr, S., Schmid, P., & Rosner, S. (2019). Winter embolism and recovery in the conifer shrub Pinus mugo L. <i>Forests</i> , 10(11), 941.
L11	45.13	5.88	France	Wang, Y., Mao, Z., Bakker, M. R., Kim, J. H., Brancheriau, L., Buatois, B., ... & Stokes, A. (2018). Linking conifer root growth and production to soil temperature and carbon supply in temperate forests. <i>Plant and Soil</i> , 426(1), 33-50.
L36	47.62	12.25	Austria	Gruber A. D. Pirkebner C. Florian and W. Oberhuber. 2011a. No evidence for depletion of carbohydrate pools in Scots pine (Pinus sylvestris L.) under drought stress. <i>Plant Biology</i> 14:142-148.

L40	46.22	7.42	Swiss	Hoch G. M. Popp and C. Körner. 2002. Altitudinal increase of mobile carbon pools in <i>Pinus cembra</i> suggests sink limitation of growth at the Swiss treeline. <i>Oikos</i> 98:361–374.
L43	46.57	7.07	Swiss	Hoch, G., Richter, A., & Körner, C. (2003). Non-structural carbon compounds in temperate forest trees. <i>Plant, Cell & Environment</i> , 26(7), 1067-1081.
L65	46.22	7.42	Swiss	Li, M., Hoch, G., & Körner, C. (2002). Source/sink removal affects mobile carbohydrates in <i>Pinus cembra</i> at the Swiss treeline. <i>Trees</i> , 16(4-5), 331-337.
L68	34.59	-80.23	US	Ludovici, K. H., Allen, H. L., Albaugh, T. J., & Dougherty, P. M. (2002). The influence of nutrient and water availability on carbohydrate storage in loblolly pine. <i>Forest Ecology and Management</i> , 159(3), 261-270.
L115	67.80	29.67	Finland	Susiluoto, S., Hiltavuori, E., & Berninger, F. (2010). Testing the growth limitation hypothesis for subarctic Scots pine. <i>Journal of Ecology</i> , 98(5), 1186-1195.
L123	43.23	-107.67	US	Woodruff, D. R., & Meinzer, F. C. (2011). Water stress, shoot growth and storage of non-structural carbohydrates along a tree height gradient in a tall conifer. <i>Plant, Cell & Environment</i> , 34(11), 1920-1930.
L125	34.72	-78.33	US	Adams, M. B., Adam, H. L., & Davey, C. B. (1986). Accumulation of starch in roots and foliage of loblolly pine (<i>Pinus taeda</i> L.): effects of season, site and fertilization. <i>Tree physiology</i> , 2(1-2-3), 35-46.
L127	45.82	-121.90	US	Billow, C., Matson, P., & Yoder, B. (1994). Seasonal biochemical changes in coniferous forest canopies and their response to fertilization. <i>Tree Physiology</i> , 14(6), 563-574.
L127	35.23	-107.61	US	Billow, C., Matson, P., & Yoder, B. (1994). Seasonal biochemical changes in coniferous forest canopies and their response to fertilization. <i>Tree Physiology</i> , 14(6), 563-574.
L128	33.33	-81.72	US	Birk, E. M., & Matson, P. A. (1986). Site fertility affects seasonal carbon reserves in loblolly pine. <i>Tree Physiology</i> , 2(1-2-3), 17-27.
L142	31.00	-92.62	US	Sayer, M. A. S., & Haywood, J. D. (2006). Fine root production and carbohydrate concentrations of mature longleaf pine (<i>Pinus palustris</i> P. Mill.) as affected by season of prescribed fire and drought. <i>Trees</i> , 20(2), 165.
L145	46.70	-92.53	US	Tjoelker, M. G., Oleksyn, J., Reich, P. B., & Żytkowiak, R. (2008). Coupling of respiration, nitrogen, and sugars underlies convergent temperature acclimation in <i>Pinus banksiana</i> across wide-ranging sites and populations. <i>Global Change Biology</i> , 14(4), 782-797.
L147	44.51	-123.55	US	Webb, W. L., & Kilpatrick, K. J. (1993). Starch content in Douglas-fir: diurnal and seasonal dynamics. <i>Forest science</i> , 39(2), 359-367.
L148	44.36	-73.90	US	Amundson, R. G., Hadley, J. L., Fincher, J. F., Fellows, S., & Alscher, R. G. (1992). Comparisons of seasonal changes in photosynthetic capacity, pigments, and carbohydrates of healthy sapling and mature red spruce and of declining and healthy red spruce. <i>Canadian Journal of Forest Research</i> , 22(11), 1605-1616.
L148	44.38	-73.07	US	Amundson, R. G., Hadley, J. L., Fincher, J. F., Fellows, S., & Alscher, R. G. (1992). Comparisons of seasonal changes in photosynthetic capacity, pigments, and carbohydrates of healthy sapling and mature red spruce and of declining and healthy red spruce. <i>Canadian Journal of Forest Research</i> , 22(11), 1605-1616.
L152	47.62	12.25	Austria	Oberhuber, W., Swidrak, I., Pirkebner, D., & Gruber, A. (2011). Temporal dynamics of nonstructural carbohydrates and xylem growth in <i>Pinus sylvestris</i> exposed to drought. <i>Canadian Journal of Forest Research</i> , 41(8), 1590-1597.
L162	60.85	16.48	Sweden	Ericsson, A., Larsson, S., & Tenow, O. (1980). Effects of early and late season defoliation on growth and carbohydrate dynamics in Scots pine. <i>Journal of applied Ecology</i> , 747-769.
L163	60.85	16.48	Sweden	Ericsson, A., Hellqvist, C., Langstrom, B., Larsson, S., & Tenow, O. (1985). Effects on growth of simulated and induced shoot pruning by <i>Tomicus piniperda</i> as related to carbohydrate and nitrogen dynamics in Scots pine. <i>Journal of Applied Ecology</i> , 105-124.
L167	46.55	7.60	Swiss	Schädler, C., Blöchl, A., Richter, A., & Hoch, G. (2009). Short-term dynamics of nonstructural carbohydrates and

				hemicelluloses in young branches of temperate forest trees during bud break. <i>Tree Physiology</i> , 29(7), 901-911.
L170	61.11	-145.25	US	Sveinbjörnsson, B., Smith, M., Traustason, T., Ruess, R. W., & Sullivan, P. F. (2010). Variation in carbohydrate source-sink relations of forest and treeline white spruce in southern, interior and northern Alaska. <i>Oecologia</i> , 163(4), 833-843.
L170	65.31	-147.19	US	Sveinbjörnsson, B., Smith, M., Traustason, T., Ruess, R. W., & Sullivan, P. F. (2010). Variation in carbohydrate source-sink relations of forest and treeline white spruce in southern, interior and northern Alaska. <i>Oecologia</i> , 163(4), 833-843.
L170	68.15	-152.22	US	Sveinbjörnsson, B., Smith, M., Traustason, T., Ruess, R. W., & Sullivan, P. F. (2010). Variation in carbohydrate source-sink relations of forest and treeline white spruce in southern, interior and northern Alaska. <i>Oecologia</i> , 163(4), 833-843.
L175	45.06	-124.01	US	Matson, P., Johnson, L., Billow, C., Miller, J., & Pu, R. (1994). Seasonal patterns and remote spectral estimation of canopy chemistry across the Oregon transect. <i>Ecological Applications</i> , 4(2), 280-298.
L175	44.58	-123.37	US	Matson, P., Johnson, L., Billow, C., Miller, J., & Pu, R. (1994). Seasonal patterns and remote spectral estimation of canopy chemistry across the Oregon transect. <i>Ecological Applications</i> , 4(2), 280-298.
L175	44.70	-122.84	US	Matson, P., Johnson, L., Billow, C., Miller, J., & Pu, R. (1994). Seasonal patterns and remote spectral estimation of canopy chemistry across the Oregon transect. <i>Ecological Applications</i> , 4(2), 280-298.
L175	44.40	-121.85	US	Matson, P., Johnson, L., Billow, C., Miller, J., & Pu, R. (1994). Seasonal patterns and remote spectral estimation of canopy chemistry across the Oregon transect. <i>Ecological Applications</i> , 4(2), 280-298.
L175	44.58	-121.18	US	Matson, P., Johnson, L., Billow, C., Miller, J., & Pu, R. (1994). Seasonal patterns and remote spectral estimation of canopy chemistry across the Oregon transect. <i>Ecological Applications</i> , 4(2), 280-298.
L175	44.64	-121.10	US	Matson, P., Johnson, L., Billow, C., Miller, J., & Pu, R. (1994). Seasonal patterns and remote spectral estimation of canopy chemistry across the Oregon transect. <i>Ecological Applications</i> , 4(2), 280-298.
L180	47.21	11.47	Austria	Gruber, A., Pirkebner, D., Oberhuber, W., & Wieser, G. (2011). Spatial and seasonal variations in mobile carbohydrates in <i>Pinus cembra</i> in the timberline ecotone of the Central Austrian Alps. <i>European journal of forest research</i> , 130(2), 173-179.
L189	31.02	-92.65	US	Sayer, M. A. S., & Haywood, J. D. (2006). Fine root production and carbohydrate concentrations of mature longleaf pine (<i>Pinus palustris</i> P. Mill.) as affected by season of prescribed fire and drought. <i>Trees</i> , 20(2), 165.
L190	40.06	-105.62	US	Hu, J. I. A., Moore, D. J., & Monson, R. K. (2010). Weather and climate controls over the seasonal carbon isotope dynamics of sugars from subalpine forest trees. <i>Plant, Cell & Environment</i> , 33(1), 35-47.
L192	64.12	19.45	Sweden	Stockfors, J., & Linder, S. (1998). The effect of nutrition on the seasonal course of needle respiration in Norway spruce stands. <i>Trees</i> , 12(3), 130-138.
L198	48.14	11.58	Germany	Fischer, C., & Höll, W. (1991). Food reserves of Scots pine (<i>Pinus sylvestris</i> L.). <i>Trees</i> , 5(4), 187-195.
L202	46.16	7.61	Swiss	Li, M. H., Hoch, G., & Körner, C. (2001). Spatial variability of mobile carbohydrates within <i>Pinus cembra</i> trees at the alpine treeline. <i>Phyton</i> , 41(2), 203-213.
L215	59.69	17.17	Sweden	Ericsson, A. (1979). Effects of fertilization and irrigation on the seasonal changes of carbohydrate reserves in different age-classes of needle on 20-year-old Scots pine trees (<i>Pinus silvestris</i>). <i>Physiologia Plantarum</i> , 45(2), 270-280.
L227	29.67	-82.16	US	Gholz, H. L., & Cropper Jr, W. P. (1991). Carbohydrate dynamics in mature <i>Pinus elliotii</i> var. <i>elliottii</i> trees. <i>Canadian Journal of Forest Research</i> , 21(12), 1742-1747.
L229	46.93	6.72	Swiss	Hoch, G. (2008). The carbon supply of <i>Picea abies</i> trees at a Swiss montane permafrost site. <i>Plant ecology & diversity</i> , 1(1), 13-20.
L230	68.35	18.74	Sweden	Hoch, G., & Körner, C. (2003). The carbon charging of pines at the climatic treeline: a global comparison. <i>Oecologia</i> , 135(1), 10-21.

L230	46.22	7.42	Swiss	Hoch, G., & Körner, C. (2003). The carbon charging of pines at the climatic treeline: a global comparison. <i>Oecologia</i> , 135(1), 10-21.
L235	47.51	8.35	Swiss	Jäggi, M., Saurer, M., Fuhrer, J., & Siegwolf, R. (2002). The relationship between the stable carbon isotope composition of needle bulk material, starch, and tree rings in <i>Picea abies</i> . <i>Oecologia</i> , 131(3), 325-332.
L270	62.60	29.72	Finland	Repo, T., Roitto, M., & Sutinen, S. (2011). Does the removal of snowpack and the consequent changes in soil frost affect the physiology of Norway spruce needles?. <i>Environmental and experimental botany</i> , 72(3), 387-396.
L275	36.02	-78.98	US	Rogers, A., & Ellsworth, D. S. (2002). Photosynthetic acclimation of <i>Pinus taeda</i> (loblolly pine) to long-term growth in elevated pCO ₂ (FACE). <i>Plant, Cell & Environment</i> , 25(7), 851-858.
L282	61.93	34.32	Russia	Kaipainen, L. K., & Sofronova, G. I. (2003). The role of the transport system in the control of the source-sink relations in <i>Pinus sylvestris</i> . <i>Russian Journal of Plant Physiology</i> , 50(1), 125-132.
L286	39.59	-76.36	US	Richardson, A. D., Carbone, M. S., Keenan, T. F., Czimczik, C. I., Hollinger, D. Y., Murakami, P., ... & Xu, X. (2013). Seasonal dynamics and age of stemwood nonstructural carbohydrates in temperate forest trees. <i>New Phytologist</i> , 197(3), 850-861.
L286	44.06	-71.30	US	Richardson, A. D., Carbone, M. S., Keenan, T. F., Czimczik, C. I., Hollinger, D. Y., Murakami, P., ... & Xu, X. (2013). Seasonal dynamics and age of stemwood nonstructural carbohydrates in temperate forest trees. <i>New Phytologist</i> , 197(3), 850-861.
L286	42.53	-72.19	US	Richardson, A. D., Carbone, M. S., Keenan, T. F., Czimczik, C. I., Hollinger, D. Y., Murakami, P., ... & Xu, X. (2013). Seasonal dynamics and age of stemwood nonstructural carbohydrates in temperate forest trees. <i>New Phytologist</i> , 197(3), 850-861.

FluxNet sites

ID	Site Name	Latitude	Longitude	Elevation
CA-Man	Manitoba - Northern Old Black Spruce (former BOREAS Northern Study Area)	55.8796	-98.4808	259
CA-NS1	UCI-1850 burn site	55.8792	-98.4839	260
CA-NS2	UCI-1930 burn site	55.9058	-98.5247	260
CA-NS3	UCI-1964 burn site	55.9117	-98.3822	260
CA-NS4	UCI-1964 burn site wet	55.9144	-98.3806	260
CA-NS5	UCI-1981 burn site	55.8631	-98.485	260
CA-Obs	Saskatchewan - Western Boreal, Mature Black Spruce	53.9872	-105.1178	628.94
CA-Qfo	Quebec - Eastern Boreal, Mature Black Spruce	49.6925	-74.3421	382
CA-SF1	Saskatchewan - Western Boreal, forest burned in 1977	54.485	-105.8176	536
CA-TP3	Ontario - Turkey Point 1974 Plantation White Pine	42.7068	-80.3483	184
CA-TP4	Ontario - Turkey Point 1939 Plantation White Pine	42.7102	-80.3574	184
CH-Dav	Davos	46.8153	9.8559	1639
CZ-BK1	Bily Kriz forest	49.5021	18.5369	875
DE-Obe	Oberbärenburg	50.7867	13.7213	734
DE-Tha	Tharandt	50.9626	13.5651	385

FI-Hyy	Hyytiala	61.8474	24.2948	181
FI-Let	Lettosuo	60.6418	23.9595	111
FI-Sod	Sodankyla	67.3624	26.6386	180
FR-LBr	Le Bray	44.7171	-0.7693	61
IT-La2	Lavarone2	45.9542	11.2853	1350
IT-Lav	Lavarone	45.9562	11.2813	1353
IT-Ren	Renon	46.5869	11.4337	1730
IT-SR2	San Rossore 2	43.732	10.2909	4
IT-SRo	San Rossore	43.7279	10.2844	6
NL-Loo	Loobos	52.1666	5.7436	25
RU-Fyo	Fyodorovskoye	56.4615	32.9221	265
US-Bl0	Blodgett Forest	38.8953	-120.6328	1315
US-GBT	GLEES Brooklyn Tower	41.3658	-106.2397	3191
US-GLE	GLEES	41.3665	-106.2399	3197
US-Me2	Metolius mature ponderosa pine	44.4523	-121.5574	1253
US-Me3	Metolius-second young aged pine	44.3154	-121.6078	1005
US-Me4	Metolius-old aged ponderosa pine	44.4992	-121.6224	922
US-Me5	Metolius-first young aged pine	44.4372	-121.5668	1188
US-Me6	Metolius Young Pine Burn	44.3233	-121.6078	998
US-NR1	Niwot Ridge Forest (LTER NWT1)	40.0329	-105.5464	3050
US-Prr	Poker Flat Research Range Black Spruce Forest	65.1237	-147.4876	210
US-Wi2	Intermediate red pine (IRP)	46.6869	-91.1528	395
US-Wi4	Mature red pine (MRP)	46.7393	-91.1663	352
US-Wi5	Mixed young jack pine (MYJP)	46.6531	-91.0858	353

5.7.3 Supplementary material 3 – Extended results

Bioclimatic Analysis

The PCA of the 81 sites in which wood formation assessments were carried out yielded eight components, of which two were significant, collectively accounting for 79.63% of the variance (Figure S5.3). The first component (PC1), which explained 49.90% of the variance, showed a strong correlation ($r > |0.7|$) with the mean temperatures of the driest, warmest, and coldest quarters (bio9, bio10, and bio11, respectively), as well as the precipitation of the warmest quarter (bio18). The second component (PC2), responsible for explaining 29.73% of the variance, displayed a strong correlation ($r > |0.7|$) with temperature seasonality (bio4). It also showed moderate correlations ($|0.5| > r > |0.7|$) with the mean temperature of the coldest quarter (bio11), precipitation seasonality (bio16), and precipitation of the driest and warmest quarters (bio17 and bio18, respectively).

Partitioning Around Medoids clustering algorithm facilitated the distinction of four bioclimatic clusters within the Northern Hemisphere, with a clear border between climatic biomes (Figure S5.3). The Mediterranean cluster showed direct correlations with the mean temperature of the driest, warmest, and coldest quarters (bio9, bio10, and bio11, respectively) while inversely correlating with precipitation seasonality (bio16) and precipitation of the driest and warmest quarters (bio17 and bio18, respectively) (Figure S5.3). The sites located in temperate biomes belonged to two main clusters, with the colder sites being directly correlated with precipitation seasonality (bio16) and precipitation of the driest and warmest quarters (bio17 and bio18, respectively), and inversely correlated with the mean temperature of the driest, warmest, and coldest quarters (bio9, bio10, bio11, respectively) (Figure S5.3). The central temperate cluster was associated with most bioclimatic variables used in the analysis. Lastly, the boreal

cluster was primarily determined by temperature seasonality (bio4) (Figure S5.3).

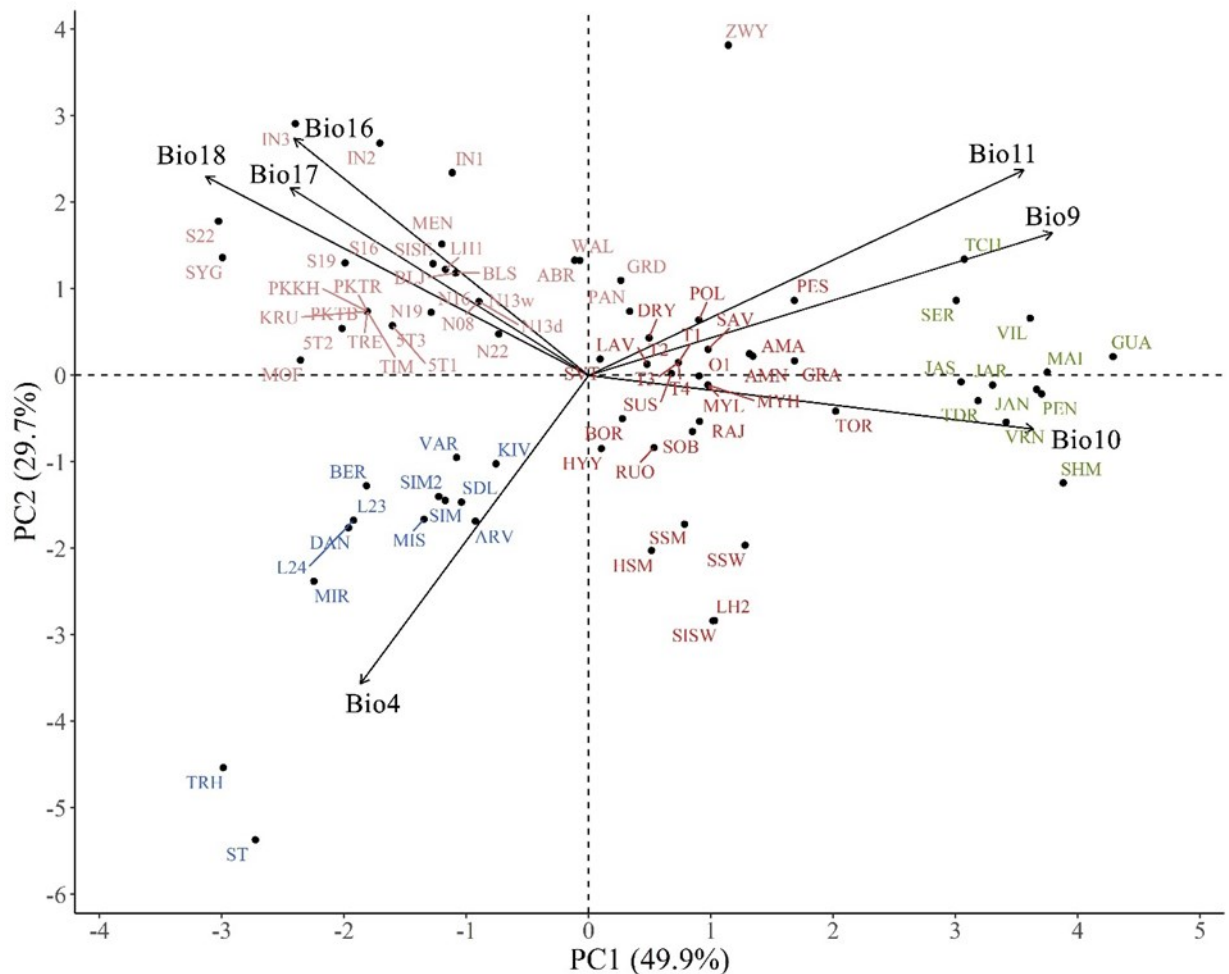


Figure S 5.3 Climate-related variability among 81 wood formation sites of 7 CHELSA (database V2.1) bioclimatic variables summarized in a PCA biplot. The color of the site ID is consistent with color codes used for bioclimatic clusters (boreal –blue labels–, temperate –red labels– and Mediterranean –green labels– biomes). Scores correspond to the first (PC1) and second (PC2) axes of the PCA.

Non-linear fittings

The seasonal dynamics of wood formation (i.e., cambial activity, cell enlargement, and cell wall thickening and lignification), NSC (i.e., starch and soluble sugars in needles, stem and roots), and carbon fluxes (i.e., NEE, GPP and RECO) were fitted with skewed normal distribution or V-type exponential curves with a residual standard error (RSE) ranging between 0.09 and 0.27 (Table S5.2). Tendentially, in each fitting in the boreal

biome, the peak is reached later than in other biomes, and the period of maximum activity (or minimum when considering soluble sugar concentrations) was shorter than in temperate and Mediterranean biomes that followed in this specific order. Therefore, the amplitude of the oscillations among biomes for each fitting was larger in Mediterranean biomes than temperate and boreal biomes.

For each curve we estimated the timing of the maximum value (or minimum when considering soluble sugar concentrations) (Tables S5.3, S5.4, and S5.5). We used 75% of the maximum value as our threshold to define the period of maximum activity (MA). When the curve presented a minimum for soluble sugar concentrations, the period of maximum activity was determined using a 25% threshold of the minimum value.

For each function, the area under the curve (AUC) was quantified, integrating the function itself (Tables S5.3, S5.4, and S5.5). The process of integration was also repeated by calculating the AUC of the period of MA for each function. This latter was obtained by using a definite integral with an interval consisting of a lower and upper limit represented by the points of intersection used to identify 75% of the maximum value of the curve and defining the period of MA (Tables S5.3, S5.4, and S5.5). Figure S5.4 presents a comparison among the AUC of the period of MA for the processes of cell enlargement, GPP, and cell wall thickening and lignification.

Table S 5.3 Summary of all curve fitting. RSE indicates the residual standard error. All fittings were significant, at least with a p-value < 0.05.

V type exponential					
Curve fitting			Parameters estimate (\pm Standard error)		
Biome	Curve	RSE	Ymax	μ	Xmax
Temperate	Needles soluble sugars	0.23	0.40(0.01)	1.02(0.01)	7.61(0.31)
Boreal	Needles soluble sugars	0.25	0.41(0.02)	1.03(0.01)	6.67(0.19)
Mediterranean	Needles starch	0.10	0.53(0.07)	0.42(0.06)	6.09(0.08)
Mediterranean	Needles soluble sugars	0.14	0.39(0.03)	1.01(0.01)	5.52(2.55)
Temperate	Stem soluble sugars	0.27	0.34(0.02)	1.01(0.01)	6.46(0.68)
Boreal	Stem starch	0.22	0.34(0.02)	0.95(0.02)	5.89(0.47)
Boreal	Stem soluble sugars	0.21	0.21(0.02)	1.02(0.01)	6.91(0.54)
Mediterranean	Stem starch	0.14	0.30(0.05)	0.97(0.02)	4.61(1.24)
Mediterranean	Stem soluble sugars	0.24	0.27(0.06)	1.02(0.01)	6.25(1.00)
Temperate	Roots soluble sugars	0.19	0.33(0.02)	1.01(0.01)	6.39(0.52)
Boreal	Roots starch	0.13	0.29(0.02)	0.95(0.01)	6.97(0.43)
Boreal	Roots soluble sugars	0.16	0.28(0.03)	1.03(0.01)	7.03(0.55)
Skewed normal					
Curve fitting			Parameters estimate (\pm Standard error)		
Biome	Curve	RSE	ξ	ω	α
Temperate	Needles starch	0.23	4.04(0.33)	2.62(0.31)	1.25(0.53)
Boreal	Needles starch	0.22	4.61(0.25)	-2.20(0.30)	-1.99(1.00)
Temperate	Stem starch	0.22	2.88(0.41)	4.47(0.68)	2.41(1.26)
Temperate	Roots starch	0.22	1.36(0.80)	6.15(1.38)	2.13(1.84)
Mediterranean	Roots starch	0.14	5.86(0.66)	3.79(1.47)	-2.44(2.01)
Temperate	Roots soluble sugars	0.25	11.76(0.57)	-5.09(1.08)	3.98(4.42)
Boreal	Cambial activity	0.18	143.78(0.72)	50.88(1.25)	2.91(0.26)
Boreal	Cell enlargement	0.20	155.63(0.54)	39.34(0.91)	2.88(0.21)
Boreal	Cell wall thickening and lignification	0.20	180.22(1.11)	43.70(1.34)	1.76(0.16)
Temperate	Cambial activity	0.21	117.39(1.02)	72.14(1.69)	2.85(0.25)
Temperate	Cell enlargement	0.20	158.48(2.72)	37.57(3.98)	0.60(0.41)
Temperate	Cell wall thickening and lignification	0.21	180.99(2.61)	54.83(2.55)	1.31(0.19)
Mediterranean	Cambial activity	0.25	27.94(19.01)	171.02(15.27)	2.63(1.99)
Mediterranean	Cell enlargement	0.23	163.83(2.39)	51.94(2.55)	0.01(2.6)
Mediterranean	Cell wall thickening and lignification	0.26	155.88(3.46)	83.25(3.98)	2.03(0.55)
Temperate	GPP	0.13	229.69(2.85)	98.90(1.44)	-0.67(0.05)
Boreal	GPP	0.11	228.37(1.20)	66.66(0.72)	-0.81(0.04)
Mediterranean	GPP	0.12	80.91(2.96)	161.98(3.18)	1.62(0.09)
Temperate	RECO	0.12	261.51(1.01)	106.65(0.90)	-1.26(0.04)
Boreal	RECO	0.09	244.30(0.72)	68.56(0.56)	-1.09(0.03)
Mediterranean	RECO	0.12	75.57(3.25)	191.75(5.82)	2.08(0.17)
Temperate	NEE	0.20	99.74(0.53)	103.16(0.88)	2.97(0.08)
Boreal	NEE	0.16	127.27(0.45)	59.98(0.81)	3.59(0.17)
Mediterranean	NEE	0.20	199.63(18.51)	96.70(10.24)	-0.71(0.38)

Cambial activity and xylem formation

Cambial activity and wood formation stages were fitted with skewed normal distribution curves with a residual standard error (RSE) ranging between 0.14 and 0.26 (Table S5.2). For cambial activity and cells differentiation stages, the peak was reached later in the boreal biome, and the period of maximum activity was shorter than in temperate and Mediterranean biomes that followed in this specific order (Figure S5.1). Cambial activity in boreal and temperate ecosystems showed a peak at the beginning of summer and end of spring, respectively. In the Mediterranean biome, the peak was substantially earlier during spring. Cell differentiation showed a peak in the number of cells around the summer solstice (i.e., middle of June – start of July), with cell enlargement peaks localized in mid-June and cell wall thickening and lignification peaks localized at the beginning of July (Figure S5.1).

The Mediterranean climate is characterised by dry and hot summers, and optimal growth conditions occur during the cooler and rainy springs and autumns. Being sensitive to drought, radial growth may cease in response to water shortage (Muller et al., 2011), leading to a bimodal growth pattern with a temporary cessation of growth in summer (Camarero et al., 2010). For this reason, we tried to fit a bimodal curve for the Mediterranean biome, but, finally, comparing the fittings, it was decided to use a skewed normal distribution that guaranteed a better fitting. Growth resumption in autumn after summer cease in response to drought is a plastic adaptation to large spatiotemporal variability in the climatic conditions in the Mediterranean region. However, even if the drought period can be temporally localized during a broad time window such as the summer season, the exact period when a moisture shortage comes into play can vary spatially and year by year in the Mediterranean region (Martins et al., 2012; Ruiz-Sinoga

et al., 2012). Moreover, it is largely recognised that different species can show different responses to the dry period (Camarero et al., 2010). For all these reasons, in this context, by considering several species and different years, it was unlikely to highlight a bimodal growth pattern in the Mediterranean biome.

Table S 5.4 Maximum value (Max), onset, ending and duration of the period of maximum activity (MA), total and period of maximum activity area under the curve (AUC) and their ratio for all the curves describing the seasonal dynamics of wood formation (i.e., cambial activity, cell enlargement, and cell wall thickening and lignification).

Wood formation								
Biome	Process	Max (DOY)	Onset MA (DOY)	Ending MA (DOY)	Duration MA (days)	Total AUC	AUC MA	AUC MA / Total AUC (%)
Boreal	Cambial activity	168.13	150.20	194.61	44.41	62.61	32.53	51.96
Temperate	Cambial activity	152.18	124.75	188.77	64.02	85.53	44.94	52.54
Mediterranean	Cambial activity	107.34	36.41	205.13	168.72	151.93	96.42	63.46
Boreal	Cell enlargement	174.53	159.66	194.47	34.81	51.73	27.16	52.50
Temperate	Cell enlargement	173.35	147.61	199.35	51.74	68.77	37.90	55.11
Mediterranean	Cell enlargement	164.50	125.04	203.85	78.81	95.85	52.95	55.24
Boreal	Cell wall thickening and lignification	203.80	182.63	227.78	45.15	69.25	37.31	53.88
Temperate	Cell wall thickening and lignification	193.47	170.31	232.76	62.45	89.56	48.85	54.54
Mediterranean	Cell wall thickening and lignification	182.95	155.23	239.32	84.09	103.92	56.27	54.15

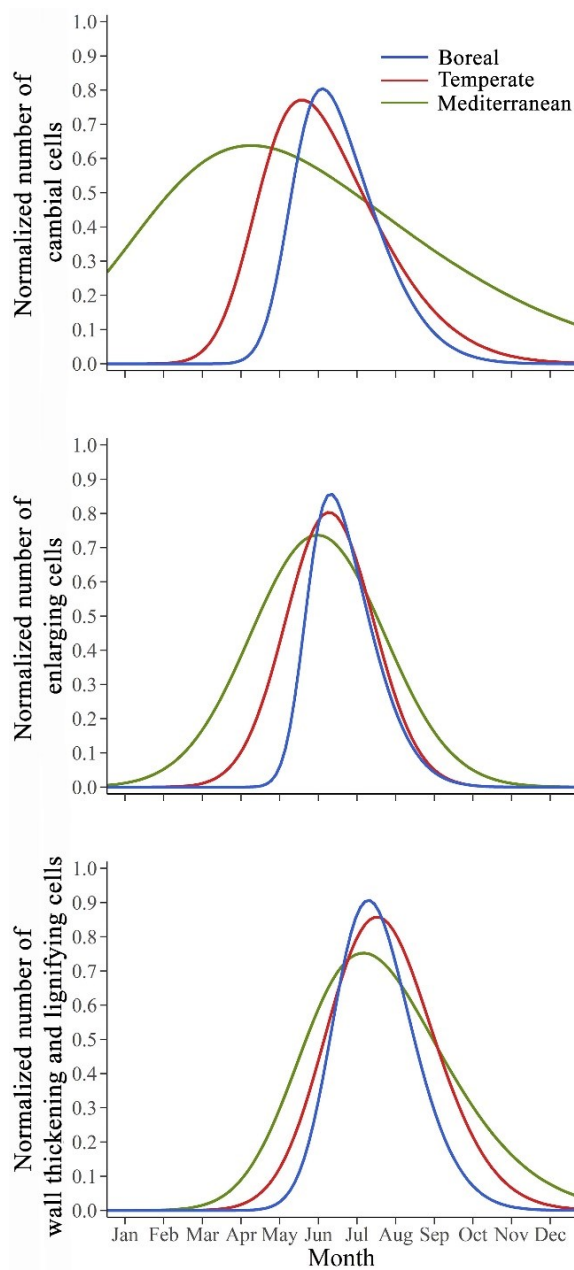


Figure S 5.4 Seasonal pattern of cambial activity and cell differentiation stages (i.e., enlargement and secondary wall thickening and lignification), normalized according to the biome and study site in conifers as a function of the biome (i.e., Boreal, Temperate and Mediterranean).

NSC

Seasonal oscillations of starch and soluble sugars for all organs in all biomes showed a residual standard error (RSE) ranging between 0.10 and 0.27 (Table S5.2). The seasonal patterns of starch and soluble sugars were characterised by opposite temporal dynamics, particularly evident in needles with a very sharp starch peak in late spring-early summer strictly followed by the seasonal minimum for soluble sugars (Figure S5.2). The amplitude of the oscillations among biomes was most prominent for starch and particularly noticeable in needles. Starch levels peaked belowground first (~early spring), then in stems (mid-spring) and finally in needles (late spring-early summer) but not regarding the boreal biome where the peak of starch in roots was later than the peak in needles and stem. Soluble sugars in roots and stems were less variable, with a hint of a seasonal minimum around late spring-early summer (Figure S5.2). However, soluble sugar concentration in roots showed a peak in autumn in the Mediterranean biome. Boreal and temperate ecosystems showed contrasting temporal dynamics for starch and soluble sugar. Starch peaked in needles, stems and roots around late spring-early summer, mid-spring, and midsummer, respectively. In contrast, soluble sugars were lowest in all organs from late spring to midsummer. Temperate biomes were characterised by maximum starch concentrations towards late spring-early summer, particularly in needles, strictly followed by minimum levels of soluble sugars in all organs. In the Mediterranean, the magnitude of such oscillation was generally lower than those observed for boreal and temperate ecosystems (Figure S5.2).

Table S 5.5 Maximum value (Max), onset, ending and duration of the period of maximum activity (MA), total and period of maximum activity area under the curve (AUC) and their ratio for all the curves describing the seasonal dynamics of NSC (i.e., starch and soluble sugars in needles, stem and roots).

Non structural carbohydrates								
Biome	Process	Max (month)	Onset MA (month)	Ending MA (month)	Duration MA (months)	Total AUC	AUC MA	AUC MA / Total AUC (%)
Boreal	Needles starch	5.78	4.77	6.95	2.18	2.05	1.10	53.66
Temperate	Needles starch	5.45	3.98	7.01	3.03	2.65	1.46	55.09
Mediterranean	Needles starch	4.79	3.03	7.55	4.52	1.03	0.66	64.08
Boreal	Needles soluble sugars	6.89	3.45	10.07	6.62	6.03	2.99	49.59
Temperate	Needles soluble sugars	6.99	3.95	11.26	7.31	5.53	3.36	60.76
Mediterranean	Needles soluble sugars	5.52	2.40	8.63	6.23	4.57	2.46	53.83
Boreal	Stem starch	5.89	3.75	8.02	4.27	2.45	1.32	53.88
Temperate	Stem starch	5.13	2.95	7.58	4.63	2.90	1.79	61.72
Mediterranean	Stem starch	4.61	1.97	7.26	5.29	2.39	1.47	61.51
Boreal	Stem soluble sugars	6.91	3.99	9.75	5.76	3.01	1.29	42.86
Temperate	Stem soluble sugars	6.46	3.34	9.28	5.94	4.19	2.09	49.88
Mediterranean	Stem soluble sugars	6.25	3.08	9.42	6.34	3.74	1.83	48.93
Boreal	Roots starch	6.97	4.93	9.01	4.08	2.07	1.10	53.14
Temperate	Roots starch	4.58	2.38	7.12	4.74	4.29	2.35	54.78
Mediterranean	Roots starch	3.94	1.99	5.51	3.52	4.76	3.14	65.97
Boreal	Roots soluble sugars	7.03	3.42	10.64	7.22	4.39	2.31	52.62
Temperate	Roots soluble sugars	6.39	3.38	9.39	6.01	4.39	2.08	47.38
Mediterranean	Roots soluble sugars	9.63	7.07	11.24	4.17	6.74	3.85	57.12

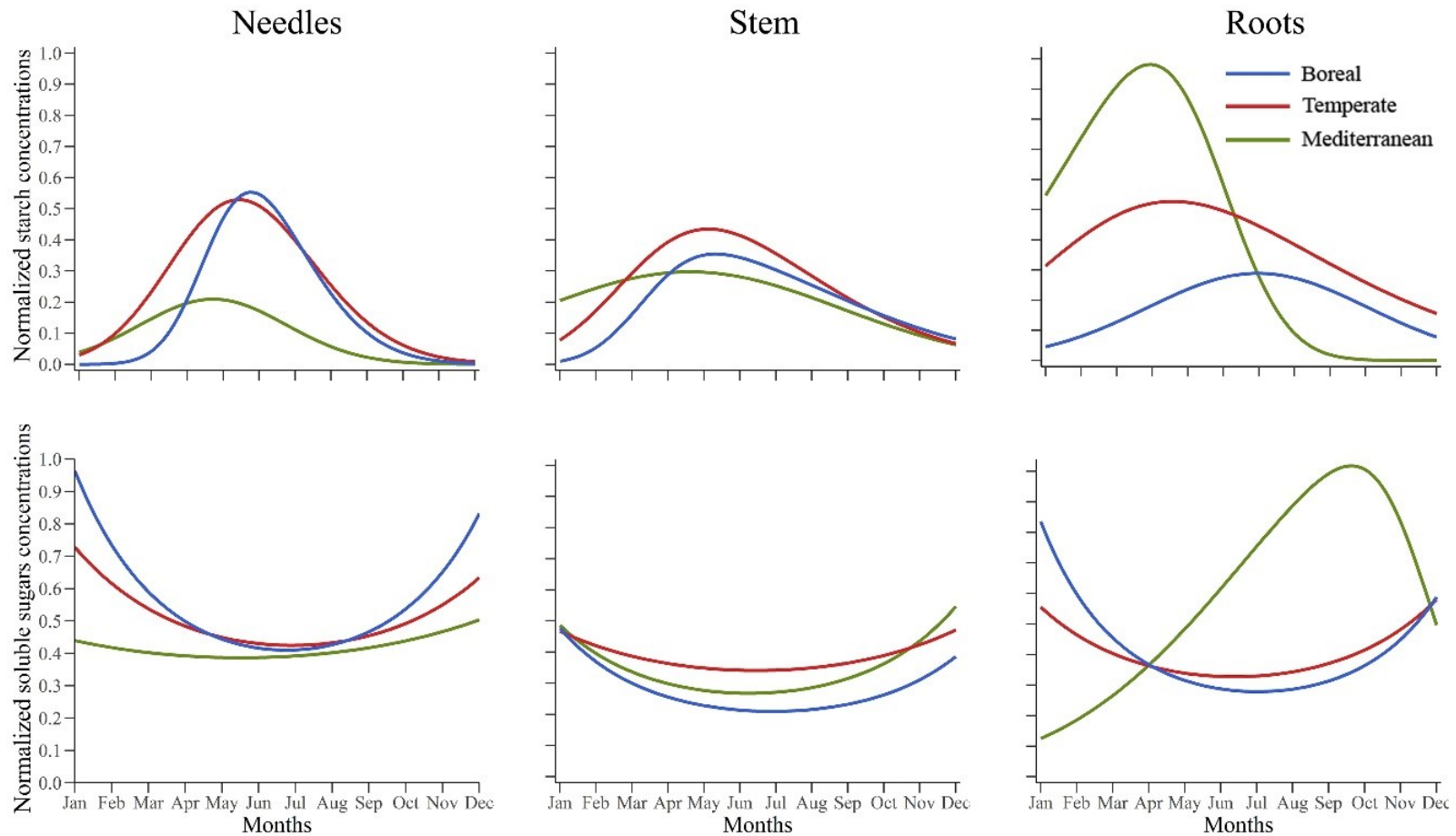


Figure S 5.5 Seasonal dynamics of NSC concentration (i.e., starch and soluble sugars, normalized according to biome, organ, study and quantification method) in conifers as a function of organ (i.e., needles, stem, roots) and biome (i.e., Boreal, Temperate and Mediterranean).

Carbon fluxes

All carbon flux dynamics (i.e., NEE, GPP, RECO) were fitted with skewed normal distribution curves with a residual standard error (RSE) ranging between 0.09 and 0.20 (Table S5.2). For each flux, in the boreal biome the peak was reached later, and the period of maximum activity was shorter, generally starting later and ending earlier than temperate and Mediterranean biomes that followed in this specific order (Figure S5.6). The NEE peak was earlier than the RECO and GPP peaks for each biome and reached a maximum at the end of spring between May and June. RECO and GPP peaked later during summer, with the peak of RECO following the peak of GPP by about two weeks in each biome (Figure S5.6).

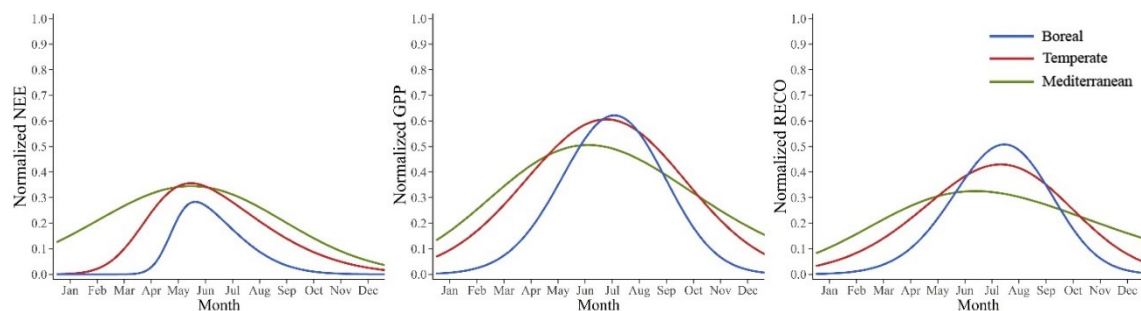


Figure S 5.6 Seasonal pattern of Net Ecosystem Exchange (NEE), Ecosystem Respiration (RECO), and Gross Primary Production (GPP), normalized according to the biome, flux type (i.e., NEE, RECO and GPP) and study site in conifers as a function of the biome (i.e., Boreal, Temperate and Mediterranean).

Table S 5.6 Maximum value (Max), onset, ending and duration of the period of maximum activity (MA), total and period of maximum activity area under the curve (AUC) and their ratio for all the curves describing the seasonal dynamics of carbon fluxes (i.e., NEE, GPP and RECO).

C fluxes								
Biome	Process	Max (DOY)	Onset MA (DOY)	Ending MA (DOY)	Duration MA (days)	Total AUC	AUC MA	AUC MA / Total AUC (%)
Boreal	GPP	197.28	153.85	239.76	85.91	89.23	48.79	54.68
Temperate	GPP	188.16	125.51	250.03	124.52	128.43	64.42	50.16
Mediterranean	GPP	168.22	103.51	238.56	135.05	129.03	69.68	54.00
Boreal	RECO	208.72	166.78	248.83	82.05	79.87	45.94	57.52
Temperate	RECO	204.51	145.47	260.22	114.75	85.81	43.07	50.19
Mediterranean	RECO	176.51	107.47	255.67	148.20	86.46	45.43	52.54
Boreal	NEE	153.59	133.64	183.42	49.78	24.91	12.85	51.59
Temperate	NEE	148.76	110.63	200.49	89.86	55.38	29.14	52.62
Mediterranean	NEE	147.58	94.47	219.73	125.26	80.57	40.58	50.37

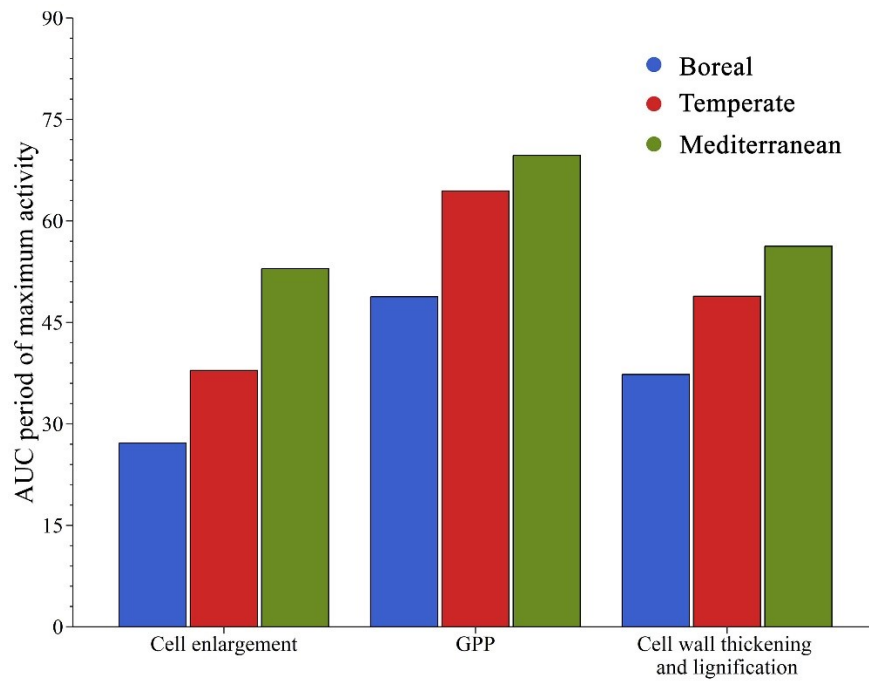


Figure S 5.7 Area under the curve (AUC) of the period of maximum activity (MA) of the processes of Gross Primary Production (GPP) and phenological phases of cell enlargement and cell wall thickening and lignification during wood formation in boreal, temperate and Mediterranean biomes.

Cambial activity and wood formation

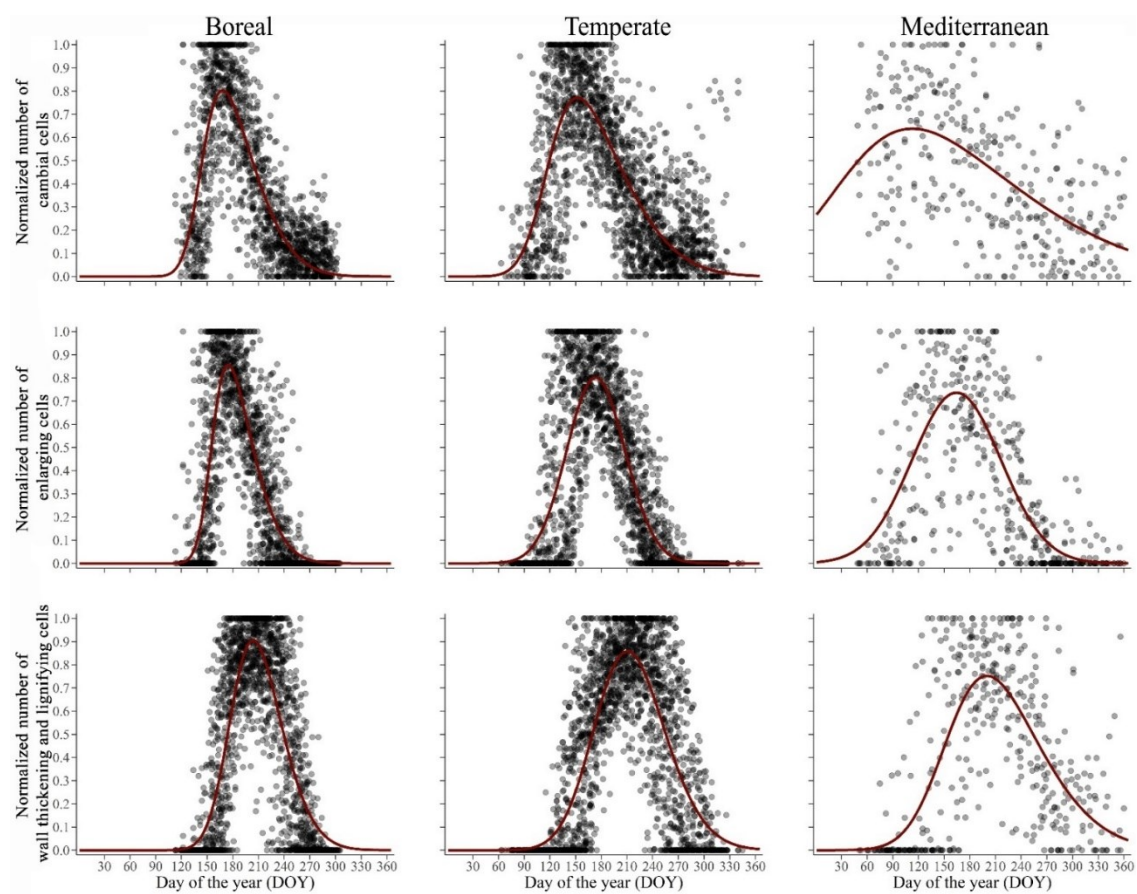


Figure S 5.8 Fitting details for cambial activity and cell differentiation phenological phase in boreal, temperate and Mediterranean biomes.

NSC seasonal dynamics

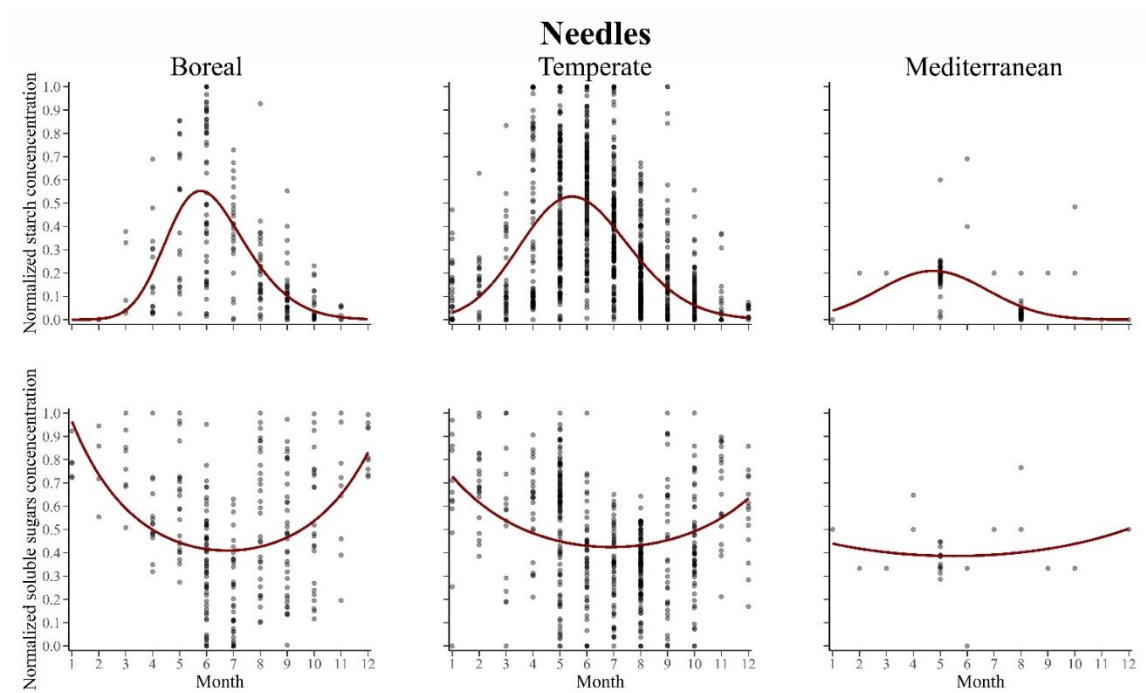


Figure S 5.9 Fitting details for starch and soluble sugars in needles in boreal, temperate and Mediterranean biomes.

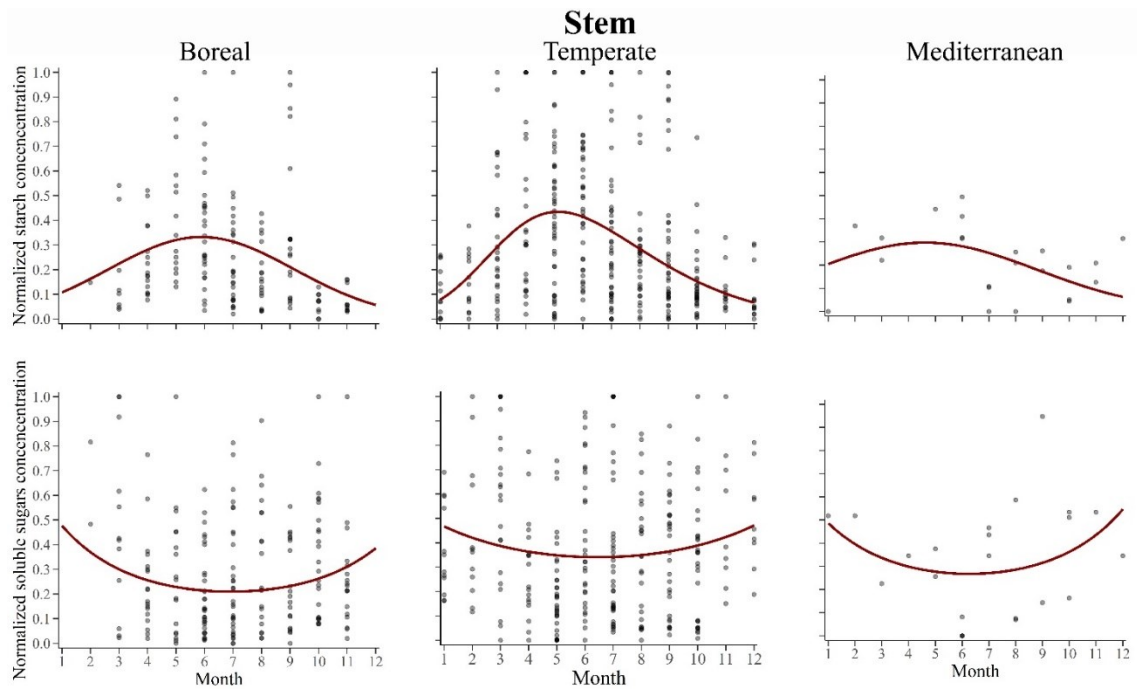


Figure S 5.10 Fitting details for starch and soluble sugars in stem in boreal, temperate and Mediterranean biomes.

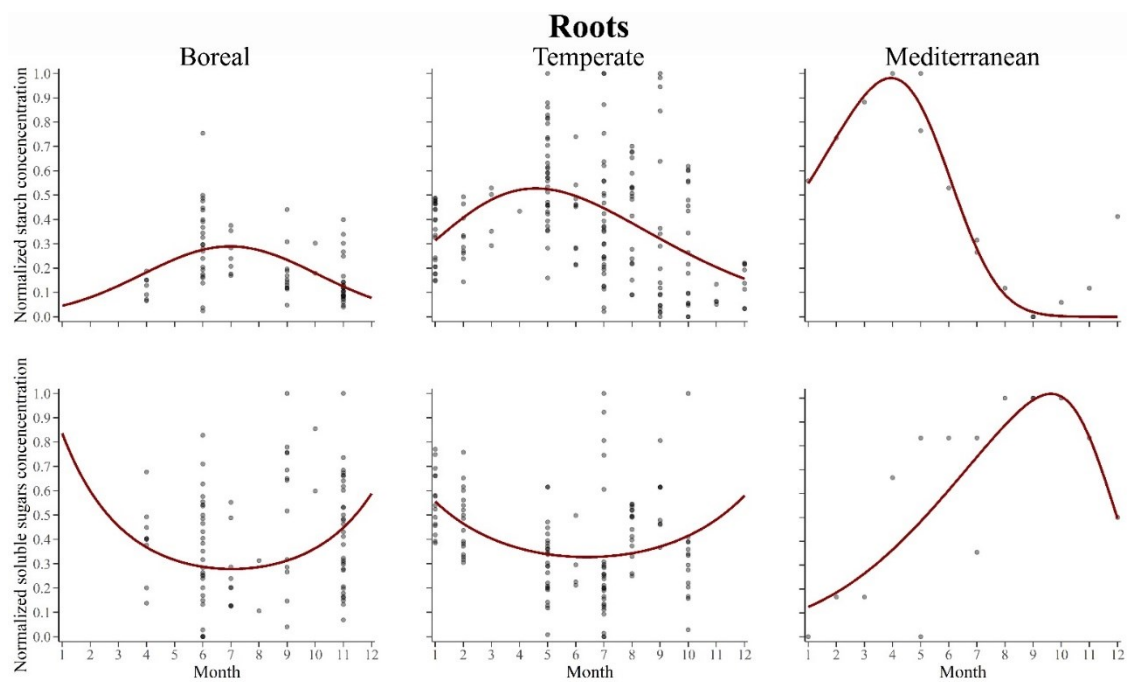


Figure S 5.11 Fitting details for starch and soluble sugars in roots in boreal, temperate and Mediterranean biomes.

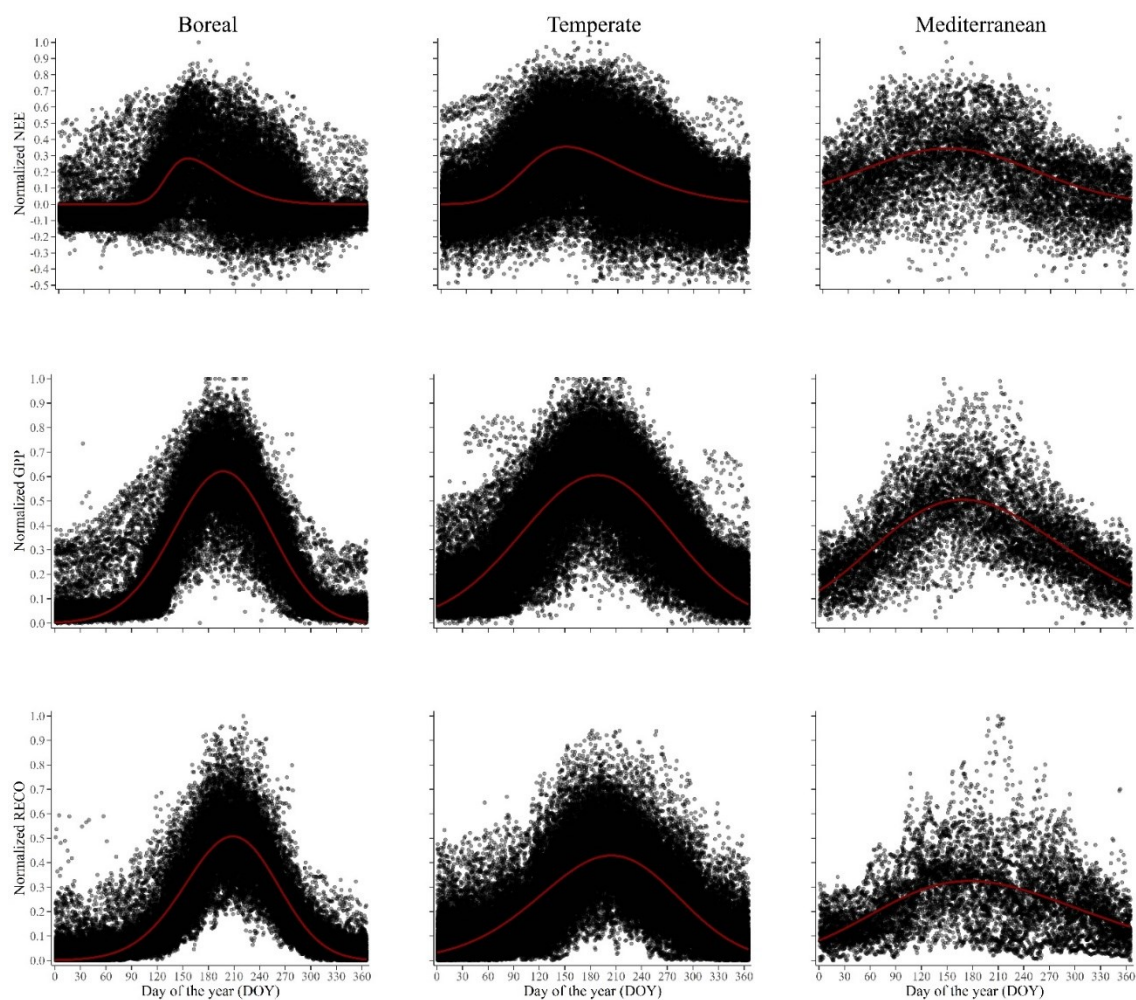
Seasonal carbon fluxes

Figure S 5.12 Fitting details for Net Ecosystem Exchange (NEE), Ecosystem Respiration (RECO) and Gross Primary Production (GPP) in boreal, temperate and Mediterranean biomes.

Table S 5.7 Delta (i.e., subtraction) between the timing of 10th, 25th, 50th, 75th, 90th percentile and peak (i.e., 100th percentile) among C fluxes, i.e., NEE, GPP, RECO and phenological phases of wood formation, i.e., cambial activity, cell enlargement and cell wall thickening and lignification in boreal, temperate and Mediterranean biomes.

C fluxes - Wood formation phases	Biome	Percentile value	Curve position	Delta
NEE - Cambial activity	Boreal	10	Ascending	-15.4
NEE - Cambial activity	Boreal	25	Ascending	-15.53
NEE - Cambial activity	Boreal	50	Ascending	-15.57
NEE - Cambial activity	Boreal	75	Ascending	-16.56
NEE - Cambial activity	Boreal	90	Ascending	-15.29
NEE - Cambial activity	Boreal	10	Descending	16.33
NEE - Cambial activity	Boreal	25	Descending	6.8
NEE - Cambial activity	Boreal	50	Descending	-2.89
NEE - Cambial activity	Boreal	75	Descending	-11.19
NEE - Cambial activity	Boreal	90	Descending	-15.64
NEE - Cambial activity	Boreal	100	Peak	-14.54
NEE - Cambial activity	Temperate	10	Ascending	-29.96
NEE - Cambial activity	Temperate	25	Ascending	-24.93
NEE - Cambial activity	Temperate	50	Ascending	-19.44
NEE - Cambial activity	Temperate	75	Ascending	-14.12
NEE - Cambial activity	Temperate	90	Ascending	-10.34
NEE - Cambial activity	Temperate	10	Descending	81.82
NEE - Cambial activity	Temperate	25	Descending	52.04
NEE - Cambial activity	Temperate	50	Descending	23.24
NEE - Cambial activity	Temperate	75	Descending	11.72
NEE - Cambial activity	Temperate	90	Descending	5.19
NEE - Cambial activity	Temperate	100	Peak	-3.42
NEE - Cambial activity	Mediterranean	10	Ascending	-37.03
NEE - Cambial activity	Mediterranean	25	Ascending	-31.03

NEE - Cambial activity	Mediterranean	50	Ascending	-9.53
NEE - Cambial activity	Mediterranean	75	Ascending	0.65
NEE - Cambial activity	Mediterranean	90	Ascending	33.06
NEE - Cambial activity	Mediterranean	10	Descending	80.37
NEE - Cambial activity	Mediterranean	25	Descending	70.37
NEE - Cambial activity	Mediterranean	50	Descending	65.36
NEE - Cambial activity	Mediterranean	75	Descending	39.22
NEE - Cambial activity	Mediterranean	90	Descending	42.1
NEE - Cambial activity	Mediterranean	100	Peak	40.24
NEE - Cell enlargement	Boreal	10	Ascending	-32.36
NEE - Cell enlargement	Boreal	25	Ascending	-30.42
NEE - Cell enlargement	Boreal	50	Ascending	-28.26
NEE - Cell enlargement	Boreal	75	Ascending	-26.02
NEE - Cell enlargement	Boreal	90	Ascending	-24.39
NEE - Cell enlargement	Boreal	10	Descending	2.42
NEE - Cell enlargement	Boreal	25	Descending	-1.84
NEE - Cell enlargement	Boreal	50	Descending	-6.38
NEE - Cell enlargement	Boreal	75	Descending	-11.05
NEE - Cell enlargement	Boreal	90	Descending	-22.51
NEE - Cell enlargement	Boreal	100	Peak	-20.94
NEE - Cell enlargement	Temperate	10	Ascending	-47.4
NEE - Cell enlargement	Temperate	25	Ascending	-44.89
NEE - Cell enlargement	Temperate	50	Ascending	-41.36
NEE - Cell enlargement	Temperate	75	Ascending	-36.98
NEE - Cell enlargement	Temperate	90	Ascending	-33.21
NEE - Cell enlargement	Temperate	10	Descending	50.69
NEE - Cell enlargement	Temperate	25	Descending	36.85
NEE - Cell enlargement	Temperate	50	Descending	23.06

NEE - Cell enlargement	Temperate	75	Descending	1.14
NEE - Cell enlargement	Temperate	90	Descending	-11.02
NEE - Cell enlargement	Temperate	100	Peak	-24.59
NEE - Cell enlargement	Mediterranean	10	Ascending	-19.99
NEE - Cell enlargement	Mediterranean	25	Ascending	-28.09
NEE - Cell enlargement	Mediterranean	50	Ascending	-44.08
NEE - Cell enlargement	Mediterranean	75	Ascending	-30.97
NEE - Cell enlargement	Mediterranean	90	Ascending	-21.42
NEE - Cell enlargement	Mediterranean	10	Descending	22.97
NEE - Cell enlargement	Mediterranean	25	Descending	24.74
NEE - Cell enlargement	Mediterranean	50	Descending	9.2
NEE - Cell enlargement	Mediterranean	75	Descending	-3
NEE - Cell enlargement	Mediterranean	90	Descending	-5.45
NEE - Cell enlargement	Mediterranean	100	Peak	-16.92
NEE - Cell wall thickening and lignification	Boreal	10	Ascending	-42.66
NEE - Cell wall thickening and lignification	Boreal	25	Ascending	-45.14
NEE - Cell wall thickening and lignification	Boreal	50	Ascending	-47.45
NEE - Cell wall thickening and lignification	Boreal	75	Ascending	-48.99
NEE - Cell wall thickening and lignification	Boreal	90	Ascending	-49.98
NEE - Cell wall thickening and lignification	Boreal	10	Descending	-20.52
NEE - Cell wall thickening and lignification	Boreal	25	Descending	-28.67
NEE - Cell wall thickening and lignification	Boreal	50	Descending	-37.24
NEE - Cell wall thickening and lignification	Boreal	75	Descending	-44.36

NEE - Cell wall thickening and lignification	Boreal	90	Descending	-47.75
NEE - Cell wall thickening and lignification	Boreal	100	Peak	-50.21
NEE - Cell wall thickening and lignification	Temperate	10	Ascending	-74.82
NEE - Cell wall thickening and lignification	Temperate	25	Ascending	-73.86
NEE - Cell wall thickening and lignification	Temperate	50	Ascending	-72.18
NEE - Cell wall thickening and lignification	Temperate	75	Ascending	-59.68
NEE - Cell wall thickening and lignification	Temperate	90	Ascending	-57.48
NEE - Cell wall thickening and lignification	Temperate	10	Descending	42.22
NEE - Cell wall thickening and lignification	Temperate	25	Descending	17.91
NEE - Cell wall thickening and lignification	Temperate	50	Descending	-4.68
NEE - Cell wall thickening and lignification	Temperate	75	Descending	-32.27
NEE - Cell wall thickening and lignification	Temperate	90	Descending	-51.67
NEE - Cell wall thickening and lignification	Temperate	100	Peak	-44.71
NEE - Cell wall thickening and lignification	Mediterranean	10	Ascending	-68.98
NEE - Cell wall thickening and lignification	Mediterranean	25	Ascending	-72.2
NEE - Cell wall thickening and lignification	Mediterranean	50	Ascending	-84.01
NEE - Cell wall thickening and lignification	Mediterranean	75	Ascending	-61.16

NEE - Cell wall thickening and lignification	Mediterranean	90	Ascending	-57.34
NEE - Cell wall thickening and lignification	Mediterranean	10	Descending	-11.75
NEE - Cell wall thickening and lignification	Mediterranean	25	Descending	-11.31
NEE - Cell wall thickening and lignification	Mediterranean	50	Descending	-18.87
NEE - Cell wall thickening and lignification	Mediterranean	75	Descending	-38.47
NEE - Cell wall thickening and lignification	Mediterranean	90	Descending	-30.2
NEE - Cell wall thickening and lignification	Mediterranean	100	Peak	-35.37
GPP - Cambial activity	Boreal	10	Ascending	-47.79
GPP - Cambial activity	Boreal	25	Ascending	-29.27
GPP - Cambial activity	Boreal	50	Ascending	-10.6
GPP - Cambial activity	Boreal	75	Ascending	3.65
GPP - Cambial activity	Boreal	90	Ascending	14.98
GPP - Cambial activity	Boreal	10	Descending	70.34
GPP - Cambial activity	Boreal	25	Descending	63.68
GPP - Cambial activity	Boreal	50	Descending	54.75
GPP - Cambial activity	Boreal	75	Descending	45.15
GPP - Cambial activity	Boreal	90	Descending	37.39
GPP - Cambial activity	Boreal	100	Peak	29.15
GPP - Cambial activity	Temperate	10	Ascending	-46.81
GPP - Cambial activity	Temperate	25	Ascending	-35.59
GPP - Cambial activity	Temperate	50	Ascending	-16.67
GPP - Cambial activity	Temperate	75	Ascending	0.76
GPP - Cambial activity	Temperate	90	Ascending	16.12
GPP - Cambial activity	Temperate	10	Descending	87.3

GPP - Cambial activity	Temperate	25	Descending	80.76
GPP - Cambial activity	Temperate	50	Descending	65.86
GPP - Cambial activity	Temperate	75	Descending	59.75
GPP - Cambial activity	Temperate	90	Descending	52.2
GPP - Cambial activity	Temperate	100	Peak	35.98
GPP - Cambial activity	Mediterranean	10	Ascending	-13.87
GPP - Cambial activity	Mediterranean	25	Ascending	-4.5
GPP - Cambial activity	Mediterranean	50	Ascending	15.92
GPP - Cambial activity	Mediterranean	75	Ascending	39.09
GPP - Cambial activity	Mediterranean	90	Ascending	39.19
GPP - Cambial activity	Mediterranean	10	Descending	97.95
GPP - Cambial activity	Mediterranean	25	Descending	74.95
GPP - Cambial activity	Mediterranean	50	Descending	59.94
GPP - Cambial activity	Mediterranean	75	Descending	58.19
GPP - Cambial activity	Mediterranean	90	Descending	58.12
GPP - Cambial activity	Mediterranean	100	Peak	60.88
GPP - Cell enlargement	Boreal	10	Ascending	-64.75
GPP - Cell enlargement	Boreal	25	Ascending	-44.16
GPP - Cell enlargement	Boreal	50	Ascending	-23.29
GPP - Cell enlargement	Boreal	75	Ascending	-5.81
GPP - Cell enlargement	Boreal	90	Ascending	5.88
GPP - Cell enlargement	Boreal	10	Descending	65.43
GPP - Cell enlargement	Boreal	25	Descending	55.04
GPP - Cell enlargement	Boreal	50	Descending	51.26
GPP - Cell enlargement	Boreal	75	Descending	45.29
GPP - Cell enlargement	Boreal	90	Descending	30.52
GPP - Cell enlargement	Boreal	100	Peak	22.75
GPP - Cell enlargement	Temperate	10	Ascending	-64.25

GPP - Cell enlargement	Temperate	25	Ascending	-55.55
GPP - Cell enlargement	Temperate	50	Ascending	-38.59
GPP - Cell enlargement	Temperate	75	Ascending	-22.1
GPP - Cell enlargement	Temperate	90	Ascending	-6.75
GPP - Cell enlargement	Temperate	10	Descending	56.17
GPP - Cell enlargement	Temperate	25	Descending	65.57
GPP - Cell enlargement	Temperate	50	Descending	65.68
GPP - Cell enlargement	Temperate	75	Descending	49.17
GPP - Cell enlargement	Temperate	90	Descending	35.99
GPP - Cell enlargement	Temperate	100	Peak	14.81
GPP - Cell enlargement	Mediterranean	10	Ascending	-37.1
GPP - Cell enlargement	Mediterranean	25	Ascending	-41.96
GPP - Cell enlargement	Mediterranean	50	Ascending	-36.52
GPP - Cell enlargement	Mediterranean	75	Ascending	-25.54
GPP - Cell enlargement	Mediterranean	90	Ascending	-15.13
GPP - Cell enlargement	Mediterranean	10	Descending	53.76
GPP - Cell enlargement	Mediterranean	25	Descending	59.36
GPP - Cell enlargement	Mediterranean	50	Descending	39.61
GPP - Cell enlargement	Mediterranean	75	Descending	39.47
GPP - Cell enlargement	Mediterranean	90	Descending	38
GPP - Cell enlargement	Mediterranean	100	Peak	3.72
GPP - Cell wall thickening and lignification	Boreal	10	Ascending	-75.05
GPP - Cell wall thickening and lignification	Boreal	25	Ascending	-58.88
GPP - Cell wall thickening and lignification	Boreal	50	Ascending	-42.48
GPP - Cell wall thickening and lignification	Boreal	75	Ascending	-28.78

GPP - Cell wall thickening and lignification	Boreal	90	Ascending	-19.71
GPP - Cell wall thickening and lignification	Boreal	10	Descending	33.49
GPP - Cell wall thickening and lignification	Boreal	25	Descending	28.21
GPP - Cell wall thickening and lignification	Boreal	50	Descending	20.4
GPP - Cell wall thickening and lignification	Boreal	75	Descending	11.98
GPP - Cell wall thickening and lignification	Boreal	90	Descending	5.28
GPP - Cell wall thickening and lignification	Boreal	100	Peak	-6.52
GPP - Cell wall thickening and lignification	Temperate	10	Ascending	-91.67
GPP - Cell wall thickening and lignification	Temperate	25	Ascending	-84.52
GPP - Cell wall thickening and lignification	Temperate	50	Ascending	-69.41
GPP - Cell wall thickening and lignification	Temperate	75	Ascending	-44.8
GPP - Cell wall thickening and lignification	Temperate	90	Ascending	-31.02
GPP - Cell wall thickening and lignification	Temperate	10	Descending	47.7
GPP - Cell wall thickening and lignification	Temperate	25	Descending	46.63
GPP - Cell wall thickening and lignification	Temperate	50	Descending	37.94
GPP - Cell wall thickening and lignification	Temperate	75	Descending	15.76
GPP - Cell wall thickening and lignification	Temperate	90	Descending	-4.66

GPP - Cell wall thickening and lignification	Temperate	100	Peak	-5.31
GPP - Cell wall thickening and lignification	Mediterranean	10	Ascending	-86.09
GPP - Cell wall thickening and lignification	Mediterranean	25	Ascending	-86.07
GPP - Cell wall thickening and lignification	Mediterranean	50	Ascending	-76.45
GPP - Cell wall thickening and lignification	Mediterranean	75	Ascending	-55.73
GPP - Cell wall thickening and lignification	Mediterranean	90	Ascending	-51.05
GPP - Cell wall thickening and lignification	Mediterranean	10	Descending	19.04
GPP - Cell wall thickening and lignification	Mediterranean	25	Descending	23.31
GPP - Cell wall thickening and lignification	Mediterranean	50	Descending	11.54
GPP - Cell wall thickening and lignification	Mediterranean	75	Descending	4
GPP - Cell wall thickening and lignification	Mediterranean	90	Descending	-12.47
GPP - Cell wall thickening and lignification	Mediterranean	100	Peak	-14.73
RECO - Cambial activity	Boreal	10	Ascending	-36.74
RECO - Cambial activity	Boreal	25	Ascending	-16.72
RECO - Cambial activity	Boreal	50	Ascending	2.42
RECO - Cambial activity	Boreal	75	Ascending	16.58
RECO - Cambial activity	Boreal	90	Ascending	27.4
RECO - Cambial activity	Boreal	10	Descending	75.62
RECO - Cambial activity	Boreal	25	Descending	69.71
RECO - Cambial activity	Boreal	50	Descending	62.46
RECO - Cambial activity	Boreal	75	Descending	54.22

RECO - Cambial activity	Boreal	90	Descending	47.54
RECO - Cambial activity	Boreal	100	Peak	40.59
RECO - Cambial activity	Temperate	10	Ascending	-46.2
RECO - Cambial activity	Temperate	25	Ascending	-26.4
RECO - Cambial activity	Temperate	50	Ascending	-1.9
RECO - Cambial activity	Temperate	75	Ascending	20.72
RECO - Cambial activity	Temperate	90	Ascending	33.36
RECO - Cambial activity	Temperate	10	Descending	98.6
RECO - Cambial activity	Temperate	25	Descending	91.79
RECO - Cambial activity	Temperate	50	Descending	77.25
RECO - Cambial activity	Temperate	75	Descending	71.45
RECO - Cambial activity	Temperate	90	Descending	66.65
RECO - Cambial activity	Temperate	100	Peak	52.33
RECO - Cambial activity	Mediterranean	10	Ascending	-13.24
RECO - Cambial activity	Mediterranean	25	Ascending	-3.19
RECO - Cambial activity	Mediterranean	50	Ascending	18.28
RECO - Cambial activity	Mediterranean	75	Ascending	37.06
RECO - Cambial activity	Mediterranean	90	Ascending	44.3
RECO - Cambial activity	Mediterranean	10	Descending	84.62
RECO - Cambial activity	Mediterranean	25	Descending	91.44
RECO - Cambial activity	Mediterranean	50	Descending	85.62
RECO - Cambial activity	Mediterranean	75	Descending	70.54
RECO - Cambial activity	Mediterranean	90	Descending	67.5
RECO - Cambial activity	Mediterranean	100	Peak	69.17
RECO - Cell enlargement	Boreal	10	Ascending	-53.7
RECO - Cell enlargement	Boreal	25	Ascending	-31.61
RECO - Cell enlargement	Boreal	50	Ascending	-10.27
RECO - Cell enlargement	Boreal	75	Ascending	7.12

RECO - Cell enlargement	Boreal	90	Ascending	18.3
RECO - Cell enlargement	Boreal	10	Descending	61.71
RECO - Cell enlargement	Boreal	25	Descending	61.07
RECO - Cell enlargement	Boreal	50	Descending	58.97
RECO - Cell enlargement	Boreal	75	Descending	54.36
RECO - Cell enlargement	Boreal	90	Descending	40.67
RECO - Cell enlargement	Boreal	100	Peak	34.19
RECO - Cell enlargement	Temperate	10	Ascending	-63.64
RECO - Cell enlargement	Temperate	25	Ascending	-46.36
RECO - Cell enlargement	Temperate	50	Ascending	-23.82
RECO - Cell enlargement	Temperate	75	Ascending	-2.14
RECO - Cell enlargement	Temperate	90	Ascending	10.49
RECO - Cell enlargement	Temperate	10	Descending	69.47
RECO - Cell enlargement	Temperate	25	Descending	76.6
RECO - Cell enlargement	Temperate	50	Descending	77.07
RECO - Cell enlargement	Temperate	75	Descending	60.87
RECO - Cell enlargement	Temperate	90	Descending	50.44
RECO - Cell enlargement	Temperate	100	Peak	31.16
RECO - Cell enlargement	Mediterranean	10	Ascending	-36.47
RECO - Cell enlargement	Mediterranean	25	Ascending	-40.65
RECO - Cell enlargement	Mediterranean	50	Ascending	-34.16
RECO - Cell enlargement	Mediterranean	75	Ascending	-17.57
RECO - Cell enlargement	Mediterranean	90	Ascending	-10.02
RECO - Cell enlargement	Mediterranean	10	Descending	59.43
RECO - Cell enlargement	Mediterranean	25	Descending	75.85
RECO - Cell enlargement	Mediterranean	50	Descending	65.29
RECO - Cell enlargement	Mediterranean	75	Descending	51.82
RECO - Cell enlargement	Mediterranean	90	Descending	51.38

RECO - Cell enlargement	Mediterranean	100	Peak	12.01
RECO - Cell wall thickening and lignification	Boreal	10	Ascending	-64
RECO - Cell wall thickening and lignification	Boreal	25	Ascending	-46.33
RECO - Cell wall thickening and lignification	Boreal	50	Ascending	-29.46
RECO - Cell wall thickening and lignification	Boreal	75	Ascending	-15.85
RECO - Cell wall thickening and lignification	Boreal	90	Ascending	-7.29
RECO - Cell wall thickening and lignification	Boreal	10	Descending	38.77
RECO - Cell wall thickening and lignification	Boreal	25	Descending	34.24
RECO - Cell wall thickening and lignification	Boreal	50	Descending	28.11
RECO - Cell wall thickening and lignification	Boreal	75	Descending	21.05
RECO - Cell wall thickening and lignification	Boreal	90	Descending	15.43
RECO - Cell wall thickening and lignification	Boreal	100	Peak	4.92
RECO - Cell wall thickening and lignification	Temperate	10	Ascending	-91.06
RECO - Cell wall thickening and lignification	Temperate	25	Ascending	-75.33
RECO - Cell wall thickening and lignification	Temperate	50	Ascending	-54.64
RECO - Cell wall thickening and lignification	Temperate	75	Ascending	-24.84
RECO - Cell wall thickening and lignification	Temperate	90	Ascending	-13.78

RECO - Cell wall thickening and lignification	Temperate	10	Descending	61
RECO - Cell wall thickening and lignification	Temperate	25	Descending	57.66
RECO - Cell wall thickening and lignification	Temperate	50	Descending	49.33
RECO - Cell wall thickening and lignification	Temperate	75	Descending	27.46
RECO - Cell wall thickening and lignification	Temperate	90	Descending	9.79
RECO - Cell wall thickening and lignification	Temperate	100	Peak	11.04
RECO - Cell wall thickening and lignification	Mediterranean	10	Ascending	-85.46
RECO - Cell wall thickening and lignification	Mediterranean	25	Ascending	-84.76
RECO - Cell wall thickening and lignification	Mediterranean	50	Ascending	-74.09
RECO - Cell wall thickening and lignification	Mediterranean	75	Ascending	-47.76
RECO - Cell wall thickening and lignification	Mediterranean	90	Ascending	-25.94
RECO - Cell wall thickening and lignification	Mediterranean	10	Descending	24.71
RECO - Cell wall thickening and lignification	Mediterranean	25	Descending	39.8
RECO - Cell wall thickening and lignification	Mediterranean	50	Descending	37.22
RECO - Cell wall thickening and lignification	Mediterranean	75	Descending	16.35
RECO - Cell wall thickening and lignification	Mediterranean	90	Descending	0.91
RECO - Cell wall thickening and lignification	Mediterranean	100	Peak	-6.44

SMA regressions following bioclimatic classification.

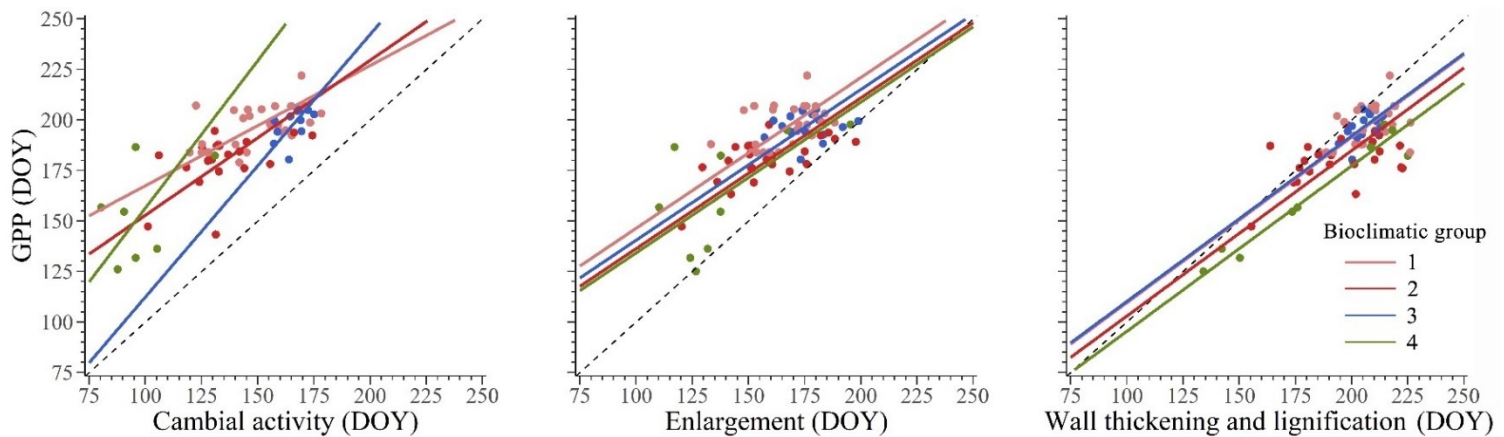


Figure S 5.13 Synchronisms among the timing of peak of Gross Primary Production (GPP) and phenological phases of wood formation (i.e., cambial activity, cell enlargement, and cell wall thickening and lignification) in 87 sites across boreal (1, blue lines and symbols), temperate (2 and 3, green lines and symbols) and Mediterranean (4, red lines and symbols) biomes. The dashed line represents a bisecting line (1:1).

Table S 5.8 Results of Standardized Major Axis (SMA) analyses of the bivariate relationships among timing of the peak of GPP and timing of cambial activity, cell enlargement and cell wall thickening and lignification in 81 sites according to their bioclimatic classification. * Indicates non-significant ($p > 0.05$) regressions.

Phenological stage	Bioclimatic group	Y-intercept	Slope	95% CI slope	R ²
Cambial activity	1	107.95	0.59	0.43 - 0.82	0.32
	2	76.12	0.77	0.50 - 1.18	0.24
	3	-17.95	1.30	0.70 - 2.40	0.12*
	4	10.73	1.46	0.59 - 3.61	0.11*
Cell enlargement	1	71.74	0.75	0.60 - 0.91	0.2
	2	61.67	0.75	0.60 - 0.91	0.38
	3	65.83	0.75	0.60 - 0.91	0.37
	4	59.57	0.75	0.60 - 0.91	0.36
Cell wall thickening and lignification	1	27.65	0.82	0.71 - 0.96	0.27
	2	21.07	0.82	0.71 - 0.96	0.22
	3	28.31	0.82	0.71 - 0.96	0.35
	4	13.51	0.82	0.71 - 0.96	0.94

Table S 5.9 Random forest regression models applied to FluxNET (i.e., NEE, GPP, RECO), FluxSat (i.e., GPP), cambial activity and xylem cell differentiation (i.e., cell enlargement and cell wall thickening and lignification timings of peaks. For each model, the table show the percentage of variance explained, the root mean squared error (RMSE) and the R^2 for both the training and test set.

	Process	Variance explained (%)	RMSE	R^2 (training set)	R^2 (test set)
C Flux	NEE (FluxNET)	44.09	37.9	0.86	0.68
	GPP (FluxNET)	27.86	18.71	0.81	0.51
	RECO (FluxNET)	23.56	22.92	0.72	0.49
	GPP (FluxSat)	54.06	21.01	0.89	0.66
Wood formation	Cambial activity	43.09	18.68	0.83	0.7
	Cell enlargement	38.09	27.26	0.76	0.83
	Cell wall thickening and lignification	39.96	26.39	0.76	0.73

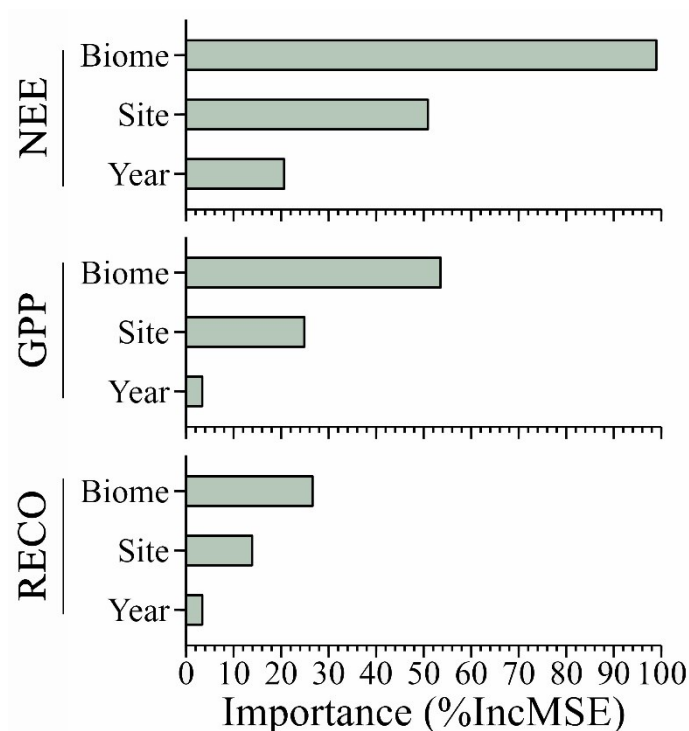


Figure S 5.14 Relative importance in terms of Mean Decrease Accuracy (%IncMSE) of predictors in the random forest regression models for the timing of peak of FluxNET Net Ecosystem Exchange (NEE), Gross Primary Production (GPP), and Ecosystem Respiration (RECO).

5.8 References

- Andreu-Hayles, L., Lévesque, M., Guerrieri, R., Siegwolf, R. T. W., & Körner, C. (2022). Limits and Strengths of Tree-Ring Stable Isotopes. In (Vol. 8, pp. 399-428). Springer, Cham. https://doi.org/10.1007/978-3-030-92698-4_14
- Azzalini, A. (2013). *The Skew-Normal and Related Families*. Cambridge University Press. https://books.google.com/books/about/The_Skew_Normal_and_Related_Families.html?hl=it&id=-tkaAgAAQBAJ
- Begum, S., Nakaba, S., Yamagishi, Y., Oribe, Y., & Funada, R. (2013). Regulation of cambial activity in relation to environmental conditions: Understanding the role of temperature in wood formation of trees. *Physiologia Plantarum*, 147(1), 46-54. <https://doi.org/10.1111/j.1399-3054.2012.01663.x>
- Blechs Schmidt-Schneider, S. (1990). Phloem transport in *Picea abies* (L.) Karst. in mid-winter - I Microautoradiographic studies on ¹⁴C-assimilate translocation in shoots. *Trees*, 4(4), 179-186. <https://doi.org/10.1007/BF00225313>
- Buttò, V., Khare, S., Drolet, G., Sylvain, J. D., Gennaretti, F., Deslaruiers, A., Morin, H., & Rossi, S. (2021). Regionwide temporal gradients of carbon allocation allow for shoot growth and latewood formation in boreal black spruce. *Global Ecology and Biogeography*, 30(8), 1657-1670. <https://doi.org/10.1111/geb.13340>
- Cabon, A., Kannenberg, S. A., Arain, A., Babst, F., Baldocchi, D., Belmecheri, S., Delpierre, N., Guerrieri, R., Maxwell, J. T., McKenzie, S., Meinzer, F. C., Moore, D. J. P., Pappas, C., Rocha, A. V., Szejner, P., Ueyama, M., Ulrich, D., Vincke, C., Voelker, S. L., . . . Anderegg, W. R. L. (2022). Cross-biome synthesis of source versus sink limits to tree growth. *Science*, 376(6594), 758-761. <https://doi.org/10.1126/science.abm4875>
- Camarero, J. J., Olano, J. M., & Parras, A. (2010). Plastic bimodal xylogenesis in conifers from continental Mediterranean climates. *New Phytologist*, 185(2), 471-480. <https://doi.org/10.1111/j.1469-8137.2009.03073.x>
- Carteni, F., Deslauriers, A., Rossi, S., Morin, H., De Micco, V., Mazzoleni, S., & Giannino, F. (2018). The physiological mechanisms behind the earlywood-to-latewood transition: A process-based modeling approach. *Frontiers in Plant Science*, 9, 1053-1053. <https://doi.org/10.3389/fpls.2018.01053>
- Chen, J., Paw U, K. T., Ustin, S. L., Suchanek, T. H., Bond, B. J., Brosofske, K. D., & Falk, M. (2004). Net ecosystem exchanges of carbon, water, and energy in young and old-growth douglas-fir forests. *Ecosystems*, 7(5), 534-544. <https://doi.org/10.1007/s10021-004-0143-6>

- Cuny, H. E., Rathgeber, C. B. K., Frank, D., Fonti, P., Makinen, H., Prislán, P., Rossi, S., Del Castillo, E. M., Campelo, F., Vavrčik, H., Camarero, J. J., Bryukhanova, M. V., Jyske, T., Gricar, J., Gryc, V., De Luis, M., Vieira, J., Cufar, K., Kirilyanov, A. V., . . . Fournier, M. (2015). Woody biomass production lags stem-girth increase by over one month in coniferous forests. *Nature Plants*, *1*(11), 1-6. <https://doi.org/10.1038/nplants.2015.160>
- Delpierre, N., Berveiller, D., Granda, E., & Dufréne, E. (2016). Wood phenology, not carbon input, controls the interannual variability of wood growth in a temperate oak forest. *New Phytologist*, *210*(2), 459-470. <https://doi.org/10.1111/NPH.13771>
- Deslauriers, A., Fournier, M. P., Carteni, F., & Mackay, J. (2019). Phenological shifts in conifer species stressed by spruce budworm defoliation. *Tree Physiology*, *39*(4), 590-605. <https://doi.org/10.1093/treephys/tpy135>
- Deslauriers, A., Huang, J. G., Balducci, L., Beaulieu, M., & Rossi, S. (2016). The contribution of carbon and water in modulating wood formation in black spruce saplings. *Plant Physiology*, *170*(4), 2072-2084. <https://doi.org/10.1104/pp.15.01525>
- Dietze, M. C., Sala, A., Carbone, M. S., Czimczik, C. I., Mantooth, J. A., Richardson, A. D., & Vargas, R. (2014). Nonstructural Carbon in Woody Plants. *Annual Review of Plant Biology*, *65*(1), 667-687. <https://doi.org/10.1146/annurev-arplant-050213-040054>
- Eilmann, B., Buchmann, N., Siegwolf, R., Saurer, M., & Rigling, P. C. (2010). Fast response of Scots pine to improved water availability reflected in tree-ring width and $\delta^{13}\text{C}$. *Plant, Cell and Environment*, *33*(8), 1351-1360. <https://doi.org/10.1111/j.1365-3040.2010.02153.x>
- Fajstavr, M., Bednářová, E., Nezval, O., Giagli, K., Gryc, V., Vavrčik, H., Horáček, P., & Urban, J. (2019). How needle phenology indicates the changes of xylem cell formation during drought stress in *Pinus sylvestris* L. *Dendrochronologia*, *56*, 125600-125600. <https://doi.org/10.1016/j.dendro.2019.05.004>
- Falk, M., Wharton, S., Schroeder, M., Ustin, S., & Paw U, K. T. (2008). Flux partitioning in an old-growth forest: Seasonal and interannual dynamics. *Tree Physiology*, *28*(4), 509-520. <https://doi.org/10.1093/treephys/28.4.509>
- Fatichi, S., Leuzinger, S., & Körner, C. (2014). Moving beyond photosynthesis: From carbon source to sink-driven vegetation modeling. *New Phytologist*, *201*(4), 1086-1095. <https://doi.org/10.1111/nph.12614>
- Friend, A. D., Eckes-Shephard, A. H., Fonti, P., Rademacher, T. T., Rathgeber, C. B. K., Richardson, A. D., & Turton, R. H. (2019). On the need to consider wood

formation processes in global vegetation models and a suggested approach. *Annals of Forest Science*, 76(2), 49-49. <https://doi.org/10.1007/s13595-019-0819-x>

- Graven, H. D., Keeling, R. F., Piper, S. C., Patra, P. K., Stephens, B. B., Wofsy, S. C., Welp, L. R., Sweeney, C., Tans, P. P., Kelley, J. J., Daube, B. C., Kort, E. A., Santoni, G. W., & Bent, J. D. (2013). Enhanced seasonal exchange of CO₂ by Northern ecosystems since 1960. *Science*, 341(6150), 1085-1089. <https://doi.org/10.1126/science.1239207>
- Gruber, A., Pirkebner, D., Oberhuber, W., & Wieser, G. (2011). Spatial and seasonal variations in mobile carbohydrates in *Pinus cembra* in the timberline ecotone of the Central Austrian Alps. *European Journal of Forest Research*, 130(2), 173-179. <https://doi.org/10.1007/s10342-010-0419-7>
- Guo, X., Klisz, M., Puchałka, R., Silvestro, R., Faubert, P., Belien, E., Huang, J., & Rossi, S. (2021). Common-garden experiment reveals clinal trends of bud phenology in black spruce populations from a latitudinal gradient in the boreal forest. *Journal of Ecology*, 1365-2745.13582. <https://doi.org/10.1111/1365-2745.13582>
- Hartmann, H., & Trumbore, S. (2016). Understanding the roles of nonstructural carbohydrates in forest trees - from what we can measure to what we want to know. *New Phytologist*, 211(2), 386-403. <https://doi.org/10.1111/nph.13955>
- Huang, J. G., Ma, Q., Rossi, S., Biondi, F., Deslauriers, A., Fonti, P., Liang, E., Mäkinen, H., Oberhuber, W., Rathgeber, C. B. K., Tognetti, R., Treml, V., Yang, B., Zhang, J. L., Antonucci, S., Bergeron, Y., Julio Camarero, J., Campelo, F., Cufar, K., . . . Ziaco, E. (2020). Photoperiod and temperature as dominant environmental drivers triggering secondary growth resumption in Northern Hemisphere conifers. *Proceedings of the National Academy of Sciences of the United States of America*, 117(34), 20645-20652. <https://doi.org/10.1073/pnas.2007058117>
- Joiner, J., & Yoshida, Y. (2021). Global MODIS and FLUXNET-derived Daily Gross Primary Production, V2. ORNL DAAC. <https://doi.org/10.3334/ORNLDAAAC/1835>
- Kagawa, A., Sugimoto, A., & Maximov, T. C. (2006). ¹³C₂ pulse-labelling of photoassimilates reveals carbon allocation within and between tree rings. *Plant, Cell and Environment*, 29(8), 1571-1584. <https://doi.org/10.1111/j.1365-3040.2006.01533.x>
- Kodama, N., Barnard, R. L., Salmon, Y., Weston, C., Ferrio, J. P., Holst, J., Werner, R. A., Saurer, M., Rennenberg, H., Buchmann, N., & Gessler, A. (2008). Temporal dynamics of the carbon isotope composition in a *Pinus sylvestris* stand: From newly assimilated organic carbon to respired carbon dioxide. *Oecologia*, 156(4), 737-750. <https://doi.org/10.1007/s00442-008-1030-1>

- Körner, C. (2003). Carbon limitation in trees. *Journal of Ecology*, 91(1), 4-17. <https://doi.org/10.1046/j.1365-2745.2003.00742.x>
- Körner, C. (2012). *Alpine treelines: Functional ecology of the global high elevation tree limits*. Springer Science & Business Media. <https://doi.org/10.1007/978-3-0348-0396-0>
- Körner, C. (2015). Paradigm shift in plant growth control. *Current Opinion in Plant Biology*, 25, 107-114. <https://doi.org/10.1016/J.PBI.2015.05.003>
- Krejza, J., Haeni, M., Darenova, E., Foltýnová, L., Fajstavr, M., Světlík, J., Nezval, O., Bednář, P., Šigut, L., Horáček, P., & Zweifel, R. (2022). Disentangling carbon uptake and allocation in the stems of a spruce forest. *Environmental and Experimental Botany*, 196, 104787-104787. <https://doi.org/10.1016/j.envexpbot.2022.104787>
- Lawlor, D. W., & Tezara, W. (2009). Causes of decreased photosynthetic rate and metabolic capacity in water-deficient leaf cells: A critical evaluation of mechanisms and integration of processes. *Annals of Botany*, 103(4), 561-579. <https://doi.org/10.1093/aob/mcn244>
- MacNeill, G. J., Mehrpouyan, S., Minow, M. A. A., Patterson, J. A., Tetlow, I. J., & Emes, M. J. (2017). Starch as a source, starch as a sink: The bifunctional role of starch in carbon allocation. *Journal of Experimental Botany*, 68(16), 4433-4453. <https://doi.org/10.1093/jxb/erx291>
- Martínez-Vilalta, J., Sala, A., Asensio, D., Galiano, L., Hoch, G., Palacio, S., Piper, F. I., & Lloret, F. (2016). Dynamics of non-structural carbohydrates in terrestrial plants: a global synthesis. *Ecological Monographs*, 86(4), 495-516. <https://doi.org/10.1002/ecm.1231>
- McKenzie, S. M., Pisaric, M. F. J., & Arain, M. A. (2021). Comparison of tree-ring growth and eddy covariance-based ecosystem productivities in three different-aged pine plantation forests. *Trees - Structure and Function*, 35(2), 583-595. <https://doi.org/10.1007/S00468-020-02061-Z/FIGURES/4>
- Metsaranta, J. M., Mamet, S. D., Maillet, J., & Barr, A. G. (2021). Comparison of tree-ring and eddy-covariance derived annual ecosystem production estimates for jack pine and trembling aspen forests in Saskatchewan, Canada. *Agricultural and Forest Meteorology*, 307, 108469-108469. <https://doi.org/10.1016/j.agrformet.2021.108469>
- Muller, B., Pantin, F., Génard, M., Turc, O., Freixes, S., Piques, M., & Gibon, Y. (2011). Water deficits uncouple growth from photosynthesis, increase C content, and

- modify the relationships between C and growth in sink organs. *Journal of Experimental Botany*, 62(6), 1715-1729. <https://doi.org/10.1093/jxb/erq438>
- Oddi, L., Migliavacca, M., Cremonese, E., Filippa, G., Vacchiano, G., Siniscalco, C., Morra Di Cella, U., & Galvagno, M. (2022). Contrasting responses of forest growth and carbon sequestration to heat and drought in the Alps. *Environmental Research Letters*, 17(4), 045015-045015. <https://doi.org/10.1088/1748-9326/ac5b3a>
- Pastorello, G., Trotta, C., Canfora, E., Chu, H., Christianson, D., Cheah, Y. W., Poindexter, C., Chen, J., Elbashandy, A., Humphrey, M., Isaac, P., Polidori, D., Ribeca, A., van Ingen, C., Zhang, L., Amiro, B., Ammann, C., Arain, M. A., Ardö, J., . . . Papale, D. (2020). The FLUXNET2015 dataset and the ONEFlux processing pipeline for eddy covariance data. *Scientific Data*, 7(1), 225-225. <https://doi.org/10.1038/s41597-020-0534-3>
- Puchi, P. F., Khomik, M., Frigo, D., Arain, M. A., Fonti, P., Arx, G. v., & Castagneri, D. (2023). Revealing how intra- and inter-annual variability of carbon uptake (GPP) affects wood cell biomass in an eastern white pine forest. *Environmental Research Letters*, 18(2), 024027-024027. <https://doi.org/10.1088/1748-9326/acb2df>
- Rinne, K. T., Saurer, M., Kirilyanov, A. V., Loader, N. J., Bryukhanova, M. V., Werner, R. A., & Siegwolf, R. T. W. (2015). The relationship between needle sugar carbon isotope ratios and tree rings of larch in Siberia. *Tree Physiology*, 35(11), 1192-1205. <https://doi.org/10.1093/treephys/tpv096>
- Rocha, A. V., Goulden, M. L., Dunn, A. L., & Wofsy, S. C. (2006). On linking interannual tree ring variability with observations of whole-forest CO₂ flux. *Global Change Biology*, 12(8), 1378-1389. <https://doi.org/10.1111/j.1365-2486.2006.01179.x>
- Rossi, S., Anfodillo, T., Čufar, K., Cuny, H. E., Deslauriers, A., Fonti, P., Frank, D., Gričar, J., Gruber, A., Huang, J. G., Jyske, T., Kašpar, J., King, G., Krause, C., Liang, E., Mäkinen, H., Morin, H., Nöjd, P., Oberhuber, W., . . . Treml, V. (2016). Pattern of xylem phenology in conifers of cold ecosystems at the Northern Hemisphere. *Global Change Biology*, 22(11), 3804-3813. <https://doi.org/10.1111/gcb.13317>
- Silvestro, R., Rossi, S., Zhang, S., Froment, I., Huang, J. G., & Saracino, A. (2019). From phenology to forest management: Ecotypes selection can avoid early or late frosts, but not both. *Forest Ecology and Management*, 436, 21-26. <https://doi.org/10.1016/j.foreco.2019.01.005>
- Sit, V., & Poulin-Costello, M. (1994). *Catalog of curves for curve fitting*. Ministry of Forests, Research Program. file://catalog.hathitrust.org/Record/101778322

<http://hdl.handle.net/2027/umn.31951d00906953d>

- Teets, A., Fraver, S., Hollinger, D. Y., Weiskittel, A. R., Seymour, R. S., & Richardson, A. D. (2018). Linking annual tree growth with eddy-flux measures of net ecosystem productivity across twenty years of observation in a mixed conifer forest. *Agricultural and Forest Meteorology*, *249*, 479-487. <https://doi.org/10.1016/j.agrformet.2017.08.007>
- Tei, S., Sugimoto, A., Kotani, A., Ohta, T., Morozumi, T., Saito, S., Hashiguchi, S., & Maximov, T. (2019). Strong and stable relationships between tree-ring parameters and forest-level carbon fluxes in a Siberian larch forest. *Polar Science*, *21*, 146-157. <https://doi.org/10.1016/j.polar.2019.02.001>
- Vicente-Serrano, S. M., Martín-Hernández, N., Camarero, J. J., Gazol, A., Sánchez-Salguero, R., Peña-Gallardo, M., El Kenawy, A., Domínguez-Castro, F., Tomas-Burguera, M., Gutiérrez, E., de Luis, M., Sangüesa-Barreda, G., Novak, K., Rozas, V., Tiscar, P. A., Linares, J. C., del Castillo, E. M., Ribas, M., García-González, I., . . . Diego Galván, J. (2020). Linking tree-ring growth and satellite-derived gross primary growth in multiple forest biomes. Temporal-scale matters. *Ecological Indicators*, *108*, 105753-105753. <https://doi.org/10.1016/j.ecolind.2019.105753>
- Waring, R. H., & Running, S. W. (2007). Carbon Cycle. In (pp. 59-98). Academic Press. <https://doi.org/10.1016/B978-012370605-8.50008-6>
- Warren, C. R., & Adams, M. A. (2004). Evergreen trees do not maximize instantaneous photosynthesis. *Trends in Plant Science*, *9*(6), 270-274. <https://doi.org/10.1016/j.tplants.2004.04.004>
- Warton, D. I., Wright, I. J., Falster, D. S., & Westoby, M. (2006). Bivariate line-fitting methods for allometry. *Biological Reviews of the Cambridge Philosophical Society*, *81*(2), 259-291. <https://doi.org/10.1017/S1464793106007007>
- Weber, R., Schwendener, A., Schmid, S., Lambert, S., Wiley, E., Landhäusser, S. M., Hartmann, H., & Hoch, G. (2018). Living on next to nothing: tree seedlings can survive weeks with very low carbohydrate concentrations. *New Phytologist*, *218*(1), 107-118. <https://doi.org/10.1111/nph.14987>
- Xu, B., Yang, Y., Li, P., Shen, H., & Fang, J. (2014). Global patterns of ecosystem carbon flux in forests: A biometric data-based synthesis. *Global Biogeochemical Cycles*, *28*(9), 962-973. <https://doi.org/10.1002/2013GB004593>
- Xu, K., Wang, X., Liang, P., An, H., Sun, H., Han, W., & Li, Q. (2017). Tree-ring widths are good proxies of annual variation in forest productivity in temperate forests. *Scientific Reports*, *7*(1), 1-8. <https://doi.org/10.1038/s41598-017-02022-6>

Yang, J., He, Y., Aubrey, D. P., Zhuang, Q., & Teskey, R. O. (2016). Global patterns and predictors of stem CO₂ efflux in forest ecosystems. *Global Change Biology*, 22(4), 1433-1444. <https://doi.org/10.1111/gcb.13188>

References annexes

Camarero, J. J., Olano, J. M., & Parras, A. (2010). Plastic bimodal xylogenesis in conifers from continental Mediterranean climates. *New Phytologist*, 185(2), 471-480. <https://doi.org/10.1111/j.1469-8137.2009.03073.x>

Joiner, J., & Yoshida, Y. (2021). Global MODIS and FLUXNET-derived Daily Gross Primary Production, V2. *ORNL DAAC*. <https://doi.org/10.3334/ORNLDAAC/1835>

Martínez-Vilalta, J., Sala, A., Asensio, D., Galiano, L., Hoch, G., Palacio, S., Piper, F. I., & Lloret, F. (2016). Dynamics of non-structural carbohydrates in terrestrial plants: a global synthesis. *Ecological Monographs*, 86(4), 495-516. <https://doi.org/10.1002/ecm.1231>

Martins, D. S., Raziei, T., Paulo, A. A., & Pereira, L. S. (2012). Spatial and temporal variability of precipitation and drought in Portugal. *Natural Hazards and Earth System Science*, 12(5), 1493-1501. <https://doi.org/10.5194/nhess-12-1493-2012>

Muller, B., Pantin, F., Génard, M., Turc, O., Freixes, S., Piques, M., & Gibon, Y. (2011). Water deficits uncouple growth from photosynthesis, increase C content, and modify the relationships between C and growth in sink organs. *Journal of Experimental Botany*, 62(6), 1715-1729. <https://doi.org/10.1093/jxb/erq438>

Pastorello, G., Trotta, C., Canfora, E., Chu, H., Christianson, D., Cheah, Y. W., Poindexter, C., Chen, J., Elbashandy, A., Humphrey, M., Isaac, P., Polidori, D., Ribeca, A., van Ingen, C., Zhang, L., Amiro, B., Ammann, C., Arain, M. A., Ardö, J., . . . Papale, D. (2020). The FLUXNET2015 dataset and the ONEFlux processing pipeline for eddy covariance data. *Scientific Data*, 7(1), 225-225. <https://doi.org/10.1038/s41597-020-0534-3>

Quentin, A. G., Pinkard, E. A., Ryan, M. G., Tissue, D. T., Baggett, L. S., Adams, H. D., Maillard, P., Marchand, J., Landhäusser, S. M., Lacointe, A., Gibon, Y., Anderegg, W. R. L., Asao, S., Atkin, O. K., Bonhomme, M., Claye, C., Chow, P. S., Clément-Vidal, A., Davies, N. W., . . . Woodruff, D. R. (2015). Non-structural carbohydrates in woody plants compared among laboratories. *Tree Physiology*, 35(11), 1146-1165. <https://doi.org/10.1093/treephys/tpv073>

- Rossi, S., Anfodillo, T., & Menardi, R. (2006). Trephor: A new tool for sampling microcores from tree stems. *IWA Journal*, 27(1), 89-97. <https://doi.org/10.1163/22941932-90000139>
- Rossi, S., Deslauriers, A., & Anfodillo, T. (2006). Assessment of cambial activity and xylogenesis by microsampling tree species: An example at the Alpine timberline. *IWA Journal*, 27(4), 383-394. <https://doi.org/10.1163/22941932-90000161>
- Ruiz-Sinoga, J. D., Garcia-Marin, R., Gabarron-Galeote, M. A., & Martinez-Murillo, J. F. (2012). Analysis of dry periods along a pluviometric gradient in Mediterranean southern Spain. *International Journal of Climatology*, 32(10), 1558-1571. <https://doi.org/10.1002/joc.2376>

GENERAL CONCLUSION

This thesis aimed to: (i) assess the phenological variability among and within sites for primary and secondary growth and (ii) deepen the relationship between phenological timings and carbon allocation during growth.

6.1 Local adaptation and phenological variability among provenances

The findings of this thesis provide strong evidence for the ecotypic variation among black spruce provenances, highlighting their long-term adaptation to diverse environmental conditions. This adaptation plays a pivotal role in forest management strategies, particularly as logging activities gradually expand to remote areas at higher latitudes. In the context of climate change, forest management aims to optimize carbon sequestration while ensuring high timber production. Our results indicate that under warming conditions, it would be challenging for northern populations to quickly achieve the growth performance levels of their southern counterparts due to their long-standing local adaptation, which results in inherently lower growth rates.

When considering phenological traits and the associated risk of late-spring frost exposure, it becomes apparent that northern provenances may face challenges in adapting to future climatic conditions. However, it is important to note that natural populations exhibit a certain degree of genetic or phenotypic variation, which opens up the possibility for evolutionary processes to come into play. In this regard, the observed maladaptation of northern populations could potentially act as a driving force for rapid local adaptation to the changing environment. Given the magnitude of the ongoing climate change, the need for swift adaptation poses a significant challenge for long-lived organisms such as trees. Interestingly, our results suggest that northern populations may have a faster generation

turnover, which can facilitate a more rapid evolutionary response to selective pressures compared to southern populations.

Overall, these findings underscore the importance of considering the genetic diversity and adaptive potential of tree populations in forest management strategies. They highlight the need for proactive measures to enhance the resilience and adaptive capacity of forests in the face of climate change, ensuring the long-term sustainability and productivity of forest ecosystems.

6.2 Within population phenological variability and wood growth

This study primarily highlighted the remarkable variability in the timing of wood formation among trees within the same stand, although the precise causes underlying these differences in xylem phenology are still partially unresolved. However, my findings provide valuable insights into the intricate relationship between the growing season length and xylem cell production, highlighting the close connection between wood formation processes and carbon uptake. This dynamic interaction ultimately leads to the production of less dense wood, characterized by larger cell sizes and a lower proportion of latewood. My thesis results offer an eco-physiological explanation that underscores the interplay between endogenous factors and environmental cues that drive xylem phenology and wood production. Temperature and precipitation are likely key drivers in determining the timing of wood formation, while the allocation pattern of carbon throughout the growing season influences the resulting wood anatomical traits.

My research also emphasizes the importance of considering sample size when assessing xylem phenology. Given the significant variability within a population, expanding the sample size becomes a critical step in further elucidating the factors contributing to this

phenological variability. By doing so, we can gain deeper insights into the underlying mechanisms and drivers of wood phenology and production. However, it is important to acknowledge that our current understanding of wood formation remains incomplete. The intricate relationships and interactions between phenological timings and the development of cell traits in wood highlight the need for further investigations. Comprehensive studies that encompass a broader range of environmental and genetic factors, as well as physiological processes are essential to unravel the complexities of wood formation and its variability among trees.

6.3 Carbon sources and sinks

In the final chapter of this thesis, the primary objective was to investigate the temporal relationship between carbon fluxes and wood growth dynamics on a global scale. The study revealed a significant finding, highlighting the synchronization between photosynthetic activity and wood differentiation. This discovery emphasizes the interconnectedness of these processes and provides valuable insights into the mechanisms underlying carbon uptake, allocation, and long-term sequestration in forest ecosystems. The main conclusion drawn from this synthesis is that gaining a comprehensive understanding of the complex relationship between carbon uptake, allocation, and long-term sequestration is crucial for reducing uncertainties in global vegetation models and advancing our knowledge of the global carbon cycle. To achieve this, it is essential to incorporate detailed intra-annual assessments of carbon pools, which can serve as a bridge between measurements of atmospheric carbon flux and assessments of forest biomass growth.

By obtaining comprehensive and accurate data on carbon pools throughout the year, we can effectively monitor and analyze the dynamics of carbon allocation, providing a more comprehensive view of the carbon cycle in forest ecosystems. This integration of intra-annual assessments of carbon pools with atmospheric carbon flux measurements will significantly contribute to refining global vegetation models and improving our understanding of carbon dynamics. Furthermore, this research highlights the importance of incorporating these findings into future studies and management practices. By considering the temporal relationships between carbon fluxes and wood growth dynamics, we can enhance our ability to predict and manage forest ecosystems in the face of climate change. This knowledge will enable us to make informed decisions regarding forest conservation, carbon sequestration strategies, and sustainable forest management.

BIBLIOGRAPHIE

- Abdul-Hamid, H., & Mencuccini, M. (2009). Age- and size-related changes in physiological characteristics and chemical composition of *Acer pseudoplatanus* and *Fraxinus excelsior* trees. *Tree Physiology*, 29(1), 27-38. <https://doi.org/10.1093/treephys/tpn001>
- Aitken, S. N., Yeaman, S., Holliday, J. A., Wang, T., & Curtis-McLane, S. (2008). Adaptation, migration or extirpation: climate change outcomes for tree populations. *Evolutionary Applications*, 1(1), 95-111. <https://doi.org/10.1111/j.1752-4571.2007.00013.x>
- Alberto, F. J., Aitken, S. N., Alía, R., González-Martínez, S. C., Hänninen, H., Kremer, A., Lefèvre, F., Lenormand, T., Yeaman, S., Whetten, R., & Savolainen, O. (2013). Potential for evolutionary responses to climate change - evidence from tree populations. *Global Change Biology*, 19(6), 1645-1661. <https://doi.org/10.1111/gcb.12181>
- Allstadt, A. J., Vavrus, S. J., Heglund, P. J., Pidgeon, A. M., Thogmartin, W. E., & Radeloff, V. C. (2015). Spring plant phenology and false springs in the conterminous US during the 21st century. *Environmental Research Letters*, 10(10), 104008.
- Anderson, K.; Gaston, K.J. (2013) Lightweight unmanned aerial vehicles will revolutionize spatial ecology. *Front. Ecol. Environ.*, 11, 138–146.
- Andreu-Hayles, L., Lévesque, M., Guerrieri, R., Siegwolf, R. T. W., & Körner, C. (2022). Limits and Strengths of Tree-Ring Stable Isotopes. In (Vol. 8, pp. 399-428). Springer, Cham. https://doi.org/10.1007/978-3-030-92698-4_14
- Anfodillo, T., Deslauriers, A., Menardi, R., Tedoldi, L., Petit, G., & Rossi, S. (2012). Widening of xylem conduits in a conifer tree depends on the longer time of cell expansion downwards along the stem. *Journal of Experimental Botany*, 63(2), 837-845. <https://doi.org/10.1093/jxb/err309>
- Antonucci, S., Rossi, S., Deslauriers, A., Morin, H., Lombardi, F., Marchetti, M., & Tognetti, R. (2017). Large-scale estimation of xylem phenology in black spruce through remote sensing. *Agricultural and Forest Meteorology*, 233, 92-100. <https://doi.org/10.1016/j.agrformet.2016.11.011>
- Antonucci, S., Rossi, S., Lombardi, F., Marchetti, M., & Tognetti, R. (2019). Influence of climatic factors on silver fir xylogenesis along the Italian Peninsula. *IAWA Journal*, 40(2), 259-275. <https://doi.org/10.1163/22941932-40190222>
- Aono Y, Kazui K (2008) Phenological data series of cherry tree flowering in Kyoto, Japan, and its application to reconstruction of springtime temperatures since the

9th century. *International Journal of Climatology: A Journal of the Royal Meteorological Society*, 28, 905-914.

Azzalini, A. (2013). *The Skew-Normal and Related Families*. Cambridge University Press.

https://books.google.com/books/about/The_Skew_Normal_and_Related_Families.html?hl=it&id=-tkaAgAAQBAJ

Balducci, L., Deslauriers, A., Giovannelli, A., Rossi, S., & Rathgeber, C. B. K. (2013). Effects of temperature and water deficit on cambial activity and woody ring features in *Picea mariana* saplings. *Tree Physiology*, 33(10), 1006-1017. <https://doi.org/10.1093/treephys/tpt073>

Belien, E., Rossi, S., Morin, H., & Deslauriers, A. (2012). Xylogenesis in black spruce subjected to rain exclusion in the field. *Canadian Journal of Forest Research*, 42(7), 1306-1315. <https://doi.org/10.1139/X2012-095>

Begum, S., Nakaba, S., Yamagishi, Y., Oribe, Y., & Funada, R. (2013). Regulation of cambial activity in relation to environmental conditions: Understanding the role of temperature in wood formation of trees. *Physiologia Plantarum*, 147(1), 46-54. <https://doi.org/10.1111/j.1399-3054.2012.01663.x>

Berra EF, Gaulton R, Barr S (2016) Use of a digital camera onboard a UAV to monitor spring phenology at individual tree level. In: *2016 IEEE International Geoscience and Remote Sensing Symposium (IGARSS)*. pp 3496-3499.

Blechschildt-Schneider, S. (1990). Phloem transport in *Picea abies* (L.) Karst. in mid-winter - I Microautoradiographic studies on ¹⁴C-assimilate translocation in shoots. *Trees*, 4(4), 179-186. <https://doi.org/10.1007/BF00225313>

Blum, B. M. (1988). Variation in the phenology of bud flushing in white and red spruce. *Canadian Journal of Forest Research*, 18(3), 315-319. <https://doi.org/10.1139/x88-048>

Bond-Lamberty, B., Wang, C., & Gower, S. T. (2004). Net primary production and net ecosystem production of a boreal black spruce wildfire chronosequence. *Global Change Biology*, 10(4), 473-487. <https://doi.org/10.1111/j.1529-8817.2003.0742.x>

Buttò, V., Deslauriers, A., Rossi, S., Rozenberg, P., Shishov, V., & Morin, H. (2020). The role of plant hormones in tree-ring formation. *Trees - Structure and Function*, 34(2), 315-335. <https://doi.org/10.1007/s00468-019-01940-4>

Buttò, V., Khare, S., Drolet, G., Sylvain, J. D., Gennaretti, F., Deslauriers, A., Morin, H., & Rossi, S. (2021). Regionwide temporal gradients of carbon allocation allow for

- shoot growth and latewood formation in boreal black spruce. *Global Ecology and Biogeography*, 30(8), 1657-1670. <https://doi.org/10.1111/geb.13340>
- Buttò, V., Rossi, S., Deslauriers, A., & Morin, H. (2019). Is size an issue of time? Relationship between the duration of xylem development and cell traits. *Annals of Botany*, 123(7), 1257-1265. <https://doi.org/10.1093/aob/mcz032>
- Buttò, V., Shishov, V., Tychkov, I., Popkova, M., He, M., Rossi, S., Deslauriers, A., & Morin, H. (2020). Comparing the Cell Dynamics of Tree-Ring Formation Observed in Microcores and as Predicted by the Vaganov–Shashkin Model. *Frontiers in Plant Science*, 11, 1268-1268. <https://doi.org/10.3389/fpls.2020.01268>
- Cabon, A., Kannenberg, S. A., Arain, A., Babst, F., Baldocchi, D., Belmecheri, S., Delpierre, N., Guerrieri, R., Maxwell, J. T., McKenzie, S., Meinzer, F. C., Moore, D. J. P., Pappas, C., Rocha, A. V., Szejner, P., Ueyama, M., Ulrich, D., Vincke, C., Voelker, S. L., . . . Anderegg, W. R. L. (2022). Cross-biome synthesis of source versus sink limits to tree growth. *Science*, 376(6594), 758-761. <https://doi.org/10.1126/science.abm4875>
- Camarero, J. J., Olano, J. M., & Parras, A. (2010). Plastic bimodal xylogenesis in conifers from continental Mediterranean climates. *New Phytologist*, 185(2), 471-480. <https://doi.org/10.1111/j.1469-8137.2009.03073.x>
- Camargo, E. L. O., Nascimento, L. C., Soler, M., Salazar, M. M., Lepikson-Neto, J., Marques, W. L., Alves, A., Teixeira, P. J. P. L., Mieczkowski, P., Carazzolle, M. F., Martinez, Y., Deckmann, A. C., Rodrigues, J. C., Grima-Pettenati, J., & Pereira, G. A. G. (2014). Contrasting nitrogen fertilization treatments impact xylem gene expression and secondary cell wall lignification in Eucalyptus. *BMC Plant Biology*, 14(1), 1-17. <https://doi.org/10.1186/s12870-014-0256-9>
- Campbell, J. L., Sun, O. J., & Law, B. E. (2004). Disturbance and net ecosystem production across three climatically distinct forest landscapes. *Global Biogeochemical Cycles*, 18(4), 1-11. <https://doi.org/10.1029/2004GB002236>
- Carteni, F., Deslauriers, A., Rossi, S., Morin, H., De Micco, V., Mazzoleni, S., & Giannino, F. (2018). The physiological mechanisms behind the earlywood-to-latewood transition: A process-based modeling approach. *Frontiers in Plant Science*, 9, 1053-1053. <https://doi.org/10.3389/fpls.2018.01053>
- Charrier, G., Ngao, J., Saudreau, M., & Améglio, T. (2015). Effects of environmental factors and management practices on microclimate, winter physiology, and frost resistance in trees. *Frontiers in Plant Science*, 6(APR), 259-259. <https://doi.org/10.3389/fpls.2015.00259>

- Chen, I. C., Hill, J. K., Ohlemüller, R., Roy, D. B., & Thomas, C. D. (2011). Rapid range shifts of species associated with high levels of climate warming. *Science*, 333(6045), 1024-1026. <https://doi.org/10.1126/science.1206432>
- Chen, J., Paw U, K. T., Ustin, S. L., Suchanek, T. H., Bond, B. J., Brosofske, K. D., & Falk, M. (2004). Net ecosystem exchanges of carbon, water, and energy in young and old-growth douglas-fir forests. *Ecosystems*, 7(5), 534-544. <https://doi.org/10.1007/s10021-004-0143-6>
- Chen, J., Ter-Mikaelian, M. T., Ng, P. Q., & Colombo, S. J. (2018). Ontario's managed forests and harvested wood products contribute to greenhouse gas mitigation from 2020 to 2100. *Forestry Chronicle*, 43(3), 269-282. <https://doi.org/10.5558/tfc2018-040>
- Chmielewski F.M, Heider S, Moryson S, E B (2013) International Phenological Observation Networks - Concept of IPG and GPM (Chapter 8). In: *Phenology: An Integrative Environmental Science*. (ed M.D. S) pp 137-153. Dordrecht, Springer Science+Business Media B.V.
- Chuine, I. (2010). Why does phenology drive species distribution? *Philosophical Transactions of the Royal Society B: Biological Sciences*, 365(1555), 3149-3160. <https://doi.org/10.1098/rstb.2010.0142>
- Clark, J.E. (1936) The History of British phenology. *Q. J. R. Meteorol. Soc.*, 62, 19–24.
- Cook, B. I., Wolkovich, E. M., & Parmesan, C. (2012). Divergent responses to spring and winter warming drive community level flowering trends. *Proceedings of the National Academy of Sciences*, 109(23), 9000-9005.
- Cuny, H. E., Fonti, P., Rathgeber, C. B. K., von Arx, G., Peters, R. L., & Frank, D. C. (2019). Couplings in cell differentiation kinetics mitigate air temperature influence on conifer wood anatomy. *Plant Cell and Environment*, 42(4), 1222-1232. <https://doi.org/10.1111/pce.13464>
- Cuny, H. E., Rathgeber, C. B. K., Frank, D., Fonti, P., & Fournier, M. (2014). Kinetics of tracheid development explain conifer tree-ring structure. *New Phytologist*, 203(4), 1231-1241. <https://doi.org/10.1111/nph.12871>
- Cuny, H. E., Rathgeber, C. B. K., Frank, D., Fonti, P., Makinen, H., Prislan, P., Rossi, S., Del Castillo, E. M., Campelo, F., Vavrčik, H., Camarero, J. J., Bryukhanova, M. V., Jyske, T., Gricar, J., Gryc, V., De Luis, M., Vieira, J., Cufar, K., Kirilyanov, A. V., . . . Fournier, M. (2015). Woody biomass production lags stem-girth increase by over one month in coniferous forests. *Nature Plants*, 1(11), 1-6. <https://doi.org/10.1038/nplants.2015.160>

- Cuny, H. E., Rathgeber, C. B. K., Lebourgeois, F., Fortin, M., & Fournier, M. (2012). Life strategies in intra-annual dynamics of wood formation: Example of three conifer species in a temperate forest in north-east France. *Tree Physiology*, *32*(5), 612-625. <https://doi.org/10.1093/treephys/tps039>
- Cuny, H. E., Rathgeber, C. B. K., Kiessé, T. S., Hartmann, F. P., Barbeito, I., & Fournier, M. (2013). Generalized additive models reveal the intrinsic complexity of wood formation dynamics. *Journal of Experimental Botany*, *64*(7), 1983-1994. <https://doi.org/10.1093/jxb/ert057>
- D'Orangeville, L., Côté, B., Houle, D., & Morin, H. (2013). The effects of throughfall exclusion on xylogenesis of balsam fir. *Tree Physiology*, *33*(5), 516-526. <https://doi.org/10.1093/treephys/tpt027>
- D'Orangeville, L., Houle, D., Côté, B., Duchesne, L., & Morin, H. (2013). Increased soil temperature and atmospheric N deposition have no effect on the N status and growth of a mature balsam fir forest. *Biogeosciences*, *10*(7), 4627-4639. <https://doi.org/10.5194/bg-10-4627-2013>
- De Frenne, P., Graae, B. J., Brunet, J., Shevtsova, A., De Schrijver, A., Chabrierie, O., Cousins, S. A., Decocq, G., Diekmann, M., & Hermy, M. (2012). The response of forest plant regeneration to temperature variation along a latitudinal gradient. *Annals of Botany*, *109*(5), 1037-1046.
- De Micco, V., Carrer, M., Rathgeber, C. B. K., Julio Camarero, J., Voltas, J., Cherubini, P., & Battipaglia, G. (2019). From xylogenesis to tree rings: Wood traits to investigate tree response to environmental changes. *IAWA Journal*, *40*(2), 155-182. <https://doi.org/10.1163/22941932-40190246>
- Delpierre, N., Berveiller, D., Granda, E., & Dufrière, E. (2016). Wood phenology, not carbon input, controls the interannual variability of wood growth in a temperate oak forest. *New Phytologist*, *210*(2), 459-470. <https://doi.org/10.1111/NPH.13771>
- Delpierre, N., Vitasse, Y., Chuine, I., Guillemot, J., Bazot, S., Rutishauser, T., & Rathgeber, C. B. K. (2016). Temperate and boreal forest tree phenology: from organ-scale processes to terrestrial ecosystem models. *Annals of Forest Science*, *73*(1), 5-25. <https://doi.org/10.1007/s13595-015-0477-6>
- Demarée, G.R.; Rutishauser, T. (2009) Origins of the word “phenology”. *Eos Trans. Am. Geophys. Union*, *90*, 291.
- Deslauriers, A., Fournier, M. P., Carteni, F., & Mackay, J. (2019). Phenological shifts in conifer species stressed by spruce budworm defoliation. *Tree Physiology*, *39*(4), 590-605. <https://doi.org/10.1093/treephys/tpy135>

- Deslauriers, A., Giovannelli, A., Rossi, S., Castro, G., Fragnelli, G., & Traversi, L. (2009). Intra-annual cambial activity and carbon availability in stem of poplar. *Tree Physiology*, 29(10), 1223-1235. <https://doi.org/10.1093/treephys/tpp061>
- Deslauriers, A., Huang, J. G., Balducci, L., Beaulieu, M., & Rossi, S. (2016). The contribution of carbon and water in modulating wood formation in black spruce saplings. *Plant Physiology*, 170(4), 2072-2084. <https://doi.org/10.1104/pp.15.01525>
- Deslauriers, A., Morin, H., & Begin, Y. (2003). Cellular phenology of annual ring formation of *Abies balsamea* in the Quebec boreal forest (Canada). *Canadian Journal of Forest Research*, 33(2), 190-200. <https://doi.org/10.1139/x02-178>
- Deslauriers, A., Rossi, S., & Liang, E. (2015). Collecting and processing wood microcores for monitoring xylogenesis. In (pp. 417-429). Springer International Publishing. https://doi.org/10.1007/978-3-319-19944-3_23
- Deslauriers, A., Rossi, S., Morin, H., & Krause, C. (2018). Analyse du développement intraannuel des cernes de croissance. In S. Payette & L. Fillion (Eds.), (pp. 772-772). Presses de l'Université Laval.
- Dethier B, Ashley M, Blair B, Hopp R (1973) Phenology satellite experiment. In: *Symposium on significant results obtained from the Earth Resources Technology Satellite-1, vol I. Technical presentations, section A.* (eds Freden S, Mercanti E, Becker M). Washington, DC, NASA.
- Dhont, P., Sylvestre, P., Gros-Louis, M. C., & Isabel, N. (2010). *Field Guide for Identifying Apical Bud Break and Bud Formation Stages in White Spruce.*
- Dietze, M. C., Sala, A., Carbone, M. S., Czimczik, C. I., Mantooth, J. A., Richardson, A. D., & Vargas, R. (2014). Nonstructural Carbon in Woody Plants. *Annual Review of Plant Biology*, 65(1), 667-687. <https://doi.org/10.1146/annurev-arplant-050213-040054>
- Dória, L. C., Sonsin-Oliveira, J., Rossi, S., & Marcatti, C. R. (2022). Functional trade-offs in volume allocation to xylem cell types in 75 species from the Brazilian savanna Cerrado. *Annals of Botany*, 130(3), 445-456. <https://doi.org/10.1093/aob/mcac095>
- Dow, C., Kim, A. Y., D'Orangeville, L., Gonzalez-Akre, E. B., Helcoski, R., Herrmann, V., Harley, G. L., Maxwell, J. T., McGregor, I. R., McShea, W. J., McMahan, S. M., Pederson, N., Tepley, A. J., & Anderson-Teixeira, K. J. (2022). Warm springs alter timing but not total growth of temperate deciduous trees. *Nature*, 608(7923), 552-557. <https://doi.org/10.1038/s41586-022-05092-3>

- Eilmann, B., Buchmann, N., Siegwolf, R., Saurer, M., & Rigling, P. C. (2010). Fast response of Scots pine to improved water availability reflected in tree-ring width and $\delta^{13}\text{C}$. *Plant, Cell and Environment*, 33(8), 1351-1360. <https://doi.org/10.1111/j.1365-3040.2010.02153.x>
- Endara, M. J., & Coley, P. D. (2011). The resource availability hypothesis revisited: A meta-analysis. *Functional Ecology*, 25(2), 389-398. <https://doi.org/10.1111/j.1365-2435.2010.01803.x>
- Eriksson, L. O., Gustavsson, L., Hänninen, R., Kallio, M., Lyhykäinen, H., Pingoud, K., Pohjola, J., Sathre, R., Solberg, B., Svanaes, J., & Valsta, L. (2012). Climate change mitigation through increased wood use in the European construction sector-towards an integrated modelling framework. *European Journal of Forest Research*, 131(1), 131-144. <https://doi.org/10.1007/s10342-010-0463-3>
- Fajstavr, M., Bednářová, E., Nezval, O., Giagli, K., Gryc, V., Vavřík, H., Horáček, P., & Urban, J. (2019). How needle phenology indicates the changes of xylem cell formation during drought stress in *Pinus sylvestris* L. *Dendrochronologia*, 56, 125600-125600. <https://doi.org/10.1016/j.dendro.2019.05.004>
- Falk, M., Wharton, S., Schroeder, M., Ustin, S., & Paw U, K. T. (2008). Flux partitioning in an old-growth forest: Seasonal and interannual dynamics. *Tree Physiology*, 28(4), 509-520. <https://doi.org/10.1093/treephys/28.4.509>
- Fang, J., Kato, T., Guo, Z., Yang, Y., Hu, H., Shen, H., Zhao, X., Kishimoto-Mo, A. W., Tang, Y., & Houghton, R. A. (2014). Evidence for environmentally enhanced forest growth. *Proceedings of the National Academy of Sciences of the United States of America*, 111(26), 9527-9532. <https://doi.org/10.1073/pnas.1402333111>
- FAO, & UNEP. (2020). *The State of the World's Forests 2020. Forests, biodiversity and people* (978-92-5-132419-6). <http://www.fao.org/documents/card/en/c/ca8642en>
- Faticchi, S., Leuzinger, S., & Körner, C. (2014). Moving beyond photosynthesis: From carbon source to sink-driven vegetation modeling. *New Phytologist*, 201(4), 1086-1095. <https://doi.org/10.1111/nph.12614>
- Filion, L., & Cournoyer, L. (1995). Variation in wood structure of eastern larch defoliated by the larch sawfly in subarctic Quebec, Canada. *Canadian Journal of Forest Research*, 25(8), 1263-1268. <https://doi.org/10.1139/x95-139>
- Fitter, A., & Fitter, R. (2002). Rapid changes in flowering time in British plants. *Science*, 296(5573), 1689-1691.

- Flynn, D. F. B., & Wolkovich, E. M. (2018). Temperature and photoperiod drive spring phenology across all species in a temperate forest community. *New Phytologist*, 219(4), 1353-1362. <https://doi.org/10.1111/nph.15232>
- Frank, A., Sperisen, C., Howe, G. T., Brang, P., Walthert, L., Clair, J. B. S., & Heiri, C. (2017). Distinct genecological patterns in seedlings of Norway spruce and silver fir from a mountainous landscape. *Ecology*, 98(1), 211-227. <https://doi.org/10.1002/ecy.1632>
- Fréjaville, T., Vizcaíno-Palomar, N., Fady, B., Kremer, A., & Benito Garzón, M. (2019). Range margin populations show high climate adaptation lags in European trees. *Global Change Biology*, 26(2), 484-495. <https://doi.org/10.1111/gcb.14881>
- Friend, A. D., Eckes-Shephard, A. H., Fonti, P., Rademacher, T. T., Rathgeber, C. B. K., Richardson, A. D., & Turton, R. H. (2019). On the need to consider wood formation processes in global vegetation models and a suggested approach. *Annals of Forest Science*, 76(2), 49-49. <https://doi.org/10.1007/s13595-019-0819-x>
- Fu, Y. S. H., Campioli, M., Vitasse, Y., De Boeck, H. J., Van Den Berge, J., Abdelgawad, H., Asard, H., Piao, S., Deckmyn, G., & Janssens, I. A. (2014). Variation in leaf flushing date influences autumnal senescence and next year's flushing date in two temperate tree species. *Proceedings of the National Academy of Sciences*, 111(20), 7355-7360. <https://doi.org/10.1073/pnas.1321727111>
- Fu, P. L., Griebinger, J., Gebrekirstos, A., Fan, Z. X., & Bräuning, A. (2017). Earlywood and latewood stable carbon and oxygen isotope variations in two pine species in Southwestern China during the recent decades. *Frontiers in Plant Science*, 7, 2050-2050. <https://doi.org/10.3389/FPLS.2016.02050/BIBTEX>
- Gao, S., Liang, E., Liu, R., Babst, F., Camarero, J. J., Fu, Y. H., Piao, S., Rossi, S., Shen, M., Wang, T., & Peñuelas, J. (2022). An earlier start of the thermal growing season enhances tree growth in cold humid areas but not in dry areas. *Nature Ecology and Evolution*, 1-8. <https://doi.org/10.1038/s41559-022-01668-4>
- Geoffrey MH, Jake FW (2015) Review of the USA National Phenology Network. In: *Circular*. (eds Glynn PD, Owen TW) pp 36, Reston, VA.
- Gonsamo, A., Chen, J. M., & Ooi, Y. W. (2018). Peak season plant activity shift towards spring is reflected by increasing carbon uptake by extratropical ecosystems. *Global Change Biology*, 24(5), 2117-2128. <https://doi.org/10.1111/gcb.14001>
- Gray, R. E. J., & Ewers, R. M. (2021). Monitoring Forest Phenology in a Changing World. *Forests*, 12(3), 297. <https://doi.org/10.3390/f12030297>

- Graven, H. D., Keeling, R. F., Piper, S. C., Patra, P. K., Stephens, B. B., Wofsy, S. C., Welp, L. R., Sweeney, C., Tans, P. P., Kelley, J. J., Daube, B. C., Kort, E. A., Santoni, G. W., & Bent, J. D. (2013). Enhanced seasonal exchange of CO₂ by Northern ecosystems since 1960. *Science*, *341*(6150), 1085-1089. <https://doi.org/10.1126/science.1239207>
- Gričar, J., Krže, L., & Čufar, K. (2009). Number of cells in xylem, phloem and dormant cambium in silver fir (*Abies alba*), in trees of different vitality. *IAWA Journal*, *30*(2), 121-133. <https://doi.org/10.1163/22941932-90000208>
- Gričar, J., Zupančič, M., Čufar, K., & Oven, P. (2007). Wood formation in Norway spruce (*Picea abies*) studied by pinning and intact tissue sampling method. *Wood Research*, *52*(2), 1-10.
- Gruber, A., Pirkebner, D., Oberhuber, W., & Wieser, G. (2011). Spatial and seasonal variations in mobile carbohydrates in *Pinus cembra* in the timberline ecotone of the Central Austrian Alps. *European Journal of Forest Research*, *130*(2), 173-179. <https://doi.org/10.1007/s10342-010-0419-7>
- Gu L, Post WM, Baldocchi D, Black TA, Verma SB, Vesala T, Wofsy SC (2003) Phenology of vegetation photosynthesis. In: *Phenology: An integrative environmental science*. pp 467-485. Springer.
- Guo, X., Klisz, M., Puchałka, R., Silvestro, R., Faubert, P., Belien, E., Huang, J., & Rossi, S. (2021). Common-garden experiment reveals clinal trends of bud phenology in black spruce populations from a latitudinal gradient in the boreal forest. *Journal of Ecology*, 1365-2745.13582. <https://doi.org/10.1111/1365-2745.13582>
- Hannerz, M., Aitken, S. N., King, J. N., & Budge, S. (1999). Effects of genetic selection for growth on frost hardiness in western hemlock. *Canadian Journal of Forest Research*, *29*(4), 509-516. <https://doi.org/10.1139/x99-019>
- Hänninen, H., & Kramer, K. (2007). A framework for modelling the annual cycle of trees in boreal and temperate regions. *Silva Fennica*, *41*(1), 167-205. <https://edepot.wur.nl/41205>
- Hansen, J., & Beck, E. (1990). The fate and path of assimilation products in the stem of 8-year-old Scots pine (*Pinus sylvestris* L.) trees. *Trees*, *4*(1), 16-21. <https://doi.org/10.1007/BF00226235>
- Harris, N. L., Gibbs, D. A., Baccini, A., Birdsey, R. A., de Bruin, S., Farina, M., Fatoyinbo, L., Hansen, M. C., Herold, M., Houghton, R. A., Potapov, P. V., Suarez, D. R., Roman-Cuesta, R. M., Saatchi, S. S., Slay, C. M., Turubanova, S. A., & Tyukavina, A. (2021). Global maps of twenty-first century forest carbon

- fluxes. *Nature Climate Change*, 11(3), 234-240. <https://doi.org/10.1038/s41558-020-00976-6>
- Hartmann, H., McDowell, N. G., & Trumbore, S. (2015). Allocation to carbon storage pools in Norway spruce saplings under drought and low CO₂. *Tree Physiology*, 35(3), 243-252. <https://doi.org/10.1093/treephys/tpv019>
- Hartmann, H., & Trumbore, S. (2016). Understanding the roles of nonstructural carbohydrates in forest trees - from what we can measure to what we want to know. *New Phytologist*, 211(2), 386-403. <https://doi.org/10.1111/nph.13955>
- Howard, C., Dymond, C. C., Griess, V. C., Tolkien-Spurr, D., & van Kooten, G. C. (2021). Wood product carbon substitution benefits: a critical review of assumptions. *Carbon Balance and Management*, 16(1), 1-11. <https://doi.org/10.1186/s13021-021-00171-w>
- Huang, J. G., Ma, Q., Rossi, S., Biondi, F., Deslauriers, A., Fonti, P., Liang, E., Mäkinen, H., Oberhuber, W., Rathgeber, C. B. K., Tognetti, R., Treml, V., Yang, B., Zhang, J. L., Antonucci, S., Bergeron, Y., Julio Camarero, J., Campelo, F., Cufar, K., . . . Ziacco, E. (2020). Photoperiod and temperature as dominant environmental drivers triggering secondary growth resumption in Northern Hemisphere conifers. *Proceedings of the National Academy of Sciences of the United States of America*, 117(34), 20645-20652. <https://doi.org/10.1073/pnas.2007058117>
- Hurme, P., Repo, T., Savolainen, O., & Pääkkönen, T. (1997). Climatic adaptation of bud set and frost hardiness in Scots pine (*Pinus sylvestris*). *Canadian Journal of Forest Research*, 27(5), 716-723. <https://doi.org/10.1139/x97-052>
- Jackson, M.T. (1966) Effects of microclimate on spring flowering phenology. *Ecology*, 47, 407–415.
- IPCC. (2019). *Climate Change and Land: an IPCC special report on climate change, desertification, land degradation, sustainable land management, food security, and greenhouse gas fluxes in terrestrial ecosystems*. [P.R. Shukla, J. Skea, E. Calvo Buendia, V. Masson-Delmo.
- Jastrzębowski, S., Ukalski, K., Klisz, M., Ukalska, J., Przybylski, P., Matras, J., Barzdaj, W., & Kowalkowski, W. (2018). Assessment of the height stability in progeny of *Fagus sylvatica* L. Populations using the GGE biplot method. *Dendrobiology*, 79, 34-46. <https://doi.org/10.12657/denbio.079.004>
- Jeffree, E. (1960) Some long-term means from The Phenological Reports (1891–1948) of the Royal Meteorological Society. *Q. J. R. Meteorol. Soc.*, 86, 95–103.

- Jeong, S. J., HO, C. H., GIM, H. J., & Brown, M. E. (2011). Phenology shifts at start vs. end of growing season in temperate vegetation over the Northern Hemisphere for the period 1982–2008. *Global Change Biology*, 17(7), 2385-2399.
- Jeong SJ, Schimel D, Frankenberg C, Drewry DT, Fisher JB, Verma M, . . . Joiner J (2017) Application of satellite solar-induced chlorophyll fluorescence to understanding large-scale variations in vegetation phenology and function over northern high latitude forests. *Remote Sensing of Environment*, 190, 178-187.
- Joiner, J., & Yoshida, Y. (2021). Global MODIS and FLUXNET-derived Daily Gross Primary Production, V2. ORNL DAAC. <https://doi.org/10.3334/ORNLDAAC/1835>
- Kagawa, A., Sugimoto, A., & Maximov, T. C. (2006). ¹³C₂ pulse-labelling of photoassimilates reveals carbon allocation within and between tree rings. *Plant, Cell and Environment*, 29(8), 1571-1584. <https://doi.org/10.1111/j.1365-3040.2006.01533.x>
- Kapeller, S., Lexer, M. J., Geburek, T., Hiebl, J., & Schueler, S. (2012). Intraspecific variation in climate response of Norway spruce in the eastern Alpine range: Selecting appropriate provenances for future climate. *Forest Ecology and Management*, 271, 46-57. <https://doi.org/10.1016/j.foreco.2012.01.039>
- Karger, D. N., Conrad, O., Böhner, J., Kawohl, T., Kreft, H., Soria-Auza, R. W., Zimmermann, N. E., Linder, H. P., & Kessler, M. (2017). Climatologies at high resolution for the earth's land surface areas. *Scientific Data*, 4. <https://doi.org/10.1038/sdata.2017.122>
- Kašpar, J., Anfodillo, T., & Treml, V. (2019). Tree size mostly drives the variation of xylem traits at the treeline ecotone. *Trees - Structure and Function*, 33(6), 1657-1665. <https://doi.org/10.1007/s00468-019-01887-6>
- Kirkwood, T. B. L., & Austad, S. N. (2000). Why do we age? *Nature*, 408(6809), 233-238. <https://doi.org/10.1038/35041682>
- Klein, T., Vitasse, Y., & Hoch, G. (2016). Coordination between growth, phenology and carbon storage in three coexisting deciduous tree species in a temperate forest. *Tree Physiology*, 36(7), 847-855. <https://doi.org/10.1093/treephys/tpw030>
- Klisz, M., Ukalska, J., Koprowski, M., Tereba, A., Puchałka, R., Przybylski, P., Jastrzębowski, S., & Nabais, C. (2019). Effect of provenance and climate on intra-annual density fluctuations of Norway spruce *Picea abies* (L.) Karst. in Poland. *Agricultural and Forest Meteorology*, 269-270, 145-156. <https://doi.org/10.1016/j.agrformet.2019.02.013>

- Klisz, M., Ukalski, K., Ukalska, J., Jastrzębowski, S., Puchałka, R., Przybylski, P., Mionskowski, M., & Matras, J. (2018). What can we learn from an early test on the adaptation of silver fir populations to marginal environments? *Forests*, *9*(7), 441-441. <https://doi.org/10.3390/f9070441>
- Koch E, Lipa W, Neumcke R, Zach S (2008) The history and current status of the Austrian phenology network. In: *COST Action 725: The history and current status of plant phenology in Europe*. (eds Nekovář J, Koch E, Kubin E, Nejedki P, Sparks T, Wielgolaski FE). COST office.
- Kodama, N., Barnard, R. L., Salmon, Y., Weston, C., Ferrio, J. P., Holst, J., Werner, R. A., Saurer, M., Rennenberg, H., Buchmann, N., & Gessler, A. (2008). Temporal dynamics of the carbon isotope composition in a *Pinus sylvestris* stand: From newly assimilated organic carbon to respired carbon dioxide. *Oecologia*, *156*(4), 737-750. <https://doi.org/10.1007/s00442-008-1030-1>
- Koga, S., & Zhang, S. Y. (2002). Relationships between wood density and annual growth rate components in balsam fir (*Abies balsamea*). *Wood and Fiber Science*, *34*(1), 146-157. <https://wfs.swst.org/index.php/wfs/article/view/127>
- Körner, C. (2003). Carbon limitation in trees. *Journal of Ecology*, *91*(1), 4-17. <https://doi.org/10.1046/j.1365-2745.2003.00742.x>
- Körner, C. (2012). *Alpine treelines: Functional ecology of the global high elevation tree limits*. Springer Science & Business Media. <https://doi.org/10.1007/978-3-0348-0396-0>
- Körner, C. (2015). Paradigm shift in plant growth control. *Current Opinion in Plant Biology*, *25*, 107-114. <https://doi.org/10.1016/J.PBI.2015.05.003>
- Körner, C., & Basler, D. (2010). Phenology under global warming. *Science*, *327*(5972), 1461-1462. <https://doi.org/10.1126/science.1186473>
- Körner, C., & Larcher, W. (1988). Plant life in cold climates. *Symposia of the Society for Experimental Biology*, *42*, 25-57.
- Kowalski, A. S., Loustau, D., Berbigier, P., Manca, G., Tedeschi, V., Borghetti, M., Valentini, R., Kolari, P., Berninger, F., Rannik, Ü., Hari, P., Rayment, M., Mencuccini, M., Moncrieff, J., & Grace, J. (2004). Paired comparisons of carbon exchange between undisturbed and regenerating stands in four managed forest in Europe. *Global Change Biology*, *10*(10), 1707-1723. <https://doi.org/10.1111/j.1365-2486.2004.00846.x>
- Kramer, K., Ducousso, A., Gömöry, D., Hansen, J. K., Ionita, L., Liesebach, M., Lorent, A., Schüler, S., Sulkowska, M., de Vries, S., & von Wühlisch, G. (2017). Chilling

- and forcing requirements for foliage bud burst of European beech (*Fagus sylvatica* L.) differ between provenances and are phenotypically plastic. *Agricultural and Forest Meteorology*, 234-235, 172-181. <https://doi.org/10.1016/j.agrformet.2016.12.002>
- Krejza, J., Haeni, M., Darenova, E., Foltýnová, L., Fajstavr, M., Světlík, J., Nezval, O., Bednář, P., Šigut, L., Horáček, P., & Zweifel, R. (2022). Disentangling carbon uptake and allocation in the stems of a spruce forest. *Environmental and Experimental Botany*, 196, 104787-104787. <https://doi.org/10.1016/j.envexpbot.2022.104787>
- Lemay, A., Krause, C., Rossi, S., & Achim, A. (2017). Xylogenesis in stems and roots after thinning in the boreal forest of Quebec, Canada. *Tree Physiology*, 37(11), 1554-1563. <https://doi.org/10.1093/treephys/tpx082>
- Larson, P. R. (1994). *The vascular cambium : development and structure*. https://books.google.ca/books?hl=it&lr=&id=7mLwCAAQBAJ&oi=fnd&pg=PA2&ots=7bxBRh1rxu&sig=IPYJhviM7U5gehvzX_y7d5O-0as&redir_esc=y#v=onepage&q&f=false
- Lawlor, D. W., & Tezara, W. (2009). Causes of decreased photosynthetic rate and metabolic capacity in water-deficient leaf cells: A critical evaluation of mechanisms and integration of processes. *Annals of Botany*, 103(4), 561-579. <https://doi.org/10.1093/aob/mcn244>
- Levin, S. A. (1992). The problem of pattern and scale in ecology. *Ecology*, 73(6), 1943-1967. <https://doi.org/10.2307/1941447>
- Li, Y., Suontama, M., Burdon, R. D., & Dungey, H. S. (2017). Genotype by environment interactions in forest tree breeding: review of methodology and perspectives on research and application. *Tree Genetics and Genomes*, 13(3), 1-18. <https://doi.org/10.1007/s11295-017-1144-x>
- Li, X., Liang, E., Gričar, J., Prislán, P., Rossi, S., & Čufar, K. (2013). Age dependence of xylogenesis and its climatic sensitivity in Smith fir on the south-eastern Tibetan Plateau. *Tree Physiology*, 33(1), 48-56. <https://doi.org/10.1093/treephys/tps113>
- Li, X., Rossi, S., & Liang, E. (2019). The onset of xylogenesis in Smith fir is not related to outer bark thickness. *American Journal of Botany*, 106(10), 1386-1391. <https://doi.org/10.1002/ajb2.1360>
- Liang, L., & Schwartz, M. D. (2009). Landscape phenology: An integrative approach to seasonal vegetation dynamics. *Landscape Ecology*, 24(4), 465-472. <https://doi.org/10.1007/s10980-009-9328-x>

- Linares, J. C., Camarero, J. J., & Carreira, J. A. (2009). Plastic responses of *Abies pinsapo* xylogenesis to drought and competition. *Tree Physiology*, 29(12), 1525-1536. <https://doi.org/10.1093/treephys/tpp084>
- Loehle, C. (1998). Height growth rate tradeoffs determine northern and southern range limits for trees. *Journal of Biogeography*, 25(4), 735-742. <https://doi.org/10.1046/j.1365-2699.1998.2540735.x>
- Logan, K. T., & Pollard, D. F. W. (1975). Mode of shoot growth in 12-year-old black spruce provenances. *Canadian Journal of Forest Research*, 5(4), 539-540. <https://doi.org/10.1139/x75-078>
- Lu X, Liu Z, Zhou Y, Liu Y, An S, Tang J (2018) Comparison of Phenology Estimated from Reflectance-Based Indices and Solar-Induced Chlorophyll Fluorescence (SIF) Observations in a Temperate Forest Using GPP-Based Phenology as the Standard. *Remote Sensing*, 10, 932; <https://doi.org/10.3390/rs10060932>.
- Lupi, C., Morin, H., Deslauriers, A., & Rossi, S. (2010). Xylem phenology and wood production: Resolving the chicken-or-egg dilemma. *Plant, Cell and Environment*, 33(10), 1721-1730. <https://doi.org/10.1111/j.1365-3040.2010.02176.x>
- Lupi, C., Morin, H., Deslauriers, A., Rossi, S., & Houle, D. (2012). Increasing nitrogen availability and soil temperature: Effects on xylem phenology and anatomy of mature black spruce. *Canadian Journal of Forest Research*, 42(7), 1277-1288. <https://doi.org/10.1139/X2012-055>
- Lupi, C., Rossi, S., Vieira, J., Morin, H., & Deslauriers, A. (2013). Assessment of xylem phenology: A first attempt to verify its accuracy and precision. *Tree Physiology*, 34(1), 87-93. <https://doi.org/10.1093/treephys/tpt108>
- Lussier, J. M., Morin, H., & Gagnon, R. (2002). Mortality in black spruce stands of fire or clear-cut origin. *Canadian Journal of Forest Research*, 32(3), 539-547. <https://doi.org/10.1139/x01-201>
- Marquis, B., Bergeron, Y., Simard, M., & Tremblay, F. (2020). Probability of Spring Frosts, Not Growing Degree-Days, Drives Onset of Spruce Bud Burst in Plantations at the Boreal-Temperate Forest Ecotone. *Frontiers in Plant Science*, 11, Article 1031. <https://doi.org/10.3389/fpls.2020.01031>
- Massad, T. J., Trumbore, S. E., Ganbat, G., Reichelt, M., Unsicker, S., Boeckler, A., Gleixner, G., Gershenson, J., & Ruelow, S. (2014). An optimal defense strategy for phenolic glycoside production in *Populus trichocarpa* - isotope labeling demonstrates secondary metabolite production in growing leaves. *New Phytologist*, 203(2), 607-619. <https://doi.org/10.1111/nph.12811>

- McMillan, C. (1957) Nature of the plant community. IV. Phenological variation within five woodland communities under controlled temperatures. *Am. J. Bot.*, 44, 154–163.
- MacNeill, G. J., Mehrpouyan, S., Minow, M. A. A., Patterson, J. A., Tetlow, I. J., & Emes, M. J. (2017). Starch as a source, starch as a sink: The bifunctional role of starch in carbon allocation. *Journal of Experimental Botany*, 68(16), 4433–4453. <https://doi.org/10.1093/jxb/erx291>
- Martínez-Vilalta, J., Sala, A., Asensio, D., Galiano, L., Hoch, G., Palacio, S., Piper, F. I., & Lloret, F. (2016). Dynamics of non-structural carbohydrates in terrestrial plants: a global synthesis. *Ecological Monographs*, 86(4), 495–516. <https://doi.org/10.1002/ecm.1231>
- Martinez del Castillo, E., Longares, L. A., Gričar, J., Prislan, P., Gil-Pelegrín, E., Čufar, K., & de Luis, M. (2016). Living on the edge: Contrasted wood-formation dynamics in *Fagus sylvatica* and *Pinus sylvestris* under mediterranean conditions. *Frontiers in Plant Science*, 7(MAR2016), 370–370. <https://doi.org/10.3389/fpls.2016.00370>
- Martins, D. S., Raziei, T., Paulo, A. A., & Pereira, L. S. (2012). Spatial and temporal variability of precipitation and drought in Portugal. *Natural Hazards and Earth System Science*, 12(5), 1493–1501. <https://doi.org/10.5194/nhess-12-1493-2012>
- McKenzie, S. M., Pisaric, M. F. J., & Arain, M. A. (2021). Comparison of tree-ring growth and eddy covariance-based ecosystem productivities in three different-aged pine plantation forests. *Trees - Structure and Function*, 35(2), 583–595. <https://doi.org/10.1007/S00468-020-02061-Z/FIGURES/4>
- Mencuccini, M., Martínez-Vilalta, J., Hamid, H. A., Korakaki, E., & Vanderklein, D. (2007). Evidence for age- And size-mediated controls of tree growth from grafting studies. *Tree Physiology*, 27(3), 463–473. <https://doi.org/10.1093/treephys/27.3.463>
- Mencuccini, M., Martínez-Vilalta, J., Vanderklein, D., Hamid, H. A., Korakaki, E., Lee, S., & Michiels, B. (2005). Size-mediated ageing reduces vigour in trees. *Ecology Letters*, 8(11), 1183–1190. <https://doi.org/10.1111/j.1461-0248.2005.00819.x>
- Menzel, A., Sparks, T. H., Estrella, N., Koch, E., Aaasa, A., Ahas, R., Alm-Kübler, K., Bissolli, P., Braslavská, O. g., Briede, A., Chmielewski, F. M., Crepinsek, Z., Curnel, Y., Dahl, Å., Defila, C., Donnelly, A., Filella, Y., Jateczak, K., Måge, F., . . . Züst, A. (2006). European phenological response to climate change matches the warming pattern. *Global Change Biology*, 12(10), 1969–1976. <https://doi.org/10.1111/j.1365-2486.2006.01193.x>

- Metsaranta, J. M., Mamet, S. D., Maillet, J., & Barr, A. G. (2021). Comparison of tree-ring and eddy-covariance derived annual ecosystem production estimates for jack pine and trembling aspen forests in Saskatchewan, Canada. *Agricultural and Forest Meteorology*, 307, 108469-108469. <https://doi.org/10.1016/j.agrformet.2021.108469>
- Messier, C., Doucet, R., Ruel, J. C., Claveau, Y., Kelly, C., & Lechowicz, M. J. (1999). Functional ecology of advance regeneration in relation to light in boreal forests. *Canadian Journal of Forest Research*, 29(6), 812-823. <https://doi.org/10.1139/x99-070>
- Milbau, A., Graae, B. J., Shevtsova, A., & Nijs, I. (2009). Effects of a warmer climate on seed germination in the subarctic. *Annals of Botany*, 104(2), 287-296.
- Muller, B., Pantin, F., Génard, M., Turc, O., Freixes, S., Piques, M., & Gibon, Y. (2011). Water deficits uncouple growth from photosynthesis, increase C content, and modify the relationships between C and growth in sink organs. *Journal of Experimental Botany*, 62(6), 1715-1729. <https://doi.org/10.1093/jxb/erq438>
- Nekovář J, Koch E, Kubin E, Nejedlik P, Sparks T, Wielgolaski F (2008) *COST Action 725-the history and current status of plant phenology in Europe*, Brussels, COST Office.
- Newman, J.E.; Beard, J.B. (1962) Phenological Observations: The Dependent Variable in Bioclimatic and Agrometeorological Studies. *Agron. J.*, 54, 399–403.
- O'Donnell, M. S., & Ignizio, D. A. (2012). *Bioclimatic predictors for supporting ecological applications in the conterminous United States: U.S. Geological Survey Data Series 691*. <https://pubs.usgs.gov/ds/691/>
- Oddi, L., Migliavacca, M., Cremonese, E., Filippa, G., Vacchiano, G., Siniscalco, C., Morra Di Cella, U., & Galvagno, M. (2022). Contrasting responses of forest growth and carbon sequestration to heat and drought in the Alps. *Environmental Research Letters*, 17(4), 045015-045015. <https://doi.org/10.1088/1748-9326/ac5b3a>
- Oleksyn, J., Modrzyński, J., Tjoelker, M. G., Zytkowski, R., Reich, P. B., & Karolewski, P. (1998). Growth and physiology of *Picea abies* populations from elevational transects: common garden evidence for altitudinal ecotypes and cold adaptation. *Functional Ecology*, 12(4), 573-590. <https://doi.org/10.1046/j.1365-2435.1998.00236.x>
- Oribe, Y., Funada, R., & Kubo, T. (2003). Relationships between cambial activity, cell differentiation and the localization of starch in storage tissues around the cambium in locally heated stems of *Abies sachalinensis* (Schmidt) Masters. *Trees* -

Structure and Function, 17(3), 185-192. <https://doi.org/10.1007/s00468-002-0231-1>

- Paixao, C., Krause, C., Morin, H., & Achim, A. (2019). Wood quality of black spruce and balsam fir trees defoliated by spruce budworm: A case study in the boreal forest of Quebec, Canada. *Forest Ecology and Management*, 437, 201-210. <https://doi.org/10.1016/j.foreco.2019.01.032>
- Pan, Y., Birdsey, R. A., Fang, J., Houghton, R., Kauppi, P. E., Kurz, W. A., Phillips, O. L., Shvidenko, A., Lewis, S. L., Canadell, J. G., Ciais, P., Jackson, R. B., Pacala, S. W., McGuire, A. D., Piao, S., Rautiainen, A., Sitch, S., & Hayes, D. (2011). A large and persistent carbon sink in the world's forests. *Science*, 333(6045), 988-993. <https://doi.org/10.1126/science.1201609>
- Parnesan, C. (2006). Ecological and evolutionary responses to recent climate change. *Annual Review of Ecology, Evolution, and Systematics*, 37(1), 637-669. <https://doi.org/10.1146/annurev.ecolsys.37.091305.110100>
- Parnesan, C., & Hanley, M. E. (2015). Plants and climate change: complexities and surprises. *Annals of Botany*, 116(6), 849-864. <https://doi.org/10.1093/aob/mcv169>
- Pasho, E., Camarero, J. J., & Vicente-Serrano, S. M. (2012). Climatic impacts and drought control of radial growth and seasonal wood formation in *Pinus halepensis*. *Trees - Structure and Function*, 26(6), 1875-1886. <https://doi.org/10.1007/s00468-012-0756-x>
- Pastorello, G., Trotta, C., Canfora, E., Chu, H., Christianson, D., Cheah, Y. W., Poindexter, C., Chen, J., Elbashandy, A., Humphrey, M., Isaac, P., Polidori, D., Ribeca, A., van Ingen, C., Zhang, L., Amiro, B., Ammann, C., Arain, M. A., Ardö, J., . . . Papale, D. (2020). The FLUXNET2015 dataset and the ONEFlux processing pipeline for eddy covariance data. *Scientific Data*, 7(1), 225-225. <https://doi.org/10.1038/s41597-020-0534-3>
- Pedlar, J. H., & McKenney, D. W. (2017). Assessing the anticipated growth response of northern conifer populations to a warming climate. *Scientific Reports*, 7. <https://doi.org/10.1038/srep43881>
- Pelletier, E., & De Lafontaine, G. (2023). Jack pine of all trades: Deciphering intraspecific variability of a key adaptive trait at the rear edge of a widespread fire-embracing North American conifer. *American Journal of Botany*, 110(2). <https://doi.org/10.1002/ajb2.16111>

- Peñuelas, J., Rutishauser, T., & Filella, I. (2009). Phenology Feedbacks on Climate Change. *Science*, 324(5929), 887-888. <https://doi.org/doi:10.1126/science.1173004>
- Perrin, M., Rossi, S., & Isabel, N. (2017). Synchronisms between bud and cambium phenology in black spruce: Early-flushing provenances exhibit early xylem formation. *Tree Physiology*, 37(5), 593-603. <https://doi.org/10.1093/treephys/tpx019>
- Piao, S., Liu, Q., Chen, A., Janssens, I. A., Fu, Y., Dai, J., Liu, L., Lian, X., Shen, M., & Zhu, X. (2019). Plant phenology and global climate change: Current progresses and challenges. *Global Change Biology*, 25(6), 1922-1940. <https://doi.org/10.1111/gcb.14619>
- Piao, S., Liu, Z., Wang, T., Peng, S., Ciais, P., Huang, M., Ahlstrom, A., Burkhardt, J. F., Chevallier, F., Janssens, I. A., Jeong, S.-J., Lin, X., Mao, J., Miller, J., Mohammad, A., Myneni, R. B., Peñuelas, J., Shi, X., Stohl, A., . . . Tans, P. P. (2017). Weakening temperature control on the interannual variations of spring carbon uptake across northern lands. *Nature Climate Change*, 7(5), 359-363. <https://doi.org/10.1038/nclimate3277>
- Piao, S., Tan, J., Chen, A., Fu, Y. H., Ciais, P., Liu, Q., Janssens, I. A., Vicca, S., Zeng, Z., Jeong, S.-J., Li, Y., Myneni, R. B., Peng, S., Shen, M., & Peñuelas, J. (2015). Leaf onset in the northern hemisphere triggered by daytime temperature. *Nature Communications*, 6(1), 6911. <https://doi.org/10.1038/ncomms7911>
- Polgar, C. A., & Primack, R. B. (2011). Leaf-out phenology of temperate woody plants: from trees to ecosystems. *New Phytologist*, 191(4), 926-941. <https://doi.org/10.1111/j.1469-8137.2011.03803.x>
- Pothier, D., Elie, J. G., Auger, I., Mailly, D., & Gaudreault, M. (2012). Spruce budworm-caused mortality to balsam fir and black spruce in pure and mixed conifer stands. *Forest Science*, 58(1), 24-33. <https://doi.org/10.5849/forsci.10-110>
- Prentice, I. C., Bondeau, A., Cramer, W., Harrison, S. P., Hickler, T., Lucht, W., Sitch, S., Smith, B., & Sykes, M. T. (2007). Dynamic Global Vegetation Modeling: Quantifying Terrestrial Ecosystem Responses to Large-Scale Environmental Change. In (pp. 175-192). https://doi.org/10.1007/978-3-540-32730-1_15
- Pretzsch, H., Biber, P., Schütze, G., Kemmerer, J., & Uhl, E. (2018). Wood density reduced while wood volume growth accelerated in Central European forests since 1870. *Forest Ecology and Management*, 429, 589-616. <https://doi.org/10.1016/j.foreco.2018.07.045>

- Pretzsch, H., Biber, P., Schütze, G., Uhl, E., & Rötzer, T. (2014). Forest stand growth dynamics in Central Europe have accelerated since 1870. *Nature Communications*, 5(1), 1-10. <https://doi.org/10.1038/ncomms5967>
- Primicia, I., Camarero, J. J., Imbert, J. B., & Castillo, F. J. (2013). Effects of thinning and canopy type on growth dynamics of *Pinus sylvestris*: Inter-annual variations and intra-annual interactions with microclimate. *European Journal of Forest Research*, 132(1), 121-135. <https://doi.org/10.1007/s10342-012-0662-1>
- Prislan, P., Gričar, J., de Luis, M., Novak, K., Del Castillo, E. M., Schmitt, U., Koch, G., Štrus, J., Mrak, P., Žnidarič, M. T., & Čufar, K. (2016). Annual cambial rhythm in *Pinus halepensis* and *Pinus sylvestris* as indicator for climate adaptation. *Frontiers in Plant Science*, 7(DECEMBER2016). <https://doi.org/10.3389/fpls.2016.01923>
- Puchalka, R., Koprowski, M., Gričar, J., & Przybylak, R. (2017). Does tree-ring formation follow leaf phenology in Pedunculate oak (*Quercus robur* L.)? *European Journal of Forest Research*, 136(2), 259-268. <https://doi.org/10.1007/s10342-017-1026-7>
- Puchi, P. F., Khomik, M., Frigo, D., Arain, M. A., Fonti, P., Arx, G. v., & Castagneri, D. (2023). Revealing how intra- and inter-annual variability of carbon uptake (GPP) affects wood cell biomass in an eastern white pine forest. *Environmental Research Letters*, 18(2), 024027-024027. <https://doi.org/10.1088/1748-9326/acb2df>
- Quentin, A. G., Pinkard, E. A., Ryan, M. G., Tissue, D. T., Baggett, L. S., Adams, H. D., Maillard, P., Marchand, J., Landhäusser, S. M., Lacoïnte, A., Gibon, Y., Anderegg, W. R. L., Asao, S., Atkin, O. K., Bonhomme, M., Claye, C., Chow, P. S., Clément-Vidal, A., Davies, N. W., . . . Woodruff, D. R. (2015). Non-structural carbohydrates in woody plants compared among laboratories. *Tree Physiology*, 35(11), 1146-1165. <https://doi.org/10.1093/treephys/tpv073>
- Rathgeber, C. B. K., Cuny, H. E., & Fonti, P. (2016). Biological basis of tree-ring formation: A crash course. *Frontiers in Plant Science*, 7(MAY2016), 734-734. <https://doi.org/10.3389/fpls.2016.00734>
- Rathgeber, C. B. K., Decoux, V., & Leban, J. M. (2006). Linking intra-tree-ring wood density variations and tracheid anatomical characteristics in Douglas fir (*Pseudotsuga menziesii* (Mirb.) Franco). *Annals of Forest Science*, 63(7), 699-706. <https://doi.org/10.1051/forest:2006050>
- Rathgeber, C. B. K., Pérez-De-Lis, G., Fernández-De-Uña, L., Fonti, P., Rossi, S., Treydte, K., Gessler, A., Deslauriers, A., Fonti, M. V., Ponton, S., Rathgeber, C. B. K., Fonti, P., Treydte, K., Gessler, A., Rossi, S., Deslauriers, A., Gessler, A., & Fonti, M. V. (2022). Anatomical, Developmental and Physiological Bases of Tree-Ring Formation in Relation to Environmental Factors. In R. T. W. Siegwolf,

- J. R. Brooks, J. Roden, & M. Saurer (Eds.), (Vol. 8, pp. 61-99). Springer, Cham. https://doi.org/10.1007/978-3-030-92698-4_3
- Rathgeber, C. B. K., Rossi, S., & Bontemps, J. D. (2011). Cambial activity related to tree size in a mature silver-fir plantation. *Annals of Botany*, 108(3), 429-438. <https://doi.org/10.1093/aob/mcr168>
- Reaumur RD (1735) Observation du thermometer, faites à Paris pendant l'année 1735, comparees avec celles qui ont été faites sous la ligne, à l'Isle de France, à Alger et en quelques-unes de nos isles de l'Amérique. Paris: Mémoires de l'Académie des Sciences.
- Rehfeldt, G. E., Tchebakova, N. M., Parfenova, Y. I., Wykoff, W. R., Kuzmina, N. A., & Milyutin, L. I. (2002). Intraspecific responses to climate in *Pinus sylvestris*. *Global Change Biology*, 8(9), 912-929. <https://doi.org/10.1046/j.1365-2486.2002.00516.x>
- Rehfeldt, G. E., Ying, C. C., Spittlehouse, D. L., & Hamilton, D. A. (1999). Genetic responses to climate in *Pinus contorta*: Niche breadth, climate change, and reforestation. *Ecological Monographs*, 69(3), 375-407. <https://doi.org/10.2307/2657162>
- Reich, P. B., Oleksyn, J., Modrzyński, J., & Tjoelker, M. G. (1996). Evidence that longer needle retention of spruce and pine populations at high elevations and high latitudes is largely a phenotypic response. *Tree Physiology*, 16(7), 643-647. <https://doi.org/10.1093/treephys/16.7.643>
- Ren, P., Néron, V., Rossi, S., Liang, E., Bouchard, M., & Deslauriers, A. (2020). Warming counteracts defoliation-induced mismatch by increasing herbivore-plant phenological synchrony. *Global Change Biology*, 26(4), 2072-2080. <https://doi.org/10.1111/gcb.14991>
- Ren, P., Ziaco, E., Rossi, S., Biondi, F., Prislan, P., & Liang, E. (2019). Growth rate rather than growing season length determines wood biomass in dry environments. *Agricultural and Forest Meteorology*, 271, 46-53. <https://doi.org/10.1016/j.agrformet.2019.02.031>
- Reyer, C., Brouwers, N., Rammig, A., Brook, B. W., Epila, J., Grant, R. F., Holmgren, M., Langerwisch, F., Leuzinger, S., Lucht, W., Medlyn, B., Pfeifer, M., Steinkamp, J., Vanderwel, M. C., Verbeeck, H., & Vilella, D. M. (2015). Forest resilience and tipping points at different spatio-temporal scales: Approaches and challenges. *Journal of Ecology*, 103(1), 5-15. <https://doi.org/10.1111/1365-2745.12337>

- Reyer, C., Lasch-Born, P., Suckow, F., Gutsch, M., Murawski, A., & Pilz, T. (2014). Projections of regional changes in forest net primary productivity for different tree species in Europe driven by climate change and carbon dioxide. *Annals of Forest Science*, 71(2), 211-225. <https://doi.org/10.1007/s13595-013-0306-8>
- Repo, T., Roitto, M., & Sutinen, S. (2011). Does the removal of snowpack and the consequent changes in soil frost affect the physiology of Norway spruce needles? *Environmental and Experimental Botany*, 72(3), 387-396. <https://doi.org/10.1016/j.envexpbot.2011.04.014>
- Richardson, A. D., Keenan, T. F., Migliavacca, M., Ryu, Y., Sonnentag, O., & Toomey, M. (2013). Climate change, phenology, and phenological control of vegetation feedbacks to the climate system. *Agricultural and Forest Meteorology*, 169, 156-173. <https://doi.org/https://doi.org/10.1016/j.agrformet.2012.09.012>
- Rinne, K. T., Saurer, M., Kirilyanov, A. V., Loader, N. J., Bryukhanova, M. V., Werner, R. A., & Siegwolf, R. T. W. (2015). The relationship between needle sugar carbon isotope ratios and tree rings of larch in Siberia. *Tree Physiology*, 35(11), 1192-1205. <https://doi.org/10.1093/treephys/tpv096>
- Rocha, A. V., Goulden, M. L., Dunn, A. L., & Wofsy, S. C. (2006). On linking interannual tree ring variability with observations of whole-forest CO₂ flux. *Global Change Biology*, 12(8), 1378-1389. <https://doi.org/10.1111/j.1365-2486.2006.01179.x>
- Rosenzweig, C.; Casassa, G.; Karoly, D.J.; Imeson, A.; Liu, C.; Menzel, A.; Rawlins, S.; Root, T.L.; Seguin, B.; Tryjanowski, P. (2007) Assessment of observed changes and responses in natural and managed systems. In *Climate Change 2007: Impacts, Adaptation and Vulnerability, Contribution of Working Group II to the Fourth Assessment Report of the Intergovernmental Panel on Climate Change*; Parry, M., Canziani, O.F., Palutikof, J., van der Linden, P., Hanson, C., Eds.; Cambridge University Press: Cambridge, UK; New York, NY, USA; Volume 2007, p. 79.
- Rossi, S. (2015). Local adaptations and climate change: converging sensitivity of bud break in black spruce provenances. *International Journal of Biometeorology*, 59(7), 827-835. <https://doi.org/10.1007/s00484-014-0900-y>
- Rossi, S., Anfodillo, T., & Menardi, R. (2006). Trephor: A new tool for sampling microcores from tree stems. *IAWA Journal*, 27(1), 89-97. <https://doi.org/10.1163/22941932-90000139>
- Rossi, S., Anfodillo, T., Čufar, K., Cuny, H. E., Deslauriers, A., Fonti, P., Frank, D., Gričar, J., Gruber, A., Huang, J. G., Jyske, T., Kašpar, J., King, G., Krause, C., Liang, E., Mäkinen, H., Morin, H., Nöjd, P., Oberhuber, W., . . . Treml, V. (2016). Pattern of xylem phenology in conifers of cold ecosystems at the Northern Hemisphere. *Global Change Biology*, 22(11), 3804-3813. <https://doi.org/10.1111/gcb.13317>

- Rossi, S., Cairo, E., Krause, C., & Deslauriers, A. (2015). Growth and basic wood properties of black spruce along an alti-latitudinal gradient in Quebec, Canada. *Annals of Forest Science*, 72(1), 77-87. <https://doi.org/10.1007/s13595-014-0399-8>
- Rossi, S., Deslauriers, A., & Anfodillo, T. (2006). Assessment of cambial activity and xylogenesis by microsampling tree species: An example at the Alpine timberline. *IWA Journal*, 27(4), 383-394. <https://doi.org/10.1163/22941932-90000161>
- Rossi, S., Deslauriers, A., Anfodillo, T., & Carrer, M. (2008). Age-dependent xylogenesis in timberline conifers. *New Phytologist*, 177(1), 199-208. <https://doi.org/10.1111/j.1469-8137.2007.02235.x>
- Rossi, S., Deslauriers, A., Anfodillo, T., Morin, H., Saracino, A., Motta, R., & Borghetti, M. (2006). Conifers in cold environments synchronize maximum growth rate of tree-ring formation with day length. *New Phytologist*, 170(2), 301-310. <https://doi.org/10.1111/j.1469-8137.2006.01660.x>
- Rossi, S., Deslauriers, A., Griçar, J., Seo, J. W., Rathgeber, C. B. K., Anfodillo, T., Morin, H., Levanic, T., Oven, P., & Jalkanen, R. (2008). Critical temperatures for xylogenesis in conifers of cold climates. *Global Ecology and Biogeography*, 17(6), 696-707. <https://doi.org/10.1111/j.1466-8238.2008.00417.x>
- Rossi, S., Deslauriers, A., & Morin, H. (2003). Application of the Gompertz equation for the study of xylem cell development. *Dendrochronologia*, 21(1), 33-39. <https://doi.org/10.1078/1125-7865-00034>
- Rossi, S., Girard, M. J., & Morin, H. (2014). Lengthening of the duration of xylogenesis engenders disproportionate increases in xylem production. *Global Change Biology*, 20(7), 2261-2271. <https://doi.org/10.1111/gcb.12470>
- Rossi, S., Morin, H., & Deslauriers, A. (2012). Causes and correlations in cambium phenology: towards an integrated framework of xylogenesis. *Journal of Experimental Botany*, 63(5), 2117-2126. <https://doi.org/10.1093/jxb/err423>
- Ruiz-Sinoga, J. D., Garcia-Marin, R., Gabarron-Galeote, M. A., & Martinez-Murillo, J. F. (2012). Analysis of dry periods along a pluviometric gradient in Mediterranean southern Spain. *International Journal of Climatology*, 32(10), 1558-1571. <https://doi.org/10.1002/joc.2376>
- Sala, A., Woodruff, D. R., & Meinzer, F. C. (2012). Carbon dynamics in trees: feast or famine? *Tree Physiology*, 32(6), 764-775. <https://doi.org/10.1093/treephys/tpr143>

- Salminen, H., & Jalkanen, R. (2005). Modelling the effect of temperature on height increment of Scots pine at high latitudes. *Silva Fennica*, 39(4), 497-508. <https://doi.org/10.14214/sf.362>
- Savolainen, O., Bokma, F., Knürr, T., Kärkkäinen, K., Pyhäjärvi, T., & Wachowiak, W. (2007). *Adaptation of forest trees to climate change* EUFORGEN Climate Change and Forest Genetic Diversity: implications for sustainable forest management in Europe, Paris, France, 15-16 March 2006, 19-30., Rome, Italy.
- Savolainen, O., Pyhäjärvi, T., & Knürr, T. (2007). Gene flow and local adaptation in trees. *Annual Review of Ecology, Evolution, and Systematics*, 38(1), 595-619. <https://doi.org/10.1146/annurev.ecolsys.38.091206.095646>
- Schnelle F, Volkert E (1974) International Phenological Gardens in Europe The Basic Network for International Phenological Observations. In: *Phenology and Seasonality Modeling*. (ed Lieth H) pp 383-387. Berlin, Heidelberg, Springer Berlin Heidelberg.
- Schrader, J., Baba, K., May, S. T., Palme, K., Bennett, M., Bhalerao, R. P., & Sandberg, G. (2003). Polar auxin transport in the wood-forming tissues of hybrid aspen is under simultaneous control of developmental and environmental signals. *Proceedings of the National Academy of Sciences of the United States of America*, 100(17), 10096-10101. <https://doi.org/10.1073/pnas.1633693100>
- Schwartz, M. D., & Hanes, J. M. (2010). Continental-scale phenology: warming and chilling. *International Journal of Climatology*, 30(11), 1595-1598.
- Seidl, R., Eastaugh, C. S., Kramer, K., Maroschek, M., Reyer, C., Socha, J., Vacchiano, G., Zlatanov, T., & Hasenauer, H. (2013). Scaling issues in forest ecosystem management and how to address them with models. *European Journal of Forest Research*, 132(5-6), 653-666. <https://doi.org/10.1007/s10342-013-0725-y>
- Shen, M., Piao, S., Cong, N., Zhang, G., & Jassens, I. A. (2015). Precipitation impacts on vegetation spring phenology on the Tibetan Plateau. *Global Change Biology*, 21(10), 3647-3656.
- Shi, J. L., Riedl, B., Deng, J., Cloutier, A., & Zhang, S. Y. (2007). Impact of log position in the tree on mechanical and physical properties of black spruce medium-density fibreboard panels. *Canadian Journal of Forest Research*, 37(5), 866-873. <https://doi.org/10.1139/X06-268>
- Slayback, D. A., Pinzon, J. E., Los, S. O., & Tucker, C. J. (2003). Northern hemisphere photosynthetic trends 1982–99. *Global Change Biology*, 9(1), 1-15.

- Silvestro, R., Brasseur, S., Klisz, M., Mencuccini, M., & Rossi, S. (2020). Bioclimatic distance and performance of apical shoot extension: Disentangling the role of growth rate and duration in ecotypic differentiation. *Forest Ecology and Management*, 477. <https://doi.org/10.1016/j.foreco.2020.118483>
- Silvestro, R., Rossi, S., Zhang, S., Froment, I., Huang, J. G., & Saracino, A. (2019). From phenology to forest management: Ecotypes selection can avoid early or late frosts, but not both. *Forest Ecology and Management*, 436, 21-26. <https://doi.org/10.1016/j.foreco.2019.01.005>
- Sit, V., & Poulin-Costello, M. (1994). *Catalog of curves for curve fitting*. Ministry of Forests, Research Program.
- Soil Classification Working, G. (1998). *The Canadian System of Soil Classification*. https://books.google.ca/books?hl=it&lr=&id=4aHVg18eDLYC&oi=fnd&pg=PR10&dq=soil+classification+working+group+1998&ots=GqFnXwNFJz&sig=9vVic8QVkrWpw1UF8l_jijQZg#v=onepage&q&f=false
- Sparks T, Carey P (1995) The responses of species to climate over two centuries: an analysis of the Marsham phenological record, 1736-1947. *Journal of Ecology*, 83, 321-329.
- St Clair, J. B., Mandel, N. L., & Vance-Borland, K. W. (2005). Genecology of Douglas fir in Western Oregon and Washington. *Annals of Botany*, 96(7), 1199-1214. <https://doi.org/10.1093/aob/mci278>
- Steltzer, H., & Post, E. (2009). Seasons and life cycles. *Science*, 324(5929), 886-887.
- Suttle, K. B., Thomsen, M. A., & Power, M. E. (2007). Species Interactions Reverse Grassland Responses to Changing Climate. *Science*, 315(5812), 640-642. <https://doi.org/doi:10.1126/science.1136401>
- Suvanto, S., Nöjd, P., Henttonen, H. M., Beuker, E., & Mäkinen, H. (2016). Geographical patterns in the radial growth response of Norway spruce provenances to climatic variation. *Agricultural and Forest Meteorology*, 222, 10-20. <https://doi.org/10.1016/j.agrformet.2016.03.003>
- Tang, J., Körner, C., Muraoka, H., Piao, S., Shen, M., Thackeray, S. J., & Yang, X. (2016). Emerging opportunities and challenges in phenology: a review. *Ecosphere*, 7(8), e01436.
- Teets, A., Fraver, S., Hollinger, D. Y., Weiskittel, A. R., Seymour, R. S., & Richardson, A. D. (2018). Linking annual tree growth with eddy-flux measures of net ecosystem productivity across twenty years of observation in a mixed conifer

- forest. *Agricultural and Forest Meteorology*, 249, 479-487. <https://doi.org/10.1016/j.agrformet.2017.08.007>
- Tei, S., Sugimoto, A., Kotani, A., Ohta, T., Morozumi, T., Saito, S., Hashiguchi, S., & Maximov, T. (2019). Strong and stable relationships between tree-ring parameters and forest-level carbon fluxes in a Siberian larch forest. *Polar Science*, 21, 146-157. <https://doi.org/10.1016/j.polar.2019.02.001>
- Templ B, Koch E, Bolmgren K, Ungersböck M, Paul A, Scheifinger H, . . . Hodzić S (2018) Pan European Phenological database (PEP725): a single point of access for European data. *International Journal of Biometeorology*, 62, 1-5.
- Thibeault-Martel, M., Krause, C., Morin, H., & Rossi, S. (2008). Cambial activity and intra-annual xylem formation in roots and stems of *Abies balsamea* and *Picea mariana*. *Annals of Botany*, 102(5), 667-674. <https://doi.org/10.1093/aob/mcn146>
- United Nations. FCCC/CP/2015/10/Add.1: Paris Agreement.
- Usmani, A., Silvestro, R., Zhang, S., Huang, J. G., Saracino, A., & Rossi, S. (2020). Ecotypic differentiation of black spruce populations: temperature triggers bud burst but not bud set. *Trees - Structure and Function*. <https://doi.org/10.1007/s00468-020-01999-4>
- Van Vliet AJ, De Groot RS, Bellens Y, Braun P, Bruegger R, Bruns E, . . . Sparks T (2003) The European phenology network. *Int J Biometeorol*, 47, 202-212.
- Verkerk, P. J., Hasegawa, M., Van Brusselen, J., Cramm, M., Chen, X., Maximo, Y. I., Koç, M., Lovrić, M., & Tegegne, Y. T. (2022). *Forest products in the global bioeconomy*.
- Vicente-Serrano, S. M., Martín-Hernández, N., Camarero, J. J., Gazol, A., Sánchez-Salguero, R., Peña-Gallardo, M., El Kenawy, A., Domínguez-Castro, F., Tomas-Burguera, M., Gutiérrez, E., de Luis, M., Sangüesa-Barreda, G., Novak, K., Rozas, V., Tíscar, P. A., Linares, J. C., del Castillo, E. M., Ribas, M., García-González, I., . . . Diego Galván, J. (2020). Linking tree-ring growth and satellite-derived gross primary growth in multiple forest biomes. Temporal-scale matters. *Ecological Indicators*, 108, 105753-105753. <https://doi.org/10.1016/j.ecolind.2019.105753>
- Vieira, J., Rossi, S., Campelo, F., Freitas, H., & Nabais, C. (2014). Xylogenesis of *Pinus pinaster* under a Mediterranean climate. *Annals of Forest Science*, 71(1), 71-80. <https://doi.org/10.1007/s13595-013-0341-5>

- Vieira, J., Rossi, S., Campelo, F., & Nabais, C. (2014). Are neighboring trees in tune? Wood formation in *Pinus pinaster*. *European Journal of Forest Research*, 133(1), 41-50. <https://doi.org/10.1007/s10342-013-0734-x>
- Wang, T., O'Neill, G. A., & Aitken, S. N. (2010). Integrating environmental and genetic effects to predict responses of tree populations to climate. *Ecological Applications*, 20(1), 153-163. <https://doi.org/10.1890/08-2257.1>
- Waring, R. H., & Running, S. W. (2007). Carbon Cycle. In (pp. 59-98). Academic Press. <https://doi.org/10.1016/B978-012370605-8.50008-6>
- Warren, C. R., & Adams, M. A. (2004). Evergreen trees do not maximize instantaneous photosynthesis. *Trends in Plant Science*, 9(6), 270-274. <https://doi.org/10.1016/j.tplants.2004.04.004>
- Warton, D. I., Wright, I. J., Falster, D. S., & Westoby, M. (2006). Bivariate line-fitting methods for allometry. *Biological Reviews of the Cambridge Philosophical Society*, 81(2), 259-291. <https://doi.org/10.1017/S1464793106007007>
- Weber, R., Schwendener, A., Schmid, S., Lambert, S., Wiley, E., Landhäuser, S. M., Hartmann, H., & Hoch, G. (2018). Living on next to nothing: tree seedlings can survive weeks with very low carbohydrate concentrations. *New Phytologist*, 218(1), 107-118. <https://doi.org/10.1111/nph.14987>
- Wei, R. P., Sang, D. H., Dhir, N. K., & Yeh, F. C. (2004). Population variation in growth and 15-year-old shoot elongation along geographic and climatic gradients in black spruce in Alberta. *Canadian Journal of Forest Research*, 34(8), 1691-1702. <https://doi.org/10.1139/X04-050>
- Wodzicki, T. J., & Zajaczkowski, S. (1970). Methodical problems in studies on seasonal production of cambial xylem derivatives. *Acta Societatis Botanicorum Poloniae*, 39(3), 519-520. <https://doi.org/10.5586/asbp.1970.040>
- Wolkovich, E. M., Cook, B. I., & Davies, T. J. (2014). Progress towards an interdisciplinary science of plant phenology: building predictions across space, time and species diversity. *New Phytologist*, 201(4), 1156-1162.
- Woodward, F. I. (1987). *Climate and Plant Distribution*. Cambridge University Press. <https://doi.org/10.2307/633873>
- Wu, J., & Li, H. (2006). Concepts of scale and scaling. In (pp. 3-15). Springer Netherlands. https://doi.org/10.1007/1-4020-4663-4_1
- Xia, J., & Wan, S. (2013). Independent effects of warming and nitrogen addition on plant phenology in the Inner Mongolian steppe. *Annals of Botany*, 111(6), 1207-1217.

- Xu, B., Yang, Y., Li, P., Shen, H., & Fang, J. (2014). Global patterns of ecosystem carbon flux in forests: A biometric data-based synthesis. *Global Biogeochemical Cycles*, 28(9), 962-973. <https://doi.org/10.1002/2013GB004593>
- Xu, K., Wang, X., Liang, P., An, H., Sun, H., Han, W., & Li, Q. (2017). Tree-ring widths are good proxies of annual variation in forest productivity in temperate forests. *Scientific Reports*, 7(1), 1-8. <https://doi.org/10.1038/s41598-017-02022-6>
- Yang, L. H., & Rudolf, V. H. W. (2010). Phenology, ontogeny and the effects of climate change on the timing of species interactions. *Ecology Letters*, 13(1), 1-10. <https://doi.org/https://doi.org/10.1111/j.1461-0248.2009.01402.x>
- Yang, J., He, Y., Aubrey, D. P., Zhuang, Q., & Teskey, R. O. (2016). Global patterns and predictors of stem CO₂ efflux in forest ecosystems. *Global Change Biology*, 22(4), 1433-1444. <https://doi.org/10.1111/gcb.13188>
- Zeng, Q., Rossi, S., & Yang, B. (2018). Effects of age and size on xylem phenology in two conifers of northwestern China. *Frontiers in Plant Science*, 8. <https://doi.org/10.3389/fpls.2017.02264>
- Zhang, J., Gou, X., Manzanedo, R. D., Zhang, F., & Pederson, N. (2018). Cambial phenology and xylogenesis of *Juniperus przewalskii* over a climatic gradient is influenced by both temperature and drought. *Agricultural and Forest Meteorology*, 260-261, 165-175. <https://doi.org/10.1016/j.agrformet.2018.06.011>
- Zhang, J.; Hu, J.; Lian, J.; Fan, Z.; Ouyang, X.; Ye, W. (2016) Seeing the forest from drones: Testing the potential of lightweight drones as a tool for long-term forest monitoring. *Biol. Conserv.*, 198, 60–69.
- Zhang X, Friedl MA, Schaaf CB, Strahler AH, Hodges JC, Gao F, . . . Huete A (2003) Monitoring vegetation phenology using MODIS. *Remote Sensing of Environment*, 84, 471-475.
- Zhuk, E., & Goroshkevich, S. (2018). Growth and reproduction in *Pinus sibirica* ecotypes from Western Siberia in a common garden experiment. *New Forests*, 49(2), 159-172. <https://doi.org/10.1007/s11056-017-9611-7>
- Zweifel, R., Eugster, W., Etzold, S., Dobbertin, M., Buchmann, N., & Häsler, R. (2010). Link between continuous stem radius changes and net ecosystem productivity of a subalpine Norway spruce forest in the Swiss Alps. *New Phytologist*, 187(3), 819-830. <https://doi.org/10.1111/j.1469-8137.2010.03301.x>